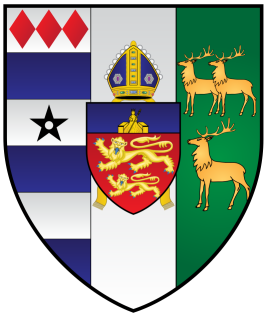
Characterisation of an “eat-me” signal on dying and HIV-1-infected T cells





A thesis submitted for the degree of Doctor of Philosophy

Michaelmas Term 2018

Niloofar Karaji

Sir William Dunn School of Pathology

Lincoln College

University of Oxford

Abstract

Niloofar Karaji
Lincoln College

Submitted for the degree of Doctor of Philosophy
Michaelmas Term 2018

Characterisation of an "eat-me" signal on dying and HIV-1-infected T cells

The clearance of dying cells by phagocytes, termed efferocytosis, is regulated by a combination of "eat-me" and "don't eat-me" signals expressed on the dying cell surface. Efferocytosis is essential for ontogeny and tissue homeostasis, but can also mediate the spread of pathogen infection, and its dysregulation leads to inflammatory disorders. The Sattentau laboratory recently reported that the macrophage efferocytic uptake of HIV-1-infected CD4+ T cells drives efficient infection of macrophages. However, the signals involved in the macrophage capture of the infected T cell remain undefined, but cell death appears to be an important component of this recognition.

In this study a novel efferocytic pathway which is based on the cleavage of the heavily sialylated glycoprotein CD43 acting as a potent 'don't eat-me' signal for macrophages is investigated. Data presented in this thesis imply that; i) CD43 shedding is mediated by ADAM10 which is activated by T cell death, and ii) cleavage of CD43 as a don't eat-me signal from the surface of dying and infected T cells triggers their engulfment by macrophages.

In the context of HIV-1infection, interventions in this pathway may have the potential of reducing targeted macrophage infection. Also, the knowledge of this novel efferocytic pathway has general implications for understanding and potentially treating unwanted inflammatory disorders.

Acknowledgment

I would like to express my gratitude to everyone who helped me during my studies. Firstly, thanks must go to my supervisors, Professor Quentin J. Sattentau and Dr. Rebecca Russell for their guidance, advice and support which helped me to develop into an independent scientist.

I would also like to thank all members of the Sattentau laboratory, in particular Dr. Amin Moghadam, for being a constant source of support and friendship. Additional thanks go to Dr. Kenny Moore for all of his scientific insights, and the generation of ADAM10 knock out T cells together with Dr. Rebecca Moore. I would also like to thank my student Rachael Harisson for her contributions to my work, Dr. Torben Schiffner for providing all the bNAbs , and everyone who contributed reagents as listed in the materials and methods section.

I have also been really lucky to have the support of my amazing friends in Oxford and Bonn. So a big thank you goes to Sara, Mayida, Alireza, Taha, Cherrelle and Kerstin. Thank you also to my family, especially Mum, Dad and, little brother, Farzan who have always supported me in “almost” everything I choose to do! Lastly, a special thank you to my partner Peter. He has literally kept me alive and sane throughout the writing process by feeding me Pepper’s burger, taking care of me while I was attacked by a variety of microorganisms, and calming my anxious and racing mind down. I genuinely could not have met the October 5th deadline without you and your Inkscaping talent.

Abbreviations

β2M	β2-microglobulin
μl	Microliter
Ab	Antibody
APAF1	Apoptotic protease activating factor 1
AIDS	Acquired immunodeficiency syndrome
APC	Allophycocyanin
APOBEC3	Apolipoprotein B messenger RNA (mRNA)-editing enzyme catalytic polypeptide-like 3
ART	Antiretroviral therapy
AZT	Azidothymidine
BAI1	Brain specific angiogenesis inhibitor 1
bNAb	Broadly neutralising antibody
CCR5	C-C chemokine receptor 5
CD	Cluster of differentiation
CFAR	Centre for aids reagents
CHO	Chinese hamster ovary cells
CNS	Central nervous system
Conc	Concentration
CRT	Calreticulin
CTC	Cell-to-cell
CXCR4	CXC chemokine receptor 4
Cytochrome c	Cyto c
DCC	DCC netrin 1 receptor
DF	Dilution factor
EGFR	Epidermal growth factor receptor
Env	Envelope glycoprotein
ELISA	Enzyme-linked immunosorbent assay
ER	Endoplasmic reticulum
ERM	ezrin-radixin-moesin
ESCRT	endosomal sorting complexes required for transport
Eto	Etoposide
FA	Formaldehyde
FACS	Fluorescence-activated cell sorting
FADD	FAS-associated death domain protein
Gag/gag	Group antigens (retroviral structural protein)
GALT	Gut associated lymphoid tissue
Gas6	Growth arrest-specific 6
Gp120	120 kDa Envelope glycoprotein surface subunit
Gp41	41 kDa Envelope glycoprotein transmembrane subunit
GSDMD	Gasdermin D

h	Hour
HEK	Human embryonic kidney
HIV-1	Human Immunodeficiency Virus-1
HLAC	Human lymphoid aggregate culture
HMGB1	High mobility group protein-1
HS	Human serum
IC_{50}	50% Inhibitory concentration
IL-2	Interleukin-2
INSTIs	Integration strand transfer inhibitors
ITIM	Immunoreceptor tyrosine-based inhibitor motif
IU	Infectious unite
kDa	kiloDalton
MAA	Maakia amurensis
LB	Liquid broth
LCs	Langerhans cells
LFA-1	Leukocyte function-associated antigen 1
LOX-1	low-density lipoprotein receptor
LPS	Lipopolysaccharide
LTR	Long Terminal Repeat
LucR	Renilla luciferase
mAb	Monoclonal antibody
Mac-1	Macrophage-1 antigen
MDM	Monocyte-derived macrophages
MFG-E8	Milk fat globule-EGF factor 8
min	Minute
ml	Millilitre
MOMP	Mitochondrial outer membrane permeabilisation
MOI	Multiplicity of infection
MPER	Membrane proximal external region
MR	Mannose receptor
mRAGE	Full-length membrane-bound form RAGE
MSM	Men-who-have-sex-with-men
MW	Molecular weight
NFAT	Nuclear Factor of Activated T cells
NF-κB	Nuclear Factor kappa-light-chain-enhancer of activated B cells
NNRTIs	Non-nucleoside RT inhibitors
NRTIs	Nucleoside RT inhibitors
NTRK3	Neurotrophic receptor tyrosine kinase 3
OD	Optical density
PAI1	Plasminogen activator inhibitor-1
PBL	Peripheral blood lymphocytes
PBMCs	Peripheral blood mononuclear cells
PBS	Phosphate buffered saline
PE	R-phycoertthrin
PEI	Polyethyleneimine
PECAM-1	Platelet-endothelial cell adhesion molecule-1
Pen Strep	P/S

PHA	Phytohaemagglutinin
PI	Protease Inhibitor
PMA	Phorbol myristate acetate
PNA	Peanut agglutinin
PS	Phosphatidylserine
PSR	Phosphatidylserine receptor
PTEF-b	Positive transcription elongation factor-b
Q-VD-OPh	(3S)-5-(2,6-difl uorophenoxy)-3-[[(2S)-3-methyl-1-oxo-2-[(2-quinolinylcarbonyl) amino]butyl]amino]-4-oxo-pentanoic acid hydrate
RBC	Red blood cells
RCD	Regulated cell death
RAGE	Receptor for advanced glycation end products
RMPI	Roswell Park Memorial Institute medium
RLU	Relative light units
RT	Room temperature
RTC	Reverse transcription complex
SAMHD1	Sterile alpha motif and HD domain protein 1
SAMC	Second mitochondria-derived activator of caspase
sec	Second
Sial	Sialic acid
Siglec-11	Sialic acid binding Ig-like lectin 11
SIRPa	Signal regulatory protein a receptor
SOC	Super optimal broth with catabolite repression
sRAGE	Soluble form RAGE
Stau	Staurosporine
T/F	Transmitted/founder
Tat	Trans-activating transcription
TIM	T cell immunoglobulin and mucin
TNF-α	Tumor necrosis factor-alpha
TRAILR	TNF-related apoptosis-inducing ligand receptor
TRIM5α	TRIpartite Motif containing family of protein 5α
UNC5A	Unc-5 netrin receptor A
US	United States
VS	Virological synapse
WT	Wild type
XIAP	X-linked inhibitor of apoptosis protein
Z-VAD-FMK	N-benzyloxycarbonyl-Val-Ala-Asp(O-Me) fluoromethylketone

Table of contents

ABSTRACT III

ACKNOWLEDGMENT IV

ABBREVIATIONS V

TABLE OF CONTENTS 9

CHAPTER 1: GENERAL INTRODUCTION 13

1.1. HUMAN IMMUNODEFICIENCY VIRUS-1 (HIV-1) 14

1.1.1. HIV/AIDS EPIDEMIOLOGY 14

1.1.2. HIV-1 STRUCTURE 16

1.1.3. HIV-1 LIFE CYCLE 17

1.1.4. HIV-1 PATHOGENESIS 24

1.1.5. CELL-TO-CELL TRANSMISSION OF HIV-1 29

1.1.6. CD4+ T CELL DEATH DURING HIV-1 INFECTION 31

1.2. CELL DEATH 35

1.2.1. APOPTOTIC CELL DEATH 35

1.2.2. PYROPTOTIC CELL DEATH 39

1.2.3. EFFEROCYTOSIS OF DYING AND PATHOGEN-INFECTED CELLS 41

1.3. LEUKOSIALIN (CD43) 53

1.3.1. CD43 STRUCTURE 53

1.3.2. CD43 FUNCTIONS 54

1.4. ADAM10 55

1.4.1. ADAM10 STRUCTURE 55

1.4.2. ADAM10 SUBSTRATES 56

1.4.3. ADAM10 REGULATION 56

1.5. FOCUS AND SCOPE OF THE THESIS 57

CHAPTER 2: MATERIALS AND METHODS 61

2.1. TISSUE CULTURE 62

2.1.1. OBTAINING PERIPHERAL BLOOD MONONUCLEAR CELLS 62

2.1.2. MONOCYTE ISOLATION AND MDM DIFFERENTIATION 62

2.1.3. ISOLATION OF $CD4^+$ T CELLS BY MAGNETIC LABELLING 63

2.1.4. NON-ADHERENT CELL MAINTENANCE 63
2.1.5. ADHERENT CELL MAINTENANCE 64
2.1.6. CRYOPRESERVATION 64
2.1.7. THAWING CELLS 64
2.1.8. GENERATION OF T AND HEK CELL LINES 67
2.2. VIRAL PREPARATION AND HIV-1 INFECTION 69
2.2.1. TRANSFORMATION 69
2.2.2. MAXI-PREPARATION OF VIRAL PLASMIDS 69
2.2.3. PEI TRANSFECTION OF HEK 293T CELLS 70
2.2.4. VIRUS CONCENTRATION 70
2.2.5. VIRAL INFECTIVITY TITRATION 70
2.2.6. CD4+ T CELL INFECTION 71
2.3. FLOW CYTOMETRY 72
2.3.1. SURFACE STAINING OF LIVE CELLS 72
2.3.2. SURFACE STAINING OF FIXED CELLS 73
2.3.3. INTRACELLULAR STAINING OF FIXED CELLS 73
2.3.4. ACQUISITION AND ANALYSIS 74
2.4. UPTAKE ASSAY 77
2.5. DIRECT ELISA 78
2.6. INDUCTION OF APOPTOSIS 79
2.6.1. CD4+ T CELL LINES 79
2.6.2. PRIMARY CD4+ T CELLS 79
2.7. INDUCTION OF PYROPTOSIS 80
2.7.1. CD4+ T CELL LINES 80
2.7.2. PRIMARY CD4+ T CELLS 80

CHAPTER 3: THE ROLE OF HIV-1 ENV AND ICAM-1 IN INTERACTIONS BETWEEN MDM AND HIV-1-INFECTED T CELLS 83

3.1. INTRODUCTION 84
3.1.1. HYPOTHESIS 85
3.1.2. SPECIFIC AIMS 85
3.2. RESULTS 86
3.2.1. THE ROLE OF ENV IN HIV-1-INFECTED CD4+ T CELL-MDM INTERACTIONS 86
3.2.2. THE ROLE OF ICAM-1 IN HIV-1-INFECTED CD4+ T CELL ENGULFMENT BY MDM 95
3.2.3. THE ROLE OF LFA-1 AND MAC-1 AS LIGANDS OF ICAM-1 IN THE ENGULFMENT OF HIV-1-INFECTED CD4+ T CELLS BY MDM 99

3.2.4. THE ROLE OF CD43 AS A LIGAND OF ICAM-1 IN MDM ENGULFMENT OF HIV-1-INFECTED CD4+ T CELLS 103
3.3. DISCUSSION 108
3.3.1. THE ROLE OF ENV IN INFECTED T CELL UPTAKE AND MDM INFECTION 108
3.3.2. THE ROLE OF ICAM-1 AND ITS LIGANDS (LFA-1, MAC-1 AND CD43) IN INFECTED T CELL UPTAKE AND MDM INFECTION 109

CHAPTER 4: CD43 MODIFICATION IN HIV-1 INFECTION AND CELL DEATH 113

4.1. INTRODUCTION 115
4.1.1. HYPOTHESIS 116
4.1.2. SPECIFIC AIMS 116
4.2. RESULTS 117
4.2.1. CD43 MODIFICATION UPON HIV-1 INFECTION 117
4.2.2. CD43 MODIFICATION UPON APOPTOTIC CELL DEATH 125
4.2.3. CD43 MODIFICATION UPON PYROPTOTIC CELL DEATH 132
4.2.4. CD45 MODIFICATION UPON HIV-1 INFECTION AND APOPTOTIC CELL DEATH 137
4.3. DISCUSSION 142

CHAPTER 5: CD43 MODIFICATION MECHANISM AND ITS IMPLICATION AS AN EAT-ME SIGNAL 147

5.1. INTRODUCTION 149
5.1.1. HYPOTHESIS 150
5.1.2. SPECIFIC AIMS 150
5.2. RESULTS 151
5.2.1. ROLE OF CASPASE ACTIVATION IN CD43 MODIFICATION DURING APOPTOTIC CELL DEATH 151
5.2.1.1. INHIBITION OF CASPASE ACTIVATION PREVENTS CD43 MDD MODIFICATION 151
5.2.2. ROLE OF CASPASE ACTIVATION IN CD43 MODIFICATION DURING HIV-1 INFECTION 159
5.2.3. THE ROLE OF CD43 INTERNALISATION IN CD43 MDD MODIFICATION 164
5.2.4. PROTEOLYTIC CLEAVAGE OF CD43 DURING CELL DEATH 165
5.2.5. PROTEASE-MEDIATED CLEAVAGE OF CD43 MDD 175
5.2.6. THE ROLE OF CD43 IN EFFEROCYTIC UPTAKE BY MACROPHAGES 186
5.3. DISCUSSION 191

CHAPTER 6: CONCLUDING REMARKS 197

6.1. SUMMARY 199
6.2. FUTURE PERSPECTIVES 201

6.2.1. CD43 SHEDDING DURING CELL DEATH 201
6.2.2. ADAM10 ACTIVITY IN CD43 SHEDDING DURING HIV-1 INFECTION AND CELL DEATH 201
6.2.3. PS AS A POTENTIAL TRIGGER OF ADAM10 ACTIVATION 202
6.2.4. ADAM10 AND CD43 MEMBRANE LOCALISATION DURING HIV-1 INFECTION, CELL DEATH AND EFFEROCYTOSIS 203
6.2.5. CD43 MEMBRANE PROXIMAL DOMAIN AND EFFEROCYTOSIS 203
6.3. CONTRIBUTION TO THE FIELD 206

REFERENCES 209

Chapter 1: General introduction

1.1. Human immunodeficiency virus-1 (HIV-1)

1.1.1. HIV/AIDS epidemiology

Over 36 million people are currently infected with the human immunodeficiency virus type 1 (HIV-1) [2]. In 1981, the acquired immunodeficiency syndrome (AIDS) which is the clinical consequence of advanced HIV-1 infection, was first recognised in the men-who-have-sex-with-men (MSM) population [3]. Doctors in the United States of America (USA) reported that the patients were profoundly lymphopenic, anergic and had a specific loss of $CD4^+$ T helper cells [4]. By 1982, patients were no longer limited to the MSM population, but women who were predominantly intravenous drug users [5], haemophiliacs [6] and Haitian immigrants were particularly at risk. At this time, AIDS cases were also reported in Europe, mostly in the MSM population and people who inject drugs similar to the USA. However, a greater burden of heterosexual infection was evident in central Africa [7, 8]. This was mainly due to genital ulcerative disease, population mobility, urbanisation, low rates of condom use and infrequent male circumcision [9]. Currently, nine southern African countries with 2% of the world's population contribute to ~30% of the HIV-1 cases as a result of the above mentioned issues and dynamics [9]. The development of effective antiretroviral therapy (ART) has helped to stabilise the HIV-1 pandemic [10], however uncontrolled transmission continues at unacceptable levels in certain risk groups such as MSM [11].

Cloning of HIV-1 [12] and full sequencing of the viral genome [13, 14] classified the virus as a member of the *Retroviridae* family, subspecies *Lentiviridae*.

Evolutionary studies provided the first evidence that HIV-1 may have emerged in humans as a consequence of a cross-species transmission events from a non-human primate natural host in Cameroon, most probably the chimpanzee [15, 16]. However, the origins of HIV-1 actually proved more difficult to elucidate. In 1999, it was recognised that the HIV-1 M and N lineages are closely related to one strain of chimpanzee (*Pan troglodytes*) SIV (SIV_{cpz}),

Cross-species transmission of SIV_{cpz} most likely occurred through cutaneous membrane exposure to infected ape blood or bodily fluid in the context of bush meat hunting [17]. The earliest identified strains from the M lineage localise the beginning of the outbreak to Leopoldville (now Kinshasa) in colonial West Central Africa [18, 19]. Unlike the M lineage, phylogenetic analyses of the P lineage suggest a gorilla (*Gorilla gorilla*) origin for this subtype. However, limited examples of natural gorilla SIV (SIV_{gor}) have made sequence comparisons to identify the exact location of the cross-species transmission event challenging [20]. Lastly, the source of the O lineage remains unclear and could be either SIV_{gor} or SIV_{cpz} [20].

As the result of these transmission events, HIV-1 has branched into four distinct lineages, known as M, N, O and P. The minor lineages include N, O and P, which form less than 1% of global HIV-1 cases and have remained geographically restricted to Cameroon [16]. However, M is the major lineage representing the pandemic form of HIV-1, which had spread to central Africa and the Americas by the 1960s, subsequently reaching Europe and Asia [9, 16]. Over this relatively short timespan, nine distinct subtypes (clades) of the

HIV-1 M lineage have been isolated (A-D, F-H, J and K) with over 40 circulating recombinant forms [15, 16]. In Africa, clade C accounts for ~50 % of infections [21], whereas in the USA and Europe clade B is predominant [22]. The genetic diversity of HIV-1 is a central feature of its rapid (duration 1-2 days) and highly mutation-prone life cycle [23]. Multiple studies have detailed the structure and life cycle of this virus (Section 1.1.2 and 3) and the pathogenesis of HIV-1 infection (Section 1.1.4).

1.1.2. HIV-1 structure

The HIV-1 genome is ~10,000 nucleotides long and encodes three proteins essential for virion structure and function, and six accessory proteins. Gag (matrix, capsid and nucleocapsid), Pol (reverse transcriptase, integrase and protease) and Env are required for the organisation and generation of new virions, whereas the accessory proteins (Tat, Rev, Vpr, Vpu, Nef, and Vif) promote viral transcription, counteract host retroviral restriction factors and evade host immunity [24]. Mature enveloped HIV-1 virions produced from infected cells are on average ~120 nm in diameter, consisting of a lipid envelope, a capsid, virally-encoded enzymes reverse transcriptase, integrase and protease, and two positive RNA strands

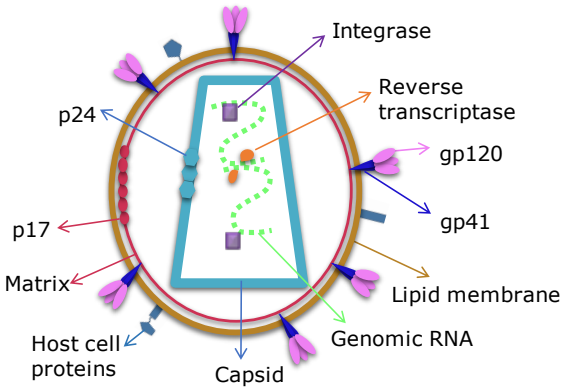


Figure 1.1. Schematic of an HIV-1 virion. Two copies of the RNA genome, including attached integrase and reverse transcriptase proteins are packaged in a cone-shaped capsid. The virion is surrounded by a lipid envelope containing the surface glycoprotein Env composed of three copies of gp120 and gp41 each in non-covalently linked heterotrimers and host cell proteins.

encoding 9 genes (Figure 1.1). The lipid envelope is composed of a host cell-derived lipid bilayer, selected host cell surface molecules and viral gp120-gp40 trimers (termed Env) [25, 26]. Env is a heavily glycosylated mushroom-like spike with the membrane proximal external region (MPER) of gp41 forming a stalk upon which three non-covalently linked gp120 subunits create a cage-like structure with an internal cavity between the subunits [27-31]. On the surface of each virion ~7-14 spikes are present [32]. However, Env is unstable and susceptible to rapid extracellular degeneration, conferring a half-life of approximately 5 hours [33].

1.1.3. HIV-1 life cycle

The life cycle of HIV-1 comprises virus transmission from HIV-1-infected to uninfected individuals followed by the infection of a cell expressing the viral entry receptors, and the production of new viral particles which involves the stages described below (Figure 1.2).

1.1.3.1. Binding and fusion

Virion attachment to the plasma membrane may occur through multiple mechanisms. Non-specific interactions occur with host cell molecules such as heparan sulfate proteoglycans [34, 35], C-type lectins [36, 37] and integrins [38, 39]. Although not necessary for infection, viral adsorption to the cell enhances the probability of subsequent engagement of the specific HIV-1 entry receptors CD4 [40, 41] and a chemokine co-receptor (usually CCR5 [42, 43] or CXCR4 [44]) by the Env receptor binding component gp120 [45] (Figure 1.2B). Viruses

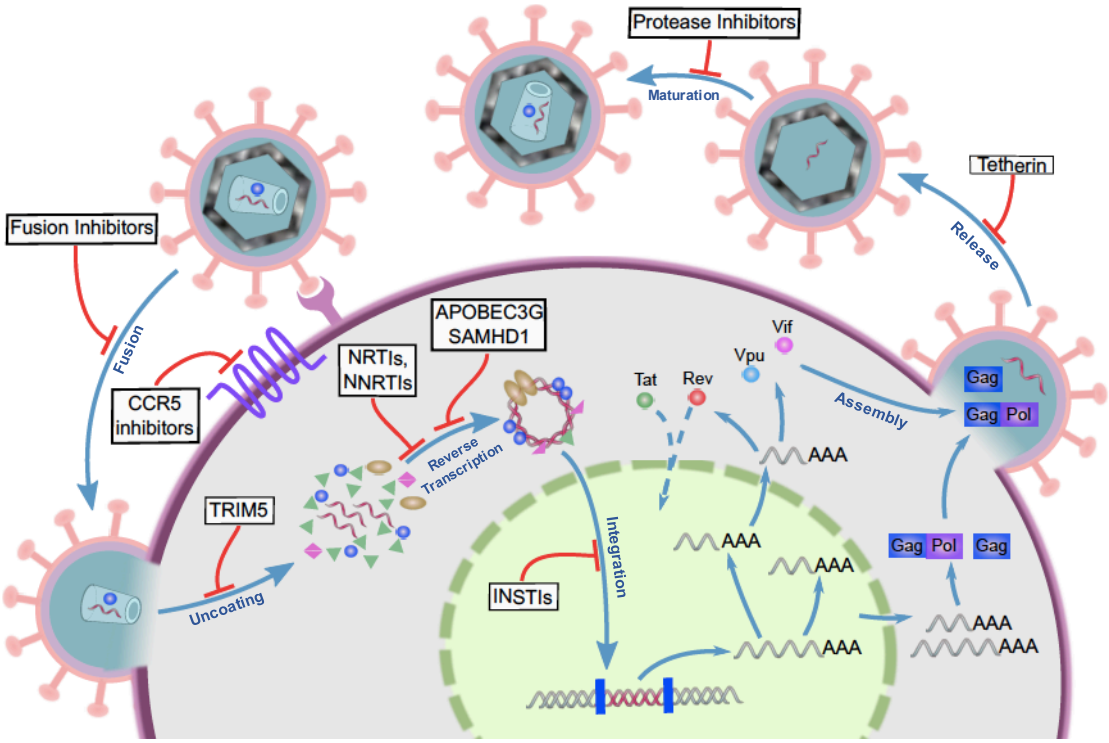


Figure 1.2. Schematic of the HIV-1 life-cycle. HIV-1 virion enters a target cell and releases its core including the RNA into the cytoplasm where reverse transcription into double-stranded DNA occurs. The DNA is imported into the nucleus and integrated into the host genome by the viral integrase protein. Transcription and nuclear export lead to formation of viral proteins and new viral RNA genomes. New virions bud from the plasma membrane (see text for details). Those host proteins that have a role in the replication cycle and are discussed in the text are also indicated. Figure is the modified version of the first Figure of Engelman et al. review article [46].

using CCR5 are termed R5 tropic, and viruses using CXCR4 are termed X4 tropic [47]. Env binding to CD4 is initially a relatively low affinity interaction [36] inducing a structural rearrangements of gp120 to increase affinity, and includes conformational changes in the gp120 variable regions, particularly V3, exposing the co-receptor binding sites [45]. The fusion event is pH-independent but it can occur at either the cell plasma membrane [45] or from within macropinocytic [48] or endosomal [49] vesicles. The relative dominance and functional implication of these differential entry routes is still unclear. Two licensed

antiretroviral compounds targeting these entry processes are maravaroc (CCR5 inhibitor [50]) and the alpha helical peptide enfurvitide (T-20, fusion inhibitor [51]).

1.1.3.2. Uncoating and reverse transcription

Once the viral envelope fuses with the host cell membrane, the viral capsid enters the cytoplasm where reverse transcription occurs. The reverse transcription of the viral genome begins within hours after viral entry, and is dictated by the availability of nucleotide precursors [23]. The phosphohydrolase activity of sterile alpha motif domain and HD domain-containing protein 1 (SAMHD1) regulates nucleotide precursor availability, particularly within myeloid cells, acting as a cell-type restriction factor [52]. SAMHD1 is antagonised by the viral accessory protein Vpx in HIV-2 and SIV, which does not exist in HIV-1. Reverse transcription happens in the reverse transcription complex, which can be destabilised by the TRIpartite Motif containing family of proteins such as 5α (TRIM5α), an inter-species restriction factor [53].

Viral DNA synthesis proceeds as follows: i) the $tRNA^{Lys3}$ primer binds to the primer binding site; ii) synthesis of long terminal repeat (LTR) cDNA minus strand (known as strong stop) and the removal of the complementary portion of the RNA strand end by RNase H domain of reverse transcriptase; iii) reverse transcriptase repositioning to complete minus strand synthesis from the 3' end; iv) RNA degradation by RNase H (sparing the polypurine tract); v) Plus-strand cDNA synthesis starting at the polypurine tract with temporary circularisation of the cDNA sequence; and vi) breakage of the cDNA circles and completion of

plus strand synthesis to generate linear dsDNA with an LTR positioned at each end [23].

The packaging of the restriction factor apolipoprotein B messenger RNA (mRNA)-editing enzyme catalytic polypeptide-like 3 protein G (APOBEC3G) into newly assembled virions induces G-to-A hypermutation in plus-strand cDNA [54] which can impair cDNA synthesis [55] or occasionally lead to sequence mutations that aid in generation of viral variation [16]. However, Vif, an HIV-1 accessory protein and potent restriction factor antagonist, degrades APOBEC proteins within the newly infected cell [56, 57]. Reverse transcription is a highly error-prone process, which generates 1-10 mutations per genome. Moreover, if the cell is simultaneously infected with more than one virus, the reverse transcriptase may switch the template resulting in genome recombination [23]. Reverse transcriptase was the earliest target for antiretroviral drugs [58]. There are two main classes of RT inhibitor. The first class includes nucleoside analogues causing cDNA chain termination, and is called nucleoside RT inhibitors (NRTIs, such as the prototype Azidothymidine (AZT)) [59]. The second class is the non-nucleoside RT inhibitors (NNRTIs, such as nevirapine) [60] which bind a non-catalytic domain on reverse transcriptase preventing chain elongation [59].

1.1.3.3. Integration

Integration occurs within 15 hours of viral entry [59]. Completion of reverse transcription gives rise to the pre-integration complex (PIC), which contains viral cDNA. In order for integration to occur, the PIC needs to migrate to the

nucleus, the mechanisms of which have not been fully understood [61]. The integration steps are as follow: i) two nucleotides are removed from the 3' ends of the blunt-end viral DNA allowing the hydroxyl groups at the 3' ends to attack a pair of phosphodiester bonds in the host DNA; ii) DNA-strand transfer begins with covalently joining 3' ends of viral to the 5' ends of the host DNA and finishes when; iii) two unpaired bases at the 5' ends of the viral DNA are removed and the single-strand gap between viral and host DNA is ligated [61]. Integration occurs preferentially at active transcription sites in order to allow transcription [62]. This preference may be due to DNA distortion promoting integration by lowering the required activation energy [63]. Host factors such as lens epithelium-derived growth factor (LEDGF/p75) facilitate this targeted integration [61, 64].

Integration strand transfer inhibitors (INSTIs) are recent additions to the antiretroviral drugs. Raltegravir is an INSTIs which blocks DNA-strand transfer by binding to the specific complex formed between integrase and the viral DNA [65].

1.1.3.4. Transcription

Once viral DNA is integrated, host regulation of transcription will determine the fate of the provirus; productive HIV-1 infection or viral latency. Proviral transcription is under the control of both host transcription factors and viral accessory proteins. Host transcription factors include nuclear factor kappa-light-chain-enhancer of activated B cells (NF-κB) [66], nuclear factor of activated T cells (NFAT) [67], positive transcription elongation factor-b (PTEF-b) [68-70], and histone deacetylation and methylation [71]. Therefore, viral transcription is linked to cellular activation status and resting infected $CD4^+$ T

cells show very low levels of virus production [71]. Initial viral transcription starts at the LTR promoter by the host RNA polymerase II [72], and is inefficient due to its dependency on trans-activating transcription (Tat, viral accessory protein) [73, 74]. However, a sufficient amount of Tat is transcribed to trigger a powerful positive feedback loop [75, 76]. Transcription elongation efficiency is enhanced if the host transcription factor PTEF-b makes a complex with Tat [68-70] which determines whether the cell goes towards latency or virus production [77]. HIV-1 RNA transcripts undergo varying degrees of co-transcriptional splicing. Unspliced RNAs function as the mRNAs for the Gag and Gag-Pro-Pol polyprotein, which are packaged into the virion as genomic RNA. Partially-spliced mRNAs encode the Env, Vif, Vpu and Vpr proteins, while completely spliced mRNAs encode Rev, Tat and Nef [78].

1.1.3.5. Assembly and budding

Virion assembly is the process in which the viral essential components are packaged into a virion for a subsequent round of infection. This includes the structural proteins Env and Gag, reverse transcriptase, integrase, protease, two ssRNA molecules and host $tRNA^{lys3}$ primer [32]. The Gag polyprotein is capable of mediating many of the steps of virion assembly. The matrix domain in the Gag oligomer (MA domain) targets the polyprotein to the plasma membrane. Targeting requires myristolation [79] and a basic patch in the MA domain [80, 81]. This basic patch binds to plasma membrane-specific lipid phosphatidyl inositol (4,5) bisphosphate ($PI_{(4,5)}P_2$) [82], inducing a structural change which exposes a myristoyl group in the N terminus of the Gag polyprotein [83], and thereby specifically targets Gag to the plasma membrane. The ability to bind the plasma membrane is not conserved in the cleaved, processed MA protein

as the myristic acid modification is lost [84]. Once at the plasma membrane, interactions between the Gag polyprotein nucleocapsid domain and RNA allow Gag molecules to align and pack. Although the membrane proteins Env and Vpu separately traffic to the plasma membrane, the precise mechanisms for the trafficking of all viral proteins to the plasma membrane is not completely defined [32].

Budding is where the virion becomes enveloped and released, and is mediated by the host ESCRT (endosomal sorting complexes required for transport) machinery. It occurs at raft-like domains as the analysis of the viral membrane revealed enrichment of lipid raft components such as sphingomyelin, phosphatidylserine (PS), phosphatidylethanolamine and cholesterol [85]. Virion maturation occurs during and after budding, is essential for conical capsid re-assembly and virion infectivity, and is viral protease-dependent [32]. The FDA has approved ten HIV-1 protease inhibitors including saquinavir, indinavir, ritonavir, nelfinavir, amprenavir, fosamprenavir, lopinavir, atazanavir, tipranavir, and darunavir. However, most of these inhibitors cause side effects in long-term treatment [86]. The host restriction factor tetherin blocks viral release following budding by tethering virions to the plasma membrane [87, 88], but is antagonised by the viral accessory protein Vpu.

1.1.4. HIV-1 pathogenesis

The pathogenesis of HIV-1 infection is governed essentially by the outcome of the battle between HIV-1 replication and the infected individual's immune responses, but almost invariably leads to AIDS in the absence of therapeutic intervention.

1.1.4.1. Stages of HIV-1 infection

Initially, it was presumed that the gradual CD4+ T cell depletion during chronic infection caused progression to AIDS during a single extended phase. Now we know that AIDS is the result of two phases; acute infection in which CD4+ T cells are massively depleted, and chronic infection in which the injured immune system gradually collapses [89]. Heterosexual infection is usually initiated by the transmission of a single viral clone called a transmitted/founder (T/F) virus followed by extensive dissemination and viral mutation due to the error-prone life cycle of HIV-1 and selection pressure by the host immune response. Although HIV-1 can use CCR5, CXCR4 or both CCR5/CXCR4 for its entry, studies have suggested that (T/F) viruses utilise almost invariably CCR5 for transmission between individuals [90, 91], the reason for which remains unclear.

Studying Initial infection in patients is clearly difficult. Therefore, using vaginal explant models, it has been shown that HIV-1 binds and infects CD4+ memory T cells expressing CCR5 within hours of viral exposure. This has been confirmed using macaque models of mucosal infection by simian immunodeficiency virus (SIV). HIV-1 RNA is undetectable in blood within 7-21 days of initial infection: this stage of infection is generally asymptomatic and is

called the eclipse period [91]. In the acute infection, the infected individual may experience fever, sore throat, lymphadenopathy and rashes. By this time, the virus has already spread in the mucosa, draining lymph nodes and the gut associated lymphoid tissue (GALT) [92]. Acute infection is characterised by immune activation and a massive depletion of CD4+ T cells (discussed in Section 1.1.4.2) in lymphoid and mucosal tissues, and particularly the GALT. Cytotoxic T lymphocyte (CTL) responses emerge in the GALT and in the peripheral lymph nodes at this stage, which are associated with reducing the viral load to the set point after the peak of viraemia [93]. In addition, viral dissemination to the CNS occurs during this period, often initiating neuropathology [94]. Establishment of HIV-1 reservoirs is thought to happen within 5-10 days of viral transmission [95], and this concept is supported by recent evidence showing that after a high dose challenge, the SIV reservoir is established in the macaque model within the first 3 days of infection [96]. Transitioning of a small proportion of infected CD4+ T cells to a resting memory phenotype has been proposed during acute infection, which could establish the long-lived reservoir of latently infected cells [71].

Chronic infection is characterised by a stable viral production period in which the immune system maintains a viral load at a relatively steady set point. During chronic infection, CD4+ T cell numbers may partially recover and this stage may persist for years before progression to AIDS occurs, defined in part by peripheral blood CD4+ T cell numbers below 200 cells per µl blood. SIV macaque studies have suggested that macrophages are preferentially infected at this stage due to extensive $CD4^+$ T cell depletion during acute infection [97,

98]. Moreover, Infected alveolar macrophages have been detected in the lungs and other tissues of patients [99]. Infection of macrophages will be discussed in more detail in Section 1.1.4.3. A number of factors have been shown to contribute to faster progression to AIDS including status of immune activation, higher viral set point during chronic infection [100], and the evolution of X4 viruses [101].

1.1.4.2. CD4+ T cells in HIV-1 infection

CD4+ T cells (known as T helper cells) are the major targets of HIV-1 infection, and are a heterogeneous population of lymphocytes coordinating cellular and humoral immune responses involved in immune regulation [102]. The earliest targets for HIV-1 infection are CCR5-expressing effector memory CD4+ T cells in the lamina propria of mucosal tissues [103]. Infected mucosal $CD4^+$ cells can be detected within two to three days of infection [104]. HIV-1-infection of CD4+T cells make them susceptible to rapid cell death via different mechanisms including direct cytopathic effects [105], $CD8^+$ T cell lysis [93], abortive infection induced pyroptosis [106], bystander apoptosis [107] and activation-induced apoptotic cell death [108]. Therefore, during acute HIV-1 infection, massive depletion of effector and memory CD4+ T cells occurs in the GALT driving intense local inflammation and tissue destruction [103]. This ultimately leads to non-specific immune activation via compromise of the mucosal epithelium and immune barrier allowing bacterial translocation, destruction of lymphoid follicular architecture, and eventually exhaustion of the immune system resulting in immunodeficiency [103]. Immune activation is driven not only by failure of mucosal barrier function, but also loss of regulatory control and/or additional effects of uninhibited replication of other pathogens such as herpes

viruses [103]. However, when it comes to SIV infections in natural hosts there is no satisfactory explanation for the absence of immune activation and immunodeficiency, despite high levels of viral replication and acute depletion of mucosal T cells [103]. Naïve $CD4^+$ T cells do not express CCR5, however they express CXCR4. Therefore, HIV-1 infection of Naïve $CD4^+$ T cells occurs in approximately 50% of individuals at the later stage as utilisation of CXCR4 evolves late in the course of HIV-1 infection [109]. HIV-1 replication in resting T cells is inefficient [110] therefore a small population of infected memory T cells can form the latent HIV-1 reservoir when they transition back to a resting state [71]. Mechanisms driving the loss of CD4+ T cells during HIV-1 infection are discussed in section 1.1.6.

1.1.4.3. Macrophages in HIV-1 infection

Macrophages are myeloid-lineage cells, essential for tissue homeostasis and repair, and sensing and removal of microbial pathogens and tumour cells (the role of macrophages as professional phagocytes is discussed in Section 1.2.3) [111]. They are dispersed in almost every organ including the CNS, lymphoid tissue, lung, gut and genital tract mucosa [112]. The lifespan of macrophages *in vivo* varies from weeks to years, since many resident macrophages such as microglia have self-renewal properties and can persist lifelong [112]. Moreover, it has recently been shown that they can be categorised in two district groups based on their origin; i) self-renewing tissue-resident macrophages derived from primitive embryonic precursors, and ii) infiltrating monocyte-derived macrophages (MDM) [113]. This knowledge has influenced our vision of macrophage function based on their location and origin in both normal and

pathologic conditions including HIV-1 infection [114], which is briefly discussed below.

Macrophages express both CD4 and chemokine co-receptors although at low levels [115]. However, most T/F and X4-tropic viruses are unable to enter or establish a productive infection in macrophages [116]. Moreover, there are post-entry obstacles that must be overcome for productive infection including expression of SAMHD1 [117, 118]. These findings are consistent with studies showing CD4+ T cells and not macrophages as the primary target of HIV-1 after transmission and explaining inefficient MDM infection compared to CD4+ T cells.

HIV-1-infected macrophages become detectable in the lymphoid tissues after two to three weeks [119]. While macrophages in different tissues share some common characteristics they also display considerable functional heterogeneity influencing HIV-1 permissiveness [120]. For example, gut macrophages appear relatively restrictive to productive infection whereas genital tract macrophages are highly susceptible [121, 122], highlighting the role of the tissue cytokine microenvironment in regulating macrophage permissiveness [123]. Another example is that macrophages proximal to the rectum present increased CCR5 expression and greater HIV-1 susceptibility compared to colon-resident cells [124].

Recent studies have shown the presence of infected tissue macrophages in brain (microglia and perivascular macrophages [125]), lung (alveolar

macrophages [126]), genital tract [127] and duodenal mucosa [128] at different stages of HIV-1 infection, which persists even under combination ART [129]. These data provide convincing evidence that HIV-1 infection of macrophages establishes reservoirs in these tissues.

Macrophage infection leads to activation of inflammatory processes associated with disease development. Inflammation in the CNS as a result of macrophage infection promotes neuropathology ranging from encephalitis to mild but progressive cognitive dysfunction. It has been shown that infected alveolar macrophages in lung have impaired phagocytic activity increasing lower respiratory tract infections [130]. The ongoing Inflammation in the GALT is in part the result of monocyte recruitment to the site of tissue damage and polarisation of GALT macrophages and recruited monocytes toward a more inflammatory M1 phenotype [131]. Moreover, inflammation due to chronic HIV-1 infection is a risk factor for cardiovascular and other inflammatory and neurodegenerative diseases in which macrophages probably play a central role [132]. Interestingly, a recent study has reported infection of osteoclasts (myeloid-lineage cells derived from blood monocytes) suggesting that inflammation associated with HIV-1 infection may have a role in osteolytic bone disease [133].

1.1.5. Cell-to-cell transmission of HIV-1

The concept of viral transmission between cells by cell-to-cell (CTC) contact was first proposed in 1992, when at sites of CTC contact between lymphocytes and epithelial cells, HIV-1 budding was observed by electron microscopy [134]. However, the "virological synapse" (VS) was first described in HTLV-1 infection

mediating efficient viral transfer between a productively infected cell and an uninfected target cell [135]. Thereafter, the Sattentau lab has shown the importance of VS for HIV-1 transmission both between T cells [136] and from HIV-infected macrophages to uninfected T cells [137]. The formation of the virological synapse can be described in a two-part process that begins with adhesion triggered by Env-CD4 interactions, and is stabilised by interactions between cellular adhesion molecules. In the infected cell, both Gag and Env polarise towards the point of CTC contact, which is mediated by the reorientation of the microtubule organising centre towards the VS junction [138]. In the target cell, CD4 and co-receptors are recruited to the VS junction in an actin-dependent manner [139]. Moreover, the members of the integrin family such as Leukocyte Function-associated Antigen (LFA)-1, ICAM-1 and ICAM-3 are reported to be involved in stabilisation of VS structure and facilitating viral transfer [140].

It has been known for more than two decades that HIV-1 spreads more efficiently by direct CTC transfer rather than cell-free diffusion [141], and is associated with an increased multiplicity of infection (MOI) in target cells [142, 143], and activation of the target cell and increasing its susceptibility to infection [144]. Estimates of the total increase in viral transfer efficiency range from two- to five-fold [145, 146] to 18,000-fold [147].

Dendritic cells (DC) are much less permissive to HIV-1 infection due to several factors including low entry receptor and co-receptor expression and the presence of host restriction factors, but are nevertheless able to efficiently

capture and transmit HIV-1 to uninfected CD4+ T cells *in trans* (reviewed in [148] [149, 150]). This interaction requires the binding of DC-SIGN to infectious virions [151] and is regulated by DC actin dynamics [152].

Neutralising antibodies are generally less efficient at blocking HIV-1 CTC infection compared to cell-free infection [153]. However, when Martin et al. used chronically infected donor T cells, the differences between neutralisation of CTC and cell-free infection were less dramatic compared to using acutely infected T cells, which may be associated with the presence of cell surface-bound cell free viral particles (reviewed in [154]). Most *in vitro* work on macrophage infection by HIV-1 is carried out using blood monocyte-derived macrophages (MDM). Duncan et al. have shown that viral transmission between infected MDM and uninfected CD4+ T cells is susceptible to the activity of CD4 binding site (CD4bs) and glycan or glycopeptide epitope-specific broadly neutralising antibodies (bNAbs) but shows resistance to bNAbs targeting the Env gp41 subunit membrane-proximal external region (MPER) [155]. Different strains of HIV-1 revealed distinct neutralisation sensitivities when CTC transmission was challenged by a panel of potent bNAbs [156]. These studies indicate that the sensitivity of HIV-1 CTC transmission to neutralising antibodies is determined by the accessibility or presence of different epitopes on the surface of the infected cell.

1.1.6. CD4+ T cell death during HIV-1 infection

T cell death plays a significant role in HIV-1 pathogenesis. In HIV-1 infection, cell death occurs by both direct viral replication-induced cytopathology and

bystander effects. Doitsh et al. recently reviewed mechanisms underlying loss of CD4+ T cells during HIV-1 infection [157], which are discussed below.

1.1.6.1. Apoptosis of HIV-1 infected T cells

Apoptosis is a regulated form of cell death that takes place to homeostatically eliminate dying cells during tissue development, but also plays a role as a mechanism to eliminate infected cells. Apoptotic cells are removed 'silently' by phagocytes as a means to prevent the triggering of inflammatory processes by release of cellular damage-associated molecular patterns (DAMPs) [158]. Mechanisms of apoptotic cell death will be described in detail in Section 1.2.1. HIV-1-infected T cells have a half-life of 12-36 hours *In vivo* [33, 159]. Apoptotic cell death triggered by direct infection was initially observed in long-term cultures of T cells [160] and activated cultures of peripheral blood cells [161] and found support in studies utilising the same models. However, the frequency of these activated CD4+ T cells appeared too limited to explain the massive loss of CD4+ T cells observed *in vivo* by either directly-induced or bystander cell death [162]. The progressive loss of productively infected CD4+ T cells was initially explained by viral cytopathic effects induced by unintegrated linear vDNA [163, 164], Vpr [165], Nef [166], viral protease [167] and more recently viral integration [168].

More recent findings from the Greene lab established an *ex vivo* human lymphoid aggregate culture (HLAC), which was described as a more physiologically relevant model than *in vitro* culture of peripheral blood mononuclear (PBMC)-derived CD4+ T cells. Using HLAC to explore T cell death during HIV-1-infection, it was shown that only ~ 5% of these CD4+ T cells

became productively infected with the virus and died by apoptotic cell death [169]. Conversely, 95% of the dying CD4+ T cells were resting, non-permissive (bystander) CD4+ T cells [169] that were not dying of apoptosis. The key question of how HIV-1 infection promotes cell death in bystander CD4+ T cell is discussed below in Section 1.1.6.2.

1.1.6.2. Pyroptosis of bystander CD4+ T cells

Pyroptosis is a proinflammatory mechanism of cell death associated primarily with pathogen infection that is caspase 1 mediated, and will be described in more detail in Section 1.2.2. In 1995, Finkel *et al.* noted that the majority of dying cells in the lymph nodes of HIV-1-infected patients were not infected, but were in close proximity to infected cells [170]. It has subsequently become clear that numerous mechanisms may induce this so-called "bystander cell death". It was assumed until recently that bystander T cell death during HIV-1 infection is due to apoptosis. However, the Greene lab has shown that bystander pyroptotic cell death probably accounts for the depletion of 95% of resting CD4+ T cells in HLAC. HIV-1-induced pyroptosis is caused by abortive infection leading to the accumulation of incomplete HIV-1 reverse transcripts, which activates a caspase 1-dependent pyroptotic pathway [171]. Moreover, the Greene lab also elucidated that cell-free infection, even at high MOI, is unable to trigger pyroptotic cell death in HLAC. However, cell-free virions are able to establish productive infection in 5% of HLAC population leading to caspase 3-dependent apoptotic cell death [172]. Another study from the Greene lab indicated that while viral spread from productively infected PBMC extensively depleted resting CD4+ T cells in HLAC, resting PBMC-derived CD4+ T cells were highly resistant to the pyroptotic cell death [173]. However, co-culturing

tonsil cells (lymphoid tissue) with resting blood-derived CD4+ T cells sensitised and depleted resting PBMC-derived CD4+ T cells, suggesting that the lymphoid microenvironment sensitises blood CD4+ T cells to depletion by caspase 1-mediated pyroptosis [173]. Co-culturing blood CD4+ T cells with supernatants from tonsil cultures instead of direct contact with tonsil cells failed to sensitise blood CD4+ T cells to pyroptosis. This indicates that cell-cell interactions between the tissue and blood-derived CD4+ T cells are required for sensitisation, which in the human body is proposed to occur when CD4+ T cells in the bloodstream traffic back to lymphoid tissue [173]. Based on these data, pyroptosis appears to make a key contribution to HIV-1-induced cell death. However these studies have been published solely by the Greene lab, thus confirmatory results from other groups are required to completely define the role of pyroptosis in HIV-1 infection.

1.1.6.3. Necroptosis during HIV-1 infection

Necroptosis is a form of regulated cellular necrosis in which plasma membrane disruption leads cells to lose their cytosolic contents [174, 175]. Moreover, necroptosis is also a controlled, pro-inflammatory cell death which requires RIPK1 and RIPK3 for phosphorylation of MLKL inducing cell membrane degradation and lysis [175]. Although pyroptotic and apoptotic cell death appear to account for most CD4+ T cell depletion, at least in vitro, a limited number of studies have implicated a role for necroptotic cell death [176, 177]. It has been shown that necrostatin-1, a RIPK1 inhibitor, reduces necroptotic cell death in HIV-infected cell lines, and in PBMC-derived CD4+ T cells [176]. Moreover, necroptosis inhibition reduces syncytia formation [176], which is the formation of multi-nucleate enlarged cells formed by the fusion of infected cells with

neighbouring cells mediated by viral proteins. Inhibition of apoptosis in HIV-infected cells increases necroptosis levels [176]. The role of necroptosis in HIV-1-induced cell death is probably small as there is no *in vivo* evidence for its involvement in human infection. However, inhibition of apoptosis in productively infected cells may theoretically drive necroptosis *in vivo*, increasing inflammation as seen in chronic infection [178], which could impact on pathogenesis.

1.2. Cell death

In January 2018, the Nomenclature committee on cell death published a comprehensive review including recent pathways and an updated classification of cell death [179]. They provided molecularly-orientated definitions of different cell death pathways including intrinsic apoptosis, extrinsic apoptosis, mitochondrial permeability transition (MPT)-driven necrosis, necroptosis, ferroptosis, pyroptosis, parthanatos, entotic cell death, NETotic cell death, lysosome-dependent cell death, autophagy-dependent cell death, and immunogenic cell death. As apoptotic and pyroptotic cell death are within the scope of my study, they will be discussed in more detail below in Sections 1.2.1 and 1.2.2, respectively.

1.2.1. Apoptotic cell death

Apoptosis is classified as a type I cell death in which cytoplasmic shrinkage, chromatin condensation (pyknosis), nuclear fragmentation (karyorrhexis), and plasma membrane blebbing occur. These events culminate with the formation of apparently intact vesicles (commonly known as apoptotic bodies) that are efficiently engulfed by phagocytes (a processes commonly known as

efferocytosis [180]) and degraded within lysosomes. Apoptosis is categorised into intrinsic and extrinsic apoptosis [181], both of which are forms of regulated cell death (RCD). Intrinsic and extrinsic apoptosis and the result of efferocytosis are generally, but not always, immunologically silent as previously thought [182, 183].

1.2.1.1. Intrinsic apoptosis

Intrinsic apoptotic cell death (Figure 1.3b) can be triggered by a variety of extracellular or intracellular microenvironmental stresses including (but not limited to) growth factor withdrawal, DNA damage, endoplasmic reticulum (ER) stress, reactive oxygen species overload, replication stress, microtubular alterations or mitotic defects [179]. Intrinsic apoptotic cell death requires irreversible and widespread mitochondrial outer membrane permeabilisation (MOMP) [184]. MOMP is mediated by pro-apoptotic BCL2 family proteins such as BAX, BID, BAD, BAK and BIM which undergo a conformational change, insert into the mitochondrial membrane, oligomerize and form protein-permeable channels [185]. However, MOMP is antagonised by anti-apoptotic members of the BCL2 family such as BCL2 itself, BCL-XL, MCL1 and BCL-W by inhibiting the conformational change or the oligomerization of BAX and BAK [186].

Following MOMP, mitochondrial intermembrane space proteins including second mitochondria-derived activator of caspases (SMAC) and cytochrome c (Cyt c) are released into the cytosol. Subsequently, Cyt c binds and triggers oligomeriasation of apoptotic protease activating factor 1 (APAF1) to form the apoptosome [187]. APAF1 then activates pro-caspase 9 (initiator

caspase), which in turn, catalyse proteolytic activation of executioner caspases including caspase 3 (mainly) and caspase 7, leading to apoptosis. Moreover, mitochondrial release of SMAC into the cytosol facilitates apoptosis by blocking the caspase inhibitor known as X-linked inhibitor of apoptosis protein (XIAP) [187].

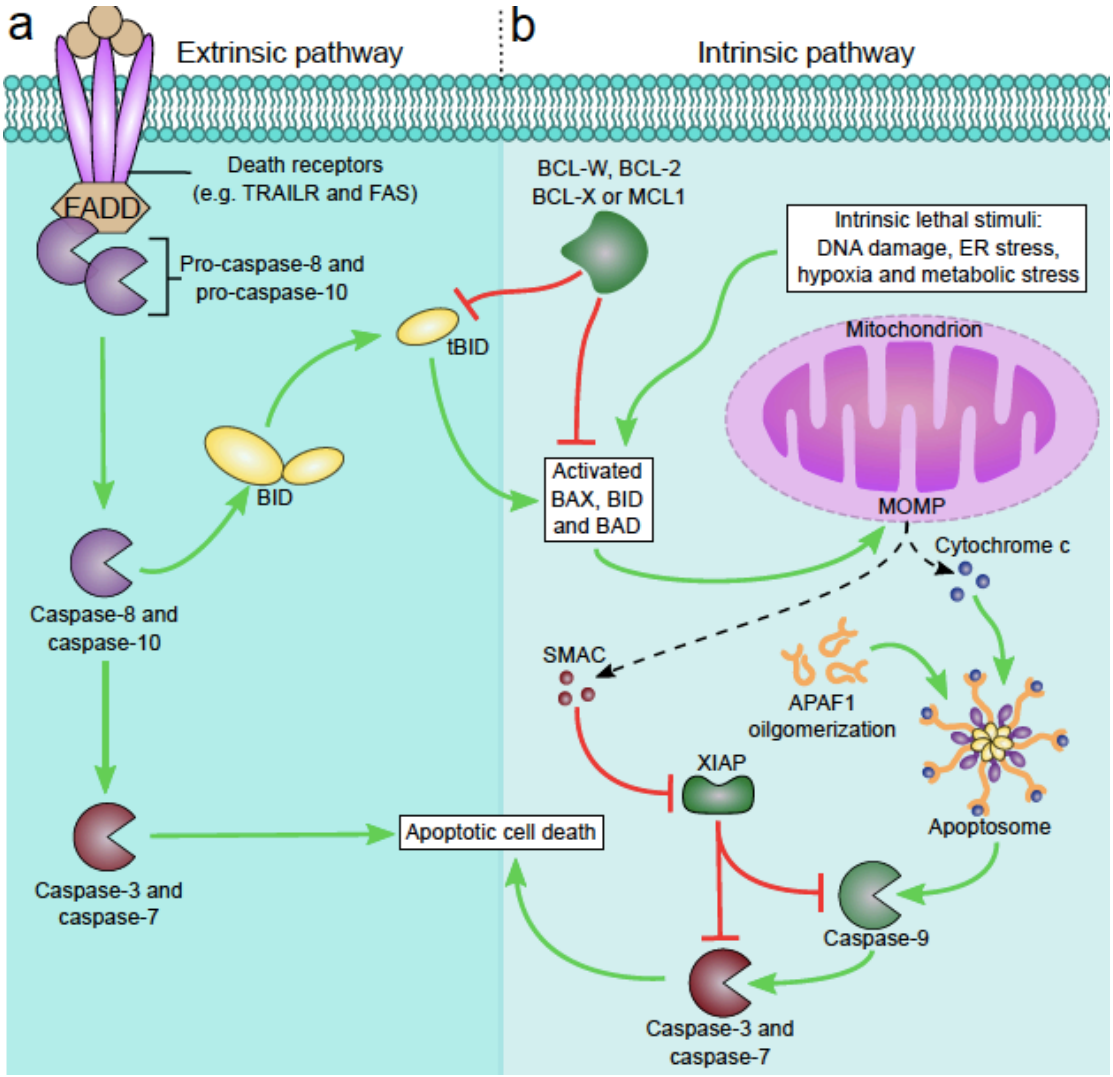


Figure 1.3. Schematic overview of extrinsic and intrinsic apoptotic signalling pathways. A caspase cascade drives apoptotic cell death in response to death ligands binding death receptors, and extrinsic or intrinsic stimuli that mediate apoptotic cell (see text for details). Figure is the modified version of the first Figure of Ichim et al. review article [187].

Notably, blocking post-mitochondrial caspase activation by either genetic means or with specific pharmacological inhibitors including pan-caspase

inhibitors (Z-VAD-fmk and Q-VD-OPH) has been shown to generally delay but not prevent intrinsic apoptosis either *in vitro* or *in vivo* in the mammalian system, as it promotes a switch to other types of RCD [188, 189].

1.2.1.2. Extrinsic apoptosis

Extrinsic apoptosis is mostly initiated by either of two types of plasma membrane receptors: i) death receptors activated after binding to their cognate ligands; and ii) dependence receptors activated when the levels of their specific ligand drop below a certain threshold [179]. Death receptors include (but are not limited to) FAS (CD95 or APO-1 [190]) and TNF receptor superfamily members (TNFR1, TRAILR1 and TRAILR2 [191]). The ligands for FAS and TRAILRs are called FASLG and TRAIL, respectively. Upon binding to their cognate ligands, death receptors activate effector caspases (caspase 8 and caspase 10) through dimerisation mediated by adaptor proteins such as FAS-associated death domain protein (FADD). Subsequently, active caspase 8 and caspase 10 then calatalyse proteolytic activation of executioner caspases (caspase 3 and caspase 7), leading to apoptosis (Figure1.3a).

Under physiological conditions, dependence receptors help with cell survival, proliferation and differentiation. However, once ligand availability falls below a specific threshold, they activate distinct lethal signaling cascades which generally involve caspase activation [192]. The family of dependence receptors includes approximately 20 members such as DCC netrin 1 receptor (DCC), unc-5 netrin receptor A (UNC5A) and neurotrophic receptor tyrosine kinase 3 (NTRK3) [179]. Moreover, cleavage of BID (member of the BCL2-family) by

activated caspase 8 during extrinsic apoptosis, triggers the mitochondrial apoptosis pathway which can be used to amplify the apoptotic signal [187].

1.2.2. Pyroptotic cell death

The term pyroptosis was firstly introduced by Cookson and Brennan to define a particular type of RCD similar to apoptosis but dependent on inflammatory caspase 1 activation [193]. Initially, pyroptotic cell death was thought to be a caspase 1-mediated monocyte death associated with invasion by certain bacteria [194]. Pyroptosis has a major role in innate immunity against intracellular pathogens [195]. However, recent studies have shown that other caspases such as caspase 3 can also trigger pyroptotic cell death [196, 197] and pyroptosis also occurs in other cell types [198, 199]. Moreover, not only microbial infection but also various pathological stimuli, such as stroke, heart attack or cancer can trigger pyroptosis [194]. The specific morphological features which differentiate pyroptosis from apoptosis are a particular form of chromatin and cellular swelling ending with plasma membrane permeabilisation [195].

In pyroptotic cell death, multiple caspases may be activated in humans depending on the stimulus including caspase 1, 3, 4 and 5 [197, 200]. Therefore, pyroptosis often (if not always) results in the secretion of IL-1β and IL18 [201]. At the molecular level, pyroptosis is triggered and driven as follows (Figure 1.4 [196]): i) diverse microbial signals (e.g. LPS (lipopolysaccharide), double cytosolic stranded DNA, bacterial flagellin [202]) are detected by pattern recognition receptors and/or canonical inflammasome sensors (e.g. AIM2/ASC,

NAIP/NLRC4 and NLRP3/ASC [202]) leading to stimulation of either ASC or NLRC4 adaptors catalysing proteolytic activation of caspase 1.

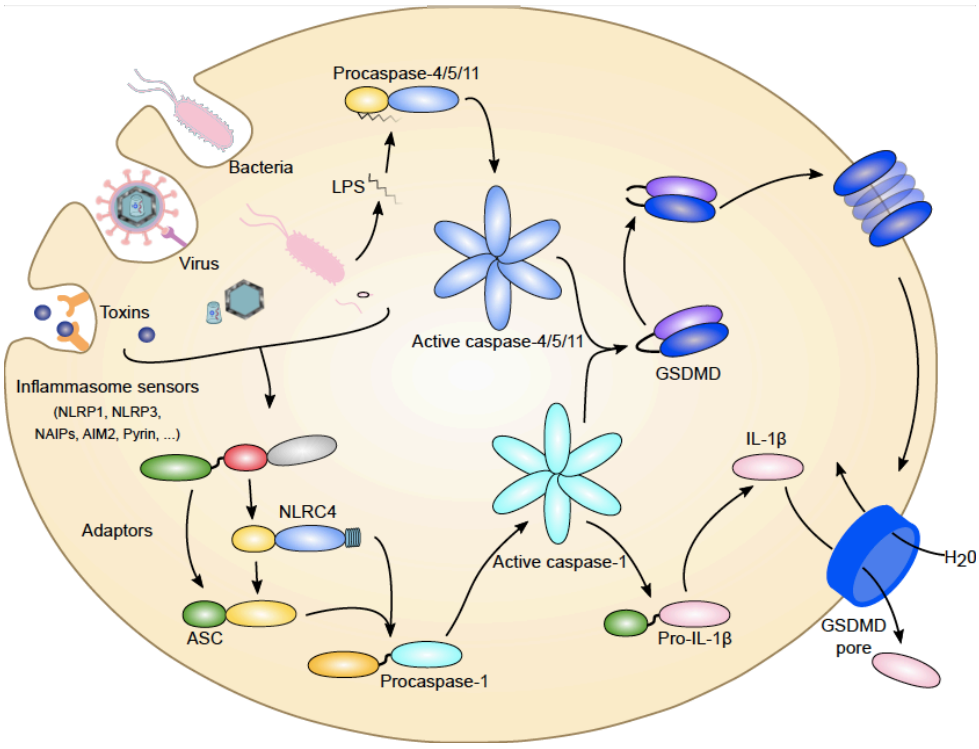


Figure 1.4. Schematic overview of pyroptotic cell death. Microbial agents can either indirectly activate caspase 1 or directly activate caspase 4/5/11 resulting in the translocation of gasdermin-N domains (blue) to plasma membrane and their oligomerisation to generate membrane pores. These pores can serve as a gate for the extracellular release of mature IL-1β (see text for details). Figure is the modified version of the first Figure of Shi et al. review article [203].

Moreover, LPS binding to pro-caspase 4/5 directly activates them. ii) Active caspase 1 and caspase 4/5 cleave gasdermin D (GSDMD) within the linker between its N-terminal (gasdermin-N shown in blue) and C-terminal (gasdermin-C showed in purple) domains eliminating the autoinhibitory interactions between the two domains. iii) Gasdermin-N is then oligomerised by binding to phosphoinositides in the plasma membrane to form membrane pores

disrupting the osmotic potential, which results in cell swelling and eventually cell lysis. Mature IL-1β, a soluble proinflammatory mediator, is released from the pyroptotic cell into the extracellular space via these pores.

1.2.3. Efferocytosis of dying and pathogen-infected cells

1.2.3.1. Phagocytes and efferocytosis

To maintain and protect themselves, multicellular organisms have to efficiently remove unwanted and abnormal cells which arise during normal tissue development and function or may be triggered by infection or sterile inflammation [204], by phagocytosis [205]. At steady state, even within tissues with high constitutive rates of apoptosis, the number of detectable apoptotic cells is relatively low, indicating that the rate of removal must be high [206-208]. This high clearance rate is vital for the constant removal of approximately one million cells undergoing apoptosis in various tissues every second in adult humans [209]. Ilya Metchnikoff, who won the Nobel Prize in 1908 for his work on phagocytes, discovered in the late 19th century, that white blood cells phagocytose bacteria [210]. A phagocyte is any cell that is able to engulf particulate matter of >1 μm [211, 212], and includes both professional and non-professional phagocytes [158]. Professional phagocytes are primarily myeloid lineage-derived macrophages and immature DC functioning in tissues such as bone marrow, spleen and thymus [213], and tissue infiltrating monocytes, neutrophils and eosinophils. Non-professional phagocytic cells can capture and engulf dying cells present in close proximity, such as epithelial cells of mammary epithelium [214] and astrocytes in the brain [215]. Efferocytosis is a term that specifically describes the cellular engulfment by phagocytes of dying

and dead cells [216, 217], and demonstrates features of both conventional phagocytosis and the fluid-phase uptake mechanism macropinocytosis [218-220]. The initial definition of efferocytosis related to clearance of apoptotic cells [220], but this has been extended to include other forms of regulated cell death including autophagic, pyroptotic and necroptotic death [221, 222].

Efferocytes identify and eliminate dying and infected cells through pathways initiated via “find me” signals, recognition via “eat me” signals and down-modulation of regulatory “don’t eat me” signals. Engulfment is subsequently mediated by cytoskeletal reorganisation that may drive phagosome formation and maturation resulting in destruction of the engulfed material. Depending on the nature of the engulfed cell, the elimination of the target cells by efferocytosis can occur in an immunologically silent manner or promote inflammatory responses.

1.2.3.2. Stages of efferocystosis

Efferocytic uptake of target cells can be divided into 4 distinct stages [158, 223]. i) Detection of the target cell by release of chemotactic ‘find-me’ signals [224, 225] including lysophosphatidylcholine, CX3CL1 (fractalkine), nucleotides adenosine triphosphate (ATP) and uridine 5’ triphosphate (UTP) and sphingosine 1-phosphate (S1P) [226-229]. ii) Exposure of “eat-me” signals [230, 231] including phosphatidylserine (PS), lyso-PS and calreticulin or loss of “don’t eat-me” signals such as CD47 [232, 233]. iii) Engagement of eat-me signals by phagocyte recognition and uptake receptors may take place via direct receptor recognition such as by TIM4, G2A, complement receptors CR3 and CR4, scavenger receptors such as SRA and CD36 or integrins such as

α5β3 and α5β5, or via indirect recognition by bridging molecules such as collectins, complement C1q, mannose binding lectin (MBL), pentraxin3, ficolins, thrombospondin and milk fat globule protein (MGF-8). iv) Engulfment of the cellular material via cytoskeletal rearrangement of the plasma membrane [208, 217, 223] and processing of the engulfed cell generally [180, 208], but not exclusively [234], leading to its elimination within a phagolysosome [235, 236]. During the target cell recognition process, phagocytes may further evaluate the target's chemical composition to evaluate the threat posed by its contents and form such as size [237], geometry [238] and topography [239]. This assessment determines: i) whether engulfment occurs or is replaced with, for example, neutrophil NETosis [240]; ii) the fate of the target cell within the phagocyte; iii) whether the clearance process is immunologically silent, such as the efferocytosis of apoptotic cells [241, 242], or stimulates an inflammatory response such as the engulfment of most pathogens, pathogen-infected cells and pyroptotic and necrotic cells [212, 243, 244]. We discussed findings regarding the efferocytosis of pathogen-infected cells in our recent review [245]. Therefore, in the following Sections I will discuss "don't eat-me" and "eat-me" signals on the surface of healthy and dying (apoptotic and pyroptotic) cells.

1.2.3.3. "Eat-me" signals on apoptotic cells

After approaching their targets via find-me signals, efferocyte recognition partially relies on interactions between eat-me signals on the target cell and receptors on the phagocyte. Phosphatidylserine (PS) is probably the best characterised eat-me signal. PS displayed on the outer leaflet of cells is an early marker of apoptosis, which is recognised by a number of well-defined receptors on the surface of efferocytes. However, the picture has become more

complex by the realisation that PS can also be expressed on the surface of viable monocytes, myocytes, mature macrophages and activated platelets independently of apoptotic cell death [242]. PS exposure on viable cells controls various processes including signal transduction, fusion and adhesion [246-249]. Notably, experimental integration of PS into the outer leaflet of live Jurkat T cells was insufficient to trigger their phagocytosis [250], implying a requirement for other signals. Similarly, constitutive induction of PS exposure on lymphoma cells via overexpression of the calcium-dependent phospholipid scramblase TMEM16F, was insufficient to trigger phagocytosis [251]. Conversely, apoptotic cells that have not lost their phospholipid asymmetry are not recognised and engulfed by phagocytes [252]. Moreover, the PS receptor (PSR), which was originally described as the principal receptor for PS binding leading to efferocytic uptake, is unable to directly mediate efferocytosis of apoptotic cells [253, 254]. Therefore, these findings suggested that exposure of PS alone appears insufficient to trigger phagocytic uptake, and the outcome will depend at least in part on the target cell type, PS topology and local density, presence of other eat-me signals, and the absence of regulatory don't eat-me signals.

As it has been known for some time, efferocytosis of apoptotic cells involves a complex interplay between a range of markers on the apoptotic cell surface and a set of phagocyte receptors with considerable functional redundancy. This functional redundancy has made it difficult to robustly identify and rank receptor-ligand interactions implicated in this process, as gain or loss of function experiments often yield inconclusive results. Moreover, some

receptors may act solely as apoptotic cell recognition receptors without uptake activity and therefore need the cooperation of an independent engulfment receptor, whereas others may combine both of these functions in a single molecule. Despite these challenges, a number of apoptotic markers and their receptors have been identified. These receptors and markers can be categorised in two main groups: PS-dependent and PS-independent recognition patterns.

1.2.3.3.1. PS-dependent recognition

PS-dependent interactions can be subcategorised into direct and indirect (opsonin-mediated) recognition patterns. The elimination of apoptotic cells is a tissue-specific activity that uses distinct receptors depending on the cellular context. Thus one of the receptors involved in direct recognition of PS is brain specific angiogenesis inhibitor 1 (BAI1), expressed on glial and neuronal cells, but also detected on macrophage cell lines and in immunological tissues such as the bone marrow, spleen, astrocytes and mouse peritoneal exudate cells [255]. It has been shown using different systems that BAI1 binds directly to PS on the apoptotic cells resulting in their uptake [255]. In another study, BAI1 on efferocytic microglia cells of live zebrafish engulfed apoptotic neurons by controlling the formation of the phagosome [256]. Another membrane protein recognising PS directly is stabilin-2 which is a scavenger receptor [257] and was originally identified as hyaluronan receptor for endocytosis on rat liver sinusoidal endothelial cells [258], but is also expressed on human MDM and a variety of reticuloendothelial cells [247, 259]. It has been shown that expression of stabilin-2 on non-phagocytic mouse fibroblast L cells resulted in their ability to recognise (Ca^{2+} dependent) and engulf aged erythrocytes and

apoptotic Jurkat and U937 cells [257, 259]. Moreover, stabilin 1 which is expressed exclusively on alternatively activated macrophages has been shown to recognise and engulf apoptotic red blood cells (RBC) [260]. Also in this study, the role of stabilin 1 as a phagocytic receptor was reported using stabilin 1-expressing mouse fibroblast L cells for the uptake of apoptotic cells [260]. Another set of PS receptors is the T cell immunoglobulin and mucin (TIM) family including TIM-1 (expressed primarily on kidney cells [261]), TIM-3 (expressed on fibroblasts and T and B cells [262]) and TIM-4 (expressed on all professional phagocytes [261]). Although the cell expression profile and PS binding of TIM-4 make it a strong candidate as a phagocytic receptor, Park et al. noted that its transmembrane region and cytoplasmic tail are dispensable for apoptotic cell internalisation, suggesting its tethering function [263]. Furthermore, DeKruyff et al. have shown that TIM-3 function is cell-type dependent; T or B cells expressing TIM-3 create conjugates with apoptotic cells but are unable to engulf them, whereas fibroblastic cells expressing TIM-3 can internalise them [262]. The most recently discovered PS receptor is the receptor for advanced glycation end products (RAGE), which is expressed in both a full-length membrane-bound form (mRAGE) and various soluble forms missing the transmembrane domain (sRAGE) [264]. RAGE is expressed in diverse cell types including endothelial cells, T cells, monocytes, and macrophages [265]. Apoptotic thymocyte-expressed PS is recognised and engulfed by RAGE on wild-type murine alveolar macrophages, but not -/-RAGE mice [266]. Interestingly, sRAGE administration impaired phagocytosis of not only wild-type murine but also -/-RAGE alveolar macrophages [266]. This suggests the possible interaction of sRAGE with other efferocytic receptors and its potential

role as an efferocytosis regulator. Another group of receptors involved in the direct recognition of PS belongs to the CD300 family, which are broadly expressed on mast cells, granulocytes, macrophages, and dendritic cells. Members of this family including CD300a [267], CD300b [268] and CD300f [269, 270] and are immunoreceptor tyrosine-based inhibitor motif (ITIM)-containing myeloid receptors binding to PS-exposed apoptotic cells in a Ca^{2+} dependent manner. However, this recognition is selective: CD300a has a higher affinity for phosphatidylethanolamine than PS while CD300f has a higher preference for PS than phosphatidylglycerol [267, 269]. Moreover, CD300a [267] and CD300b [268] proteins act as tethering receptors and regulate efferocytosis while CD300f acts as an efferocytic receptor [270]. Last but not least, the class E scavenger receptor, lectin like oxidised low-density lipoprotein receptor (LOX-1) has been shown to recognise and engulf apoptotic RBC [271]. In this study, LOX-1 expressing Chinese hamster ovary cells (CHO) were able to efferocytose aged RBC but not the wild-type CHO [271]. Additionally, this interaction could be inhibited by administration of PS liposomes suggesting the role of LOX-1 in the uptake of apoptotic RBC via recognition of PS [271].

Indirect recognition of PS on apoptotic cells requires linker molecules (opsonins) that bridge PS with efferocyte receptors. These bridging proteins include calreticulin (CRT), C1q, Milk fat globule-EGF factor 8 (MFG-E8), growth arrest-specific 6 (Gas6), HMGB1, β2-GP1 and protein S. CRT is another major eat-me signal and its plasma membrane expression can trigger efferocytosis of both viable and apoptotic cells [272]. This protein is rapidly translocated from the ER to the plasma membrane under ER stress conditions including

apoptosis, and colocalises with PS on the outer plasma membrane leaflet [273]. Moreover, it has been shown that CRT binds not only to PS but also C1q which is another PS-biding opsonin enhancing uptake of apoptotic cells [274, 275]. However, CRT binding to PS is 10-fold higher in affinity than C1q [274]. This complex interaction can trigger the uptake of apoptotic cells via recognition of CRT by a phagocytic receptor called LDL-receptor-related protein (LRP1 and CD91) on the phagocyte [272, 276]. MFG-E8, a well-studied bridging protein is expressed by a variety of cells and tissues, especially professional and non-professional phagocytes including macrophages, immature DCs, mammary gland epithelial cells and epididymis [277]. The MFG-E8 C1 and C2 domains bind with high affinity to PS on apoptotic cells and its RGD motif associates with efferocytic integrin $\alpha_v\beta_{3/5}$ on phagocytes transducing PS-dependent efferocytic signals [278-280]. Gas6 and protein S are two other PS binding proteins, which are the members of vitamin K-dependent protein family present in blood serum in low (subnanomolar) and high concentration, respectively [281-283]. Gas6 binds to all three TAM receptors including Tyro3, Axl and Mer with different affinity (Mer < Axl, Tyro3) while the protein S interaction seems to be restricted to Mer and Tyro3 [284]. TAM family receptors are expressed on the surface of macrophages and macrophages from Mer knockout mice were incapable of engulfing apoptotic thymocytes [206]. Interestingly, the engagement of natural IgM with PS exposed on early apoptotic cells has been reported to induce efferocytosis via recruitment of C1q leading to the engagement of C1q and Fc receptors on efferocytes [285]. Furthermore, like calreticulin, involvement of another intracellular protein called high mobility group protein-1 (HMGB1), has been reported in the PS-dependent engulfment of apoptotic cells. HGMB1 is a

nuclear non-histone DNA-binding protein acting as a DNA chaperone in the nucleus, regulating autophagy in the cytoplasm and modulating inflammatory responses outside the cell. It has been shown that pre-incubation of macrophages with HMGB1 inhibits engulfment of apoptotic neutrophils in vivo and in vitro [286]. HMGB1 inhibits efferocytosis by binding to PS exposed on the apoptotic neutrophils and blocking MGF-E8 interaction with PS on apoptotic neutrophils and $\alpha_v\beta_3$ (but not $\alpha_v\beta_5$) on macrophages [287]. Finally, β2-glycoprotein 1 (β2-GP1) has been reported as a PS-binding protein mediating uptake of apoptotic cells by macrophages [288, 289]. β2-GP1 is a member of the complement control protein family and a soluble single chain plasma glycoprotein, which interacts with ionic phospholipids including PS and PG [286, 290]. β2-GP1 mediates the uptake of apoptotic cells by binding to PS resulting in its conformational change which allows the interaction of its cryptic motif with LRP on the macrophage [289].

1.2.3.3.2. PS-independent recognition

In the recognition of apoptotic cells by efferocytes, a number of PS-independent receptor-ligand interactions have been described including both soluble and membrane-anchored receptors. Mannose receptor (MR/CD206) binds to mannose, fucose or acetylglucosamine sugar residues on the surfaces of microorganisms [291]. It has been reported that macrophage MR is involved in the recognition and efferocytosis of apoptotic bronchial epithelial cells in chronic obstructive pulmonary disease [292]. Moreover, It has been shown that MR-transfected Cos-1 cells can engulf yeast (*Candida albicans* or *Pneumocystis carinii*) and that the cytoplasmic tail of MR is involved in efferocytic signalling [293]. However, Le Cabec et al. challenged the role of MR as an efferocytic

receptor. In their study, stably transfected CHO cells with hMR were unable to phagocytose zymosan, the mycobacterium *M. kansasii*, or Man3 BSA-coated latex beads, all known to be internalised using the MR in human macrophages [294]. Therefore, further research is required to clarify whether the MR is an efferocytic receptor and if so what its ligand(s) on the apoptotic cell is/are. CD14, the lipopolysaccharide receptor on macrophages interacts with the intercellular adhesion molecule-3 (ICAM3/CD50), which is upregulated on apoptotic cells [295, 296]. A combination of thrombospondin receptor (CD36) with $\alpha_v\beta_{3/5}$ integrins binding thrombospondin-1 (TSP-1) [297, 298], conjugation of α2 macroglobulin receptor (LRP1/CD91) with calreticulin (CRT) binding complement protein C1q [275, 299], and complement receptor 3 (CR3/Mac-1) binding serum protein iC3b [300]. It has been shown that P2 purinergic receptors such as $P2X_1$ and $P2X_3$ are stimulated by extracellular nucleotides released from apoptotic cells with potential for recognition by efferocytes [301]. In addition, $P2X_7$ [302] and hyaluronate receptor CD44 [303] on phagocytes are also involved in the recognition and uptake of apoptotic cells, however their target(s) on the surface of the apoptotic cell remains unknown.

1.2.3.4. Eat-me signals on pyroptotic cells

As described in Section 1.2.2, pyroptosis is a form of RCD in which inflammatory caspases (caspase-1 and/ or caspase 4/5) are activated. Up to date only one study, conducted by Wang et al. ,investigated the exposure of eat-me signals on pyroptotic cells leading to their efficient clearance by macrophages [304]. In this study, macrophages derived from the THP-1 human monocyte line or mouse peritoneal macrophages efficiently engulfed pyroptotic bacterium-infected THP-1 cells and an MDP-treated CLC12N2-Pyr cell line.

This engulfment was PS-dependent as the application of PS-binding protein MFG-E8 significantly inhibited macrophage uptake. Moreover, they showed that MDP-treated CLC12N2-Pyr cells bound to the plate coated with Tim4-Fc, another PS-binding protein. Whilst informative, it is clear that more work needs to be done to reveal eat-me signals exposed on the surface of pyroptotic cells resulting in their efferocytic uptake.

1.2.3.5. Don't eat-me signals and regulation of efferocytosis

Cells actively protect themselves from engulfment by exposing don't eat-me signals including CD47, CD200, surface sialic acid, CD46, CD31 and plasminogen activator inhibitor-1 (PAI1), which are discussed in this Section. Whether a cell is efferocytosed or not is regulated by the net eat-me/don't eat-me balance, and availability of corresponding receptors on the efferocyte. CD47 is one of the major don't eat-me signals expressed not only on the surface of most normal cells, but frequently over-expressed on cancerous cells as a mechanism to prevent their clearance by phagocytes [305]. CD47 inhibits efferocytosis by stimulation of Signal Regulatory Protein-a receptor (SIRPa) on the efferocyte [306]. Antibodies against CD47 lead to uptake and clearance of leukaemic cells by macrophages in vitro and inhibition of tumor engraftment *in vivo,* providing a novel anti-cancer therapeutic approach [307].

Another example is a cell surface glycoprotein, CD200 (OX-2), which plays a role in maintenance of tissue homeostasis by suppression of immune responses through its corresponding receptor, CD200R (expressed mainly on myeloid cells). It was proposed by Stumpfova et al. that the interaction between CD200 and CD200R follows the same model as has been demonstrated between CD47 and SIRPa. Therefore, this interaction is a double-edged sword

as it is crucial for maintenance of homeostasis by supressing myeloid cell activation, but the ability of CD200 to suppress myeloid cell activation can allow the survival of migratory neoplastic cells by disrupting their uptake [308].

Sialic acid has been suggested to be a don't eat-me signal, since enzymatic removal of sialic acid residues using neuraminidase is sufficient to trigger macrophage efferocytosis of viable lymphoblasts [309]. Moreover, it has been shown that apoptotic lymphoblasts lose surface sialic acid [309]. Binding of complement C1q to desialylated mouse neurites results in CR3/Mac-1-mediated macrophage removal [310]. Additionally, it has been reported that Siglec-11 (Sialic acid binding Ig-like lectin 11) is a receptor on microglia that binds poly-sialic acid residues on neurons leading to inhibition of efferocytosis [311].

The loss of complement regulatory protein CD46 on various cell types during apoptosis results in complement opsonisation, which can lead to efferocytic recognition [312]. CD31/PECAM-1 (platelet-endothelial cell adhesion molecule-1) is a cell surface molecule that blocks efferocytic uptake of viable leukocytes by induction of 'detachment' signals; apoptosis disables CD31-mediated detachment leading to tight binding and macrophage uptake of apoptotic leukocytes [313]. Loss of co-localisation of CRT and PAI-1 on apoptotic neutrophils results in their efferocytosis, suggesting that PAI-1 may act as a don't eat-me signal [314]. Finally, a recently discovered don't eat-me signal is the common MHC class I component β2-microglobulin (β2M) [315]. Barkal et al. have shown that the expression of β2M on cancerous cells protects them

from efferocytic uptake by macrophages, and this protection is mediated by LILRB1 on the surface of macrophages.

1.3. Leukosialin (CD43)

1.3.1. CD43 structure

CD43 (leukosialin, sialophorin, Figure 1.5) is one of the most abundant transmembrane glycoproteins on the surface of T cells [316]. Its gene has only one exon, encoding a 400 amino acid polypeptide. Therefore, the predicted molecular weight (MW) of the CD43 polypeptide backbone is ~44 kDa [317]. However, human T cells express two CD43 glycoforms decorated with either core 1 (115 kDa) or core 2 (130 kDa) O-glycans meaning that ~62-66% of CD43 mass is due to its glycans [318]. CD43 has a 235 amino acid rod-shaped extracellular domain, which extends ~45 nm from the T cell surface and is decorated with 70 - 85 O-linked sialic acid-terminated glycans and only one N-linked glycan [319, 320]. Loss or defective CD43 expression has been reported in lymphocytes of patients with Wiskott–Aldrich syndrome which is an inherited deficiency of T-lymphocyte function and of platelets [321].

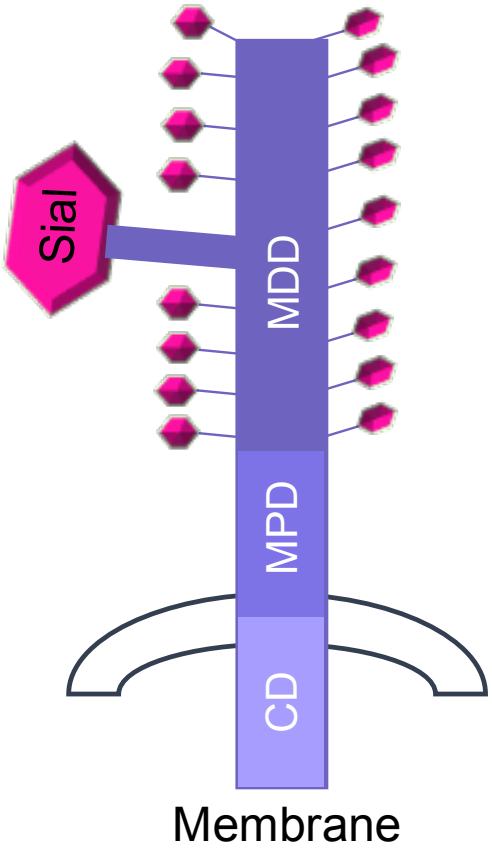


Figure 1.5. CD43 Schematic structure. MDD, membrane distal domain; MPD, membrane proximal domain; CD, cytoplasmic domain.

1.3.2. CD43 functions

1.3.2.1. Cytoplasmic domain

The CD43 cytoplasmic domain interacts with members of the ezrin-radixin-moesin (ERM) family of cytoskeleton linker proteins, regulating T cell migration [322], activation [323, 324], and proliferation [324]. ERM cytoskeletal adaptor protein interaction with the CD43 cytoplasmic domain in activated T cells leads to active exclusion of CD43 from the immunological synapse [323] and regulates IL-2 production [324]. Also, CD43-KO CEM present hyperproliferation phenotype which could be reversed by the expression of the CD43 cytoplasmic tail [324]. It has been demonstrated that ERM binding to the CD43 cytoplasmic domain is crucial for phosphorylation of this domain mediating T-cell trafficking and migration [322]. Moreover, inhibition of the CD43 cytoplasmic domain nuclear translocation or its release by γ-secretase was suggested to have a pro-apoptotic role in murine T cells [325].

1.3.2.2. Extracellular domain

The extracellular domain of CD43 covers ~20% of the entire T cell surface and has been proposed to impart substantial steric and electrostatic properties to the cell surface due to its size and high density of O-linked glycans [320]. According to the literature, CD43 can impose both pro- and anti-adhesive properties ON the cells [326]. This apparent contradiction might be due to a combination of CD43 ligand-specific adhesive interactions, and non-ligand specific repulsive properties resulting from its size and charge, yielding different functional outcomes depending on the systems used for analysis [326, 327].

The role of the CD43 extracellular domain will be discussed in detail in the following chapters.

1.4. ADAM10

1.4.1. ADAM10 structure

A disintegrin and metalloprotease (ADAM) 10 is also known as Kuzbanian from its orthologous gene, kuz, in Drosophila. ADAM10 is a ubiquitous single-pass transmembrane sheddase cleaving a variety of membrane-anchored proteins with roles in cell adhesion, proliferation, differentiation, migration, immunity, and receptor-ligand signalling [328]. The ectodomain of ADAM10 has an N-terminal signal sequence and an adjacent prodomain, followed by metalloprotease, disintegrin, and cysteine-rich domains (Figure 1.6) [329]. It has been suggested that disintegrin, and cysteine-rich domains supress the metalloprotease activity in the absence of substrates [330]. Moreover, these domains may also direct the enzymatic activity by binding directly to the substrates [331].

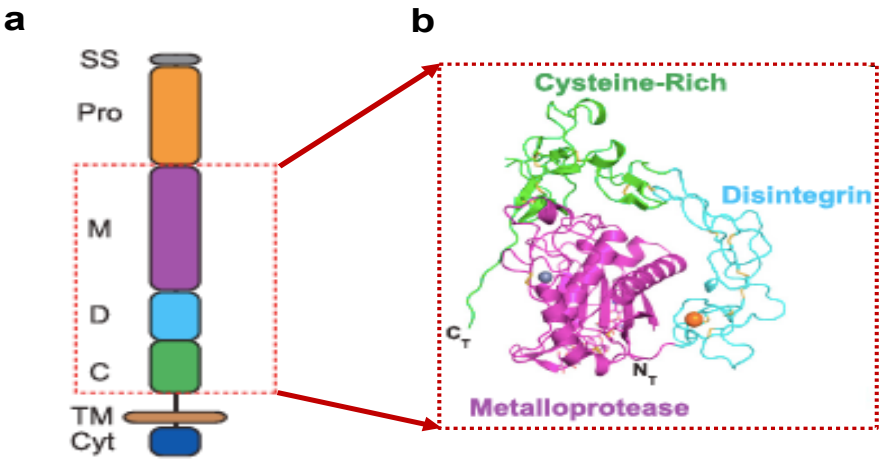


Figure 1.5. ADAM10 structure. a) Schematic structure. SS, signal sequence; Pro, prodomain; M, metalloproteinase; D, disintegrin; C, cysteine-rich; TM, transmembrane; Cyt, cytoplasmic tail. **b)** X-ray structure of the red box in a. Image adapted from Seegar et al. study **[329].**

1.4.2. ADAM10 substrates

ADAM10 acts as "molecular scissors" proteolytically cleaving the extracellular regions of more than 40 other transmembrane proteins having crucial roles in health and disease [328]. These include the Notch cell fate regulators, Alzheimer's precursor protein (APP), cellular prion protein, epidermal growth factor receptor (EGFR) ligands betacellulin and EGF, adhesion molecules E-cadherin, N-cadherin, VE-cadherin, CD44, transmembrane chemokines CX3CL1 and CXCL16, the low-affinity immunoglobulin E receptor CD23, and vascular endothelial growth factor receptor 2. It has been shown that ADAM10-deficient mice phenocopy Notch-deficient mice dying at embryonic day 9.5 with multiple defects of the somites, cardiovascular, and neuronal systems, highlighting the key role of ADAM10 in the activation of Notch proteins [332].

Dysregulation of ADAM10 activity is associated with pathological processes in cancer and a variety of human brain and immune disorders [333]. These include T cell acute lymphoblastic leukaemia, glioblastoma, breast cancer, oral squamous cell carcinoma, Alzheimer, Huntington, fragile X-syndrome, psoriasis (chronic skin inflammation), systemic lupus erythematosus, rheumatoid arthritis, chronic liver inflammation and *Staphylococcus aureus* infections [333].

1.4.3. ADAM10 regulation

ADAM10 appears to have constitutive activity toward some substrates, but its activity can be up-regulated by certain stimuli that induce intracellular signaling. However, the mechanisms by which ADAM10 activity is regulated are not fully understood. It has been reported that the ADAM10 transmembrane region, and not the cytoplasmic tail, is important in this process [334]. Moreover, in the last

four years, the role of multi-transmembrane proteins called TspanC8 has been explored as regulators of ADAM10 activity as reviewed by Matthews et al. [335]. TspanC8 is the subgroup of tetraspanins which have been shown to co-immunoprecipitate with ADAM10 in multiple studies [335]. Moreover, knockdown or knockout of the most highly expressed member of TspanC8 prevented ADAM10 to exit from ER and be transported to the plasma membrane in a cell type dependent manner, whereas overexpression promoted ADAM10 ER exit and enzymatic maturation [336-338].

1.5. Focus and scope of the thesis

The work that I have carried out for my DPhil studies started with a study carried out by previous members of the laboratory [339], showing that uptake of HIV-1-infected T cells by macrophages led to efficient macrophage infection. My project was to attempt to define the signals that govern recognition and uptake of HIV-1-infected T cells by macrophages, using model *in vitro* systems. My initial studies were designed to address the idea that infected T cell recognition might be via virus-specific eat-me signals, in particular interactions of HIV-1 Env, the only viral antigens exposed on the infected T cell surface, with macrophage receptor(s). Having excluded this, I then went on to investigate whether ICAM-1 might be implicated as a ligand for HIV-1-infected T cell recognition by macrophages, since previous lab members had demonstrated inhibition of this process by ICAM-1 antibodies. However, despite confirming the prior results, I was unable to identify a functional ligand for ICAM-1. This work makes up the majority of results in chapter 1.

Since Baxter et al. [339] had also shown that dying and dead HIV-1-infected cells were particularly susceptible to uptake by macrophages, I then moved towards the idea that cell death might be a trigger for macrophage efferocytic recognition, and worked towards identifying eat-me signals on the infected dying CD4+ T cell. A serendipitous observation that HIV-1-infected T cells appeared to express lower levels of the leukocyte sialoglycoprotein CD43 compared to uninfected healthy cells led me to investigate whether HIV-1 infection and cell death modulated expression of this molecule, which I showed was indeed the case. I showed that loss of CD43 from T cells was sufficient to mediate their uptake by macrophages, and therefore CD43 acts as a don't eat-me signal. I then carried out a detailed analysis of CD43 modification during HIV-1 infection and cell death, culminating in the conclusion that the glycosylated CD43 extracellular domain was rapidly cleaved during HIV-1 infection and apoptotic and pyroptotic cell death. These results make up the majority of results chapter 2.

I then focussed on trying to identify the mechanism by which CD43 was cleaved from infected and dying T cells. Reviewing the literature led me to suspect that a cell surface 'sheddase' might be responsible for the loss of CD43 ectodomain, and subsequent studies using pharmacological inhibitors confirmed that a disintegrin and metalloprotease 10 (ADAM10) was most likely responsible. Use of gene edited T cells confirmed this idea, and allowed me to propose a new model in which CD43 is a don't eat-me signal that is removed during cell death resulting in efferocytic recognition and uptake by macrophages. Whilst this work was initiated in the context of HIV-1 infection, it clearly has implications that go

beyond this, with potential for understanding how dying cells are cleared, and how pharmacological intervention might influence this process with potential for intervention in inflammatory and infectious diseases.

Chapter 2: Materials and Methods

2.1. Tissue culture

2.1.1. Obtaining peripheral blood mononuclear cells

Leukocyte cones derived from human peripheral blood were obtained from the Blood Service at the John Radcliffe Hospital, Oxford. Whole leukocyte cone material was layered onto 15 millilitres (ml) of Histopaque ficoll (Sigma Aldrich, USA), and centrifuged at 500 g for 25 min at room temperature (RT). The middle layer containing peripheral blood mononuclear cells (PBMCs) was collected and washed 3 times with 25 ml phosphate-buffered saline (PBS, Sigma Aldrich) at 500 g for 5 min at RT. Total PBMCs were counted and frozen at $1x10^8$ cells per mL of freezing medium (10% Dimethyl Sulphoxide (DMSO, Sigma Aldrich), 90% fetal bovine serum (FBS, (Gibco, Life technologies, USA)) at -80^oC for later use. For immediate use of the isolated PMBCs, RBCs were lysed. For this purpose, the PBMC pellet was suspended in 5 ml of RBC Lysis Buffer (Invitrogen, Life Technologies, USA) and incubated IN a 37^oC water bath for 3 min followed by a wash with 20 mL complete Roswell Park Memorial Institute medium (cRPMI, RPMI (Sigma Aldrich) containing 10% FBS and 1% penicillin/streptomycin (P/S, 1%, (Gibco)). Subsequently PMBCs were used for monocyte and CD4+ T cell isolations.

2.1.2. Monocyte isolation and MDM differentiation

Monocytes were isolated from PMBCs (fresh or thawed) using MACS Monocyte Isolation (Miltenyi Biotech, Germany) as described in the manufacturer's instructions. To prevent antibody binding causing nonspecific activation and receptor blockage, negative selection was performed. Eluted CD14+ cells (monocytes) were counted and plated at $2x10^5$ cells per 200 microliters (μL) of

X-vivo (Lonza, Switzerland) containing 1 % human serum (HS, H4522, Sigma Aldrich) per well of a flat bottom 96-well plate to differentiate into MDMs. 100 μL of the medium was exchanged at day 3 or 4, and at day 6 or 7 the whole medium was replaced to differentiate monocytes into MDM using plastic-adherence within 10 days. The purity of isolated monocytes was checked by flow cytometry after staining for their specific cell surface marker, CD14. Based on the staining, the mean purity of isolated monocytes obtained from 4 donors was 95.45% ± 1.51 (Figure 3.2b).

2.1.3. Isolation of $CD4^+$ T cells by magnetic labelling

PBMCs (fresh or thawed) were activated with 1 μg/mL Phytohaemagglutinin (PHA, Sigma Aldrich) and 10 U/ mL IL-2, (Centre For AIDS Reagents, National Institute of Biological Standards and Controls (CFAR, NIBSC)) for 72 h in cRPMI ($4x10^6$ cells/mL). On day 3, cells were collected and processed with MACS CD4 negative cell isolation Kit (Miltenyi Biotech) as described in the manufacturer's instructions. The eluted CD4+ T cells were maintained in cRPMI containing 10 U/mL IL-2 ($2x10^6$ cells/mL) for 24 h, prior being infected or used for the cell death experiments.

2.1.4. Non-adherent cell maintenance

Non-adherent cell lines were maintained in 75 cm^2 tissue culture flasks at 37°C with 5 % CO_2 in 20-25 mL cRPMI (Table 2.1). Cells were split 1:15 every 3-4 days into fresh medium.

2.1.5. Adherent cell maintenance

Adherent cell lines were maintained in 75 cm^2 tissue culture flasks at 37^oC with 5 % CO_2 in 15 mL complete (Dulbecco's Modified Eagles Medium (cDMEM, DMEM (Sigma) containing 10% FBS + 1 %P/S) or cDMEM containing selection antibiotic. Every 3-4 days, cells were lifted by being incubated in 2 mL EDTA Trypsin (0.25%, (gibco)) for 1-3 min, and resuspended in 15 mL cDMEM. Subsequently, they were split 1:15 into fresh appropriate cDMEM (Table 2.1). HEK 293T cells were maintained for a maximum of 25 passages.

2.1.6. Cryopreservation

To freeze the cell lines, cells were centrifuged at 500 g for 5 min at RT and resuspended at $5x10^6$ - $1x10^7$ cells/mL in freezing medium. Cells were stored in Mr. Frosty freezing container (NALGENE^{TM}, Sigma Aldrich) for 24 h at -80^oC. Afterwards, the frozen vials were either stored at at -80^oC for short-term storage or in liquid nitrogen for long-term storage.

2.1.7. Thawing cells

Frozen vials of cell lines stored either at -80^oC or in liquid nitrogen, were quickly (45-90 sec) thawed in a 37^oC water bath, then diluted into pre-warmed appropriate complete medium without selection antibiotic. Cells were centrifuged at 500 g for 5 min at RT, and non-adherent and adherent cells were then resuspended in 5 mL fresh cRPMI (25 cm^2 tissue culture flask) and 15 mL fresh cDMEM (75 cm^2 tissue culture flask), respectively. After reaching confluence, cultures were scaled up and a selection antibiotic was added if required (Table 2.1).

Table 2.1. List of primary cells and cell lines used including their applications and culture conditions. UA = Uptake assay in which MDM uptake of HIV-1-infected or healthy T cells by MDM was investigated. FS = FACS staining. Wild type (WT)-CEM and CD43-knock out (KO) CEM cells were kindly donated by Dr. Linda Baum (UCLA Medical Centre). ADAM10-KO HEK and their WT counterpart were kindly donated by Prof. Matthew Freeman (Sir William Dunn School of Pathology). ADAM10-KO CEM and ADAM10-KO CD43-Myc CEM T cells were generated and kindly donated by Dr. R.A. Russell and Dr. M.D. Moore (Sir William Dunn School of Pathology).

Name	Cell type	Culture medium and condition	Application
WT-CEM	T cell line	RPMI + 10% FCS + 1% P/S	UA, FS
WtT-CEM Luc	CEM cell line, expressing Renilla luciferase after transduction	RPMI + 10% FCS + 1% P/S + 100 μg/mL blasticidin (TOKU-E, USA)	UA, FS
ADAM10-KO CEM	CEM cell line deficient in ADAM10	RPMI + 10% FCS + 1% P/S	FS
CD43-KO CEM	CEM cell line deficient in CD43.	RPMI + 10% FCS + 1% P/S +0.450 mg/mL G418	UA, FS
CD43-KO Luc *	CEM cell line deficient in CD43 expressing Renilla luciferase	RPMI +10% FCS + 1% P/S +100 μg/mL blasticidin	UA, FS

Name	Cell type	Culture medium and condition	Application
Myc-CD43 CEM*	CEM cell line deficient in CD43 expressing Myc-CD43	RPMI + 10% FCS + 1% P/S + 5 μg/ml puromycin (company)	FS
ADAM10-KO Myc-CD43 CEM	CEM T cell line deficient in ADAM10, expressing Myc-CD43	RPMI+10% FCS+ 1% P/S + 5 μg/mL puromycin	FS
Human PBMCs	Peripheral blood mononuclear cells isolated from leucocyte cone (single donor)/ buffy coats (multiple donors)	RPMI+10% FCS+ 1% P/S + IL-2 (10 U/mL) PHA 1µg/mL	- Production of wild type virus after PHA activation Source of human primary CD4+ T cell after activation with PHA & IL-2, and negatively-selected monocytes before differentiation
Human CD4+ T cells	Primary T cells isolated from PBMCs obtained from leucocyte cones	$2x10^6$ - $4x10^6$ cells/mL of RPMI containing 10% FCS, 1% P/S, 10 U/mL IL-2	UA, FS
Human monocytes	Monocytes isolated from PBMCs obtained from leucocyte cone.	$1x10^6$ cells/mL of X-VIVO 10 containing 1% HS	UA, FS
TZM-bl	Adherent cells	DMEM + 10% FCS + 1% P/S	Virus titration
HEK 293T	Adherent human embryonic kidney (HEK) cells	DMEM + 10% FCS + 1% P/S	Transfection Virus production
WT-HEK	HEK cells	DMEM + 10% FCS + 1% P/S	FS

Name	Cell type	Culture medium and condition	Application
Myc-CD43 WT-HEK*	HEK cells expressing Myc-CD43	DMEM + 10% FCS + 1% P/S+ 2.5 μg/mL	FS
ADAM10-KO HEK	HEK cells deficient in ADAM10	DMEM + 10% FCS + 1% P/S	FS
Myc-CD43 ADAM10-KO HEK*	HEK cells deficient in ADAM10 expressing Myc-CD43	DMEM + 10% FCS + 1% P/S+ 2.5 μg/mL	FS

2.1.8. Generation of T and HEK cell lines

Cell lines which were generated by me in this study are marked with * in Table 2.1.

2.1.8.1. Myc-CD43 cell lines

CD43 cDNA (NCBI reference sequence: NM_001030288.1) with an N-terminal Myc-tag was purchased from Sino Biological Inc (catalogue number: HG13108-CM). Subsequently, Myc-CD43 was cloned in a plasmid allowing lentivirus production and encoding puromycin as a selection marker (PEF1, donated by Dr. M.D. Moore). Unfortunately, the CD43 purchased plasmid had an incorrect Kozak sequence which led to multiple unsuccessful attempts in the generation of Myc-CD43 CEM using different nucleofection, transfection and transduction protocols. The incorrect Kozak sequence was detected with the help of Dr. M.D. Moore, and with the supervision and guidance of Dr. R.A. Russell, I re-cloned Myc-CD43 into the lentiviral plasmid encoding the correct Kozak sequence (PEF1 Myc-CD43). Afterwards, I produced Myc-CD43 lentiviral

particles by polyethyleneimine (PEI) transfection of $1x10^6$ HEK 293T cells per well of 6-well plate using the plasmid mixture including 2μg pQ8.91, 2μg pMD-G and 2μg PEF1 Myc-CD43. Lentiviral particles were then used for transduction of CD43-KO CEM, WT and ADAM10-KO HEK cells. Forty-eight hours after transduction, different concentrations of puromycin were added to wild type and transduced cells to determine cell type-based puromycin sensitivity curve. Subsequently puromycin was added to the culture of transduced cells at the concentrations specified in Table 2.1. After puromycin selection, generation of Myc-CD43 CEM, Myc-CD43 ADAM10-KO and WT HEK cells was characterised and confirmed by flow cytometry described and presented in Chapter 5.

2.1.8.2. Renilla luciferase reporter (Luc) cell lines

A lentiviral plasmid encoding Renilla luciferase and blasticidin as a selection marker (pLenti.PKG.blast-Renilla_Luciferase; PKG-Luc) was purchased from Addgene (ID: 74444). Subsequently, Luc lentiviral particles were produced by PEI transfection of $1x10^6$ HEK 293T cells per well of 6-well plate using the plasmid mixture including 2μg pQ8.91, 2μg pMD-G and 2μg PKG-Luc. Lentiviral particles were then used for transduction of WT-CEM and CD43-KO CEM. Forty-eight hours after transduction, different concentrations of blasticidin were added to wild type and transduced cells to determine cell type-based blasticidin sensitivity curve. Subsequently blasticidin was added to the culture of transduced cells at the concentrations specified in Table 2.1. After blasticidin selection, generation of Myc-CD43 CEM, Myc-CD43 WT and ADAM10-KO HEK cells were characterised and confirmed by T cell line-based uptake assay described and presented in Chapter 5.

2.2. Viral preparation and HIV-1 infection

Infectious HIV-$1_{NL4.3\text{-}Luc}$ and HIV-$1_{Bal\text{-}Luc}$ were produced from plasmids listed in Table 2.2 as described below.

2.2.1. Transformation

One-Shot Stbl3 *E. coli* cells (Invitrogen) were incubated with 1-20 ng of DNA on ice for 30 min followed by a heat-shocked for 45 sec at 42^{o}C, and 2 min incubation on ice. Subsequently, 1 mL super optimal broth with catabolite repression (SOC) medium was added and bacteria were shaken at 225 rpm for 1 h at 37^{o}C. Afterwards, bacteria were pelleted by centrifugation at 500 g for 45 sec. Subsequently, the pellet was resuspended in 20µL SOC medium and plated onto a pre-warmed liquid broth (LB) containing a selection antibiotic followed by overnight incubation at 37^{o}C.

2.2.2. Maxi-preparation of viral plasmids

A single colony was picked from the selection plate prepared as described in Section 2.2.1 and used for inoculation of 2 mL LB containing the selection antibiotic (starter culture). The starter culture was incubated at 37^{o}C with vigorous shaking at 225p rpm overnight. The starter culture was then used to inoculate 200 mL culture, which was incubated at 37^{o}C with vigorous shaking (225 rpm) overnight. Endo-free QIAgen Maxi-prep kit (QIAgen, the Netherlands) was used for plasmid preparation as described in manufacturer's instructions. Plasmid concentration was determined using a NanoDrop 2000c (Thermo Scientific, USA).

2.2.3. PEI Transfection of HEK 293T cells

HEK 293T cells were seeded at $6x10^6$ cells/10 cm^2 tissue culture plate in 8 mL cDMEM and incubated for 24 h prior to transfection at 37°C to achieve 70-80 % confluency. On the next day, 10 µM polyethylenimine (PEI, Sigma Aldrich) was prepared in DMEM from a 10 mM stock (1:1000 dilution). For each transfection, 2 tubes were set up, the first tube contained 2.5 ml DMEM with 0.4 µM PEI which was prepared fresh on the day of use from a 10 mM stock solution. The second tube contained 20-25 µg plasmid DNA diluted in 2.5 mL. DMEM added drop-wise to the first tube whilst vortexing. The DNA-PEI mixture was incubated for 20 min at RT. Subsequently, the culture medium of HEK 293T cells was replaced with 5 mL of the DNA-PEI mixture followed by incubation for 4 h at 37°C. Afterwards, the transfection mixture was replaced with 5 mL fresh cDMEM. The plate was incubated for a further 48 h at 37°C. The supernatant was collected after 48 h, filtered through a disposable 0.45 µm pore filter (Sartorius, Germany) and concentrated as described below (2.2.4).

2.2.4. Virus concentration

Filtered virus-containing supernatant was concentrated 10-40 fold using LentiX™ concentrator (Clontech, France) according to the manufacturer's instructions. The pellet was resuspended in 100 µL fresh cRPMI and stored at 120°C.

2.2.5. Viral infectivity titration

Infectivity of viral stocks was assessed using TZM-bl cells based on a standard protocol [340]. Briefly, viral stock was thawed and diluted 1:2 into 100 µL cDMEM, and added to the first column of a 96-well plate. A 3-fold dilution series

was set up across the plate, leaving the final column without virus. $1x10^4$ TZM-bl cells/100 μL/well were added to each well followed by incubation for 24 - 36 h at 37°C. The following day, supernatant was removed and cells were washed once with 100 μL PBS, and then lysed with 100 μL reporter lysis buffer (E397A, Promega, USA) followed by overnight storage at -80°C. For luciferase quantification, the cell lysate was thawed in the dark and mixed 1:1 (50 μL) with Bright-Glo luciferase assay solution (E2620, Promega) into the wells of a white luciferase plate. The plate was incubated for 2 min at RT before reading with a SpectraMax M3 or M5 plate reader (Molecular Devices Inc., USA) with 1000 ms^{-1} integration (i.e. luciferase expression from each well was read for 1 sec) to determine the relative light units (RLU). Background values from uninfected wells were multiplied by two and subtracted from the luciferase read-outs obtained from the virus-containing wells. Infectious unit calculations were done using ID-50 version 5.0 (John L. Spouge) using a Poisson model. This information was used to calculate the number of infectious unit in 50 µL of virus (IU) and MOI.

2.2.6. CD4+ T cell infection

Primary CD4+ T cells were isolated as described in Section 2.1.3 and pelleted at 500 g for 10 min at RT. Subsequently, they were resuspended in cRPMI containing IL-2 (10 U/mL) to achieve $1x10^7$ cells/mL, and incubated with the CCR5 tropic Renilla luciferase reporter virus $HIV_{BaL\text{-}Luc}$ at a MOI of 0.01 for 4 h. Cells were then topped up with fresh cRPMI containing IL-2 (10 U/mL) to achieve $1x10^6$ cells/mL and incubated for 7 days at 37°C. To maintain IL-2 in the culture, the medium was topped up with 10 U/mL IL-2 4 days post-infection. For infecting WT-CEM and CD43-KO CEM, the same protocol was applied,

except using cRPMI as culture medium and CXCR4 tropic Renilla luciferase reporter virus $HIV_{NL4.3\text{-}Luc}$ at a MOI of 0.01. Moreover, WT-CEM and CD43-KO CEM were incubated for 3 and 4 days, respectively.

Table 2.2. List of viruses. LucR= Renilla luciferase, CHAVI=The Centre for HIV/AIDS Immunology, IMCs= molecular clones generated and kindly provided by C. Ochsenbauer and J. Kappes, University of Alabama, Birmingham.

Virus	Plasmid	Clade	Type	Env	Insert	Source
$HIV\text{-}1_{Bal\text{-}Luc}$	NL-LucR-T2A.ecto	B	IMC Ref	BaL	LucR	CHAVI
$HIV\text{-}1_{NL4.3\text{-}Luc}$	NL-LucR-T2A.ecto	B	IMC X4 Ref	NL4.3	LucR	CHAVI

2.3. Flow Cytometry

2.3.1. Surface staining of live cells

Live cells were pelleted and the culture medium was aspirated. The pellet was then washed with 200 µL - 1 mL FACS wash buffer (FWB, PBS containing 1% FBS and 0.09% NaN_3 (sodium azide, Sigma Aldrich)) at 500 g for 5 min at 4°C, and pelleted in wells of round bottom 96-well plate. Staining was performed for 1 h in 100 µL primary unconjugated or directly conjugated antibody solution at 4°C with gentle agitation followed by three washes in 200 µL FWB. For primary unconjugated antibodies, live cells were incubated for 1 h with 100 µL relevant fluorochrome-conjugated secondary antibody solution at 4°C with gentle agitation in the dark followed by three washes in 200 µL FWB. Cells were then

fixed with 4% formaldehyde (FA (Sigma Aldrich)) for 15 min at RT followed by two washes in 200 µL FWB. Afterwards, the pellet was resuspended in either 200 µL FWB to acquire data using FACS tube, or 60 µL FWB for acquiring data using round bottom 96-well plate. Cells were either analysed immediately or stored at 4^{o}C overnight. Antibodies and the used concentrations are summarised in table 2.3.

2.3.2. Surface staining of fixed cells

Live cells were pelleted and the culture medium was aspirated. The pellet was then washed with 200 µL-1 mL FACS wash buffer at 500 g for 5 min at 4^{o}C. The cell pellet was fixed with 4% FA for 15 min at RT followed by two washes with 200 µL-1 mL FWB. Subsequently, cells were pelleted in wells of round bottom 96-well plate and antibody incubations were performed for 1 h at RT with the same washes as described in Section 2.3.1. Antibodies and the concentrations used are summarised in table 2.3.

2.3.3. Intracellular staining of fixed cells

Cells were either immediately fixed with 4% FA for 15 min at RT or stained with cell surface proteins as described in Sections 2.3.1 and 2. Afterwards, fixed cells were permeabilised in permeabilisation wash buffer (PWB, PBS containing 30% FBS, 0.1% saponin (S4521, Sigma Aldrich) and 0.09% NaN_3) for 30 min, and intracellular staining and washing performed for 1 h at RT in PWB instead of FWB. Antibodies and the concentrations used are summarised in table 2.3.

2.3.4. Acquisition and analysis

Flow cytometry data were acquired on a FACS Calibur (BD Biosciences) and analysed using FlowJo (Tree Star, USA).

Table 2.3. List of antibodies, their specifications and applications. UA = Uptake assay in which the uptake of HIV-1-infected T cells by MDMs and their subsequent infection was investigated; Abs used in this assay were free from preservative ($NaN_{3)}$ and were prepared in the medium appropriate for the cell type they were incubated with. FS = FACS staining; for detection of cell surface molecules and cytoplasmic proteins. EL = direct ELISA; for detection of soluble cell surface proteins in the supernatant. Ab concentrations for staining and blocking purposes were chosen based on the manufacturer's data sheet and provided citations. All the Abs against the HIV-1 Env spike were produced and kindly donated by former lab member, Dr. T. Schiffner; they were used at 50µg/mL, a super-saturating concentration since all bNAbs have IC50 values of much less than 50µg/mL [341].

Ab name/ clone	Target	Application	Source
ICRF44	CD 11b of human Mac-1	UA (10 µg/mL)	Biolegend, Cat: 301311
CBRM1/5	CD11b of activated Mac-1	UA (10 µg/mL)	Biolegend, Cat: 301407
H1III	CD 11a of human LFA-1	UA (10 µg/mL)	Biolegend, Cat: 301214
HA58	D1 domain of human ICAM-1	UA, FS (10 µg/mL)	Biolegend, Cat: 353104
R6.5	D2 domain of human ICAM-1	UA (10 µg/mL)	eBioscience, Cat: BMS1011
DFT-1	Sialic acid-dependent epitope on CD43 [342]	UA (10 µg/mL) FS (2 µg/mL)	UA: Abcam, Cat: ab76524 FS: Santa Cruz, Cat: sc-6256
Biotinylated DFT-1	Sialic acid-dependent epitope on CD43	EL (2 µg/mL)	Ancell, Cat:192-030

Ab name/ clone	Target	Application	Source
1D4	Sialic acid-dependent epitope on CD43 [343]	FS (5 µg/mL)	Antibodies-online Cat: ABIN1106370
C-20	Sialic acid-independent epitope on CD43 [343, 344]	FS (4 µg/mL)	Santa Cruz, Cat: sc-7052
Asp175	Cleaved caspase 3	FS (1:400)	Cell signalling Cat: 9661
Asp391 (18C8)	Cleaved caspase 8	FS (1:100)	Cell signalling Cat: 9496
Asp315 (D8I9E)	Cleaved caspase 9	FS (1:100)	Cell signalling Cat: 20750
136-4B5	Sialic acid-dependent epitope on CD45 [345]	FS (10 µg/mL)	Biotium Cat: BNUB0173-100
FITC conjugated MEM-28	Sialic acid-independent epitope on CD45	FS (1:100)	Immuno tools Cat: 21270453x2
11G2	Human ADAM10	FS (1:400)	Abcam, Cat: ab59482
9E10	Myc-tag	FS (2 µg/mL)	Santa Cruz, Cat: sc-40
Biotinylated-9E10	Myc-tag	EL (1 µg/mL)	Santa Cruz, Cat: sc-40 B
HIT3a	Human CD3	MS (10 µg/mL)	BD Pharmingen Cat: 555336
V450 conjugated UCHT1	Human CD3	FS (5 µL/test)	BD Horizon Cat: 560365
APC conjugated mouse anti human CD14 (61D3)	Human CD14	FS (5 µg/mL)	eBioscience, Cat: 17-0149-41
37G12	Human anti HIV-1 p24	FS, MS (26 µg/mL)	Polymun scientific Lot: 271113A
KC57-FITC	Human anti HIV-1 P24	FS (10 µg/mL)	Beckman coulter Cat: 6604665
R-phycoertthrin (PE)	Goat anti mouse IgG2a	FS (5 µg/mL)	Life Technology, Cat: P21139

Ab name/ clone	Target	Application	Source
PE	Goat anti rabbit IgG	FS (5 µg/mL)	Life Technology, Cat: A10542
Alexa 488	Goat anti mouse IgG1	FS (5 µg/mL)	Life Technology, Cat: A21121
Alexa 488	Goat anti rabbit IgG	FS (10 µg/mL)	Life Technology, Cat: A11008
Alexa 488	Donkey anti goat IgG	FS (20 µg/mL)	Life Technology, Cat: A11055
Alexa 647	Goat anti human IgG	MS,FS (5 µg/mL)	Life Technology, Cat: A21445
Alexa 647	Goat anti rabbit IgG	FS (10 µg/mL)	Life Technology, Cat: A21245
Alexa 647	Donkey anti goat IgG	FS (10 µg/mL)	Life Technology, Cat: A21447
Allophycocyanin (APC)	Goat anti mouse IgG (H+L)	FS (5 µg/mL)	Life Technology, Cat: A865
IgG1	Human IgG1 isotype control	UA, FS (10 µg/mL)	BD Biosciences Cat: 554721
IgG2a	Human IgG2a isotype control	UA (10 µg/mL)	eBiosciences Cat: 16-4724-85
Goat IgG	Goat IgG isotype control	FS (4 µg/mL)	Santa Cruz, Cat: sc-2028
Rabbit IgG (DA1E)	Rabbit IgG isotype control	FS (as the main primary Ab)	Cell signalling Cat: 3900
Mouse IgG1	Mouse IgG1 isotype control	FS (as the main primary Ab)	Santa Cruz, Cat: sc-3877
FITC conjugated mouse IgG1 isotype control	Mouse IgG1 isotype control	FS (10 µg/mL)	eBiosciences Cat: 11-4714-42
APC conjugated mouse IgG1 isotype Ctrl	Mouse IgG1 isotype control	FS (10 µg/mL)	Biolegend, Cat: 400121
APC conjugated Goat anti mouse IgG (H+L)	mouse IgG	FS (5 µg/mL)	Jackson , Cat: 115-135-164
FITC conjugated Goat anti mouse IgG (H+L)	mouse IgG	FS (5 µg/mL)	Jackson , Cat: 115-096-146
10E8 [346]	HIV-1 Env gp41 MPER	UA (50 µg/mL)	
2F5 [347, 348]	HIV-1 Env gp41 MPER	UA (50 µg/mL)	
7b2 [349]	HIV-1 Env-gp41 MPER	UA (50 µg/mL)	
35O22 [350]	HIV-1 Env-quaternary gp120/41 interface	UA (50 µg/mL)	

Ab name/ clone	Target	Application	Source
PGT151 [351]	HIV-1 Env-quaternary gp120/41 interface	UA (50 µg/mL)	
3BC315 [352]	HIV-1 Env-quaternary gp120/41 interface	UA (50 µg/mL)	
PGT121 [353, 354]	HIV-1 Env-V3 glycan	UA (50 µg/mL)	
PGT128 [353, 354]	HIV-1 Env-V3 glycan	UA (50 µg/mL)	
19b [349]	HIV-1 Env-V3 non neutralising	UA (50 µg/mL)	
PGT145 [354]	HIV-1 Env-quaternary V1/V2	UA (50 µg/mL)	
VRC01 [355]	HIV-1 Env CD4 binding site	UA (50 µg/mL)	
VRC03 [355]	HIV-1 envelope spike-CD4 binding site	UA (50 µg/ml)	
17b [356]	HIV-1 Env-CD4i non neutralising	UA (50 µg/mL)	
A32 [357]	HIV-1 Env-CD4i non neutralising	UA (50µg/mL)	
2G12 [358]	HIV-1 Env-Glycan N332	UA (50 µg/mL)	

2.4. Uptake Assay

Treated or untreated HIV-$1_{BaL\text{-}Luc}$ infected primary CD4+ T cells and HIV-$1_{NI4.3\text{-}Luc}$ WT-CEM and CD43-KO CEM were co-cultured with MDM in triplicate wells per condition for 1-3 h depending on the experiment. Subsequently, extensive washes with PBS containing 10 mM EDTA were applied to remove unbound/unengulfed T cells followed by MDM-lyse with 60 µL Glo-Lysis buffer (E266A, Promega) per well of flat-bottom 96-well plate. The plate was stored at

least for 4 h at -80°C. To measure the MDM capture of infected T cells, 50 μL cell lysate was mixed with 50 μL Ren-Glo Luciferase Assay solution (E2720, Promega) at RT in white 96 well plates. Luciferase activity was then measured at 1000 ms^{-1} integration with a SpectraMax M3 or M5 plate reader (Molecular Devices). Background values in uninfected wells were subtracted, and the uptake index in test wells was calculated relative to relevant untreated/control peptide/control solution/isotype control and reported either in the form of inhibition of uptake (%) or uptake as fold-increase.

2.5. Direct ELISA

$1x10^8$ T cells were incubated for 3 h in the 1 mL RPMI either with/without 100 μM staurosporine. Afterwards, T cells were centrifuged at 500 g for 5 min at 4°C, and supernatants were collected and 1:100 tissue culture protease inhibitor cocktail (P1860, Sigma) was added. Subsequently, supernatants were aliquoted and stored at -20ºC. Enzyme-linked immuno-sorbent assays (ELISAs) were performed by coating T cell supernatant onto ELISA plates (High protein binding Spectraplate™, PerkinElmer, USA) at 4°C overnight at different dilutions in 50 μL 100 mM Na_2CO_3 buffer pH 8.5 per well. Wells were washed 3 times with PBS-T (PBS containing 0.005% Tween-20 (Sigma Aldrich) in a hydrospeed plate washer (TECAN, Switzerland) and blocked with 200 μL blocking buffer (PBS-T + 1% BSA (Sigma Aldrich)) for >30 min at RT. Plates were washed once with PBS-T, then incubated with 50 μL biotinylated primary mAb (table 2.3) per well in blocking buffer at RT for 1 h. Plates were washed 3 times with PBS-T and incubated with 50 μL HRP-coupled secondary antibodY (GE Healthcare UK limited) per well were added at 1:10,000 in blocking buffer.

After 30 min, plates were washed 3 times with PBS-T and 50 µL 1-Step Ultra TMB (Thermo Fisher, USA) substrate was added. After the required optical density (OD) had been reached, 50 µL 0.5 M H_2SO_4 were added to stop the reaction and absorption was read at 450 nm on a Spectramax M3 or M5 plate reader. Background subtraction was performed by subtracting the average of control wells (supernatant of CD43-KO CEM) from the values of test wells (supernatant of Myc-CD43 CEM).

2.6. Induction of apoptosis

2.6.1. CD4+ T cell lines

T cells were resuspended at $2x10^6$- $3x10^6$ cells/mL in cRPMI containing 1 µM staurosporine (191400, MP biomedical, France) and incubated for 4 h at 37°C to induce caspase 3 activation in 70-80% of the population. Subsequently, T cells were washed with FWB and, depending on the experiment, were either fixed with 4% FA or went through a live staining protocol as described in Section 2.3.1.

2.6.2. Primary CD4+ T cells

CD4+ T cells were isolated from whole blood and activated and infected as described in Section 2.1.3. On Day 3, cells were washed with 20 mL cRPMI at 500 g for 5 min at RT. T cells were resuspended at $2x10^6$- $3x10^6$ cells/mL in cRPMI containing 10 µM staurosporine and incubated for 4 h at 37°C to induce caspase 3 activation in 70-80% of the population. Subsequently, T cells were washed with FWB and, depending on the experiment, were either fixed with 4% FA or went through the live staining protocol (Section 2.3.1).

2.7. Induction of pyroptosis

2.7.1. CD4+ T cell lines

T cells were resuspended at $7x10^6$ cells/ml in cRPMI containing 75 μM nigericin (N7143, Sigma Aldrich) and incubated for 4 h at 37°C to induce caspase 1 activation in 30-40% of the population. Subsequently, T cells were stained for cleaved caspase 1 using FAM FLICA™ caspase-1 kit (Bio-Rad, USA) as described in the manufacturer's instruction and depending on the experiment either stored at 4°C or fixed using the protocol as described in Section 2.3.2 and 3.

2.7.2. Primary CD4+ T cells

CD4+ T cells were isolated from whole blood, and activated and infected as described in Section 2.1.3. On Day 3, cells were washed with 20 mL cRPMI at 500 g for 5 min at RT. T cells were resuspended at $7x10^6$ cells/mL in cRPMI containing 50 μM nigericin and incubated for 4 h at 37°C to induce caspase 1 activation in 30-40% of the population. Subsequently, T cells were stained for cleaved caspase 1 using FAM FLICA™ caspase-1 kit as described in the manufacturer's instruction and, depending on the experiment, either stored at 4°C or fixed using the protocol as described in Section 2.3.2 and 3.

Table 2.4. List of inhibitors and enzymes, their specifications and applications. Inf = used in HIV-1 infection assay. Apo = used in apoptotic cell death assay. Pyro= used in pyroptotic cell death assay. FS= flow cytometry. EL=ELISA

Name	Function	Application	Source
Q-VD-OPH peptide	Pan-caspase inhibitor	Apo (20 μM), Inf (50 μM)	Calbiochem Cat: 551476
Q-VD-OPH peptide	Pan-caspase inhibitor	Apo (20 μM), Inf (50 μM)	Cayman Cat: 15260

Name	Function	Application	Source
Q-VE-OPH peptide	Pan-caspase control	Apo (20 μM), Inf (50 μM)	Santa Cruz, Cat: SC-396537
Z-VAD-FMK peptide	Pan-caspase inhibitor	Apo (100 μM)	BD pharmingen Cat: 550377
Z-FA-FMK peptide	Pan-caspasec contol	Apo (100 μM)	BD pharmingen Cat: 550411
Z-DEVD-FMK peptide	caspase 3 inhibitor	Apo (200 μMl)	Selleckchem, S7312
Ac-LEHD-CMK peptide	caspase 9 inhibitor	---	Santa Cruz, Cat: SC-300327
Z-IETD-FMK peptide	caspase 8 inhibitor	Apo (25 μM)	Selleckchem, S7314
GI254023X	ADAM 10 inhibitor	Apo, FS (10 μM) Apo, EL (100 μM)	AOBIOUS, Cat: AOB3611
GW280264X	ADAM 10 and 17 inhibitor	Apo (10 μM)	AOBIOUS, Cat: AOB3632
1,10-Phenanthroline	General metalloprotease inhibitor	Apo (1 mM)	Sigma Aldrich Cat: 131377
α_1-anti chymotrypsin	General serine protease inhibitor	---	Sigma Aldrich Cat: A9285
α_1-antitrypsin	General serine protease inhibitor	---	Sigma Aldrich Cat: SRP6312
3,4-dich-loroisocoumarin	General serine protease inhibitor	Apo (100 μM)	Sigma Aldrich Cat: D7910
GM6001	General metalloprotease inhibitor	Apo (100 μM)	Donated by Prof. Yoshi Itoh Lab
Marimastat	General metalloprotease inhibitor	Apo (10 μM)	Donated by Prof. Yoshi Itoh Lab
Jasplakinolide	Actin polymerisation inhibitor	Apo (5 μM)	
Nocodazole	Microtubule polymerisation inhibitor	Apo (10 μM)	
Brefeldin	Golgi to cell membrane inhibitor	Apo (10 μg/mL)	
Arthrobacter ureafaciens	Sialidase		Amsbio Cat:AMS.24229-74

Name	Function	Application	Source
Vibrio cholerae	Sialidase		Sigma Aldrich Cat: 72197-1ml

Chapter 3: The role of HIV-1 Env and ICAM-1 in interactions between MDM and HIV-1-infected T cells

3.1. Introduction

Treating HIV-1 infection in ~50% of the world's population is still a challenge, and the establishment of viral reservoirs is a major obstacle to eliminating the disease. The virus primarily targets CD4+ T cells leading to their progressive elimination. However, infected macrophages may disseminate infection by forming viral reservoirs within tissues where antiretroviral drugs may not penetrate well [359]. It has been shown that the establishment of HIV-1 reservoirs occurs within 5-10 days of viral transmission, and this hypothesis is supported by recent evidence showing that the SIV reservoir is established in the macaque model within the first 3 days of infection [96, 150].

Cell-free infection of macrophages is not an efficient process due to several entry and post-entry restrictions in these cells. MDM express 10-20 and 22-330 fold lower levels of CD4 and dNTP precursors, respectively [115, 117]. There is also substantial donor-dependent variation in MDM permissiveness that may result from variation in receptor and restriction factor expression [360]. Macrophages express specific restriction factors including tetherin, SAMHD1 and APOBEC3G [361]. As a result, many viruses capable of entering CD4+ T cells fail to efficiently infect and replicate in MDM *in vitro.* Despite these restrictions, infected macrophages can be identified in regional lymph nodes of acutely infected individuals, and post-mortem brain of chronically infected individuals [362-364]. This raises the question of how these macrophages become infected *in vivo* with viruses that are so inefficient at infecting MDM *in vitro*.

In 2014, our laboratory reported that the engulfment of HIV-1 infected CD4+ T cells by MDM leads to efficient MDM infection [339]. To investigate the role of HIV-1 Env, which is the only viral product expressed on the surface of virions or infected cells, they used Env-deficient HIV-1 pseudovirus and different Env-receptor inhibitors including some bNAbs against Env and receptor/coreceptor antagonists. Neither use of Env-deficient HIV-1 nor Env-receptor inhibitors could reproducibly and significantly block MDM uptake of infected T cells [339]. Moreover, inhibitors of ICAM-1-LFA-1 adhesion molecule interactions, strongly implicated in the spread of HIV-1 across VS, failed to inhibit HIV-1-infected T cell capture by MDM (unpublished data R. Russell, A. Baxter, C. Duncan). Puzzlingly, some ICAM-1-specific antibodies did show significant inhibitory activity on MDM uptake of infected T cells, apparently independent of the ICAM-1-LFA-1 interaction, the mechanism of which remains unclear.

3.1.1. Hypothesis

Based on the previous observations outlined above, I hypothesised that the recognition and engulfment of HIV-1-infected T cells by MDM is mediated by specific molecular interactions and that identification of these cell surface receptors and/or signals (including virally-encoded proteins such as Env) driving these interactions will inform future attempts to inhibit this process and reduce macrophage infection.

3.1.2. Specific aims

In this chapter, I further investigated the role of Env in the capture of HIV-1-infected CD4+ T cells by MDM and their subsequent infection, using 10 recently discovered broadly neutralising antibodies (bNAbs) targeting different regions

of Env. Moreover, I further interrogated the implication of ICAM-1 in MDM uptake of HIV-1-infected T cells.

3.2. Results

3.2.1. The role of Env in HIV-1-infected CD4+ T cell-MDM interactions

Although our laboratory published preliminary findings suggesting that Env-receptor interactions were not implicated in HIV-1-infected T cell uptake by MDM [339], these required further confirmation, since only a small panel of inhibitors was available at the time. Baxter et al. showed that Env-receptor inhibitors could not reproducibly and significantly prevent the uptake of infected T cells. However, within the last 3 years, new potent bNAbs have been generated targeting different epitopes of Env. Therefore, to further probe the role of Env in macrophage recognition and capture of infected T cells, I investigated the effect of 11 recently discovered bnAbs (Figure 3.2c and Table 2.3) on MDM isolated from PBMCs of 6 different donors using the approach described in Figure 3.1.

In brief, CD4+ T cells and monocytes were isolated from human leukocyte cones using negative isolation procedures by magnetic bead sorting. The efficiency of the isolation procedure was evaluated by staining CD3 and CD14 on the isolated CD4+ T cells and monocytes, respectively. Isolated CD4+ T cells and monocytes from 4 human leukocyte cones showed combined means of 95.4% and 98.2% purity, respectively (Figure 3.2b).

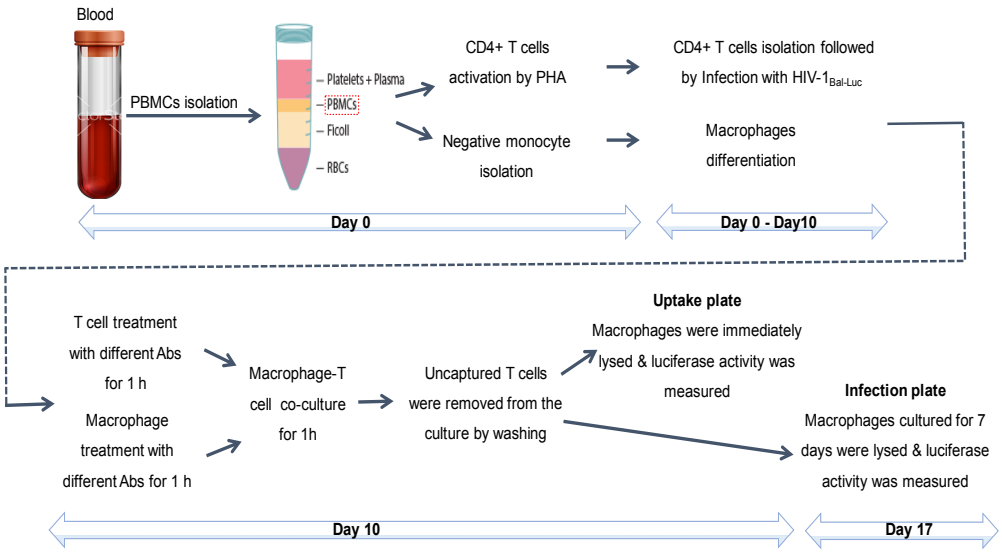
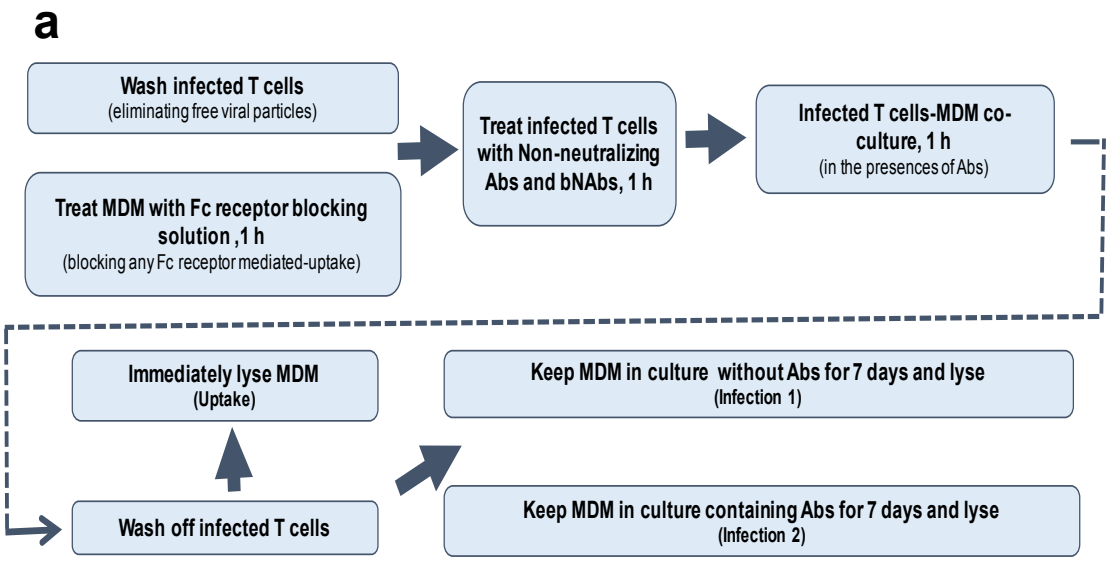
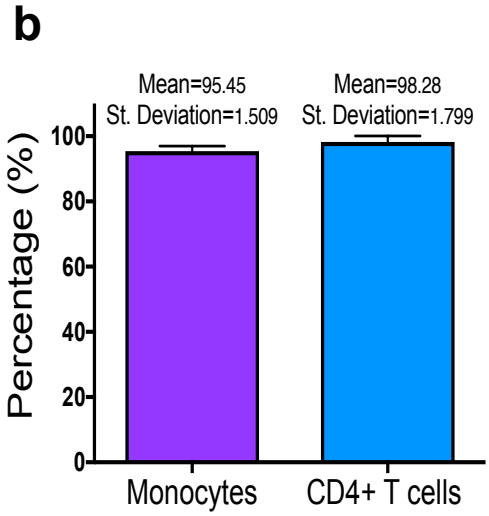


Figure 3.1. The schematic experimental strategy for isolation, infection, co-culture and analysis of the uptake of HIV-1-infected CD4+ T cells by MDM and their subsequent infection. CD4+ T cells and monocytes were isolated from blood (leukocyte cones) using negative isolation procedures by magnetic bead sorting. CD4+ T cells were activated with PHA and IL-2 three days before infection with an infectious CCR5-using (R5) luciferase reporter virus molecular clone, strain BaL (HIV-$1_{BaL\text{-}Luc}$). Monocytes were differentiated by plastic adherence in the presence of 1% human serum and the absence of any additional cytokines for 10 days. On the day of the assay, infected T cells were added to MDM for 1 h in the presence of non-neutralising Abs or bNAbs, and non-captured T cells were vigorously washed off. To measure the uptake of infected T cells by MDM, MDM washed free of non-captured infected T cells were lysed, and luciferase assayed. Luciferase activity represents infected T cells captured by MDM since insufficient time had elapsed for MDM to become productively infected and generate a de-novo luciferase signal. For the MDM infection assay, MDM washed free of non-captured infected T cells were cultured for 7 days then lysed, and luciferase assayed. In this case, the luciferase signal represents the sum of the residual captured infected T cell signal and the infected MDM signal.

After the isolation procedure, activated CD4+ T cells were infected with HIV-$1_{Bal\text{-}Luc}$ and monocytes differentiated into MDM. On the day of the assay, infected T cells (5% positive for intracellular Gag p24 using FACS staining and analysis) and MDM were treated with non-neutralising control Abs and bNAbs for 1 h before co-culture. Afterwards, infected T cells were added to MDM in the presence of non-neutralizing Abs or bNAbs for 1 h at the ratio of 2 to 1. Unbound/unengulfed T cells were extensively washed away and MDM were immediately lysed, and luciferase (which is expressed following viral integration and therefore is only produced by infected CD4+ T cells) was measured.





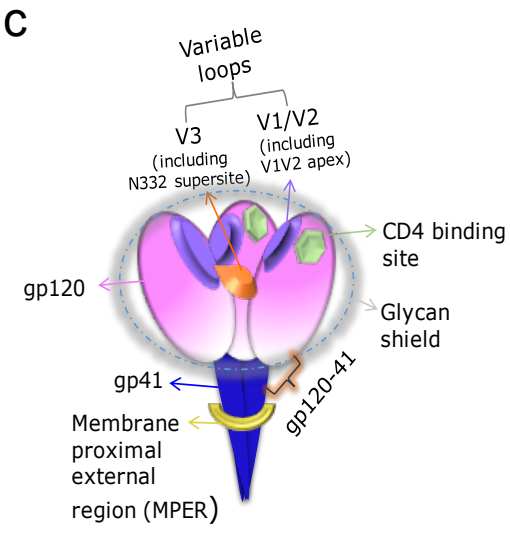


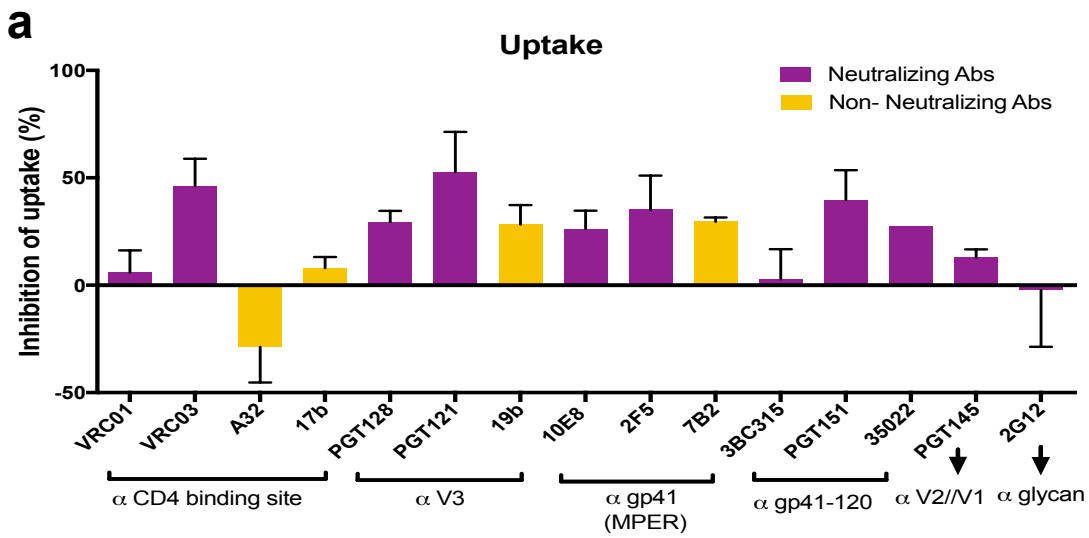
Figure 3.2. a) The schematic experimental strategy for the uptake of HIV-1-infected T cells treated with bNAbs and non-neutralising Abs by MDM and their subsequent infection. HIV-1-infected CD4+ T cells were washed thoroughly to remove cell free viral particles and treated with 50 μg/mL (a super-saturating dose based on previous experiments carried out in the laboratory) of bNAbs and non-neutralising Abs for 1 h. Meanwhile, MDM were treated with 10 μg/mL Fc receptor blocking solution for 1 h. Subsequently, infected T cells were co-cultured with MDM for 1 h, and infected T cells were then removed with vigorous washing. Uptake: after removing infected T cells, MDM were lysed, and luciferase assayed. Infection 1: after removing infected T cells, the plate was kept in culture for 7 days, MDM were lysed and luciferase assayed. Infection 2: after removing infected T cells, the plate was kept in culture containing bNAbs and non-neutralising Abs for 7 days, and MDM were lysed, and luciferase assayed**. b) Purity of CD4+ T cells and monocytes isolated from human leukocyte cones.** CD4+ T cells and monocytes were isolated from human leukocyte cones using MACS cell separation kits. Isolated T cells and monocytes were stained with anti CD3 and CD14 mAbs, respectively. Bars = mean CD3 and CD14 positive T cells and monocytes (%) + SD for 4 donors. **c) The schematic close-up of viral Env showing major structural features involved in immune evasion and regions targeted by bNAbs.**

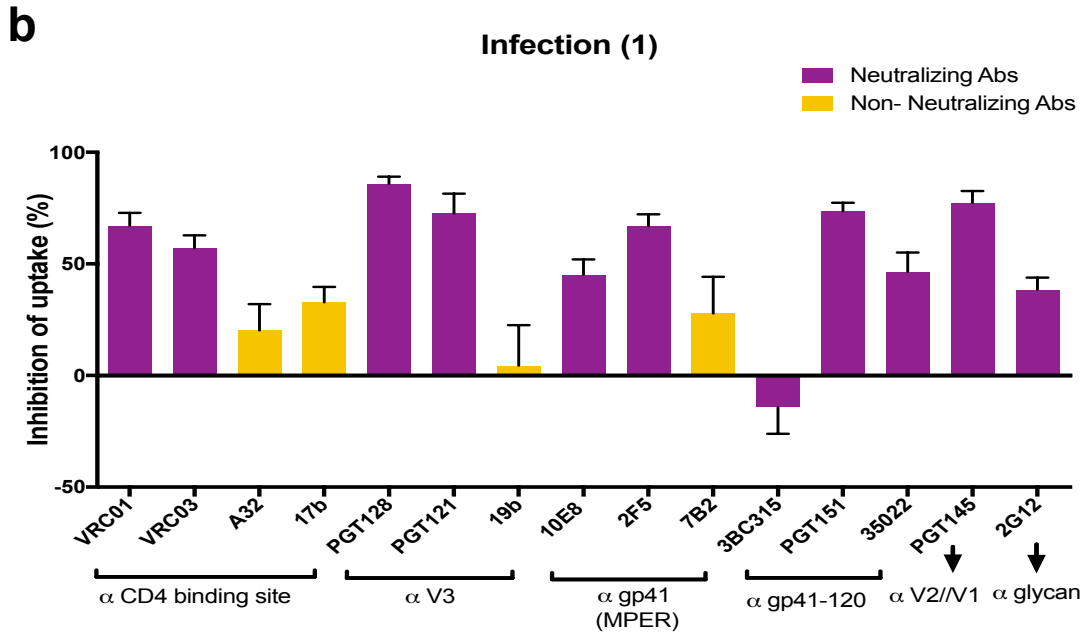
As the first pilot experiment, CD4+ T cells were infected with HIV-$1_{Bal\text{-}Luc}$ and monocytes were differentiated into MDM over 10 days, respectively (Figure 3.1). To investigate the role of Env on the MDM capture of infected T cells and subsequent MDM infection, as described in Figure 3.2a, infected T cells were treated with bNAbs and non-neutralising Abs on day 10. If Env is implicated in MDM recognition and/or uptake of infected T cells, uptake should be inhibited by bNAbs. Afterwards, infected T cells were co-cultured with MDM for 1 h, and unbound/unengulfed infected T cells were then removed with vigorous washing. To measure the uptake of infected T cells by MDM, MDM were lysed, and luciferase assayed (Figure 3.3a). To measure MDM infection due to the

uptake of infected T cells after washing, the plate was kept in culture for 7 days, MDM were then lysed, and luciferase assayed (Figure 3.3b). To investigate infection of MDM by infected T cell uptake, bNAbs and non-neutralising Abs were maintained in culture for 7 days, and MDM were then lysed, and luciferase assayed (Figure 3.3c).

Preliminary data showed ~40% reduction in the MDM capture of infected T cells treated with VRC03 (anti-CD4 binding site), PGT121 (anti-V3 loop), 2F5 (anti-MPER) and PGT151 (anti-quaternary gp120-41 interface). However, other bNAbs targeting the same epitopes did not show the same inhibitory effect. 7B2 and 19b which are non-neutralising Abs showed ~30% inhibitory effect targeting MPER and V3 loop, respectively. Keeping MDM for 7 days in culture without bNAbs reduced subsequent MDM infection by at least 50%, suggesting that bNAbs bound to infected T cells may have been carried over into the MDM to partially reduce MDM infection, since these reductions were more than their inhibitory effects on the uptake of infected T cells by MDM. Maintaining the presence of bNAbs during the entire 7 day-culture reduced HIV-1 infection of MDM by at least 98%. This was anticipated since the presence of bNAbs would prevent fusion of HIV-1 released from the infected T cells with the MDM [339]. Interestingly, non-neutralising Abs revealed a range of inhibition when maintained in the culture. A32 (anti-CD4-induced site) and 7B2 (anti-MPER) showed the lowest (39%) and the highest inhibitory effects (78%), respectively. To investigate whether any of the observed patterns could reach significance in the face of substantial donor-dependent variation, I repeated this experiment three times, each time with two donors. However, I did not further

investigate subsequent MDM infection in the presence of bNAbs and non-neutralising Abs during the 7 day-culture, as the results obtained from this donor confirmed what previously reported by Baxter et al. [339].


a
Uptake
Neutralizing Abs
Non- Neutralizing Abs
Inhibition of uptake (%)
100
50
0
-50
VRC01
VRC03
A32
17b
PGT128
PGT121
19b
10E8
2F5
7B2
3BC315
PGT151
35022
PGT145
2G12
α CD4 binding site
α V3
α gp41 (MPER)
α gp41-120
α V2//V1
α glycan


b
Infection (1)
Neutralizing Abs
Non- Neutralizing Abs
Inhibition of uptake (%)
100
50
0
-50
VRC01
VRC03
A32
17b
PGT128
PGT121
19b
10E8
2F5
7B2
3BC315
PGT151
35022
PGT145
2G12
α CD4 binding site
α V3
α gp41 (MPER)
α gp41-120
α V2//V1
α glycan

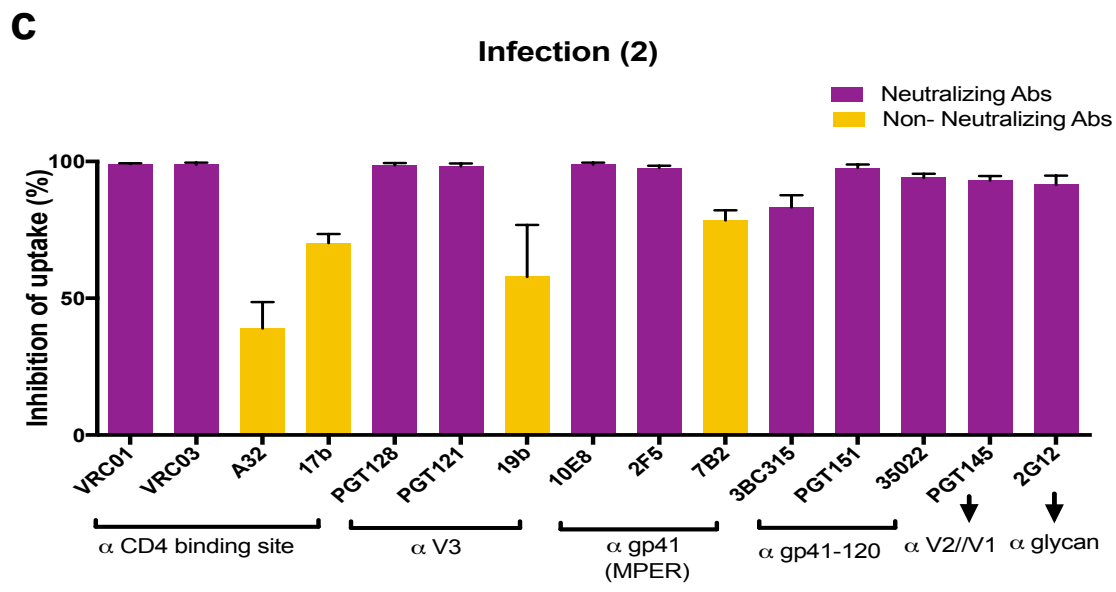

c
Infection (2)
Neutralizing Abs
Non- Neutralizing Abs
Inhibition of uptake (%)
100
50
0
VRC01
VRC03
A32
17b
PGT128
PGT121
19b
10E8
2F5
7B2
3BC315
PGT151
35022
PGT145
2G12
α CD4 binding site
α V3
α gp41 (MPER)
α gp41-120
α V2//V1
α glycan

Figure 3.3. The effect of bNABs and non-neutralizing Abs on MDM uptake of HIV-1-infected T cells and subsequent MDM infection. CD4+ T cells and monocytes were isolated and treated as described above. (Figure 3.2a) HIV-1-infected CD4+ T cells were treated for 1 h with 50μg/mL of bNAbs and non-neutralising Abs binding to the different epitopes of HIV-1 Env. Afterwards, infected T cells and MDM were co-cultured for 1 h, and infected T cells were then removed with vigorous washing. **a) Uptake:** after removing infected T cells, MDM were lysed, and luciferase assayed. **b) Infection 1:** after removing infected T cells, the plate was kept in culture for 7 days, and MDM were then lysed and luciferase assayed. **c) Infection 2:** after removing infected T cells, the plate was kept in culture containing bNAbs and non-neutralising Abs for 7 days, and MDM were then lysed and luciferase assayed. Bars = mean inhibition of uptake or infection (%) + SD for triplicate.

As summarised in Figure 3.4a, I observed no significant inhibitory effect from bNAbs on the uptake of infected T cells by MDM, although some non-significant inhibitory trends were observed. This might represent non-specific inhibition of T cell uptake by the accumulation of IgG at the T cell-MDM interface that inhibits other ligand-receptor interactions. Interestingly 19b, a weakly-neutralising antibody binding to the gp120 V3 loop, was the only mAb to show a significant inhibitory effect. The reason for this is presently unclear, but a specific inhibitory effect would be inconsistent with the failure of other antibodies (PGT121 and PGT128), targeting a spatially related epitope cluster, to inhibit MDM capture of infected T cells.

Although my results, in agreement with Baxter et al [339], do not support a role for Env in infected T cell uptake by MDM, I did find that several bNAbs including PGT151 (anti-quaternary gp120-41 interface), PGT128 and PGT121 (anti-N332 supersite) significantly decreased subsequent infection of MDM caused

by the capture of infected T cells (Figure 3.4b). This is consistent with the idea that once the infected T cell has been captured by the MDM, virus is released by the T cell and fuses with an MDM membrane to initiate infection via canonical Env-receptor interactions. Therefore, any residual bNAb, present even at low concentration during the process of virus entry into the MDM, may prevent viral fusion.

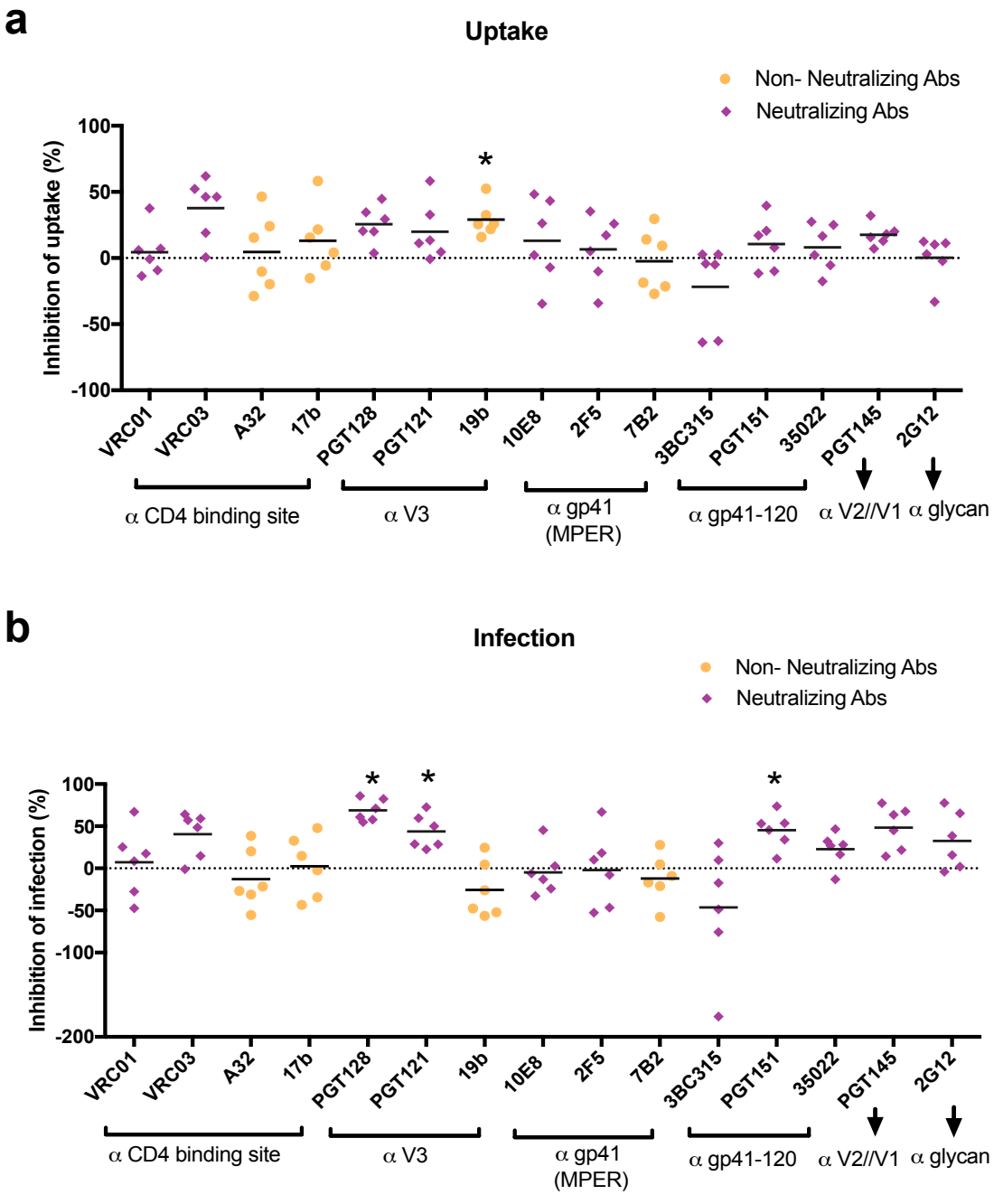


Figure 3.4. The effect of neutralising and non-neutralising antibodies on MDM uptake of HIV-1-infected T cells and subsequent MDM infection. HIV-1-infected CD4+ T cells were treated for 1 h with 50 µg/mL (a super-saturating dose based on previous experiments carried out in the laboratory) of bNAbs and non-neutralising Abs binding to the different epitopes of HIV-1 Env. Afterwards, infected T cells and MDM were co-cultured for 1 h, and infected T cells were then removed with vigorous washing. **a) Uptake:** after removing infected T cells, MDM were lysed, and luciferase assayed. **b) Infection:** after removing infected T cells, the plate was kept in culture for 7 days and MDM were lysed and luciferase assayed. Bars = mean inhibition of uptake or infection (%) + SD for six donors, each in triplicate. *p < 0.05, by one-sample t-test, comparing each condition to a hypothetical value of 0 with Sidak's multiple comparison post hoc test.

3.2.2. The role of ICAM-1 in HIV-1-infected CD4+ T cell engulfment by MDM

Intercellular cell adhesion molecule-1 (ICAM-1; CD54) is a member of the immunoglobulin superfamily with 5 extracellular domains (D1-5), a transmembrane region and a short intracellular domain (Figure 3.5a) [1]. As described above, our lab showed that unlike a conventional VS, the ICAM-1-LFA-1 interaction played no obvious role in MDM capture and engulfment of infected CD4+ T cells. However, during the course of these experiments, it became clear that ICAM-1 mAb directed specifically to the first domain (D1) significantly inhibited infected T cell capture when maintained in the co-culture. Therefore, I aimed to confirm or refute the role of ICAM-1 in MDM capture of HIV-1-infected T cells and to further probe this by attempting to define the function of ICAM-1 in this model. For this, I used primary MDM and HIV-$1_{Bal\text{-}Luc}$-infected primary autologous CD4+ T cells in the previously described luciferase uptake assay (Figure 3.1).

To probe which domain of ICAM-1 was functioning to modulate T cell uptake and on which cell type (T cell or MDM), I treated infected CD4+ T cells and/or MDM isolated from a human leukocyte cone with either D1 ICAM-1 mAb (HA58) or D2 ICAM-1 mAb (R6.5) for 1 h.

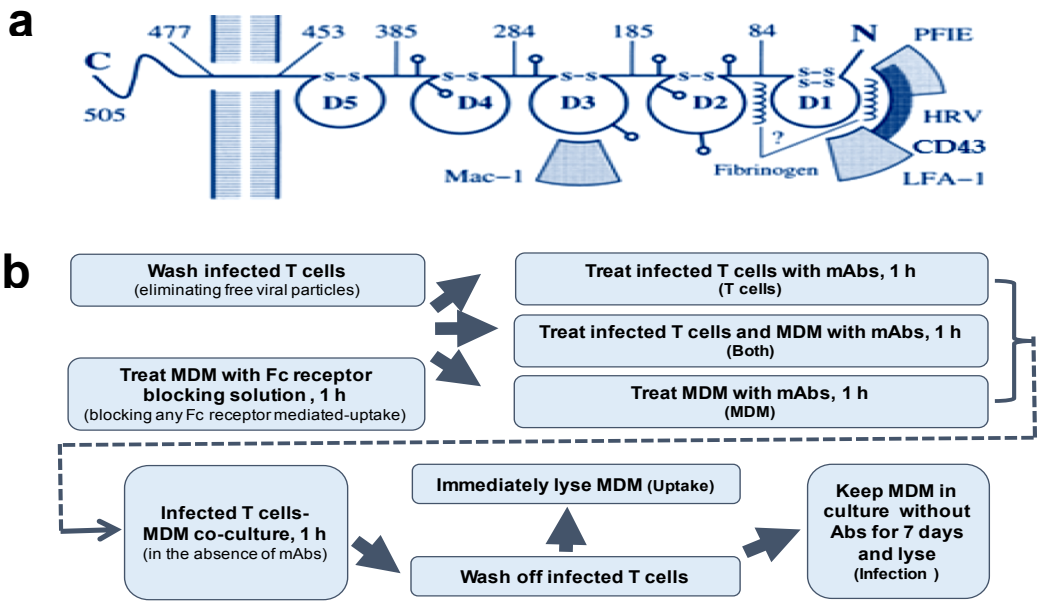


Figure 3.5. The role of ICAM-1 in the engulfment of HIV-1-infected T cells by MDM and their subsequent infection. a) The schematic structure of ICAM-1 (adapted from [1]). b) The schematic experimental strategy for the uptake of HIV-1-infected T cells treated with D1 and D2 ICAM-1 mAbs by MDM and their subsequent infection. CD4+ T cells and monocytes were isolated from a human leukocyte cone (Figure 3.1). HIV-1 infected T CD4+ T cells were washed thoroughly to remove cell free viral particles. Meanwhile, MDM were treated with 10μg/mL Fc receptor blocking solution for 1 h. Afterwards, infected T cells and/or MDM were treated with 10μg/mL of either H58 mAb or R6.5 mAb blocking ICAM-1 D1 and D2, respectively. Treated cells were then washed to remove the residual mAb. Subsequently, infected T cells were co-cultured with MDM for 1 h, and infected T cells were then removed with vigorous washing. **c) Uptake:** after removing infected T cells, MDM were lysed, and luciferase assayed. **d) Infection:** after removing infected T cells, the plate was kept in culture for 7 days and MDM were lysed and luciferase assayed. Bars = mean inhibition of uptake or infection (%) + SD for triplicate.

I then washed these cells to remove the residual mAb, and co-cultured them for 1 h. Subsequently, I vigorously washed off the non-captured T cells, lysed the MDM and assayed the luciferase activity representing the infected T cell capture by MDM (Figure 3.5b). As presented in Figure 3.5c, treatment of infected T cells and MDM with HA58 showed 65% and 51% inhibition of MDM capture of infected T cells and subsequent MDM infection, respectively. This is consistent with the result obtained when only MDM were treated with HA58; 67% inhibition of MDM capture of infected T cells and 65% reduction in MDM subsequent infection. However, T cell treatment with HA58, showed no inhibition but rather an increase in MDM capture of infected T cells and subsequent MDM infection. Thus HA58 appears to be acting by interfering with ICAM-1 function on MDM rather than T cells. By contrast, the treatment of MDM and/or infected T cells with D2 ICAM-1 mAb (R6.5) showed maximum ~20%

inhibitory effect on the MDM uptake of infected T cells when both infected T cells and MDM were treated. Individual treatment of MDM or T cells with R6.5 led to enhancement of T cell uptake. Moreover, the infection plate failed to show any inhibition of subsequent MDM infection by R6.5, rather ~60% enhancement of MDM infection. These preliminary data suggest that D1 ICAM-1 on MDM could play a role in the MDM capture of infected T cells and subsequent MDM infection, whereas a role for D2 ICAM-1 was less clear.

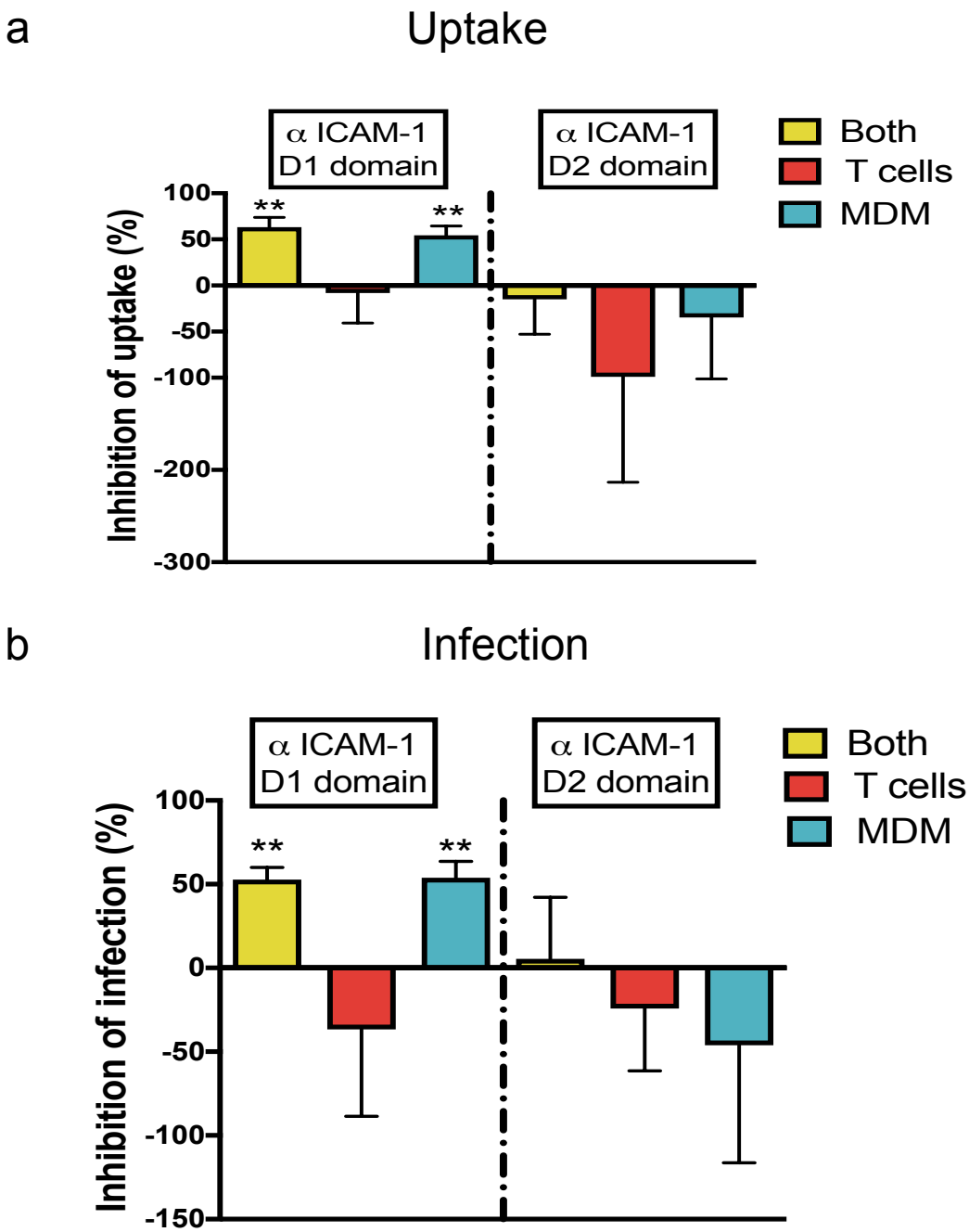


Figure 3.6. The role of ICAM-1 in the engulfment of HIV-1-infected T cells by MDM and their subsequent infection. HIV-1-infected CD4+ T cells and/or MDM were treated for 1 h with 10µg/mL of ICAM-1 mAb. Clone H58 and R6.5 block ICAM-1 D1 and D2, respectively. Subsequently, cells were washed 3 times to eliminate unbound mAb and co-cultured for 1 h. Afterwards, infected T cells were removed with vigorous washing (Figure 3.5b). **a) Uptake:** after washing away free infected T cells, MDM were lysed. **b) Infection:** after removing infected T cells, the plate was kept in culture for 7 days, and MDM were lysed. Bars = mean inhibition of uptake or infection (%) + SD for 6 donors for HA58 Ab and 4 donors for R6.5 Ab, each in tripµicate. **p < 0.01 by one-sample t-test, comparing each condition to a hypothetical value of 0 with Sidak's multiple comparison post hoc test.

Since these primary cell assays exhibit substantial inter-donor variation, I repeated this experiment using multiple donors to obtain a statistically robust outcome.

Therefore, I treated the infected CD4+ T cells and/or MDM isolated from 6 different donors with HA58 and from 4 different donors with R6.5 for 1 h. I then washed these cells to remove the residual mAb, and co-cultured them for 1 h. Subsequently, I vigorously washed off the non-captured T cells, lysed the MDM and assayed luciferase activity representing infected T cell capture by MDM (Figure 3.5b). As presented in Figure 3.6a, treatment of co-cultured infected T cells and MDM significantly inhibited ~40-60% MDM capture of infected T cells, consistent with the results previously seen in the lab, and the implication of D1 as a functional site on ICAM-1. Moreover, I confirmed that there is a significant inhibitory effect when pre-treating the MDM but not the T cells with HA58 prior to the co-culture (Figure 3.6a). Thus as I previously hypothesised, ICAM-1

appears to function on the MDM rather than on the T cell. Also according to Figure 3.6b, maintaining MDM in culture for 7 days after washing off unbound/unengulfed T cells to measure MDM infection showed that the D1 ICAM-1 mAb inhibited not only infected T cell capture, but also subsequent MDM infection. This was expected as infected T cells were less well taken up by the MDM.

3.2.3. The role of LFA-1 and Mac-1 as ligands of ICAM-1 in the engulfment of HIV-1-infected CD4+ T cells by MDM

In the literature, leukocyte-associated function antigen 1 (LFA-1; CD11a/CD18) and macrophage-1 antigen (Mac-1; CR3; CD11b/CD18) have been reported as ligands for ICAM-1 (Figure 3.5a) [365]. Both are heterodimeric transmembrane proteins termed integrins [365]. As mentioned earlier in this chapter, former lab members have shown that a blocking mAb to LFA-1, the ligand for ICAM-1 in the conventional VS, does not inhibit the capture of HIV-1-infected T cells by MDM – indeed capture was enhanced. Moreover, neither a blocking mAb to Mac-1, the other major ligand for ICAM-1, nor siRNA knockdown of Mac-1, showed any consistent inhibitory effect on the uptake of infected T cells by MDM. Thus we were left with the apparently paradoxical observation of ICAM-1 modulating infected T cell capture, but without implication of either of its conventional integrin ligands. Therefore, to confirm or refute the role of ICAM-1 conventional ligands on HIV-1-infected CD4+ T cells, I thoroughly tested blocking mAbs against the different conventional ICAM-1 ligands (LFA-1 and Mac-1) in the luciferase uptake assay using primary MDM and HIV-$1_{Bal\text{-}Luc}$-

infected primary autologous T cells. For this purpose, I treated infected CD4+ T cells and/or MDM isolated from 4 different donors with blocking mAbs specific for activated Mac-1 (CBRM1/5), or both active and inactive Mac-1 (ICRF44), or to LFA-1 (H1III). Infected T cells were subsequently washed to remove the residual mAb followed by their co-culture with MDM for 1 h. Afterwards, I vigorously washed off the non-captured T cells, lysed the MDM, and assayed luciferase activity representing the capture of infected T cells by MDM (Figure 3.5b). As previously observed, neither blocking LFA-1 nor Mac-1 has a significant inhibitory effect on HIV-1-infected T cell uptake by MDM (Figure 3.7a). Interestingly, the blocking mAb to LFA-1 tended to enhance infected T cell uptake, although this effect did not achieve significance. The reasons for this enhancement are currently unclear. Also as expected, based on Figure 3.7b, maintaining MDM in culture for 6 days after washing off unbound/unengulfed T cells as a measure of MDM infection showed no inhibitory effect on subsequent MDM infection. These results do not support a role for either LFA-1 or Mac-1 as an interaction partner of ICAM-1 in the capture of HIV-1-infected T cells by MDM.

Sialophorin (CD43) has been described as an unconventional ligand for ICAM-1 [366]. Therefore, I decided to investigate the role of CD43 in HIV-1-infected T cell capture by MDM.

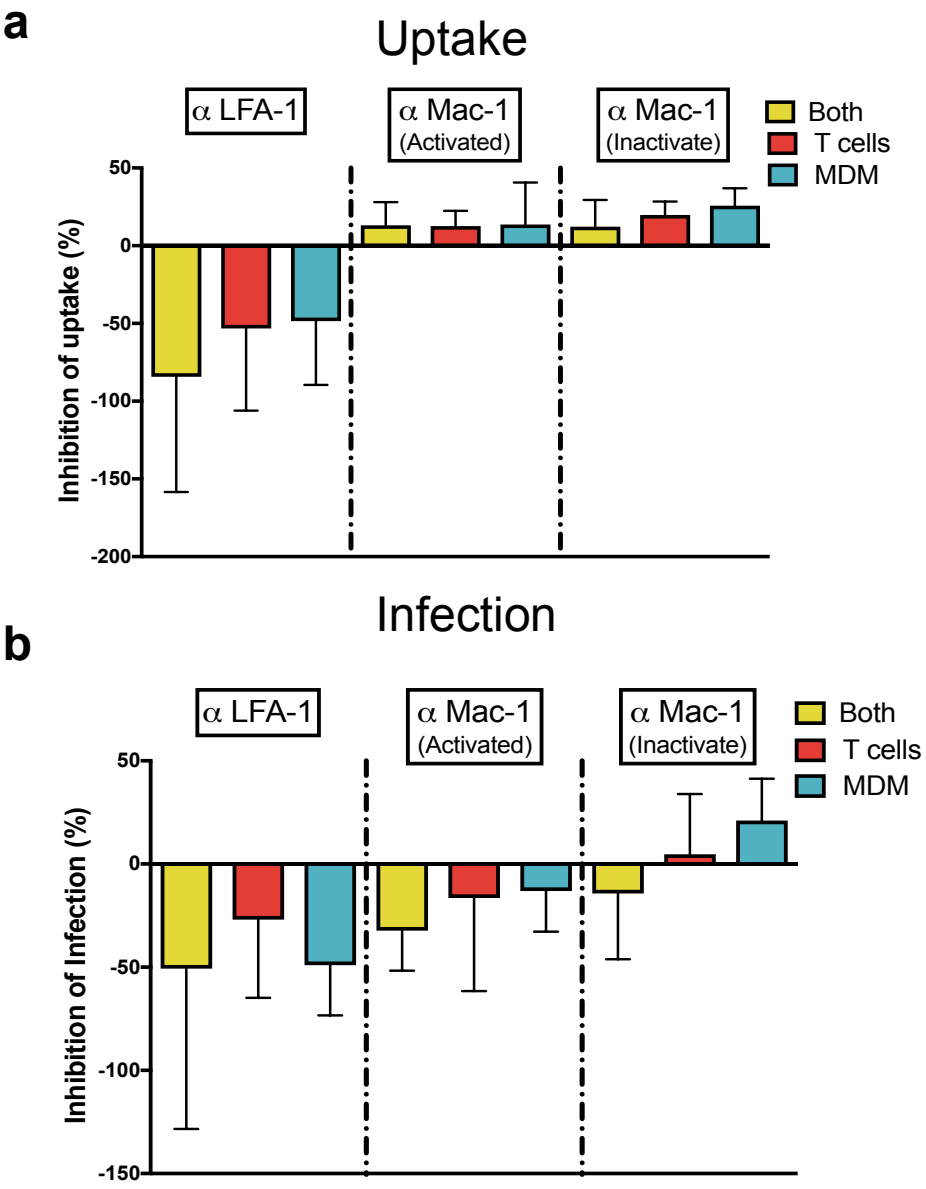


Figure 3-7. The inhibitory effect of blocking mAbs against ICAM-1 ligands (LFA-1 and Mac-1) on the uptake of CD4+ T cells by MDM and their subsequent infection. a) and b) HIV-1-infected CD4+ T cells and/or MDM were treated for 1 h with 10μg/mL of LFA-1, activated and inactivate Mac-1 mAb. Subsequently, cells were washed 3 times to eliminate unbound mAb and co-cultured for 1 h. Afterwards, infected T cells were removed with vigorous washing. Uptake: after washing away free infected T cells, MDM were lysed (Figure 3.5b). Infection**:** after removing infected T cells, the plate was kept in culture for 7 days, and MDM were lysed. Bars = mean inhibition of uptake or infection (%) + SD 4 donors, each in triplicate. Significance was investigated by one-sample t-test, comparing each condition to a hypothetical value of 0 with Sidak's multiple comparison post hoc test.

3.2.4. The role of CD43 as a ligand of ICAM-1 in MDM engulfment of HIV-1-infected CD4+ T cells

CD43 has been reported as a negative regulator of intercellular adhesion, and it has been shown that mAbs blocking CD43 function can overcome this regulation causing T cells to aggregate [367, 368]. As T cell aggregation in the presence of CD43 blocking mAbs might complicate interpretation of any data obtained for MDM engulfment, we instead obtained a CD43 knock-out (KO) CEM T cell line (from hereon termed CD43-KO). CD43-KO was generated from the WT CD4+ CEM T cell line (from hereon termed WT-CEM), giving us the advantage of a stable CD43-/- line for further studies [369]. To obtain this clone via homologous recombination, N. Manjunath et al. first generated a heterozygous clone by electroporating the WT-CEM T line with a plasmid containing the CD43 sequence interrupted at the coding region by a neomycin gene cassette. Afterwards, they screened for clones expressing 30-50% less CD43 on their cell surface. Subsequently, they generated CD43-/- (3-22 XX) by transfecting the CD43-/+ clone (3-22 X) with the same plasmid followed by CD43 negative selection using immunomagnetic beads. The 3-22 XX clone showed no expression or transcription of CD43 [369].

I infected CD43-KO and WT-CEM T lines with HIV-$1_{NL4.3\text{-}Luc}$ and also substituted them for primary T cells in the previousely described uptake assay (Figure 3.1). A time-course was conducted to optimise the infected T cell line-MDM uptake assay. As presented in Figure 3.8a, approximately 20% of CD43-KO CEM were infected after 1 day, and 2 days post-infection, 90% of the cells were infected. By 3 days post-infection the percentage of infected CD43-KO

CEM had dropped to 50% and by day 5 hardly any infected cells were detectable. By contrast, WT-CEM T cells showed the highest percentage of infected cells at day 3 post infection (68%) which was sustained for 24 h, then reduced to less than 1% by day 7. These data suggest that the absence of CD43 on the surface of the T cell makes it more susceptible to HIV-1 infection resulting in rapid cell death, as previously reported by Srinivas et al [370]. Moreover, CD43-KO and WT-CEM T cells showed the highest percentage of infected cells on day 2 (90%) and day 3 (68.5%), respectively (Figure 3.8b).

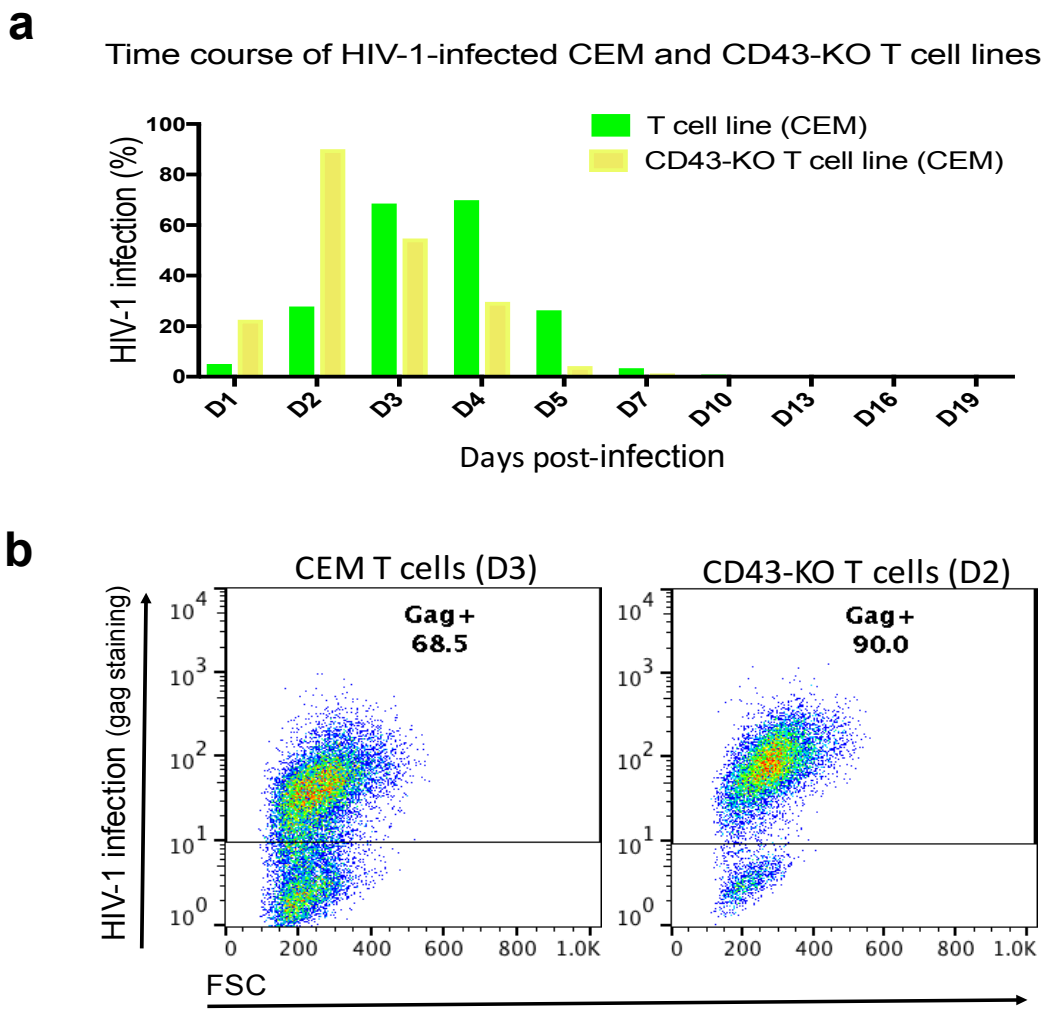


Figure 3.8. HIV-1 infection time-course of CD43-KO and WT-CEM. a) Percentage of HIV-1-infected cells at different post-infection days acquired using FACS staining and analysis. CD43-KO and WT-CEM T cells were infected with HIV-$1_{NL4.3\text{-}Luc}$ at MOI of 0.01. Fixed HIV-1-infected T cells were stained for the intracellular HIV-1 p24 indicating HIV-1 infection. **b) Intracellular HIV-1 P24 of HIV-1-infected CD43-KO and WT-CEM T cells co-cultured with MDM in the uptake assay (FACS).** CD43 KO and WT- CEM T cells were infected with HIV-$1_{NL4.3\text{-}Luc}$ 2 and 3 days' post-infection, respectively.

Therefore, CD43-KO and WT-CEM T cells were used at day 2 and day 3 respectively for co-culture with MDM. After 1 h co-culture, unbound/unengulfed T cells were removed with vigorous washing followed by MDM lysis and luciferase measurement. As CD43-KO and WT-CEM were not equally infected, the same number of infected T cells used in the co-culture was separately lysed, and luciferase assayed. This signal was used to normalise the fold difference obtained from the MDM uptake assay (Figure 3.9a). As presented in Figure 3.9b, approximately 2-fold more infected CD43 KO T cells were captured compared to the infected WT-CEM line when used in the MDM capture assay.

To investigate what role CD43 plays in relation to ICAM-1 in the uptake of infected T cells by MDM, infected CD43-KO and WT-CEM were co-cultured with MDM from 5 donors pre-treated with D1 ICAM-1 mAb (HA58) (Figure 3.10a).

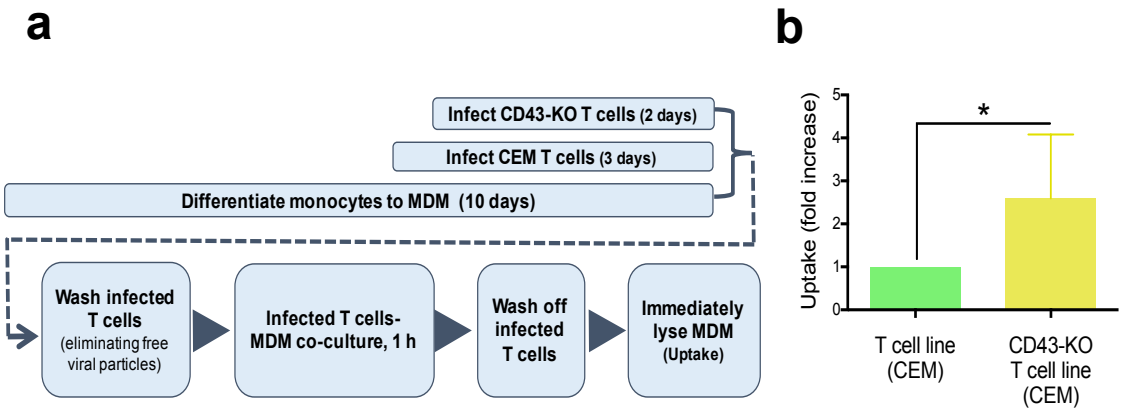


Figure 3.9. The role of CD43 as a ligand of ICAM-1 in the uptake of HIV-1-infected T cells by MDM. a) The schematic experimental strategy for the uptake of HIV-1-infected CD43-KO and WT-CEM T cells by MDM. Monocytes were differentiated in to MDM during 10 days and in the meantime CD43-KO and WT-CEM T cells were infected with HIV-$1_{NL4.3\text{-}Luc}$ at MOI of 0.01 for 2 and 3 days, respectively. On day 10, infected T cells were washed thoroughly to remove cell free viral particles. Subsequently, infected T cells were co-cultured with MDM for 1 h, and infected T cells were then removed with vigorous washing. **b) Uptake:** After removing infected T cells, MDM were lysed, and luciferase assayed. Luciferase signal representing the uptake of infected T cells by MDM. Bars = Mean luciferase signal of MDM co-cultured with infected T cells divided by the mean luciferase signal of infected T cells (%). SD for 7 donors, each in triplicate. *$p < 0.05$ by one-sample t-test, comparing infected CD43-KO T cells uptake to a hypothetical value of 1.

As presented in Figure 3.10b, the MDM capture of infected WT-CEM was approximately 50% inhibited, similar to that observed for infected primary CD4+ T cells (Figure 3.6a). Conversely, the inhibitory effect of ICAM-1 D1 was significantly reduced (to ~23%) when infected CD43-KO CEM were co-cultured with MDM in the uptake assay (Figure 3.10b), implying that the absence of CD43 on the surface of infected T cells reduces the inhibitory effect of D1 ICAM-1 blocking of MDM uptake of T cells. These data suggest that CD43 on the

surface of infected T cells does not interact with ICAM-1 on MDM, as if CD43 would be an ICAM-1 ligand in the MDM recognition and capture of infected T cells, blocking or absence of either side of this interaction should result in ~50% inhibition of uptake. However, it is difficult to fully define the interactions between ICAM-1 and CD43 as CD43-KO cells are stickier and form clumps which maybe overriding any effects that inhibiting D1 of ICAM-1 may be having.

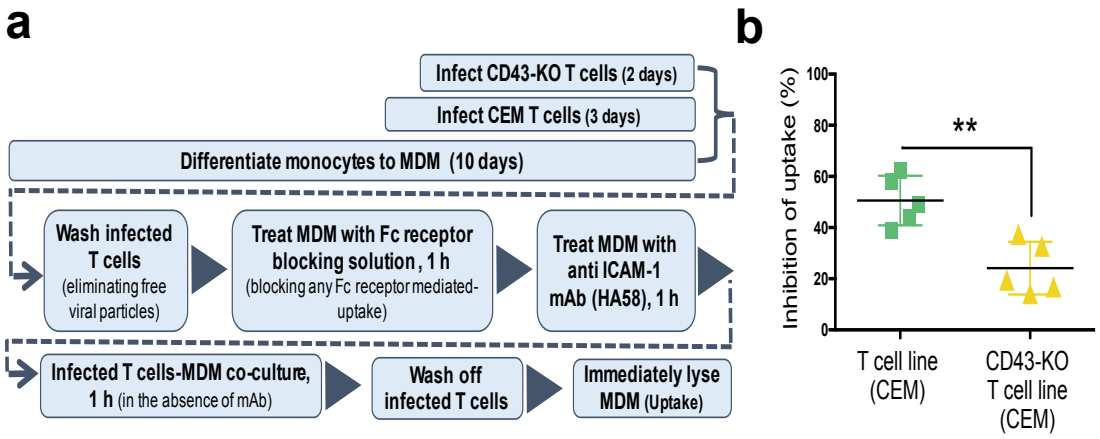


Figure 3.10. The role of CD43 as a ligand of ICAM-1 in the uptake of HIV-1-infected T cells by MDM. a) The schematic experimental strategy for the uptake of HIV-1-infected CD43-KO and WT-CEM T cells by MDM. Monocytes were differentiated in to MDM during 10 days and in the meantime CD43-KO and WT-CEM T cells were infected with HIV-$1_{NL4.3\text{-}Luc}$ at MOI of 0.01 for 2 and 3 days, respectively. On day 10, infected T cells were washed thoroughly to remove cell free viral particles. Meanwhile, MDM were treated with 10μg/mL Fc receptor blocking solution for 1 h. Afterwards, MDM were treated with 10μg/mL D1 ICAM-1 blocking mAb (HA58), and were then washed to remove the residual mAb. Subsequently, infected T cells were co-cultured with MDM for 1 h, and infected T cells were then removed with vigorous washing. **b) Uptake:** After removing infected T cells, MDM were lysed, and luciferase assayed. Luciferase signal representing the uptake of infected T cells by MDM. Bars = Mean luciferase signal of MDM co-cultured with infected T cells divided by the mean luciferase signal of infected T cells (%). SD for 7 donors, each in triplicate. **$p < 0.01$ by one-sample t-test, comparing each condition to a hypothetical value of 0 with Sidak's multiple comparison post hoc test.

3.3. Discussion

In this chapter, I investigated the role of HIV-1 Env and ICAM-1 and its proposed ligands (LFA-1, Mac-1 and CD43) in the recognition and engulfment of HIV-1-infected T cells by MDM.

3.3.1. The role of Env in infected T cell uptake and MDM infection

The results obtained from investigation of the effect of HIV-1 bNAbs and non-neutralising mAbs on the MDM uptake of HIV-1-infected T cells and subsequent MDM infection showed that with one exception, there was no significant inhibitory effect on the infected CD4+ T cell uptake by MDM with any of the mAbs used. The exception was V3 mAb 19b, which significantly inhibited the MDM uptake of infected CD4+ T cells. This mAb is non-neutralising for so-called difficult to neutralise 'Tier-2' viruses that represent the circulating pandemic, but neutralises neutralisation-sensitive Tier-1 viruses such as the BaL isolate Env used here [371]. The V3 loop forms a component of the epitope cluster known as the N332 supersite (Figure 3.2c), of which two other representative bNAbs used here are PGT121 and PGT128 [354, 372]. Interestingly these two bNAbs showed a trend towards inhibition (20-25%), suggesting that this region of Env may have some role in MDM recognition or uptake of infected T cells. However, at present I have no further insight into the mechanism of this effect, and if it is real. By contrast, several bNAbs did have a significant inhibitory effect on MDM infection after the extended culture. This might have occurred via two possible mechanisms. The bNAbs which inhibited to a significant degree (PGT128, PGT121 and PGT151) are very potent and

have the highest affinity of all bNAbs tested [373]. Therefore, even after several washes, a residual amount of these bNAbs in the culture might inhibit viral entry into the MDM. Alternatively or additionally, during MDM uptake of infected T cells, these bNAbs might be captured along with the infected T cell within the phagosome. Thus any virus particles released from the infected T cells would be neutralised prior to MDM infection. As presented in Figure 3.3c, These findings are consistent with the effect of bNAb-mediated inhibition of MDM infection by the capture of HIV-1-infected T cells when the bNAbs were left in the culture throughout the 7-day culture period [339].

3.3.2. The role of ICAM-1 and its ligands (LFA-1, Mac-1 and CD43) in infected T cell uptake and MDM infection

Investigation of the role of ICAM-1 using blocking mAbs showed that blocking D1 ICAM-1 on MDM led to approximately 40%-60% inhibition of MDM uptake of infected CD4+ T cells and subsequent MDM infection. This reveals that the D1 domain of ICAM-1 on MDM may be playing a role in the recognition of infected CD4+ T cells. However, inhibition of LFA-1 and Mac-1, ligands of ICAM-1, using blocking mAbs, did not result in significant inhibition of either infected CD4+ T cell uptake or subsequent MDM infection. Indeed mAbs to LFA-1 enhanced T cell uptake and MDM infection via as yet undefined mechanisms.

The investigation of the role of CD43 as a potential ligand of ICAM-1 using infected CD43-KO CEM T cells showed approximately 2-fold higher MDM uptake of infected CD43-KO CEM compared with the uptake of infected WT-CEM T cells. The higher uptake of CD43-KO CEM by MDM could be caused

by the non-specific adhesive nature of these cells; the loss of the heavily sialylated negatively charged CD43, which contributes a significant part of the leucocyte glycocalyx [374] and covers ~20% of the T cell area results in a less electrostatically repulsive phenotype [320, 369]. Moreover, probing the role of CD43 in relation to ICAM-1 using the uptake assay showed that blocking D1 of ICAM-1 on MDM significantly reduced the capture of infected WT-CEM T cells by approximately 50%, similar to that observed for infected primary CD4+ T cells. By contrast, the uptake of infected CD43-KO CEM T cells was not significantly inhibited (~25%) by blocking D1 of ICAM-1 on MDM (Figure 3.11). These data imply that CD43 on the surface of infected T cells does not interact with ICAM-1 on MDM, as if CD43 would be an ICAM-1 ligand in the MDM recognition and capture of infected T cells, blocking or absence of either side of this interaction should result in ~50% inhibition of uptake. However, it is difficult to fully define the interactions between ICAM-1 and CD43 due to the confounding 'stickyness' of the CD43 KO cells which maybe overriding any effects that inhibiting D1 of ICAM-1 may be having.

Moreover, these data suggest that CD43 may act as a don't eat-me signal on the surface of infected T cells, the absence of which may act as an "eat-me" signal, sufficient to partially bypass the inhibitory effect of D1 ICAM-1 blocking on MDM. Taken together, these data suggest that in the uptake and recognition of HIV-1-infected T cells by ICAM-1 on MDM, the ICAM-1 conventional ligands (LFA-1 and MAC-1) do not appear to act as the counterpart to ICAM-1 in this process. However, the role of CD43 in the recognition and uptake of infected T cells by MDM requires further study, which will be investigated and discussed in the following chapters.

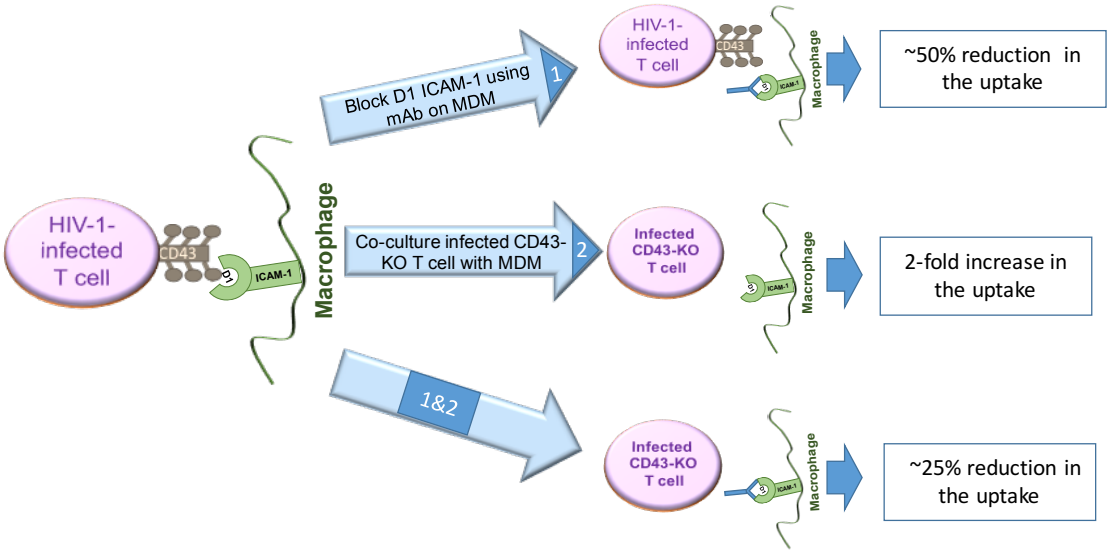


Figure 3.11. Schematic summary of CD43- ICAM-1 as the counterparts driving recognition and uptake of infected T cells by MDM. Blocking D1 domain of ICAM-1 on MDM using mAb (HA58) inhibited ~50% of the MDM uptake of infected WT-CEM T cells. Infected CD43-KO CEM were engulfed 2-fold more compared with WT-CEM T cells by MDM. Blocking D1 ICAM-1 on MDM did not significantly inhibit (~25%) the uptake of infected CD43-KO CEM T cells.

Chapter 4: CD43 modification in HIV-1 infection and cell death

4.1. Introduction

As described in Section 1.3, CD43 is a major transmembrane sialomucin on the surface of T cells, of which its extracellular domain forms ~20% of the entire T cell area [316, 320]. According to the literature, the CD43 extracellular domain can be modified either by proteolytic cleavage or enzymatic desialylation (loss of sialic acid).

Studies suggesting proteolytic cleavage of CD43 upon TNF-α and PMA activation were mainly carried out using neutrophils [375-378], such as the study conducted by Rieu et al. in which soluble CD43 was detected in the supernatant of PMA-activated neutrophils [379]. In another study (Bazil et al.) PMA activation and CD43 antibody crosslinking provoked CD43 shedding from the surface of granulocytes and lymphocytes, respectively [380].

CD43 hyposialylation has been reported in studies investigating T cell activation and HIV-1 infection [342, 381], and moreover, T cell apoptotic cell death results in general surface glycoprotein desialylation [309, 382]. Taken together, these studies suggest that CD43 on the surface of T cells may be desialylated during acute HIV-1 infection and apoptotic cell death, with the underlying mechanism being enzymatic removal of sialic acid and/or cleavage of CD43 from the cell surface.

CD45 (T200, LCA, PTPRC and Ly-5) is another major transmembrane glycoprotein, which expresses different isoforms on all nucleated hematopoietic cells. These isoforms are the result of alternative splicing of exon 4-6 at the N-

terminus of the CD45 extracellular domain and include CD45RA (exon 4 spliced out), CD45RB (exon 5 spliced out), CD45RC (exon 6 spliced out) and CD45RO (exons 4 to 6 spliced out) [383-385]. Depending on the isoform, the CD45 predicted MW is between ~123k-141kDa, whereas its observed MW is between ~180-230kDa suggesting that ~32-36% of CD45 mass is due to glycosylation. All the different isoforms of CD45 are decorated with 11 N-linked glycans. However, the CD45 extracellular domain is decorated with ~8-47 O-glycans depending on the isoforms [316]. This glycoprotein forms up to ~13% of the entire T cell area [320]. Analogous to CD43, it has been reported that sialylation of CD45 on the surface of latently HIV-1-infected CEM T cells is altered [386]. Therefore, to determine whether the desialylation was an event specific to CD43, or more generally applicable, I also studied whether CD45 is modified upon apoptosis and acute HIV-1 infection in a manner similar to CD43.

4.1.1. Hypothesis

Based on my findings described in the previous chapter and the literature outlined above, I hypothesised that HIV-1 infection and/or cell death can modify CD43 on T cells, the mechanism of which may help us understand the signals underlying MDM capture of HIV-1-infected T cells.

4.1.2. Specific aims

1. Investigation of whether HIV-1 infection and/or cell death (apoptosis/ pyroptosis) mediate CD43 modification.

2. Comparison of specificity of CD43 modification with another highly expressed leukocyte glycoprotein, CD45.

4.2. Results

4.2.1. CD43 modification upon HIV-1 infection

As shown and discussed in chapter 3, the absence of CD43 on the surface of HIV-1-infected CD43-KO CEM significantly increased their capture by MDM. Moreover, as discussed in the introduction, Lefebvre et al. previously reported that CD43 on the surface of latently infected CEM T cells was partially desialylated [342]. Therefore, I initially intended to investigate CD43 sialylation status upon acute HIV-1 infection. For this purpose, I looked through the literature to find antibodies allowing me to investigate the sialylation status of CD43. Based on the literature, I purchased the DFT-1 mAb and C-20 Ab to detect sialic acid-dependent (termed CD43-Sial) and -independent (termed CD43) epitopes, respectively on CD43 (Figure 4.2a) [342-344]. C20 recognises an epitope close to the membrane (Figure 4.2a), which from here on I call the membrane proximal domain (MPD).

To confirm that DFT-1 recognises a sialic acid-dependent epitope, I treated WT-CEMs with different concentrations of sialidase purified from either *Arthrobacter ureafaciens* (Arth) *or Vibrio cholera* (Vib) for 1 h at 37ºC. As presented in Figure 4.1, treatment of WT-CEMs with either Vib or Arth sialidase reduced DFT-1 labeling in a dose-dependent manner to background levels as

a function of geometric mean fluorescence (GMFI, Figure 4.1a) and to undetectable as a percentage of the total population (Figure 4.1b).

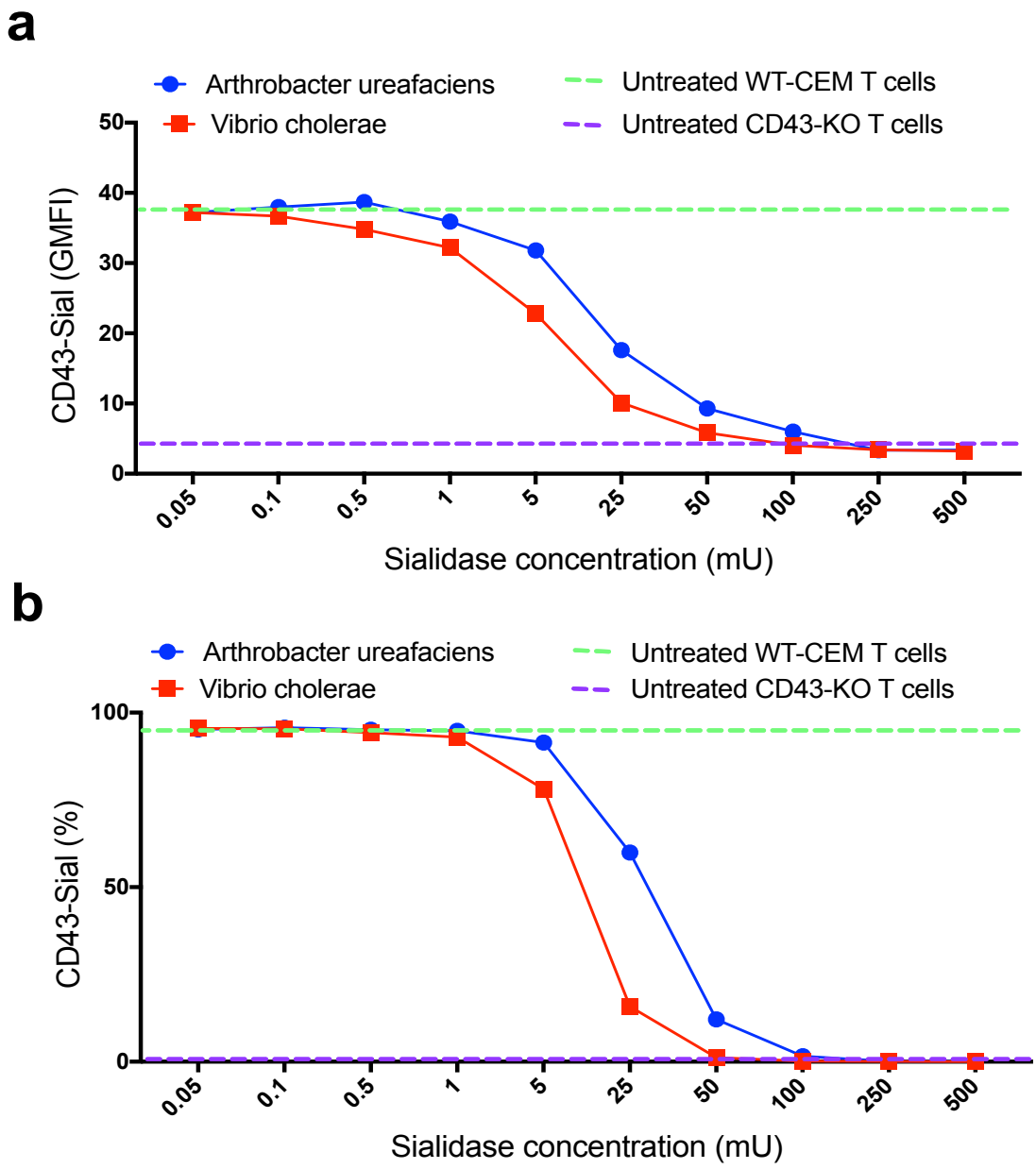


Figure 4.1. CD43-Sial mAb (DFT-1) recognises a sialic acid-dependent epitope on CD43. WT-CEMs were treated with different concentrations of two different sialidases purified from *Arthrobacter ureafaciens* and *Vibrio cholerae* for 1 h at 37ºC. Untreated CD43-KO and WT-CEM (presented as dotted lines), and treated WT-CEMs were fixed and stained with 2 µg/mL DFT-1. **a) Geometric mean of CD43-Sia acquired by FACS analysis. b) Percentage of T cells stained with DFT-1 mAb acquired by FACS analysisl.**

To confirm that C-20 Ab recognises a sialic acid-independent epitope on CD43, I treated WT-CEMs with 100 mU Vib sialidase for 1 h at 37ºC. As presented in Figure 4.2b and c, treating T cells with this concentration of Vib sialidase completely abolished CD43-Sial mAb binding but did not obviously alter C-20 Ab detection. Having established that DFT-1 and C-20 recognise CD43 sialic acid-dependent and -independent epitopes, respectively, I sought to investigate the sialylation and expression of CD43 on the surface of HIV-1-infected WT-CEMs. For this purpose, a time-course experiment was conducted. WT-CEMs were infected with HIV-$1_{NL4.3\text{-}Luc}$ followed by 4% FA fixation and staining for the intracellular Gag p24 and surface CD43 using DFT-1 mAb at 24 h intervals.

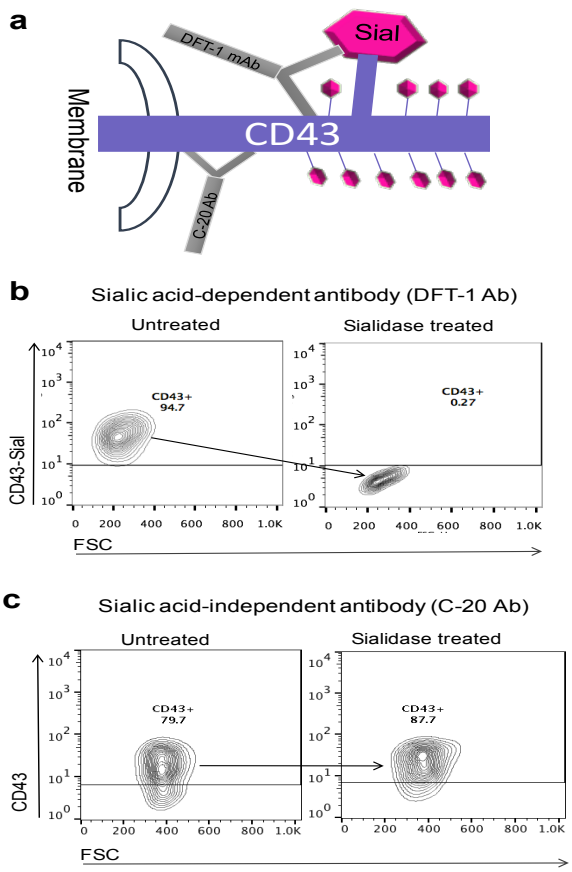


Figure 4.2. DFT-1 mAb (CD43-Sial) and C-20 Ab (CD43) recognise sialic acid-dependent and independent epitopes on CD43, respectively. WT-CEMs were treated with 100 mU of Vib sialidase for 1 h at 37ºC. **a) Schematic structure of DFT-1 mAb (CD43-Sial) and C-20 Ab (CD43 Ab) epitopes on CD43. b) CD43 sialic acid-dependent antibody (DFT-1):** Sialidase treated and untreated WT-CEMs were fixed and stained with DFT-1 (2 µg/mL). **c) CD43 sialic acid-independent antibody (C-20):** Sialidase treated and untreated WT-CEMs were fixed and stained with C-20 (4 µg/mL).

As presented in Figure 4.3, at day 2 and 3 approximately 80% of T cells were infected. Interestingly, approximately one-third of infected T cells did not stain with DFT-1 mAb (gated in red, from hereon termed CD43-Sial negative) at 3 days post-infection. By day 4, the population of infected cells was reduced to ~55% and the CD43-Sial negative population to ~13%, respectively. By 6 days post-infection few infected cells (~8%) were present, and the CD43-Sial negative population was reduced to ~2%. These preliminary data suggested that CD43 on a subpopulation of HIV-1-infected T cells (CD43-Sial negative) either had a modification of the sialylated DFT-1 epitope, or CD43 expression was in some way reduced.

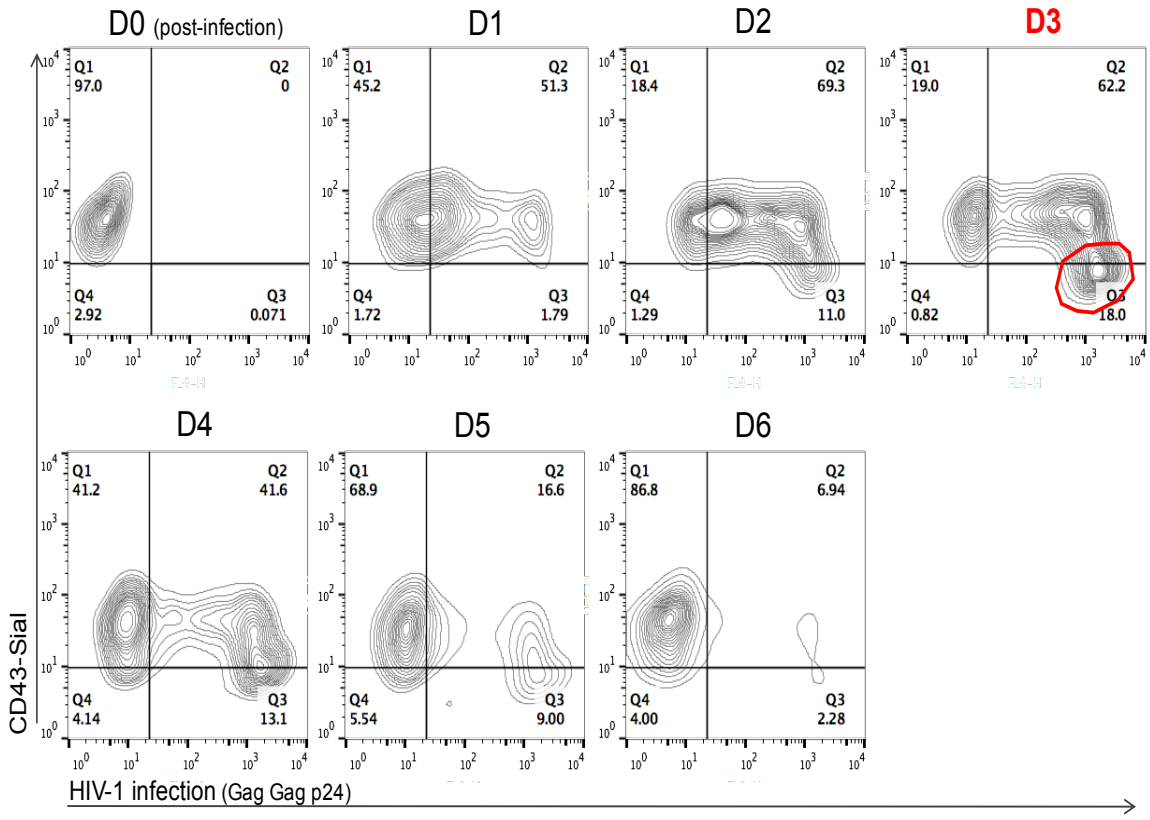


Figure 4.3. HIV-1 infection time-course of WT-CEMs. WT-CEMs were infected with HIV-$1_{NL4.3\text{-}Luc}$ at an MOI of 0.01. Fixed HIV-1-infected T cells were stained with DFT-1 mAb then permeabilised and stained for anti Gag p24 representing sialylation of surface CD43 and HIV-1 infection, respectively. The population in highlighted in red at D3 represents a sub-population of HIV-1-infected T cells which is DFT-1 negative.

To attempt to differentiate between local changes in CD43 that modify the DFT-1 epitope, or down-regulation or loss of CD43, I fixed WT-CEMs infected for 3 days and stained for surface CD43 with either DFT-1 mAb or C-20 Ab. In the same experiment I also treated half of the fixed cells with Vib sialidase to re-confirm that DFT-1 mAb recognises a sialic acid-dependent epitope on CD43. As presented in Figure 4.4a, population 1 (Pop 1) comprised uninfected T cells, and Pop 2 was a subpopulation of infected T cells, negative for DFT-1 mAb staining. The pooled data from four independent experiments showed that DFT-1 staining of Pop 2 was significantly reduced in comparison with Pop 1, and the CD43-Sial levels for Pop2 and CD43 are not significantly different (Figure 4.4b). By contrast, staining with C-20 Ab revealed no difference between the expression of CD43 on Pop 1 and 2 (Figure 4.4c, d). Based on the proposed membrane-proximal epitope of C-20 (Figure 4.2a) and the above data, we assumed that the CD43 membrane proximal domain (MPD) continued to be expressed on the surface of HIV-1-infected WT-CEMs. By contrast, the heavily sialylated membrane distal domain (MDD) of CD43 was clearly modified on HIV-1-infected WT-CEMs. These results could be due to the activity of either a sialidase leading to the desialylation of CD43 MDD, or a protease resulting in the cleavage of CD43 MDD but leaving the MPD intact.

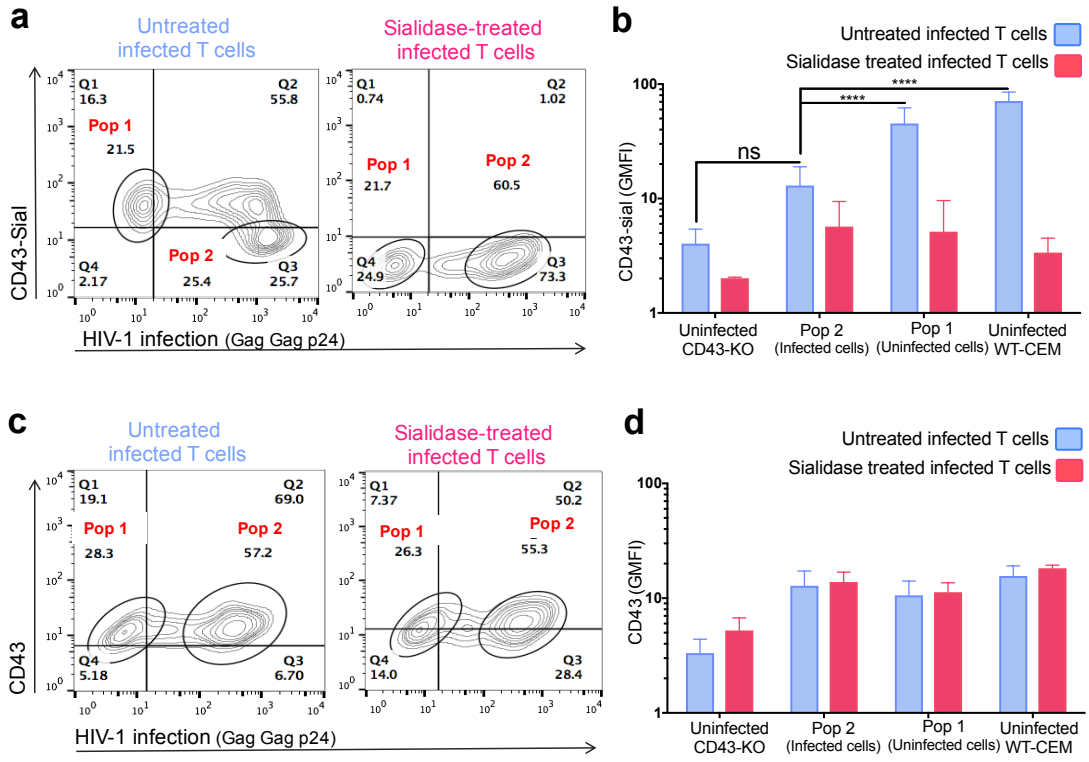


Figure 4.4. CD43 expression on the surface of HIV-1-infected WT-CEMs 3 days post-infection. WT-CEMs were infected with HIV-$1_{NL4.3\text{-}Luc}$ at an MOI of 0.01 for 3 days followed by 4% FA fixation. Afterwards half of the fixed cells were treated with 100mU Vib sialidase for 1 h. **a) and b) CD43-sial staining:** Fixed sialidase treated or untreated HIV-1-infected T cells were stained with DFT-1 mAb then permeabilised and stained with anti Gag p24. Two populations were defined by the gating strategy shown. Population 1 (Pop 1) represents uninfected T cells. population 2 (Pop 2) represents a subpopulation of infected T cells. **c) and d) CD43 staining:** As described in a, except CD43 was stained with C-20 Ab representing CD43 expression on the T cell surface. The graphs represent the data obtained from 4 independent experiments. ****P < 0.0001 tested using two-way ANOVA multiple comparisons with Sidak post-test correction.

HIV-1 infection of CD4+ T cells may modify cellular phenotype and function via the direct effects of virally-encoded proteins, or may do this indirectly by HIV-1-induced cell death. It has been reported that HIV-1 infection induces either pyroptotic or apoptotic cell death depending upon the activation state of the cell

[387, 388]. Productively infected activated T cells tend to die by apoptosis, whereas abortively infected resting T cells tend to die by pyroptotic cell death. Therefore, I sought to investigate whether CEM T cells undergo apoptotic cell death upon HIV-1 infection, and if so whether this could trigger CD43 modification. I infected WT-CEMs for 3 days with HIV-$1_{NL4.3\text{-}Luc}$ followed by 4% FA fixation. Subsequently, I investigated the relationship between HIV-1 infection, caspase 3 activation and CD43 modification. For this purpose, I measured the level of intracellular Gag p24 and cleaved caspase 3 by specific antibody staining, and CD43 modification by DFT-1 mAb staining. As presented in Figure 4.5a, I gated on 4 different populations (Pop 1-4), Pop 1-3 were gated based on their level of HIV-1 infection (intracellular Gag p24), and their staining with DFT-1 mAb was assessed within those gates. As shown in Figure 4.5b, DFT-1 labeling of Pop 4 was significantly modified in comparison with Pop 1-3 and uninfected WT-CEMs. The extent of this modification appeared slightly higher but was statistically indistinguishable from the absence of CD43 on CD43-KO CEM. Moreover, there was no significant difference between the level of intracellular Gag p24 and cleaved caspase 3 in Pop 3 and 4 (Figure 4.5c and d). However, the levels of intracellular Gag p24 and cleaved caspase 3 of Pop 3 were significantly higher than Pop 2. These data suggested that the modification of the DFT-1 epitope on the surface of Pop 4 was not directly linked to Gag p24 or cleaved caspase 3 levels in Pop 3 and 4. However, I hypothesised that if the activation of caspase 3 passed a certain threshold, this might be sufficient for activation of a pathway resulting in the modification of CD43. Therefore, I next sought to investigate CD43 modification on the surface of apoptotic T cells.

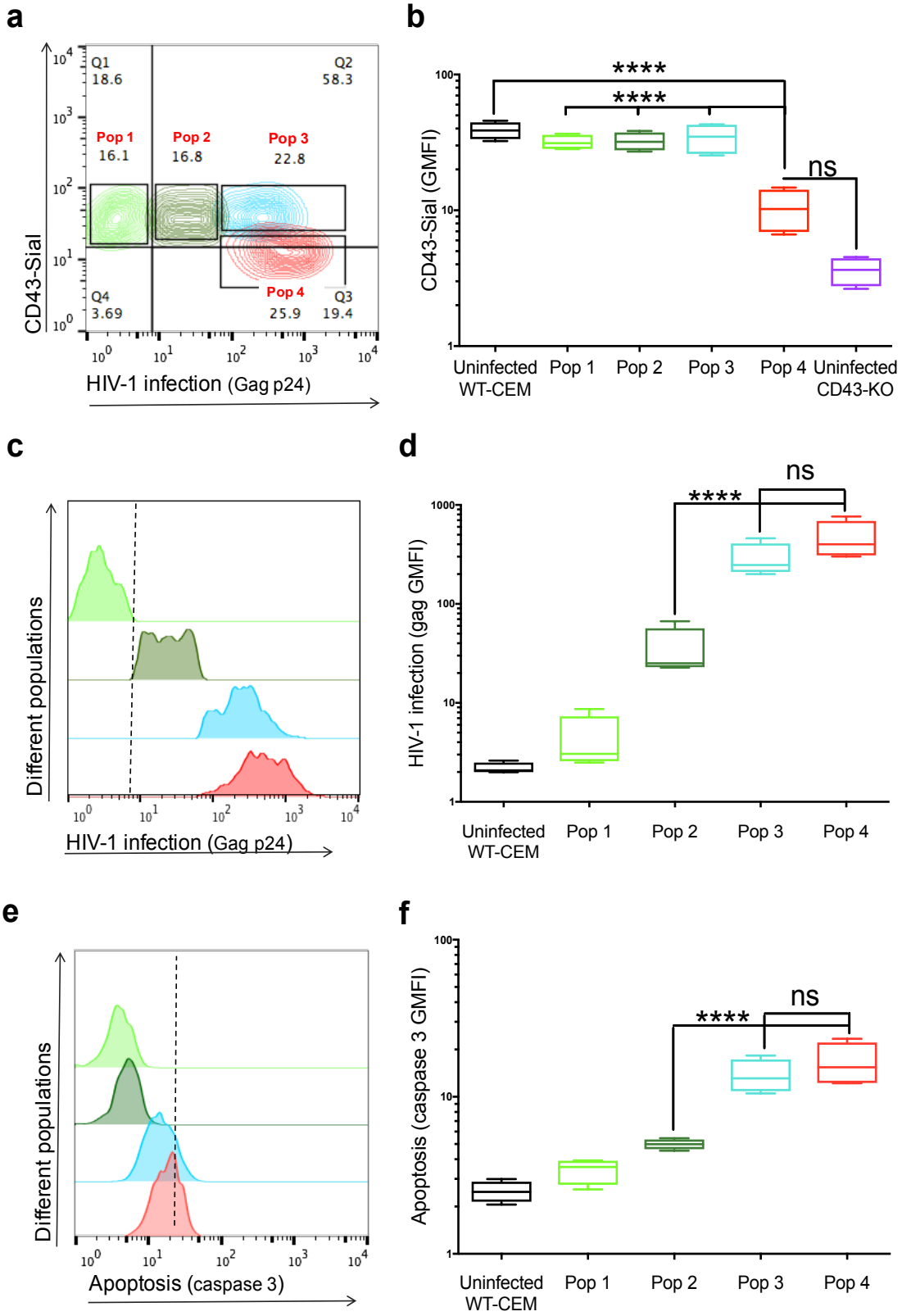

a
Q1
18.6
Q2
58.3
Pop 1
16.1
Pop 2
16.8
Pop 3
22.8
Pop 4
25.9
Q4
3.69
Q3
19.4
CD43-Sial
HIV-1 infection (Gag p24)
b
****
****
ns
CD43-Sial (GMFI)
Uninfected WT-CEM
Pop 1
Pop 2
Pop 3
Pop 4
Uninfected CD43-KO
c
Different populations
HIV-1 infection (Gag p24)
d
ns
****
HIV-1 infection (gag GMFI)
Uninfected WT-CEM
Pop 1
Pop 2
Pop 3
Pop 4
e
Different populations
Apoptosis (caspase 3)
f
ns
****
Apoptosis (caspase 3 GMFI)
Uninfected WT-CEM
Pop 1
Pop 2
Pop 3
Pop 4

Figure 4.5. CD43 sialylation and caspase 3 activation of HIV-1-infected WT-CEMs 3 days post-infection. WT-CEMs were infected with HIV-$1_{NL4.3\text{-}Luc}$ at an MOI of 0.01 for 3 days followed by 4% FA fixation. **a) CD43-sial and Gag p24 staining of infected T cells:** Fixed HIV-1-infected T cells were stained with DFT-1 mAb then permeabilised and stained for Gag p24. Four populations were defined by their level of intracellular Gag p24 and CD43-Sial staining. Population 1 (Pop 1) represents uninfected T cells. Populations 2,3 and 4 (Pop 2, 3 and 4), each represents a subpopulation of infected T cells. **b) CD43 sialylation of Pop 1-4. c) and d) HIV-1 infection of Pop 1-4.** Intracellular Gag p24 staining of Pop 1-4. Graphs were prepared as described in **a**. **e) and f) caspase 3 activation of Pop 1-4.** Cleaved caspase 3 staining of Pop 1-4. Graphs were prepared as described in **a**. The graphs represent the data obtained from 4 independent. ****P < 0.0001 tested using two-way ANOVA multiple comparisonswith Sidak post-test correction.

4.2.2. CD43 modification upon apoptotic cell death

To investigate whether CD43 on T cells is modified upon apoptosis induction, I initially tested staurosporine and etoposide, two chemical compounds reported in the literature as apoptosis inducers. It has been described in the literature, that 1 μM staurosporine and 100 μM etoposide treatment induce apoptosis in the Jurkat T cell line within 4 and 17 h, respectively [389, 390]. Therefore, to investigate the effect of these two compounds, I treated WT-CEMs with different concentrations of staurosporine and etoposide for 4 and 17 h, respectively. As presented in Figure 4.6a, etoposide treatment resulted in ~40% of the population separating into cells with a dying or dead phenotype. I decided to look at caspase 3 activation within the live cell population based on forward scatter (FSC) and side scatter (SSC), since dead cells may present complications with regard to interpretation of membrane labeling and autofluorescence. When treated with etoposide, ~36% of cells were gated as dead, and of the live cells only ~10% of WT-CEMs showed staining for cleaved

caspase 3 at 50μM (Figure 4.6a), and a similar result was obtained at 150 μM etoposide (Figure 4.6b).

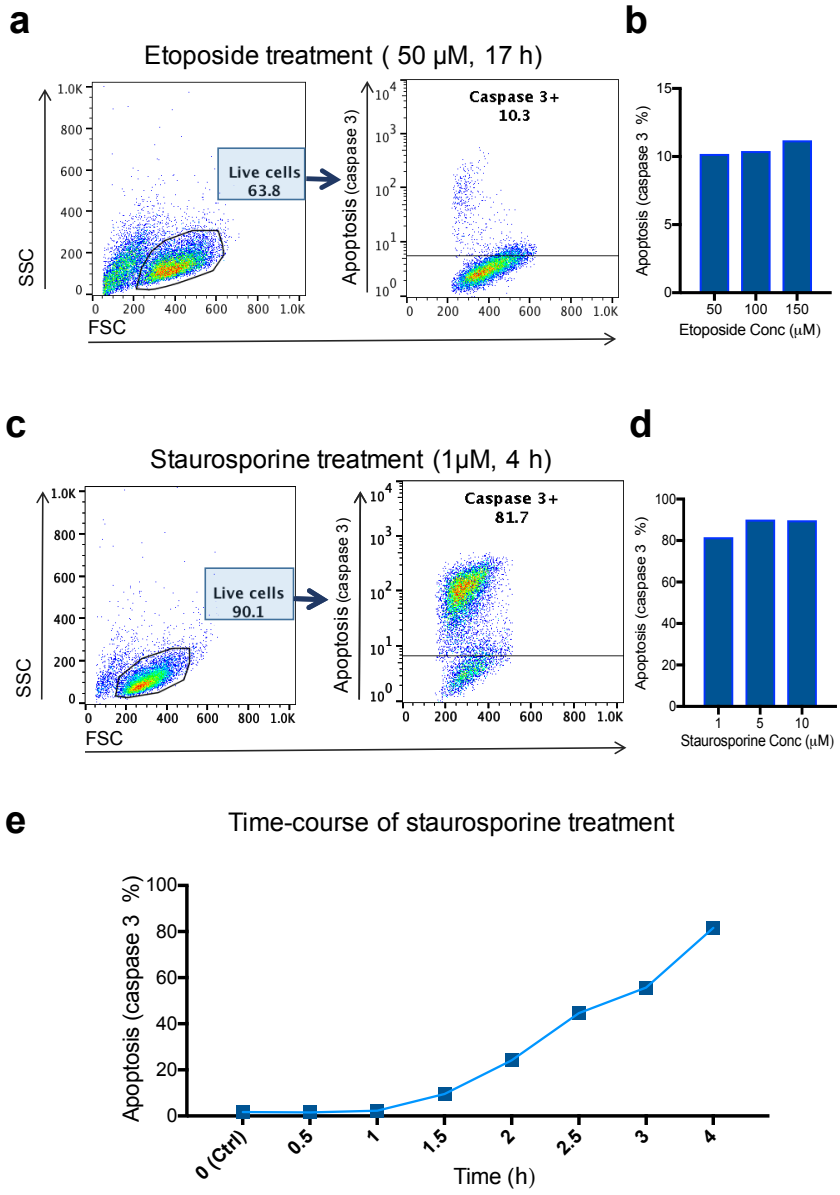


Figure 4.6. Apoptosis induction of WT-CEMs. a) and b) Etoposide treatment: Histograms in **a** represent WT-CEMs treated with 50 μM etoposide. Diagram in **b** represents WT-CEMs treatment with different concentrations of etoposide for 17 h. **c and d) Staurosporine treatment:** Histograms in **c)** represent WT-CEMs treated with 1 μM staurosporine. Diagram in **d)** represents WT-CEMs treatment with different concentrations of staurosporine for 4 h. **e) Staurosporine treatment time-course:** WT-CEMs were treated with 1 μM staurosporine and were fixed with 4% FA at different time-points followed by permeabilisation and cleaved caspase 3 staining.

By contrast to the etoposide treatment, treatment for 4 h with 1 μM staurosporine resulted in approximately 90% of T cells within the live gate (Figure 4.6c). Moreover, cleaved caspase 3 was detected in ~80% of live-gated WT-CEMs, which did not substantially change with increasing the staurosporine concentration to 10 μM (Figure 4.6d). Based on these preliminary data, I decided to treat WT-CEMs with 1 μM staurosporine for apoptosis induction. As the next step, I sought to find a time-point which activates caspase 3 in ~50% of WT-CEMs to study CD43 modification in caspase 3 negative and positive cells within the same sample. As shown in Figure 4.6e, caspase 3 was activated after 90 min in ~10% of staurosporine-treated WT-CEM, and increased over time to a maximum of ~80% at 4 h. For subsequent experiments I therefore chose to treat WT-CEMs with 1 μM staurosporine for 3 h as this gave ~50% caspase 3 +ve and –ve populations.

Using these conditions, I explored the relationship between caspase 3 activation and the modification of DFT1 binding over time. The data obtained from this experiment suggested a close correlation between activation of caspase 3 and reduction in DFT-1 mAb staining (Figure 4.7a). After 3 h of staurosporine treatment, approximately half the population did not stain with DFT-1 mAb and showed activated caspase 3. To investigate whether these two processes occur on the same population of cells, I treated WT-CEMs with 1 μM staurosporine for 3 h followed by 4% FA fixation and labeled for caspase 3 activation and with DFT-1. As shown in Figure 4.7.b, Pop 2 represents T cells with both activated caspase 3 and reduced staining of DFT-1 mAb. Moreover, the pooled data showed that the DFT-1 epitope on apoptotic T cells (Pop 2) was significantly modified by comparison with the non-apoptotic (Pop 1) and

untreated T cells (Figure 4.7.c). Also, the extent of this modification appeared slightly higher but was statistically indistinguishable from the absence of CD43 on the surface of CD43-KO CEM (Figure 4.7c).

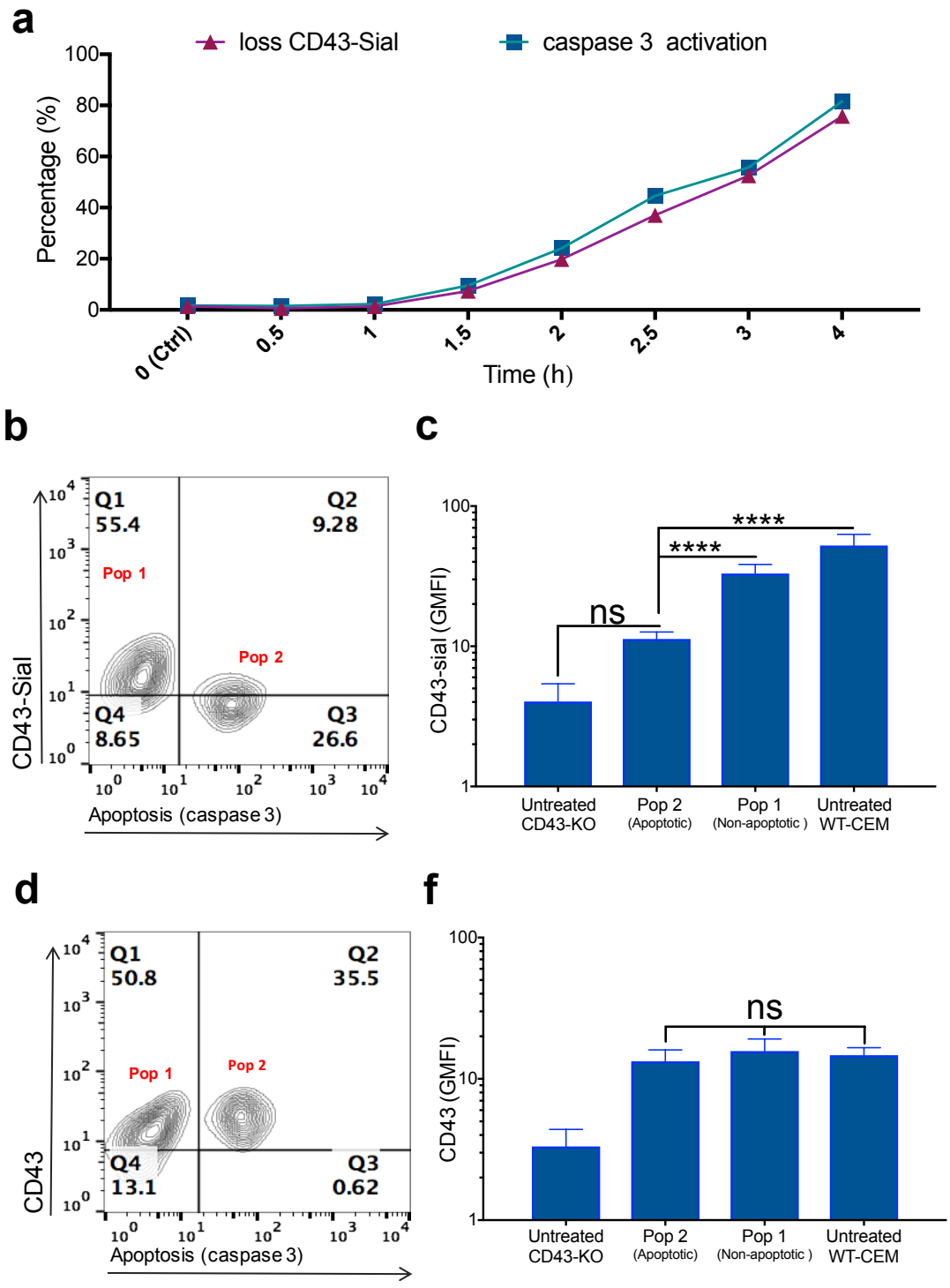


Figure 4.7. Staurosporine treatment of WT-CEM results in apoptosis induction and CD43 modification. a) Staurosporine treatment time-course: WT-CEMs were treated with 1 μM staurosporine and were fixed with 4% FA at different time-points. Afterwards, fixed T cells were stained with DFT-1 mAb representing CD43 sialylation status and for cleaved caspase 3 representing apoptosis. **b) and c) CD43-Sial staining:** WT-CEMs were treated with 1 μM staurosporine for 3 h, and then fixed wit 4% FA. CD43 on fixed T cells was stained with DFT-1 mAb followed by permeabilisation and cleaved caspase 3 staining. Two populations were defined by a gating strategy. Pop 1 and 2 represent non-apoptotic and apoptotic T cells, respectively. **d and f) CD43 staining:** As described in **b**, except CD43 being stained with C-20 Ab representing CD43 expression on the T cell surface. The graphs represent the data obtained from 4 independent experiments. ****P < 0.0001 tested using one-way ANOVA multiple comparisons with Sidak post-test correction.

To further investigate whether the loss of DFT-1 mAb staining was due to either the modification or down-regulation of CD43 upon apoptosis, I stained CD43 on the surface of staurosporine treated WT-CEMs with C-20. As presented in Figure 4.7d and f, C-20 staining revealed no difference between CD43 expression on Pop 1 and 2. These data imply that the CD43 MDD on WT-CEMs was modified upon apoptotic cell death induced by staurosporine treatment.

I next wished to extend my observations of CD43 modification on the surface of WT-CEMs to primary CD4+ T cells. Firstly, I treated primary CD4+ T cells with different concentrations of staurosporine to find the optimal concentration for apoptosis induction. Primary CD4+ T cell treatment with 1 μM staurosporine resulted in caspase 3 activation in ~10% of the population, whereas 10 μM staurosporine resulted in ~50% caspase 3 activation after 3 h of treatment (Figure 4.8a and b). In subsequent experiments, I treated primary CD4+ T cells with 10 μM staurosporine for 4 h followed by 4% FA fixation and labeling with

DFT-1 and for cleaved caspase 3. As shown in Figure 4.8c, Pop 2 represents primary CD4+ T cells with activated caspase 3 and reduced staining of DFT-1. Data pooled from 5 independent donors showed that the DFT1 epitope on the apoptotic primary CD4+ T cells (Pop 2) was significantly modified compared with the non-apoptotic (Pop 1) and untreated primary CD4+ T cells (Figure 4.8d).

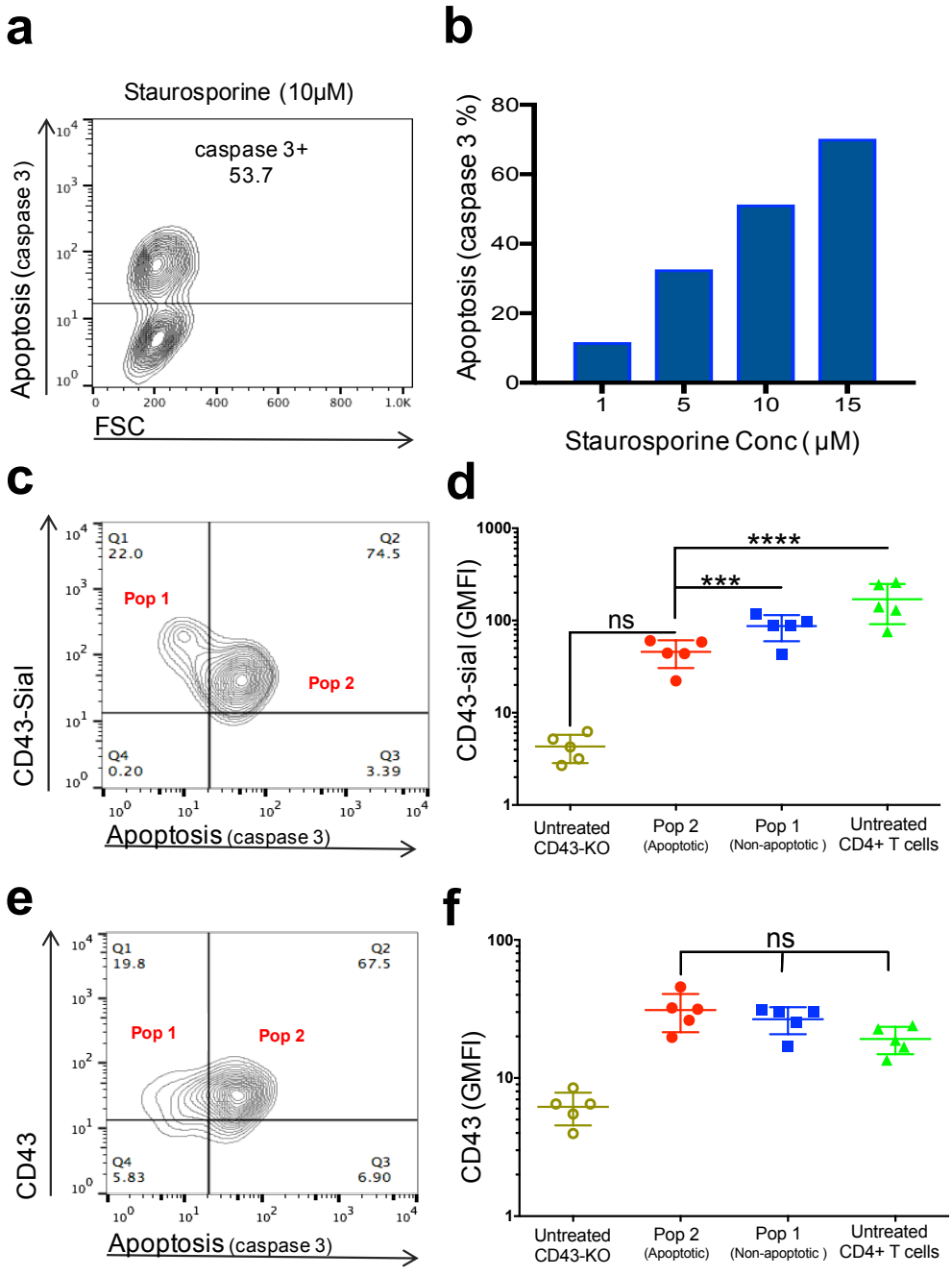


Figure 4.8. Staurosporine treatment of primary CD4+ T cells results in apoptosis induction and CD43 modification. a) and b) Staurosporine treatment: Primary CD4+ T cells were treated with different concentrations of staurosporine for 3 h followed by 4% FA fixation. Fixed T cells were permeabilised and stained for cleaved caspase 3 representing apoptosis. **a)** represents the gating strategy for diagram **b). c) and d) CD43-Sial staining:** primary CD4+ T cells were treated with 10 μM staurosporine for 4 h, and then fixed with 4% FA. CD43 on fixed cells was stained with DFT-1 mAb followed by permeabilisation and cleaved caspase 3 staining. Two populations were defined by the gating strategy shown in **c)**. Pop 1 and 2 represent non-apoptotic and apoptotic T cells, respectively. **e) and f) CD43 staining:** As described in **c**, except CD43 which was stained with C-20 Ab representing CD43 expression on the T cell surface. The graphs represent the data obtained from 5 donors. **P < 0.01 and ***P < 0.001 tested using one-way ANOVA multiple comparisons with Sidak post-test correction.

Similar to apoptotic WT-CEMs, the extent of this modification was statistically indistinguishable from the absence of CD43 on the surface of CD43-KO CEM. To further investigate whether the reduction in DFT-1 staining was due to either the modification or down-regulation of CD43 upon apoptosis, I stained CD43 on the surface of staurosporine treated CD4+ T cells with C-20. As presented in Figure 4.8e and f, C-20 staining revealed no significant difference between the expression of CD43 on Pop 1 and 2. These data show that the CD43 MDD on primary CD4+ T cells was modified upon apoptotic cell death induced by staurosporine treatment, similar to apoptotic WT-CEMs.

During my DPhil studies, I supervised an Oxford final undergraduate year medical student (Rachael Harrison) for her FHS project in which she optimised the induction of apoptotic cell death in WT-CEM and Jurkat T cell lines using etoposide. She successfully demonstrated the modification of the DFT1 epitope

on etoposide treated WT-CEM and Jurkat T cells (data not shown), confirming and extending my results to another T cell line and an alternative inducer of apoptosis. Taken together, these data indicate that apoptotic cell death results in the modification of the CD43 MDD on the surface of apoptotic T cells, and that this modification is generalisable to both compounds used for apoptosis induction and immortalised and primary and CD4+ T cells.

4.2.3. CD43 modification upon pyroptotic cell death

As discussed in detail in Section 1.1.6.2 and mentioned above, the Greene laboratory showed that most CD4+ T cells isolated from tonsil and HIV-1-infected in vitro were depleted as a result of pyroptotic cell death [387]. Therefore, I sought to investigate whether the DFT-1 epitope of CD43 is modified upon pyroptotic cell death. According to the literature, nigericin activates the inflammasome and caspase 1 resulting in pyroptotic cell death [387, 391]. To establish this system, I treated WT-CEMs with different concentrations of nigericin. As presented in Figure 4.9a, treatment with 75 μM nigericin activated caspase 1 in ~50% of the population, and this could be detected in all cells at 100 μM. Moreover, activation was largely specific for caspase 1 as nigericin treatment at 75 μM only resulted in ~10% of the population being caspase 3 positive (Figure 4.9b). I next explored whether there is a temporal relationship between caspase 1 activation and the modification of the DFT1 epitope on CD43 by conducting a time-course experiment. For this purpose, I treated WT-CEMs with 75 μM nigericin for up to 5 h. As presented in Figure 4.9c, ~45% of the T cells were DFT-1 negative after 2 h of pyroptosis induction, whereas only ~15% were caspase 1 positive. Even after 5 h, 20% of the T cells which were DFT1 negative remained caspase 1

negative (Figure 4.9c). These preliminary data suggested that modification of the DFT1 epitope during pyroptotic cell death may occur more rapidly than, or partially independently of, caspase 1 activation. However, all the pyroptotic T cells with activated caspase 1 showed loss of DFT1 binding (Figure 4.9d).

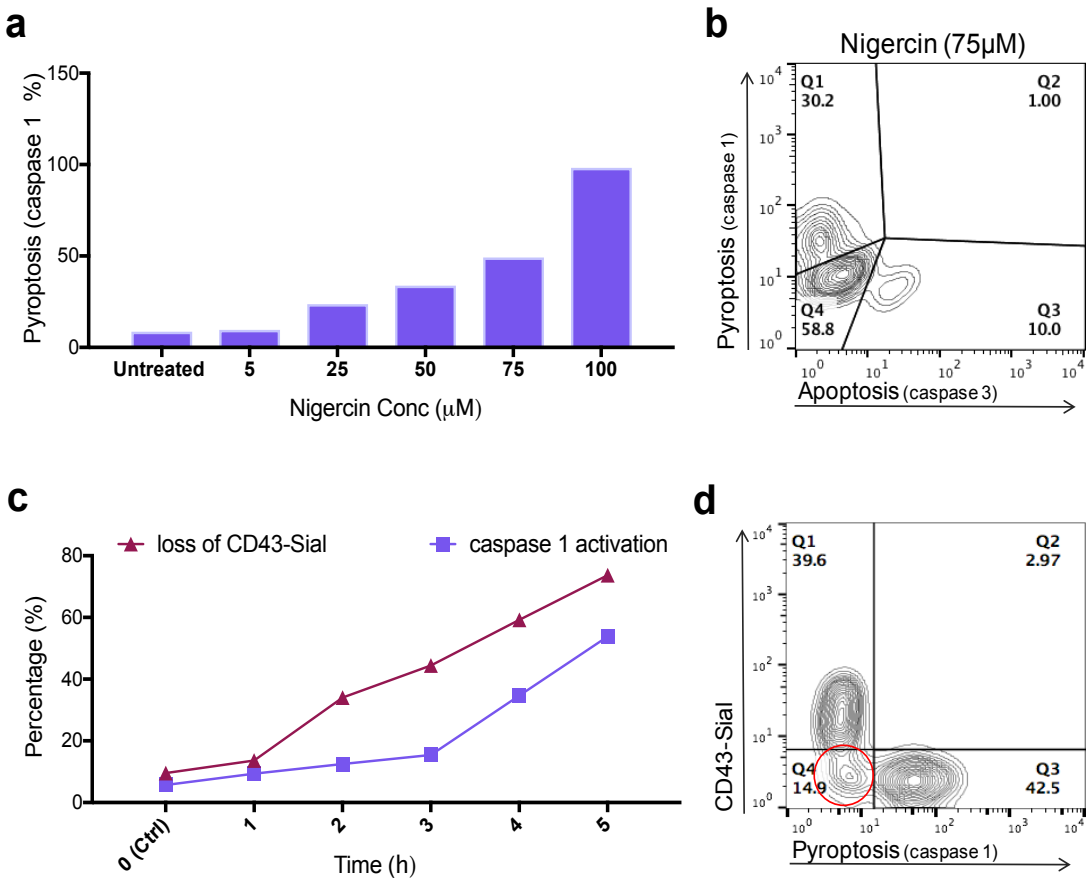


Figure 4.9. Pyroptosis induction of WT-CEMs. a) Nigericin treatment: WT-CEMs were treated with different concentrations of nigericin for 4 h followed by cleaved caspase 1 staining representing pyroptosis. **b) caspase activation of nigericin treated T cells:** WT-CEMs were treated with 75 μM nigericin for 4 h followed by caspase 1 and 3 co-staining. **c) Nigericin treatment time-course:** WT-CEMs were treated with 75 μM nigercin and stained for cleaved caspase 1 followed by CD43 staining using DFT-1 mAb. **d) Caspase 1 activation and CD43-Sial staining of nigercin treated cells:** WT-CEMs were incubated with 75μM nigercin for 4 h and stained as described in **c**.

To further investigate CD43 modification during pyroptosis, WT-CEMs were treated with 75 µM nigericin for 4 h followed by caspase 1 staining. Subsequently, T cells were fixed and stained with DFT-1 (Figure 4.10a and b). As I observed in the time-course experiment, data pooled from 4 independent experiments showed that caspase 1 positive WT-CEMs were DFT-1 negative suggesting modification of the CD43 sialylated epitope during pyroptotic cell death. As with apoptotic cells, staining with C-20 revealed no significant difference between CD43 MPD expression on the surface of pyroptotic and non-pyroptotic WT-CEMs (Figure 4.10c and d). These data imply that the CD43 MDD on WT-CEMs was modified upon pyroptotic cell death induced by nigercin treatment without complete loss of membrane CD43.

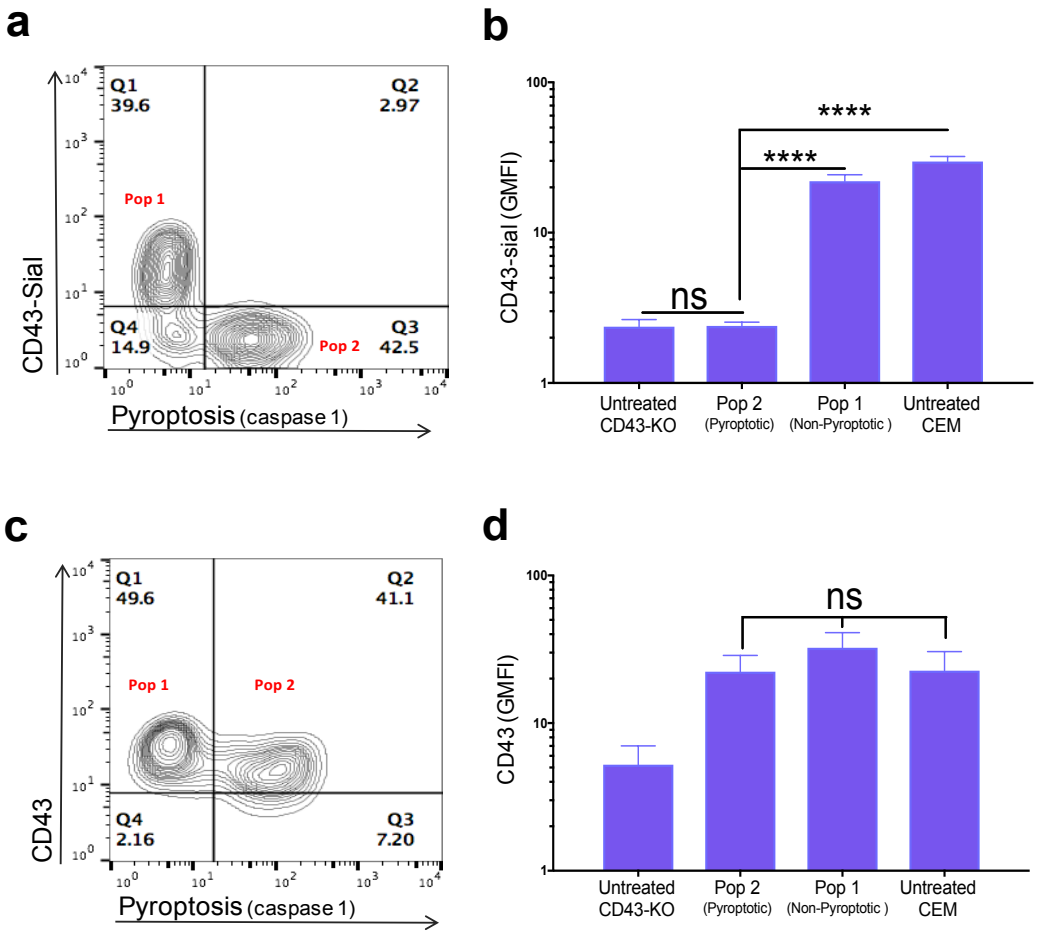


Figure 4.10. Nigerlcin treatment of WT-CEM results in pyroptosis induction and CD43 modification. a) and b) CD43-Sial staining: WT-CEMs were treated with 75 μM nigercin for 4 h followed by activated caspase 1 staining. Afterwards, T cells were fixed and stained for CD43 with DFT-1 mAb. Two populations were defined by the gating strategy shown in **a**. Pop 1 and 2 represent non-pyroptotic and pyroptotic T cells, respectively. **c) and d) CD43 staining:** As described in **a**, except CD43 being stained with C-20 Ab representing CD43 expression on the T cell surface. The graphs represent the data obtained from 4 independent experiments. ****P < 0.0001 tested using one-way ANOVA multiple comparisonswith Sidak post-test correction.

I next sought to investigate modification of the DFT1 epitope on the surface of primary CD4+ T cells during pyroptotic cell death. After testing different concentrations of nigericin, I treated primary CD4+ T cells with 75 μM nigericin for 4 h followed by caspase 1 staining (Figure 4.11). As shown in Figure 4.11a, Pop 2 represents T cells with activated caspase 1, which were DFT-1 negative. Based on the pooled data from 3 donors, DFT1 labeling on pyroptotic T cells (Pop 2) was significantly reduced compared to the non-pyroptotic (Pop 1) and untreated primary CD4+ T cells (Figure 4.11b). Moreover, like pyroptotic WT-CEMs (Figure 4.10), the extent of this modification was statistically indistinguishable from the absence of CD43 on the surface of CD43-KO CEM. To investigate as before whether the reduction in DFT-1 mAb staining was due to the specific modification or down-modulation of CD43 upon pyroptosis, I stained CD43 on the surface of nigericin treated primary CD4+ T cells with C-20. As presented in Figure 4.11c and d, C-20 staining revealed no significant difference between the expression of CD43 on Pop 1 and 2. These data confirmed my observations made using CEM, that the DFT-1 epitope is lost on

primary CD4+ T cells upon pyroptotic cell death, but CD43 is not completely removed from the cell membrane.

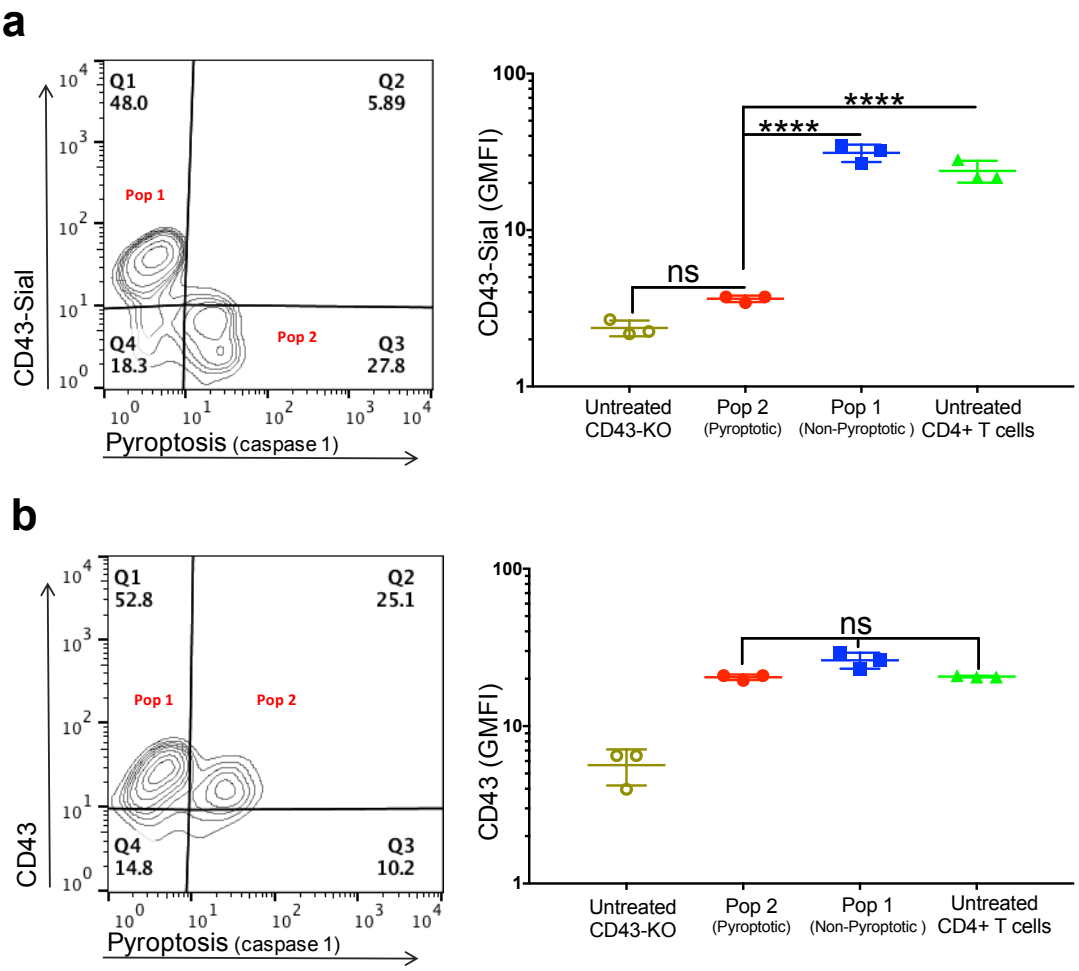
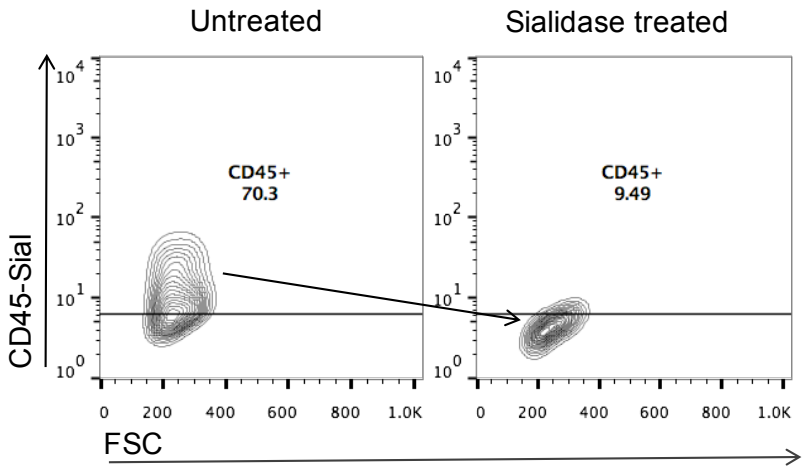


Figure 4.11. Nigericin treatment of primary CD4+ T cell results in pyroptosis induction and CD43 modification. a) and b) CD43-Sial staining: Primary CD4+ T cells were treated with 50 μM nigercin for 4 h followed by activated caspase 1 staining. Afterwards T cells were fixed and stained for CD43 with DFT-1 mAb. Two populations were defined by the gating strategy shown in **a**. Pop 1 and 2 represent non-pyroptotic and pyroptotic T cells, respectively. **c) CD43 staining:** As described in **b**, except CD43 was stained with C-20 Ab representing CD43 expression on the T cell surface. The graphs represent the data obtained from 3 donors. ****P < 0.0001 tested using one-way ANOVA multiple comparisonswith Sidak post-test correction.

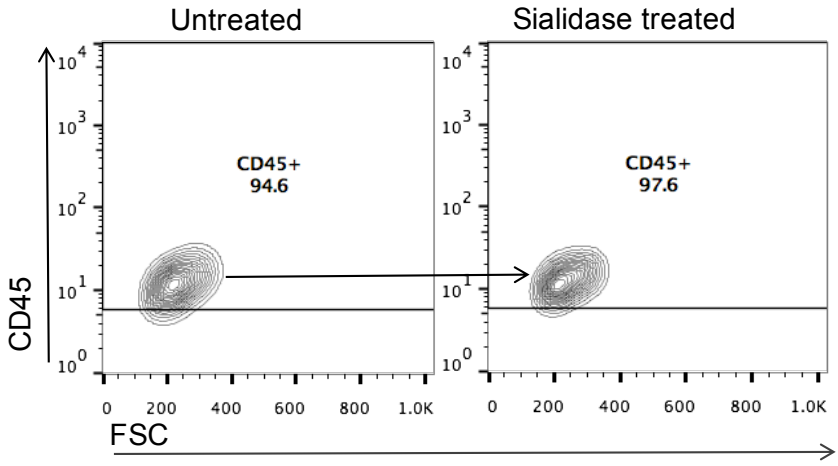
4.2.4. CD45 modification upon HIV-1 infection and apoptotic cell death

Since CD45 is a glycoprotein with an extended form present on leukocytes, that has been reported to have altered sialylation on latently HIV-1-infected CEM T cells [386], I sought to study whether, like CD43, CD45 is modified upon apoptosis and acute HIV-1 infection. This was to establish whether glycoprotein modification is specific to CD43 or is a more generalisable phenomenon. For probes, I found the mAbs 136-4B5 and MEM-28 that recognise sialic acid-dependent and -independent epitopes on CD45, respectively [345]. I treated WT-CEMs with 100 mU Vib sialidase and stained treated and untreated T cells with MEM-28 or 136-4B5 mAb. As presented in Figure 4.12a and b, MEM-28 mAb staining did not alter with sialidase treatment, whereas 136-4B5 mAb staining was abolished. These data confirmed that 136-4B5 (CD45-Sial) and MEM-28 (CD45) mAbs recognise CD45 sialic acid-dependent and -independent epitopes, respectively. Moreover, as DFT-1 and 136-4B5 isotypes are both mouse IgG1, in order to investigate the CD45 sialylation on the subpopulation of HIV-1-infected T cells having modified CD43 (Figure 4.4), I found an alternative (Alt) mAb for the detection of a sialic acid-dependent epitope on CD43 called 1D4, that is of the IgG2a isotype [343] (Figure 4.12c).

a Sialic acid-dependent antibody (CD45-Sial Ab)



b Sialic acid-independent antibody (CD45 Ab)



c Sialic acid-dependent antibody (CD43-Sial Ab)

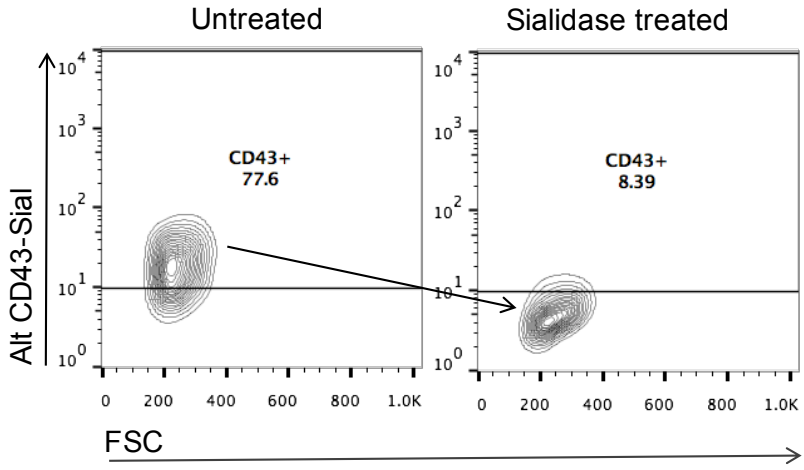


Figure 4.12. The antibody panel recognising sialic acid-dependent and independent epitopes on CD45 and CD43. WT-CEMs were treated with 100 mU of Vib sialidase for 1 h at 37ºC. **a) CD45 sialic acid-dependent antibody (136-4B5):** live sialidase treated and untreated WT-CEMs were stained with 136-4B5 mAb. Contour plots showing detection of CD45-Sial with (right) and without (left) sialidase treatment. **b) CD45 sialic acid-independent antibody (MEM-28):** live sialidase treated and untreated WT-CEMs were stained with MEM-28 mAb. Contour plots showing detection of CD45 with (right) and without (left) sialidase treatment. **c) Alternative CD43 sialic acid-dependent antibody (1D4):** live sialidase treated and untreated WT-CEMs were stained with 1D4 mAb. Contour plots showing detection of CD43-Sial with (right) and without (left) sialidase treatment.

To investigate whether CD45 is modified upon apoptotic cell death, I treated WT-CEMs with 1 μM staurosporine for 3 h followed by 100 mU Vib sialidase treatment on half the population for 1 h at 37ºC. Subsequently, the sialidase-treated and -untreated T cells were stained for either CD45 or CD43 followed by 4% FA fixation. The fixed T cells were then stained for intracellular cleaved caspase 3 representing apoptosis. As presented in Figure 4.13a and b, there is no significant difference between either CD45-Sial or CD45 on non-apoptotic (Pop 1) and apoptotic (Pop 2) T cells. However, the sialidase treatment significantly reduced 136-4B5 mAb staining, whereas MEM-28 mAb staining did not alter. These data show that the sialic acid-dependent epitope of 136-4B5 mAb (CD45-Sial) on CD45 is not modified upon apoptotic cell death, whereas Alt CD43-Sial labeling was significantly reduced on apoptotic T cells in comparison with non-apoptotic T cells (Figure 4.13c). These data suggest that unlike for CD43, cell death does not induce modification of a sialic acid-dependent mAb on CD45.

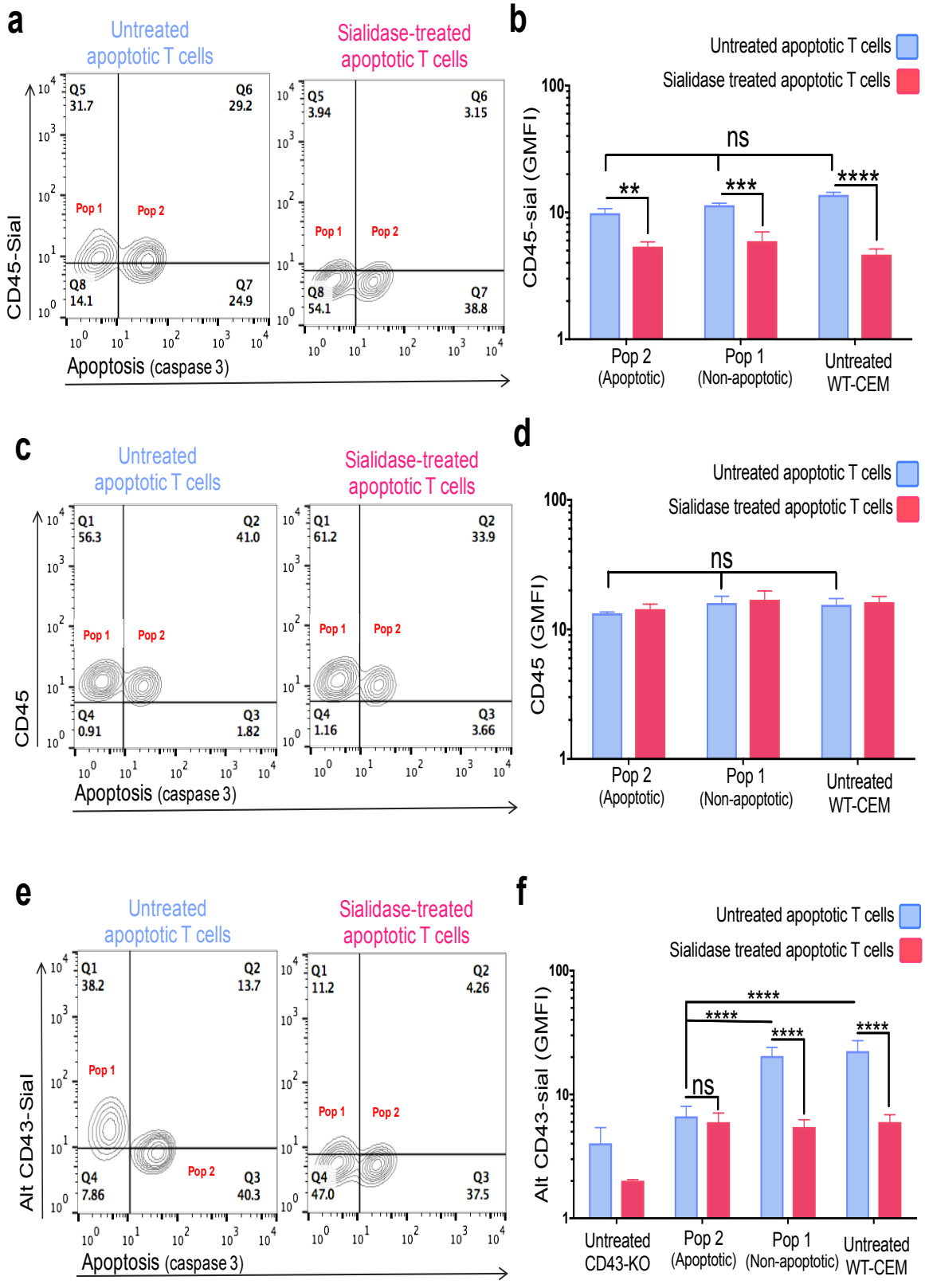

a
Untreated apoptotic T cells
Sialidase-treated apoptotic T cells
CD45-Sial
Apoptosis (caspase 3)
Q5 31.7
Q6 29.2
Q8 14.1
Q7 24.9
Pop 1
Pop 2
Q5 3.94
Q6 3.15
Q8 54.1
Q7 38.8
b
Untreated apoptotic T cells
Sialidase treated apoptotic T cells
CD45-sial (GMFI)
ns
**
***
****
Pop 2 (Apoptotic)
Pop 1 (Non-apoptotic)
Untreated WT-CEM
c
Untreated apoptotic T cells
Sialidase-treated apoptotic T cells
CD45
Apoptosis (caspase 3)
Q1 56.3
Q2 41.0
Q4 0.91
Q3 1.82
Q1 61.2
Q2 33.9
Q4 1.16
Q3 3.66
d
Untreated apoptotic T cells
Sialidase treated apoptotic T cells
CD45 (GMFI)
ns
Pop 2 (Apoptotic)
Pop 1 (Non-apoptotic)
Untreated WT-CEM
e
Untreated apoptotic T cells
Sialidase-treated apoptotic T cells
Alt CD43-Sial
Apoptosis (caspase 3)
Q1 38.2
Q2 13.7
Q4 7.86
Q3 40.3
Q1 11.2
Q2 4.26
Q4 47.0
Q3 37.5
f
Untreated apoptotic T cells
Sialidase treated apoptotic T cells
Alt CD43-sial (GMFI)
ns
****
Untreated CD43-KO
Pop 2 (Apoptotic)
Pop 1 (Non-apoptotic)
Untreated WT-CEM

Figure 4.13. CD45 and CD43 expression on the apoptotic WT-CEM. WT-CEMs were treated with 1 μM staurosporine followed by 100 mU Vib sialidase treatment on half of the population for 1 h at 37ºC. **a) and b) CD45-sial staining:** live untreated or sialidase treated apoptotic T cells were stained with 136-4B5 mAb representing CD45R sialylation followed by 4% FA fixation. Fixed T cells were permeabilised and stained with anti cleaved caspase 3 Ab representing apoptosis induction. Two populations were defined by the gating strategy shown in a. Pop 1 and 2 represent non-apoptotic and apoptotic T cells, respectively. **c) and d) CD45 staining:** as described in **a**, except CD45 being stained with MEM-28 mAb representing expression of CD45R on the cell surface. **e) and f) Alt CD43-Sial staining:** As described in **a**, except CD43 was stained with 1D4 mAb representing the sialylation status of CD43. The graphs represent the data obtained from 3 independent experiments. **P < 0.01, ***P < 0.001 and ****P < 0.0001 tested using two-way ANOVA multiple comparisons with Sidak post-test correction.

To investigate whether CD45 is modified upon HIV-1 infection of CD4+ T cells, I infected WT-CEMs with HIV-$1_{NL4.3\text{-}Luc}$ for 3 days followed by CD45 and CD43 staining. Live infected T cells were co-stained for either Alt CD43-Sial and CD45-Sial or Alt CD43-Sial and CD45. Subsequently, T cells were fixed with 4%FA, and then stained for intracellular Gag p24. As presented in Figure 4.14a, Pop 1 and 2 were defined based on the intracellular Gag p24 expression and modification of CD43 sialylation. Pop 2 represents a subpopulation of infected T cells that showed significant modification of the sialylated epitope of CD43 in comparison with Pop 1 representing uninfected T cells. However, probing CD45 with the sialic acid-dependent mAb showed no significant difference between Pop 1 and 2 (Figure 4.14b). These data show that the epitope of 136-4B5 mAb (CD45-Sial) on CD45 is modified neither upon apoptosis nor acute HIV-1 infection.

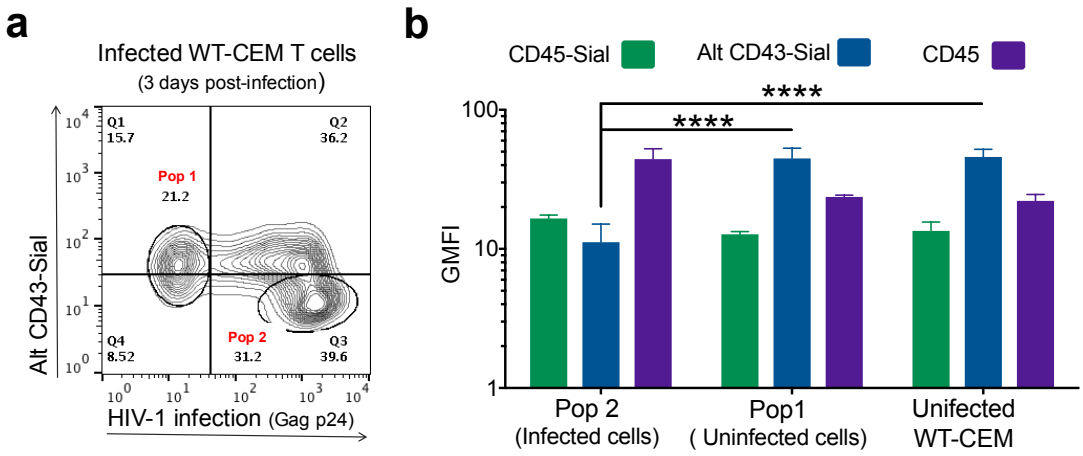


Figure 4.14. CD45 and CD43 expression on HIV-1-infected WT-CEM. WT-CEMs were infected with HIV-$1_{NL4.3\text{-}Luc}$ at MOI of 0.01 for 3 days followed by CD45 and CD43 staining. Live T cells were co-stained with either 1D4 and 136-4B5 mAbs or 1D4 and MEM-28 mAbs. T cells were then fixed with **4%** FA followed by permeabilisation and Gag p24 staining. Two populations were defined by the gating strategy shown in **a**. Pop 1 and 2 represent uninfected and a subpopulation of infected T cells, respectively. The graphs represent the data obtained from 3 independent experiments. ****P < 0.0001 tested using two-way ANOVA multiple comparisons with Sidak post-test correction.

4.3. Discussion

In this chapter, I investigated the status of sialic acid-dependent mAb epitopes of the glycoproteins CD43 and CD45 on the surface of CD4+ T cells either HIV-1-infected and/or dying by apoptosis and pyroptosis. My results are consistent with the model shown in Figure 4.15 that HIV-1 infection and cell death promote modification of sialic acid-dependent epitopes of two mAbs (DFT-1 and 1D4) on CD43 without completely removing CD43 from the cell surface, whereas the epitope of a sialic acid-dependent mAb (136-4B5) to CD45 remains unmodified.

Since CD43 is the dominant glycoprotein on the leukocyte surface with a strong influence on cell-cell interactions, the modification of sialic acid content on this molecule may have important implications in a number of immunological processes including T cell activation and migration (discussed in Section 1.3.2)

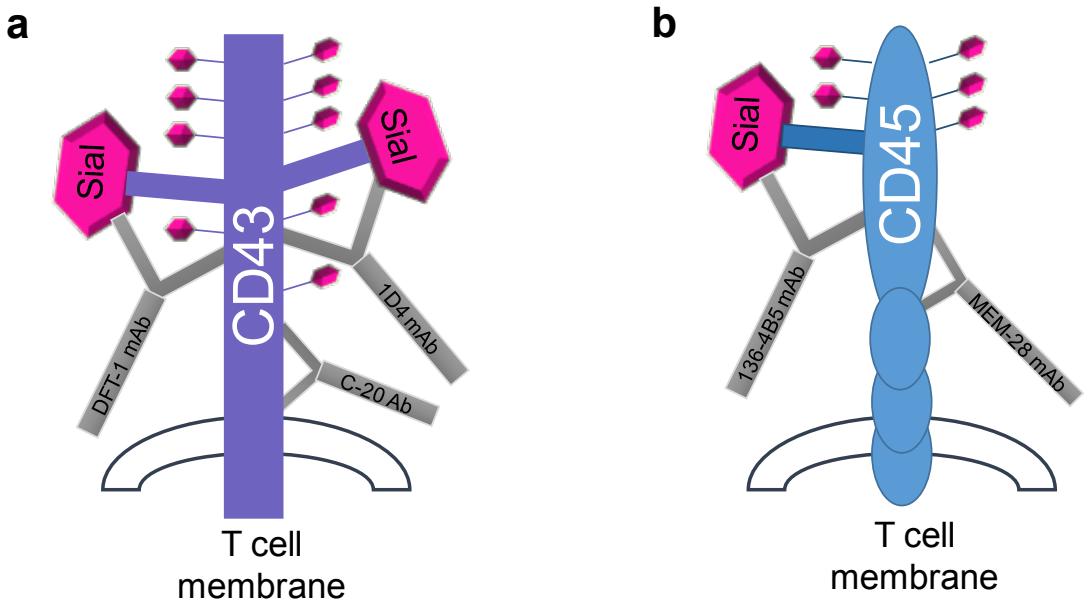


Figure 4.15. Schematic summary showing recognition of sialic acid-dependent and –independent epitopes of CD43 and CD45 on HIV-1-infected and dying (apoptotic and pyroptotic) T cells by antibodies. a) CD43: DFT-1 and 1D4 mAbs recognising sialic acid-dependent epitopes on CD43 is modified during HIV-1 infection, apoptotic and pyroptotic cell death, whereas C-20 epitope (siaic acid-independent) remains unmodified. **b) CD45:** Staining of 136-4B5 and MEM-28 mAbs recognising sialic acid-dependent and –independent epitopes on CD45, respectively, do not alter during neither HIV-1 infection nor apoptotic cell death.

The finding that CD43 sialylation status was modified upon HIV-1 infection and cell death, but that CD45 was not, suggests that this is not a generalised phenomenon at the lymphocyte surface. These results imply that the molecular events that are mediating modification of CD43 do not apply to CD45. Reasons for this might be that CD43 and CD45 are spatially segregated at the lymphocyte surface, giving differential exposure to either sialidase or protease

enzymes. Alternatively, enzymatic modification might be a protein sequence- or structure-specific effect, allowing selective modification of CD43 but not CD45. In either case, the differential modification suggests different functional outcomes for these two molecules during infection and cell death.

A major remaining question is, what is the precise molecular modification taking place on CD43? Two possibilities exist: i) that the sialic acid content of CD43 is modified, either in an epitope-specific manner or in a more general manner, on CD43 but not on CD45; ii) that the CD43 ectodomain is lost from the cell surface, potentially by proteolytic cleavage, leaving behind the membrane proximal region labelled by C20. Some clues regarding this may be taken from the existing literature.

Alterations in CD43 glycosyation and sialylation have been reported upon T cell activation and stimulation. In the studies conducted by Elies et al. and Jones et al., they used S7 and 1B11 mAbs recognising core 1 and core 2 O-glycans on murine CD43, respectively, to characterise glycoform expression of CD43 throughout thymocyte development and T cell activation [392, 393]. They have shown that immature thymocytes express CD43 decorated with both core 1 and core 2 O-glycans, whereas mature thymocytes only express CD43 with core 1 O-glycans [392, 393]. In the human and murine periphery, activated T cells express core 1 and 2 O-glycosylated CD43, whereas, naïve T cells only express core 1 O-glycosylated CD43 [393-396]. Moreover, it has been shown that the activation of murine CD4+ T cells results in a general desialylation and an increase in core 2 O-glycans, which is suggested to be due to de

novo synthesis of hyposialylated CD43 [381]. Bazil et al. reported shedding of CD43 from the surface of lymphocytes ligated with anti CD43 mAb (MEM-59) [380]. However, they failed to show CD43 shedding upon PMA activation of lymphocytes [380].

There are studies that have investigated sialylation of CD43 on the surface of T cells in the context of HIV-1 infection and death. In the study conducted by Lefebvre et al. [342] the electrophoretic mobility of CD43 on the surface of latently HIV-1-infected WT-CEMs was reduced. This was partially restored by enzymatic re-sialylation of the CD43 molecule suggesting that CD43 is desialylated during latent HIV-1 infection [342]. However, they were unable to observe the same phenomenon on HIV-1-infected peripheral blood lymphocytes. Ten years later, the Lefebvre laboratory reported that down-regulation of UDP-N-acetylglucosamine 2-epimerase/N- acetylmannosamine kinase (GNE) resulted in CD43 desialylation on latently HIV-1-infected CEM T cells [397]. Moreover, the binding of MAL lectin to the surface of apoptotic Jurkat T cells and lymphoblasts was reduced comparing with the healthy T cells. As MAL lectin recognises terminal sialic acid, this indicated that the apoptotic cell death might lead to general desialylation of the T cell surface [309, 382]. However, no further studies have elucidated the mechanisms underlying modification of CD43 sialylation on CD4+ T cells during acute HIV-1 infection and cell death. Thus my subsequent chapter describes the work I have undertaken to define the molecular cause of the loss of CD43 sialic acid-dependent epitopes during HIV-1 infection and cell death.

Chapter 5: CD43 modification mechanism and its implication as an eat-me signal

5.1. Introduction

As shown in my previous chapter, HIV-1 infection and cell death (apoptosis and pyroptosis) mediate modification of the CD43 MDD on CD4+ T cells. There are two major hypotheses that can be formulated to explain this observation.

Firstly, this modification could have occurred due to either perturbation in de-novo synthesis and/or transfer of sialic acid, or second, the activation of cell-intrinsic or extrinsic sialidases. The study conducted by the Lefebvre laboratory supports the first hypothesis as they reported that the underlying mechanism for CD43 desialylation on latently HIV-1-infected CEM T cells is via the down-regulation of GNE, the key enzyme in the biosynthesis of CMP-N-acetylneuraminic acid, the donor substrate of all sialyltransferases [397]. However, observation of CD43 MDD modification on the surface of T cells 90 minutes after staurosporine treatment (Figure 4.7a), suggests that CD43 MDD desialylation during apoptosis is probably not due to GNE down-regulation. Another clue from the literature is the study by Billy et al. in which they have shown that apoptosis increases the activity of Jurkat T cell sialidase 1, resulting in general surface desialylation [382]. Moreover, in this study, caspase 3 activation was proposed to trigger sialidase 1 activity in apoptotic Jurkat T cells [382]. One can hypothesise from this study that CD43 might have been one of the glycoproteins desialylated on the surface of T cells during apoptotic cell death.

In the second hypothesis, protease activity could have mediated proteolytic cleavage of the CD43 MDD during HIV-1 infection and cell death. The advocate

of this hypothesis from the literature is the study by Bazil et al. in which they observed CD43 shedding due to CD43 antibody crosslinking on the surface of lymphocytes. In this study lymphocyte treatment with metalloprotease and serine protease inhibitors blocked CD43 shedding [380]. Similarly, it has been shown that the release of CD43 fragments into the supernatant of activated neutrophils and mast cells can be blocked by serine protease inhibitors [379, 398]. These studies imply that proteolytic cleavage of CD43 occurs during leukocyte activation.

5.1.1. Hypothesis

Based on my findings described in the previous chapter and the literature outlined above, I hypothesised that cell death could trigger either sialidase removal of CD43-associated sialic acid, or proteolytic cleavage of the CD43 MDD upon HIV-1 infection and/or cell death. Loss of CD43 sialylation or MDD may act as an eat-me signal for efferocytic uptake of dying or infected T cells.

5.1.2. Specific aims

1. Investigation of the relationship between caspase activation, modification of the CD43 MDD upon apoptotic cell death and HIV-1 infection, and the MDM uptake of HIV-1-infected CD4+ T cells.
2. Analysis of cellular sialidase and protease activity in the modification of CD43 MDD.
3. Probing the role of CD43 as a don't eat-me signal on the surface of healthy and HIV-1-infected CD4+ T cells.

5.2. Results

5.2.1. Role of caspase activation in CD43 modification during apoptotic cell death

As presented in chapter 4, the heavily sialylated CD43 MDD is modified upon apoptotic and pyroptotic cell death. Moreover, I studied the correlation between caspase 3 or caspase 1 activation during apoptosis or pyroptosis, respectively, and CD43 modification. Here, I sought to further investigate the role of caspase activation in the modification of the CD43 MDD on apoptotic T cells.

5.2.1.1. Inhibition of caspase activation prevents CD43 MDD modification

It has been reported in the literature that two pan-caspase inhibitory peptides, Z-VAD-FMK and Q-VD-OPH, block the cleavage of different caspases in vivo and in vitro with varying potency [399]. Therefore, I titrated these two inhibitory peptides for their effect on caspase 3 activation and CD43 modification during apoptosis. I included Z-FA-FMK and Q-VA-OPH control peptides for Z-VAD-FMK and Q-VD-OPH, respectively. WT-CEMs were pre-treated with different concentrations of each of the above mentioned peptides for 45 min at 37ºC. Subsequently, T cells were incubated with 1 µM staurosporine for 3 h to induce apoptosis and after fixation with 4% FA, they were stained with DFT-1 and then permeabilised and stained for cleaved caspase 3, representing sialylated CD43 and apoptosis induction, respectively. As presented in Figure 5.1, treatment of apoptotic WT-CEMs with either Z-VAD-FMK or Q-VD-OPH reduced cleavage of caspase 3 to undetectable levels in a dose-dependent manner as a

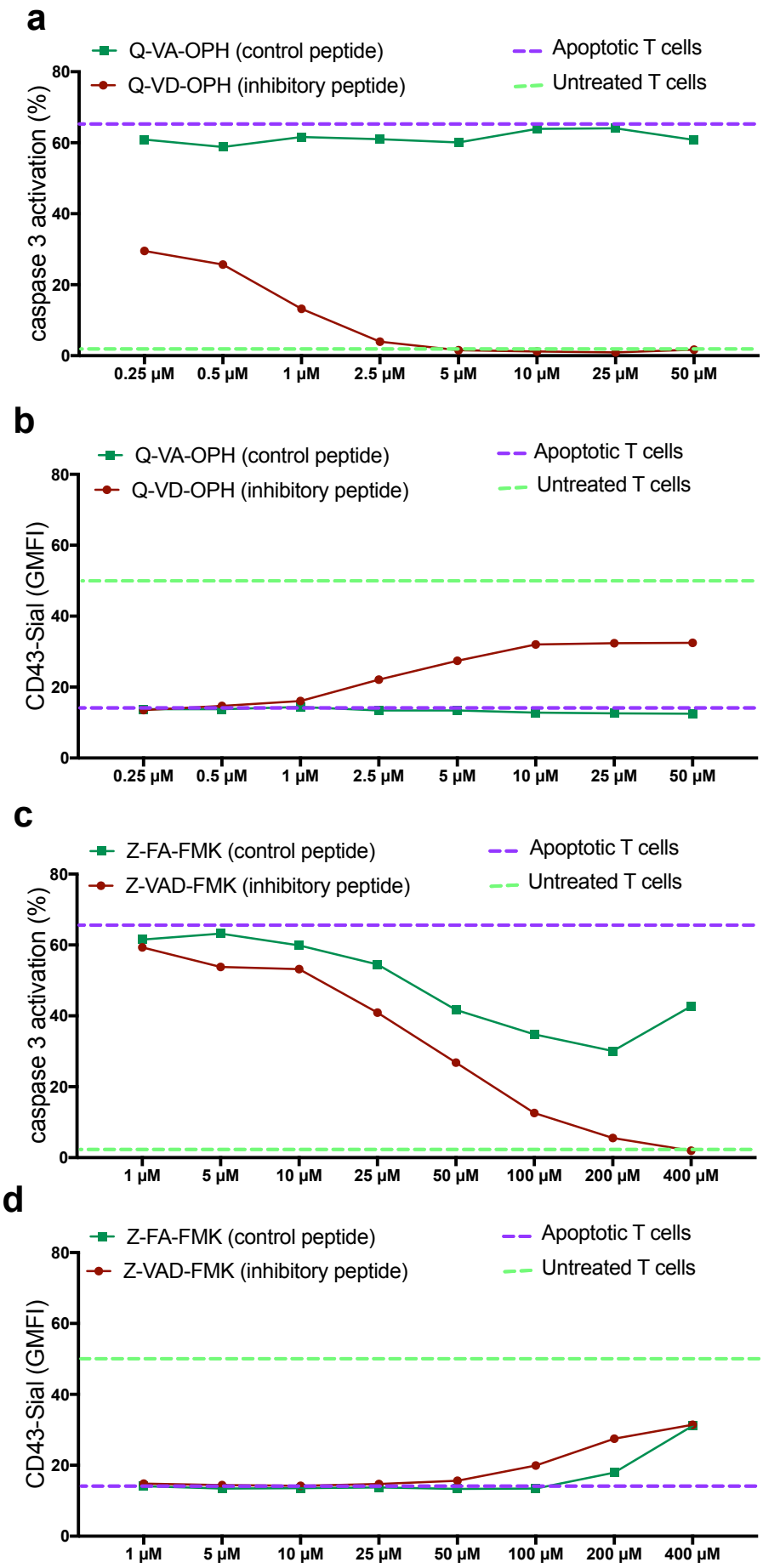

a
Q-VA-OPH (control peptide)
Q-VD-OPH (inhibitory peptide)
Apoptotic T cells
Untreated T cells
caspase 3 activation (%)
0
20
40
60
80
0.25 µM
0.5 µM
1 µM
2.5 µM
5 µM
10 µM
25 µM
50 µM
b
Q-VA-OPH (control peptide)
Q-VD-OPH (inhibitory peptide)
Apoptotic T cells
Untreated T cells
CD43-Sial (GMFI)
0
20
40
60
80
0.25 µM
0.5 µM
1 µM
2.5 µM
5 µM
10 µM
25 µM
50 µM
c
Z-FA-FMK (control peptide)
Z-VAD-FMK (inhibitory peptide)
Apoptotic T cells
Untreated T cells
caspase 3 activation (%)
0
20
40
60
80
1 µM
5 µM
10 µM
25 µM
50 µM
100 µM
200 µM
400 µM
d
Z-FA-FMK (control peptide)
Z-VAD-FMK (inhibitory peptide)
Apoptotic T cells
Untreated T cells
CD43-Sial (GMFI)
0
20
40
60
80
1 µM
5 µM
10 µM
25 µM
50 µM
100 µM
200 µM
400 µM

Figure 5.1**. Figure 5.1. Effect of pan-caspase inhibitors on caspase 3 activation and CD43 modification of apoptotic T cells.** WT-CEMs were pre-treated with different concentrations of either control or inhibitory pan-caspase peptides for 45 min followed by 1 μM staurosporine treatment for 3 h in the presence of peptides. Subsequently, T cells were fixed with 4% FA and stained with DFT-1 mAb representing the sialylation status of CD43 and, then permeabilised and stained for cleaved caspase 3 representing apoptosis. **a)** and **b) Q-VD-OPH and Q-VA-OPH were used as inhibitory and control pan-caspase peptides, respectively. c)** and **d) Z-VAD-FMK and Z-FA-FMK were used as inhibitory and control pan-caspase peptide, respectively.** The graphs show the effect of these peptides on caspase 3 activation (**a** and **c**) and sialylation status of CD43 (**b** and **d**).

percentage of the total population (Figure 5.1a and c), and enhanced DFT-1 labeling as a function of GMFI (Figure 5.1b and d). Interestingly DFT-1 labeling in staurosporine treated, caspase 3 inhibitor-treated cells failed to achieve more than 50% of non-apoptotic cells, suggesting that caspase 3 activation was only partially correlated with CD43 MDD modification. However, the control Z-FA-FMK peptide also decreased caspase 3 activation in a dose-dependent manner, suggesting residual inhibitory activity or off-target effects (Figure 5.1c), and rescued DFT-1 labeling at 400 μm similar to its inhibitory counterpart (Figure 5.1d). Therefore I assumed that the Q-VD-OPH and its control peptide were more reliable inhibitors of caspase 3 in T cells.

Having established that pan-caspase inhibitors effectively reduce caspase 3 activation and enhance DFT-1 labelling, I picked two concentrations of these inhibitors which could abolish caspase 3 activation and were non-toxic for WT-CEMs: 10 and 20 μM of Q-VD-OPH and control, and 100 and 200 μM Z-VAD-FMK and control. As presented in Figure 5.2a, pre-treatment of staurosporine

treated T cells with 20 μM Q-VD-OPH and 200 μM Z-VAD-FMK inhibited caspase 3 cleavage and prevented loss of DFT-1 labeling during apoptosis induction. Pooled data from 4 independent experiments showed that both Q-VD-OPH and Z-VAD-FMK significantly inhibited caspase 3 activation and prevented CD43 modification by comparison with their control counterparts (Figure 5.2b and c).

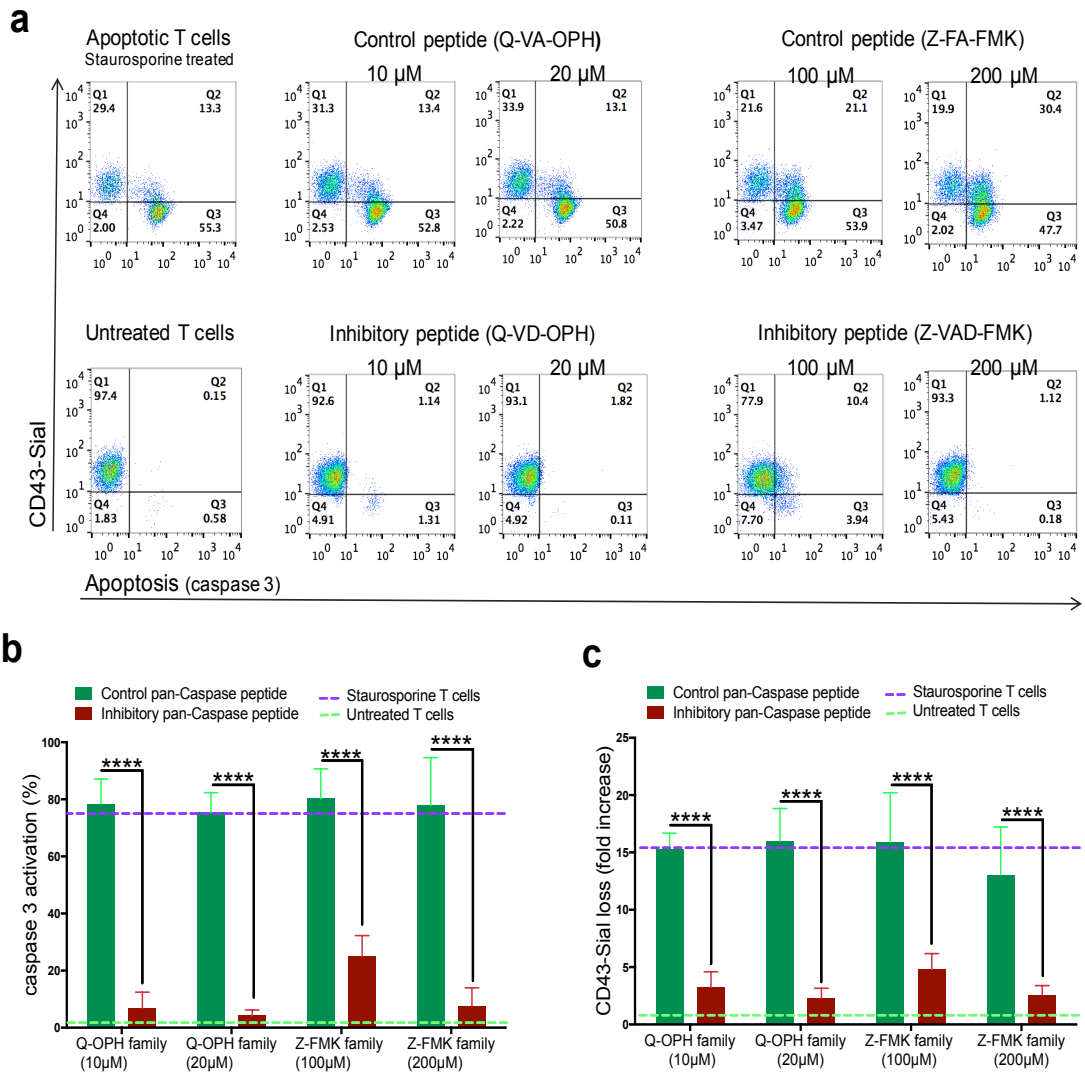


Figure 5.2. Effect of pan-caspase inhibitors on caspase 3 activation and CD43 modification of apoptotic T cells. WT-CEMs were pre-treated or not with different concentrations of either control or inhibitory pan-caspase peptides for 45 min followed by 1 µM staurosporine treatment for 3 h in the presence or absence of peptides. Subsequently, T cells were fixed with 4% FA and stained with DFT-1 mAb representing the sialylation status of CD43, and then permeabilised and stained for cleaved caspase 3 representing apoptosis. **a) Correlation of caspase 3 activation with sialylation status of CD43.** Representative FACS plots of one experiment to show gating strategy for **b**) and **c**). **b) caspase 3 activation. c) Modification of CD43 sialylation.** The graphs represent the data obtained from 4 independent experiments. ****P < 0.0001 tested using two-way ANOVA multiple comparisons with Sidak post-test correction.

To further investigate whether application of these peptides might have affected overall CD43 expression at the cell surface, I stained CD43 with antibody C-20 on staurosporine treated WT-CEMs, which were pre-treated with pan-caspase peptides. As presented in Figure 5.3b, C-20 staining revealed no significant difference between staurosporine treated T cells pre-treated with either pan-caspase inhibitory peptides or control peptides before apoptosis induction. These data imply that blocking caspase cleavage using pan-caspase inhibitory peptides significantly inhibited caspase 3 activation and partially rescued the modification on CD43 sialylated MDD during apoptosis induction of CD4+ T cells.

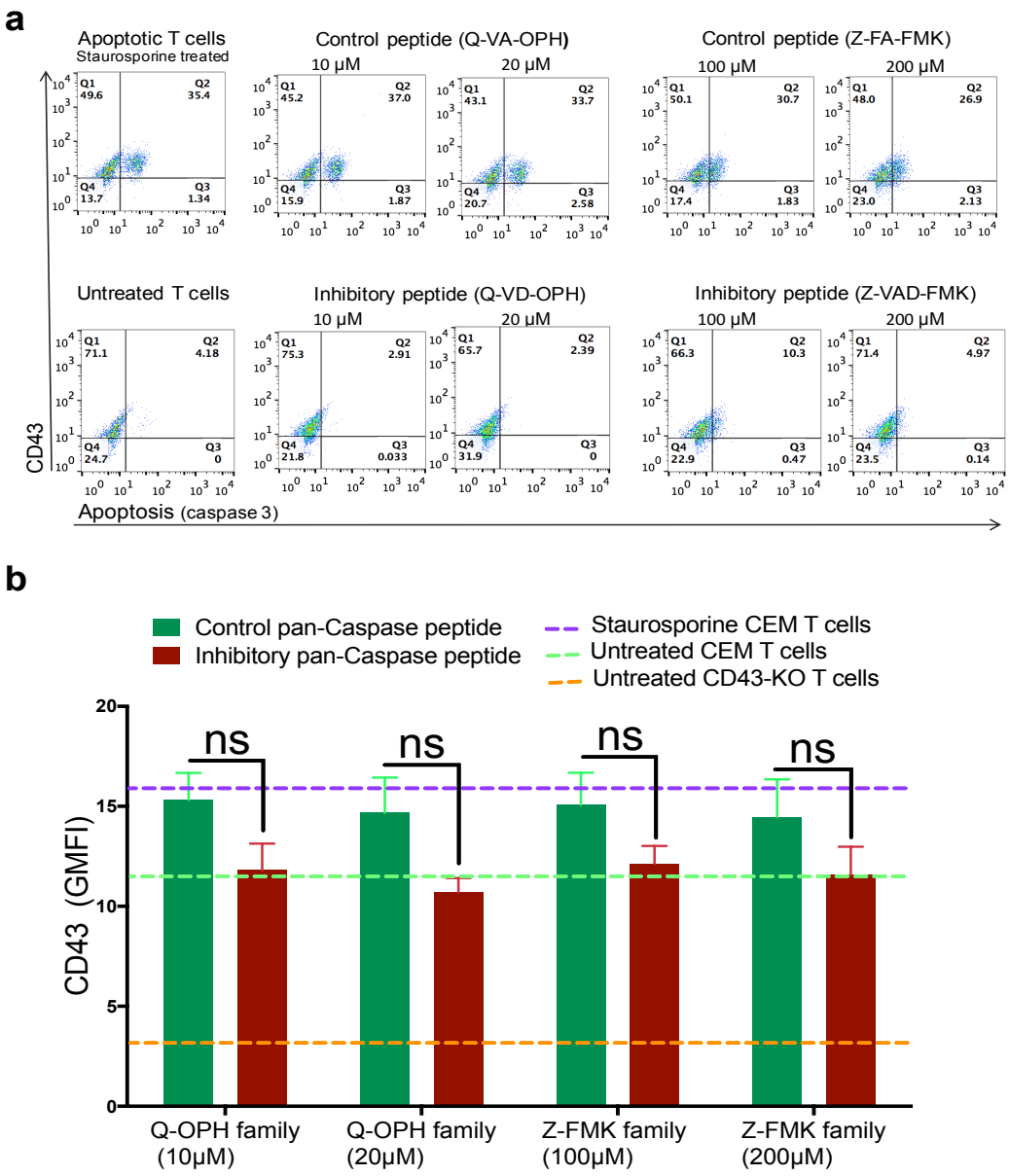


Figure 5.3. Effect of pan-caspase inhibitors on caspase 3 activation and CD43 modification of apoptotic T cells. WT-CEMs were pre-treated or not with different concentrations of either control or inhibitory pan-caspase peptides for 45 min followed by 1 μM staurosporine treatment for 3 h in the presence or absence of peptides. Subsequently, T cells were fixed with 4% FA and stained with C-20 Ab representing CD43 expression and then permeabilised and stained for cleaved caspase 3 representing apoptosis. **a) Correlation between caspase 3 activation and sialylation status of CD43:** Representative FACS plots of one experiment to show gating strategy for **b**). **b) Expression of CD43.** The graph represents the data obtained from 4 independent experiments tested using two-way ANOVA multiple comparisons with Sidak post-test correction, ns = non significant.

5.2.1.2. Caspase 3 but not caspase 8 activation is important for CD43 MDD modification.

According to the literature, during apoptotic cell death caspases 8 and 9 (initiator caspases) are activated which lead to cleavage of caspase 3, 6 and 7 (executioner caspases) [400]. However, it has been reported that caspase 3 is the major executioner/effector caspase during apoptosis [401]. Therefore, I sought to pin down which caspases might be specifically involved in the modification of the CD43 MDD. Firstly, I pre-treated WT-CEMs with different concentrations of the caspase 3-specific inhibitory peptide Z-DEVD-FMK [382], the caspase 8 inhibitory peptide Z-IETD-FMK [402] and the caspase 9 inhibitory peptide Ac-LEHD-CMK [403] for 45 min before apoptosis induction. Subsequently, T cells were incubated with 1 μM staurosporine for 3 h to induce apoptosis and after fixation with 4% FA, were permeabilised and stained for target caspases. As presented in Figure 5.4a, pre-treatment of staurosporine treated WT-CEMs with either Z-DEVD-FMK or Z-IETD-FMK inhibitory peptides before apoptosis induction reduced cleavage of caspase 3 and 8 respectively, to undetectable levels in a dose-dependent manner as a percentage of the total population, whereas Ac-LEHD-CMK did not inhibit caspase 9 cleavage even at 200 μM (>200 μM was toxic to CD4+ T cells). Having established that 100-200 μM Z-DEVD-FMK and 10-25 μM Z-IETD-FMK could strongly inhibit activation of caspase 3 and 8, respectively, I investigated the correlation of caspase 3 or 8 activation with the CD43 MMD modification (Figure 5.4b and c).

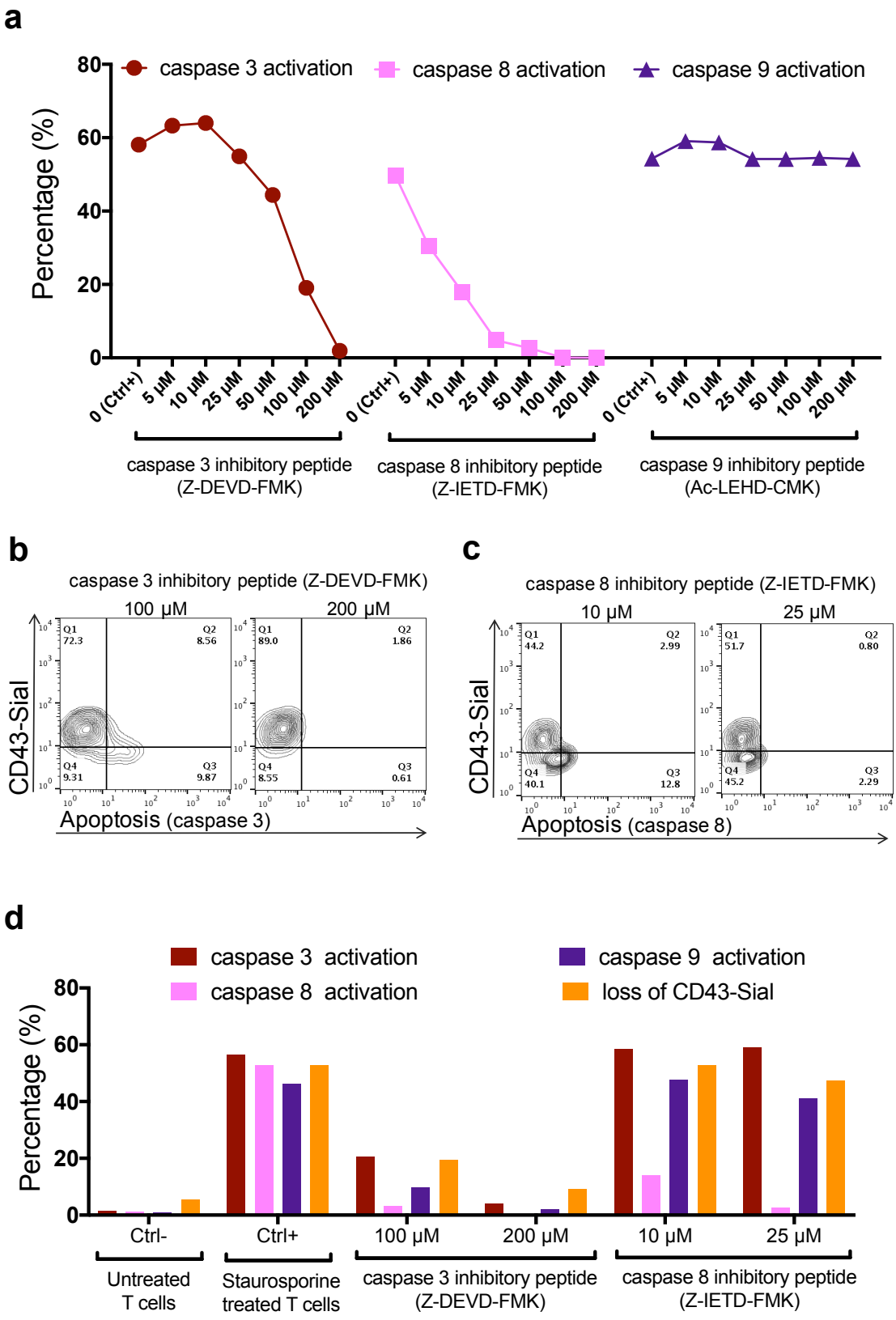

a
caspase 3 activation
caspase 8 activation
caspase 9 activation
Percentage (%)
0 (Ctrl+)
5 μM
10 μM
25 μM
50 μM
100 μM
200 μM
caspase 3 inhibitory peptide (Z-DEVD-FMK)
caspase 8 inhibitory peptide (Z-IETD-FMK)
caspase 9 inhibitory peptide (Ac-LEHD-CMK)
b
caspase 3 inhibitory peptide (Z-DEVD-FMK)
100 μM
200 μM
CD43-Sial
Apoptosis (caspase 3)
c
caspase 8 inhibitory peptide (Z-IETD-FMK)
10 μM
25 μM
CD43-Sial
Apoptosis (caspase 8)
d
caspase 3 activation
caspase 8 activation
caspase 9 activation
loss of CD43-Sial
Percentage (%)
Ctrl-
Ctrl+
Untreated T cells
Staurosporine treated T cells
caspase 3 inhibitory peptide (Z-DEVD-FMK)
caspase 8 inhibitory peptide (Z-IETD-FMK)

Figure 5.4. Effect of caspase 3, 8 and 9 inhibitors on caspase activation and CD43 modification of staurosporine treated T cells. WT-CEMs were pre-treated with different concentrations of inhibitory caspase 3, 8 and 9 peptides for 45 min followed by 1 μM staurosporine treatment for 3 h in the presence of peptides. Subsequently, T cells were fixed with 4% FA and after permeabilisation stained for cleaved caspase 3, 8 and 9. **a) Titration of caspase 3, 8 and 9 inhibitory peptides:** The graph shows the effect of different concentrations of the specific caspase inhibitory peptides on the activation of their target caspase. **b)** and **c) Correlation of caspase 3 and 8 activations with sialylation status of CD43:** Representative FACS plots of one experiment to show gating strategy for **d**). **d) Effect of caspase 3 and 8 inhibition on modification of CD43 sialylation and activation of caspase 3, 8 and 9**: the graph represents the data obtained from one experiment.

As presented in Figure 5.4b, pre-treatment with 200 μM Z-DEVD-FMK reduced both caspase 3 activation and loss of DFT-1 labelling. However, pre-treatment with 25 μM Z-IETD-FMK only inhibited caspase 8 activation but did not prevent loss of DFT-1 labeling (Figure 5.4c). I probed the off-target effect of Z-DEVD-FMK and Z-IETD-FMK at concentrations where they strongly inhibit the activation of their target caspases. As presented in Figure 5.4d, inhibition of caspase 3 activation with Z-DEVD-FMK also blocked the cleavage of caspase 8 and 9 in staurosporine treated WT-CEMs, whereas pre-treatment with Z-IETD-FMK only inhibited the activation of caspase 8. These data suggest that caspase 8 activation is not required for modification of CD43 MDD in staurosporine treated CD4+ T cells.

5.2.2. Role of caspase activation in CD43 modification during HIV-1 infection

As discussed in Section 1.1.6.1, apoptotic cell death is responsible for removal of HIV-1-infected activated peripheral CD4+ T cells. In this context, I sought to investigate the effect of pan-caspase inhibitory peptide on the modification of CD43 MDD on CD4+ T cells during activation and HIV-1 infection.

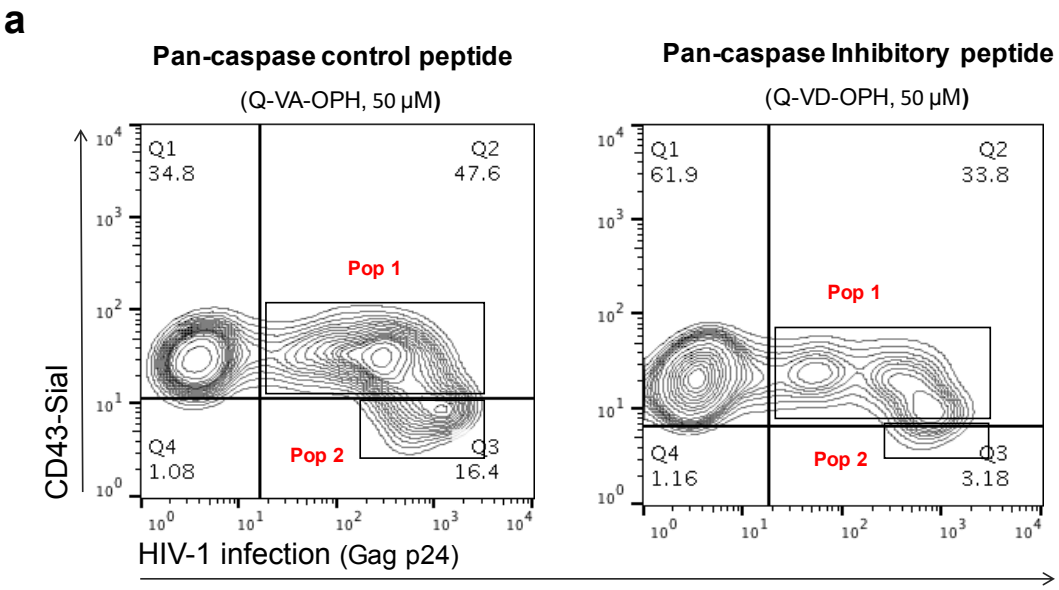
5.2.2.1. Caspase activation is important for HIV-1-induced CD43 MDD modification.

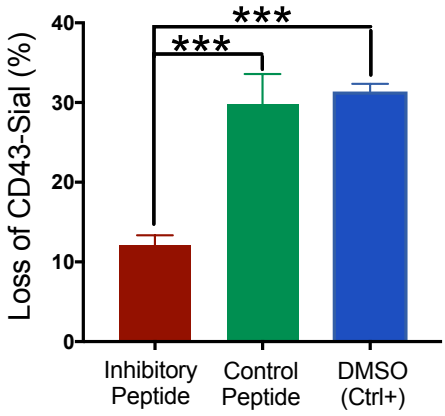
Having confirmed that Q-VD-OPH pan-caspase inhibitory peptide could significantly inhibit caspase 3 activation and CD43 MDD modification during apoptosis induction, I aimed to investigate the effect of Q-VD-OPH on the CD43 MDD modification on HIV-1-infected T cells. Thus CD43-KO and WT-CEM were pre-treated with 50 μM Q-VD-OPH (pan-caspase inhibitory peptide) and Q-VA-OPH (pan-caspase control peptide) for 45 min followed by HIV-$1_{NL4.3\text{-}Luc}$ infection in the presence of pan-caspase peptides for 2 and 3 days, respectively. WT-CEMs were fixed with 4% FA 3 days post-infection, Subsequently, fixed T cells were labeled with DFT-1 and stained for intracellular Gag p24 after permeabilisation. As presented in Figure 5.5a, treatment with pan-caspase inhibitory peptide resulted in ~37% HIV-1 infection, whereas pre-treatment with control peptide led to 64% infection. Thus inhibiting caspase activation reduces apparent HIV-1 infection efficiency, perhaps by preventing bystander cell death resulting in a higher proportion of non-infected cells in the culture. Therefore, I gated on 2 different populations (Pop 1 and 2). Pop 1 was

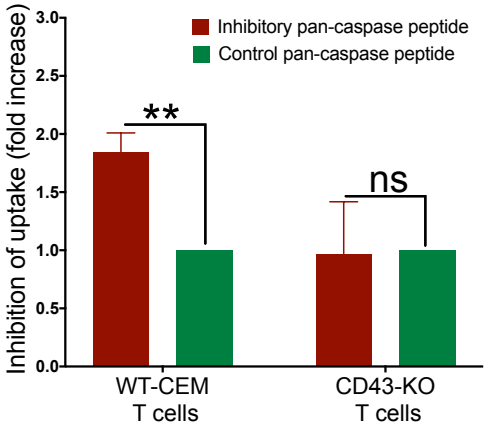
gated on HIV-1 infected cells expressing WT levels of the DFT-1 epitope on the cell surface, whereas Pop 2 represents HIV-1 infected cells with reduced DFT-1 labeling. This allowed me to include the alteration in infection rate to investigate the effect of pan-caspase peptides on CD43 modification during HIV-1 infection, by plotting percentage of [Pop 2/ (Pop 2+1)] instead of absolute percentage of Pop 2. As presented in Figure 5.5b, pooled data from 4 independent experiments showed that pre-treatment with Q-VD-OPH significantly rescued DFT-1 labeling on HIV-1-infected WT-CEMs compared to treatment with Q-VD-OPH or DMSO (vehicle control). These data suggest that treatment with the pan-caspase inhibitory peptide could inhibit modification of CD43 sialylated MDD during HIV-1 infection.

5.2.2.2. Caspase activation is important for MDM efferocytosis of HIV-1-infected T cells

To probe whether MDM efferocytosis of HIV-1-infected T cells would be influenced by inhibition of caspase activation, I isolated MDM from 3 donors and co-cultured them with HIV-1-infected CD43-KO and WT-CEM pre-treated with either Q-VD-OPH (inhibitory peptide) or Q-VA-OPH (control peptide). MDM uptake of caspase-inhibited CEM cells was significantly reduced by comparison with cells pre-treated with the control inhibitor (Figure 5.5c), demonstrating that caspase activation is required for efficient efferocytosis. Moreover, MDM capture of HIV-1-infected CD43-KO CEM did not significantly change after caspase inhibitor treatment (Figure 5.5c). Together these data show that inhibiting caspase activation reduces both CD43 MDD modification and MDM engulfment of HIV-1-infected CD4+ T cells.


a
Pan-caspase control peptide
(Q-VA-OPH, 50 µM)
Pan-caspase Inhibitory peptide
(Q-VD-OPH, 50 µM)
Q1
34.8
Q2
47.6
Pop 1
Q4
1.08
Pop 2
Q3
16.4
Q1
61.9
Q2
33.8
Pop 1
Q4
1.16
Pop 2
Q3
3.18
CD43-Sial
HIV-1 infection (Gag p24)


b
Loss of CD43-Sial (%)
***
***
Inhibitory Peptide
Control Peptide
DMSO (Ctrl+)


c
Inhibition of uptake (fold increase)
Inhibitory pan-caspase peptide
Control pan-caspase peptide
**
ns
WT-CEM T cells
CD43-KO T cells

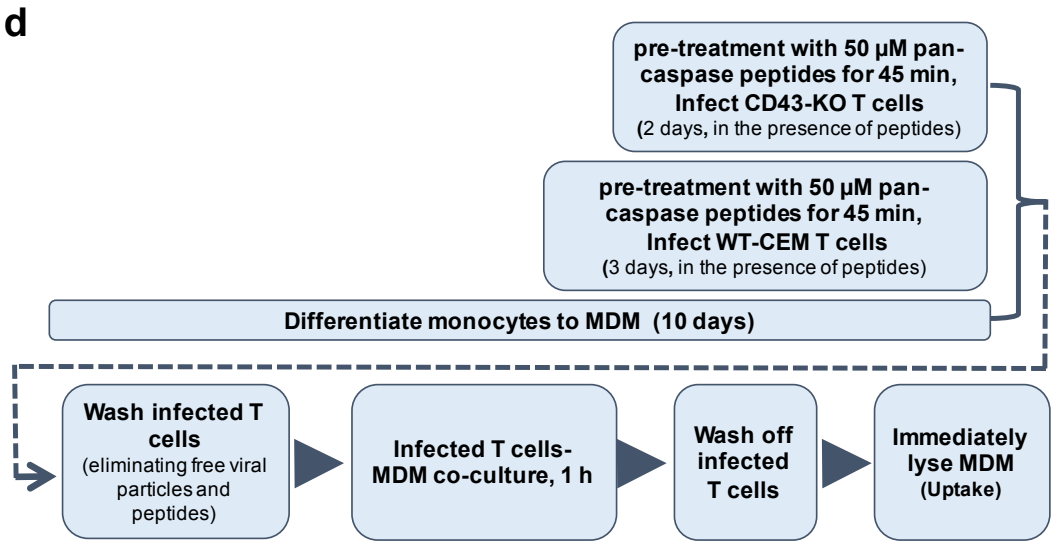

d
pre-treatment with 50 µM pan-caspase peptides for 45 min, Infect CD43-KO T cells
(2 days, in the presence of peptides)
pre-treatment with 50 µM pan-caspase peptides for 45 min, Infect WT-CEM T cells
(3 days, in the presence of peptides)
Differentiate monocytes to MDM (10 days)
Wash infected T cells
(eliminating free viral particles and peptides)
Infected T cells-MDM co-culture, 1 h
Wash off infected T cells
Immediately lyse MDM
(Uptake)

Figure 5.5. Effect of pan-caspase inhibitors on modification of CD43 MDD on HIV-1-infected CEM, and MDM capture of infected CEM. a) CD43-sial and Gag p24 staining: WT-CEMs were untreated or pre-treated with 50 μM either control or inhibitory pan-caspase peptide for 45 min followed by HIV-$1_{NL4.3-Luc}$ infection at MOI of 0.01 for 3 days in the presence or absence of peptides. Subsequently, cells were fixed with 4% FA and stained with DFT-1 representing sialylation of surface CD43 and for intracellular Gag p24 after permeabilisation, representing HIV-1 infection. **b) Effect of pan-caspase inhibitors on CD43 modification:** T cells were treated, infected and stained as described in **a**. Two populations were defined by a gating strategy as shown in **a**. Pop 1 represents infected T cells with WT levels of DFT-1 epitope. Pop 2 represents infected T cells with reduced DFT-1 labeling. Each column shows the percentage of Pop 2 to total population of infected cells (Pop 1+2) per treatment. The graphs represent the data obtained from 4 independent experiments. ***P < 0.001 tested using two-way ANOVA multiple comparisons with Sidak post-test correction. **c)** and **d) MDM uptake of HIV-1 infected CEM.** Monocytes were differentiated into MDM for 10 days and in the meantime CD43-KO and WT-CEM were pre-treated with 50 μM either control or inhibitory pan-caspase peptide for 45 min followed by HIV-$1_{NL4.3-Luc}$ infection at MOI of 0.01 in the presence of peptides for 2 and 3 days, respectively. On day 10, infected CEM were washed thoroughly to remove cell free viral particles and free peptides. Subsequently, infected CEM were co-cultured with MDM for 2 h, and infected cells were then removed with vigorous washing. After removing infected CEM, MDM were lysed, and luciferase assayed. The luciferase signal represents the uptake of infected CEM by MDM. Bars = mean luciferase signal of MDM co-cultured with infected CEM divided by the mean luciferase signal of infected CEM with the relevant treatment (%). Error bars represent SD for 3 donors, each tested in triplicate. **p < 0.01 tested using two-way ANOVA multiple comparisons with Sidak post-test correction.

5.2.3. The role of CD43 internalisation in CD43 MDD modification

Whilst the data above clearly reveal that caspase 3 and 8 activation, which is an essential component of apoptotic cell death, are correlated with CD43 MDD modification and MDM uptake, they do not reveal the underlying mechanisms. As outlined in the introduction of this chapter, the study by Lefebvre proposed that the mechanism for CD43 desialylation on latently HIV-1-infected CEM T cells is down-regulation of GNE resulting in the biosynthesis of hyposialylated CD43 instead of the sialylated form of CD43 [397]. Therefore, I decided to investigate whether CD43 sialylated MDD modification might have occurred due to the transfer of hyposialylated CD43 to the cell membrane during acute HIV-1 infection and cell death. For this purpose, I investigated the role of the cytoskeleton and Golgi to cell membrane transport during apoptotic cell death. The actin polymerisation inhibitor jasplakinolide (Jasp), the microtubule polymerisation inhibitor nocodasole (Noc), and the secretory pathway inhibitor brefeldin A (Bref) were used at concentrations previously shown in the literature to be effective with minimal toxicity [339, 404, 405]. WT-CEMs were pre-treated with 5 μM Jasp, 10 μM Noc or 10 μg/ml Bref before apoptosis induction. As presented in Figure 5.6a, these compounds neither interfered with caspase 3 cleavage nor DFT-1 labeling during staurospaurine-induced apoptosis. Similarly, pre-treatment with Jasp, Noc or Bref failed to influence CD43 expression revealed by C-20 labeling (Figure 5.6b). These data show that CD43 modification during cell death is unlikely to require involvement of the T cell cytoskeleton or secretory pathways, and is therefore most likely taking

place at the cell surface rather than by a pathway involved in the transport or recycling of surface glycoproteins.

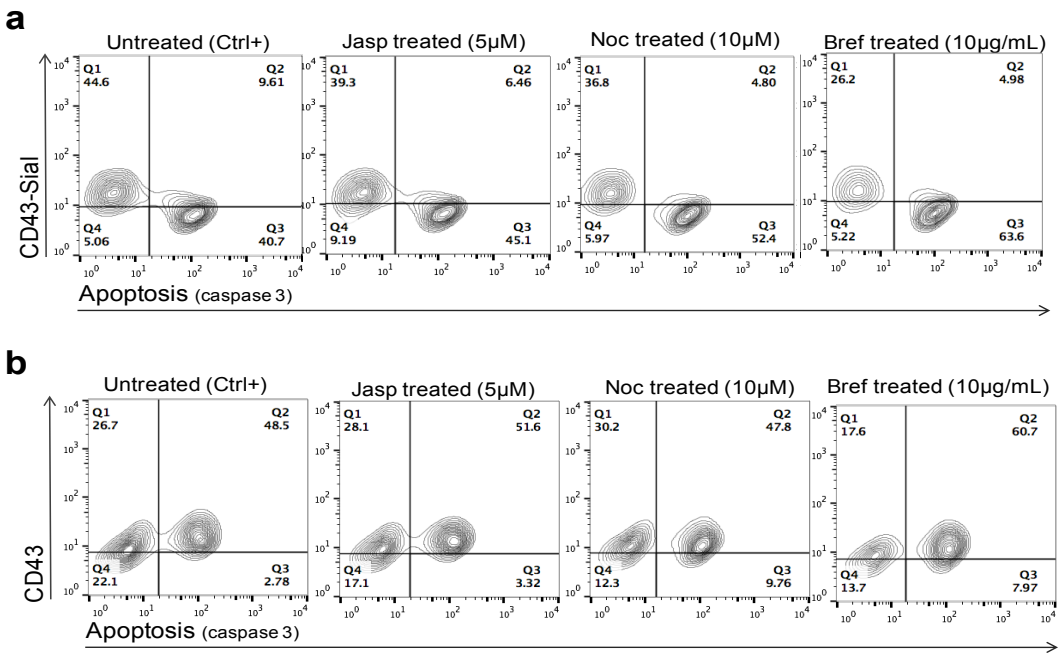


Figure 5.6. Role of the cytoskeleton and Golgi to cell membrane transport in CD43 modification during apoptosis. WT-CEMs were pre-treated with 5 µM Jasplakinolide (Jasp), 10 µM Nocodazole (Noc) or 10 µg/mL Brefeldin A (Bref) for 30 min. Subsequently, cells were treated with 1µM staurosporine for 3 h in the presence of those compounds followed by 4% FA fixation. **a) CD43-Sial staining:** Fixed cells were stained with DFT-1 mAb representing the sialylation status of CD43 and for cleaved caspase 3 after permeabilisation, which represents apoptosis. **b) CD43 staining:** as described in **a**, except CD43 was stained with C20 Ab representing CD43 surface expression..

5.2.4. Proteolytic cleavage of CD43 during cell death

As outlined in the introduction of this chapter, Bazil et al. reported CD43 shedding as a result of CD43 antibody crosslinking on the surface of lymphocytes [380]. Therefore, I sought to to investigate whether the modification of CD43 MDD during HIV-1 infection and cell death is due to the proteolytic cleavage of the CD43 MDD.

5.2.4.1. Generation of Myc-tagged CD43 transgenic CEM cells

Since the DFT-1 mAb cannot discriminate between modified sialylation of the CD43 MDD or its proteolytic cleavage, and C20 does not bind the MDD, I introduced an N-terminally Myc-tagged version of CD43 into CD43-KO CEM, allowing detection of CD43 expression independently of sialic acid composition. For this purpose, I transduced CD43-KO CEM T cells with lentiviral particles carrying the CD43 gene with an N-terminal Myc-tag and puromycin-resistance selectable marker as described in Section 2.1.8.1. After puromycin selection, I characterised these CD4+ T cells (termed Myc-CD43 CEM from hereon) by antibody labeling as shown in Figure 5.7a. DFT-1 labeling of Myc-CD43 CEM showed that these cells express approximately 2-fold more cell surface CD43-Sial epitope compared to WT-CEMs, a significant difference (Figure 5.7b). To confirm that binding of the DFT1 mAb to the transgenic CD43 molecule was sialic acid-dependent, I exposed the Myc-CD43 CEM to different concentrations of Arth. sialidase. As shown Figure 5.7c, 200 mU Arth. sialidase completely abolished DFT-1 labeling, whereas 100 mU Arth. sialidase was sufficient for the elimination of WT-CEM DFT-1 labeling, consistent with the expression of more CD43-Sial on Myc-CD43 CEM (Figure 5.7b). These results confirm that DFT1 binding is sialic acid dependent on both WT and CD43 transgenic CEM lines. Arth. sialidase treatment did not alter binding of the Myc tag-specific mAb 9E10, an expected result since 9E10 binding to the Myc-tag should not be sialic acid dependent (Figure 5.7d).

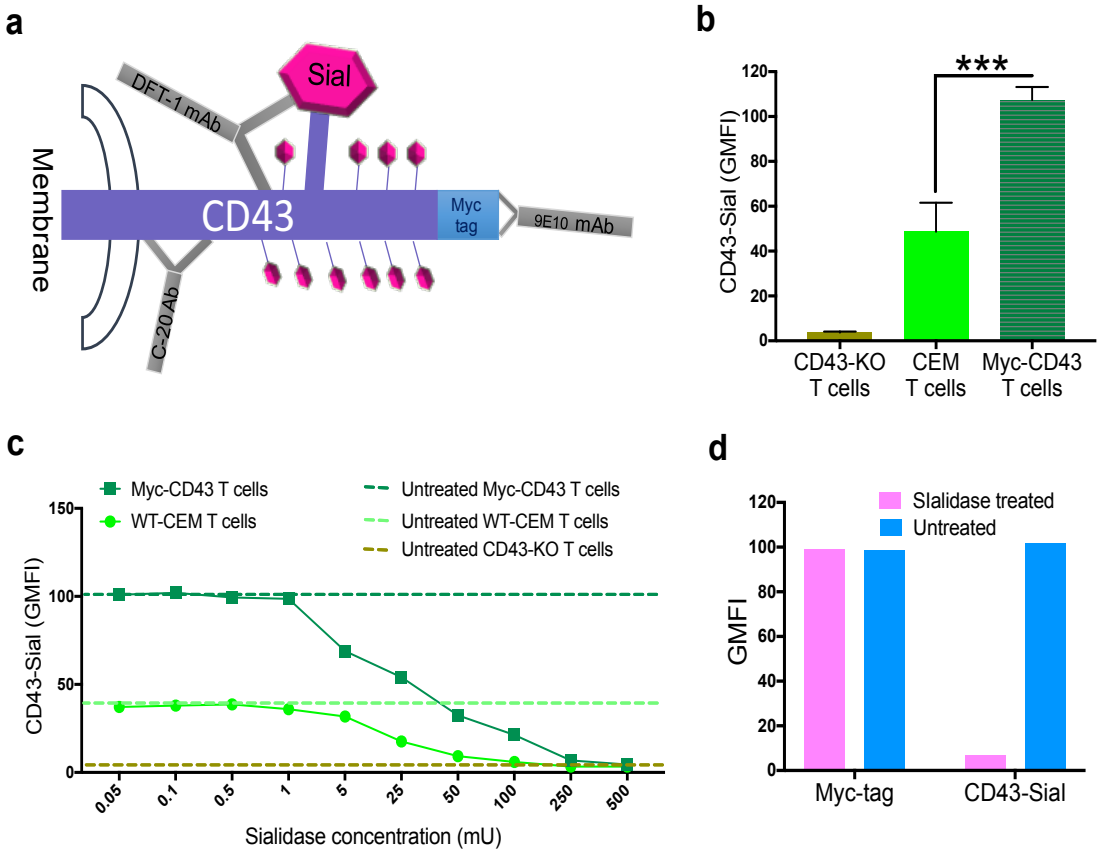


Figure 5.7. Characterisation of the Myc-CD43 CEM line. a) Schematic structure of DFT-1 mAb (CD43-Sial), C-20 Ab (CD43) and 9E10 (Myc-tag) epitopes on Myc-CD43 CEM. b) CD43-Sial expression. CD43-KO, Myc-CD43 and WT-CEM were fixed with **4%** FA and stained with DFT-1 mAb representing expression of the CD43 sialylated MDD epitope on the surface of T cells. The graph shows the data obtained from 3 independent experiments, ***P < 0.001 tested using one-way ANOVA with Sidak post-test correction. **c) CD43 sialylation status.** WT-CEM and Myc-CD43 CEM were treated with different concentrations of Arth. sialidase for 1 h at 37ºC. Untreated CD43-KO, WT-CEM and Myc-CD43 CEM (presented as dotted lines), and treated WT-CEM and Myc-CD43 CEM were fixed and stained with DFT-1. The graph presents the geometric mean of CD43-Sial. **d) Sialidase treatment effect on Myc-tag expression**: Myc-CD43 CEM were treated with 200 mU Arth. sialidase for 1 h at 37ºC. Untreated and sialidase treated Myc-CD43 CEM were fixed and stained with DFT-1 or 9E10 mAbs representing sialylation of CD43 and Myc-tag at CD43 N-terminus, respectively. The graph presents the geometric mean of CD43-Sial of one experiment.

5.2.4.2. Apoptosis drives cleavage of CD43 MDD from the cell surface

Having completed this preliminary characterisation, I then probed the effect of apoptosis induction on transgenic Myc-CD43 expression. I treated Myc-CD43 CEM with 1 μM staurosporine for 3 h and after 4% FA fixation, labeled them with C-20 and then permeabilised to stain for cleaved caspase 3.

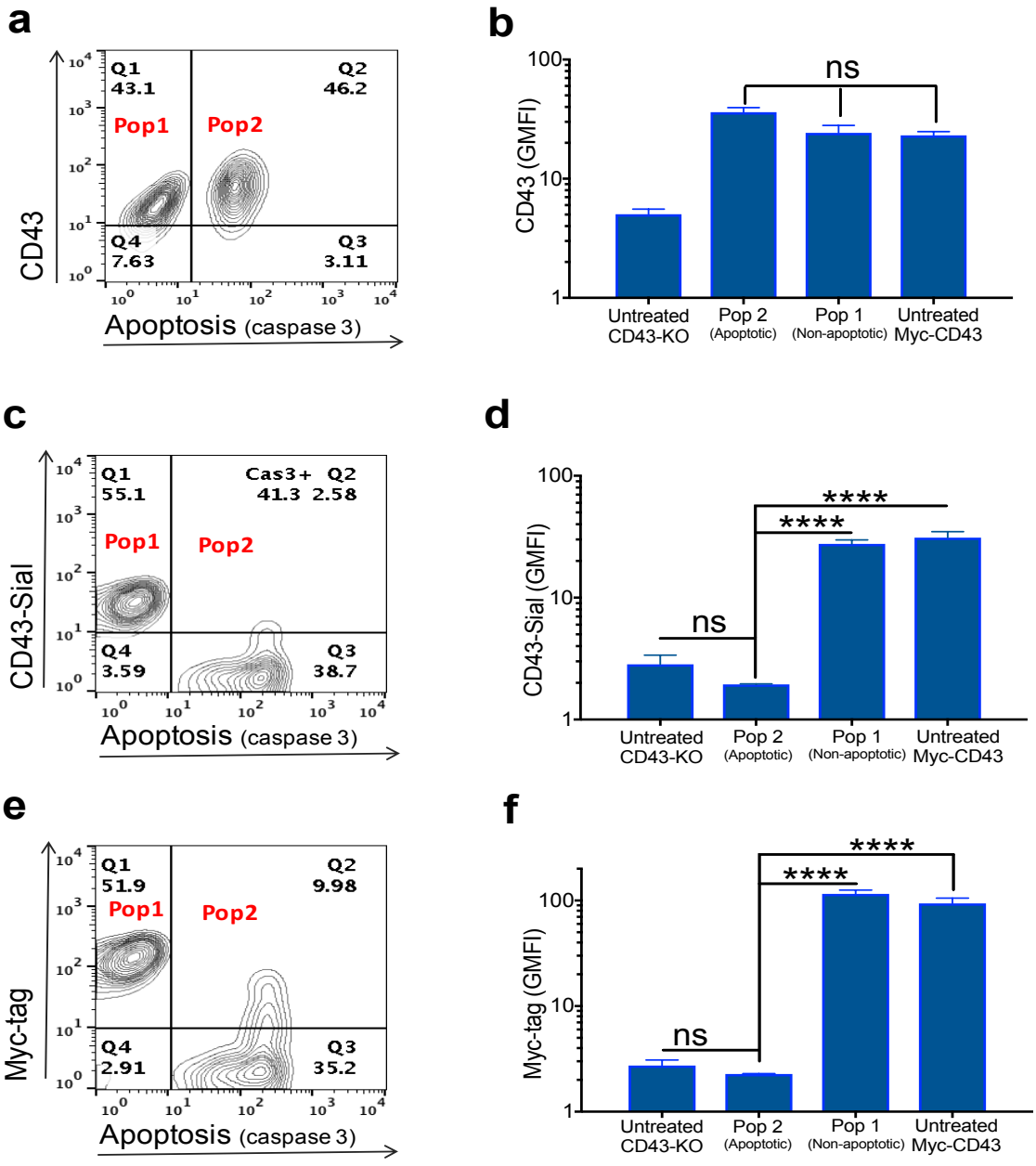


Figure 5.8. Apoptosis induction of Myc-CD43 CEM results in proteolytic cleavage of CD43. a) and **b) CD43 staining:** Myc-CD43 CEM were treated with 1 μM staurosporine for 3 h, and then fixed with 4% FA. CD43 on fixed T cells were stained with C-20 Ab followed by permeabilisation and cleaved caspase 3 staining. The FACS plot shows the gating strategy for defining non-apoptotic (Pop 1) and apoptotic (Pop 2) used in graph b). **c)** and **d) CD43-Sial staining:** As described in **a**, except CD43 was stained with DFT-1 mAb representing the CD43 sialylation status on the T cell surface. **e)** and **f) Myc-tag staining:** As described in **a**, except instead of CD43 staining, fixed T cells stained for N- terminal Myc-tag on CD43 with 9E10 mAb. The graphs represent the data obtained from 3 independent experiments. ns and ****P < 0.0001 tested using one-way ANOVA multiple comparisons with Sidak post-test correction.

As presented in Figure 5.8a and b, apoptosis induction did not affect CD43 C20 epitope expression on the surface of Myc-CD43 CEM. By contrast, apoptosis induction significantly reduced DFT-1 and 9E10 labeling on Myc-CD43 CEM compared to their non-apoptotic counterparts (Figure 5.8d and f). Since the Myc tag is N-terminally located on CD43 and 9E10 binding is not sialic acid dependent, these data strongly imply that the MDD, or at least a component of it, is proteolytically cleaved during apoptotic cell death.

Further analysis with pan-caspase inhibition revealed that blocking apoptosis induction prevented loss of both DFT-1 and 9E10 labeling by comparison with control peptide treatment (Figure 5.9). These data strongly support a requirement for caspase activation in apoptosis leading to cleavage of the CD43 MDD.

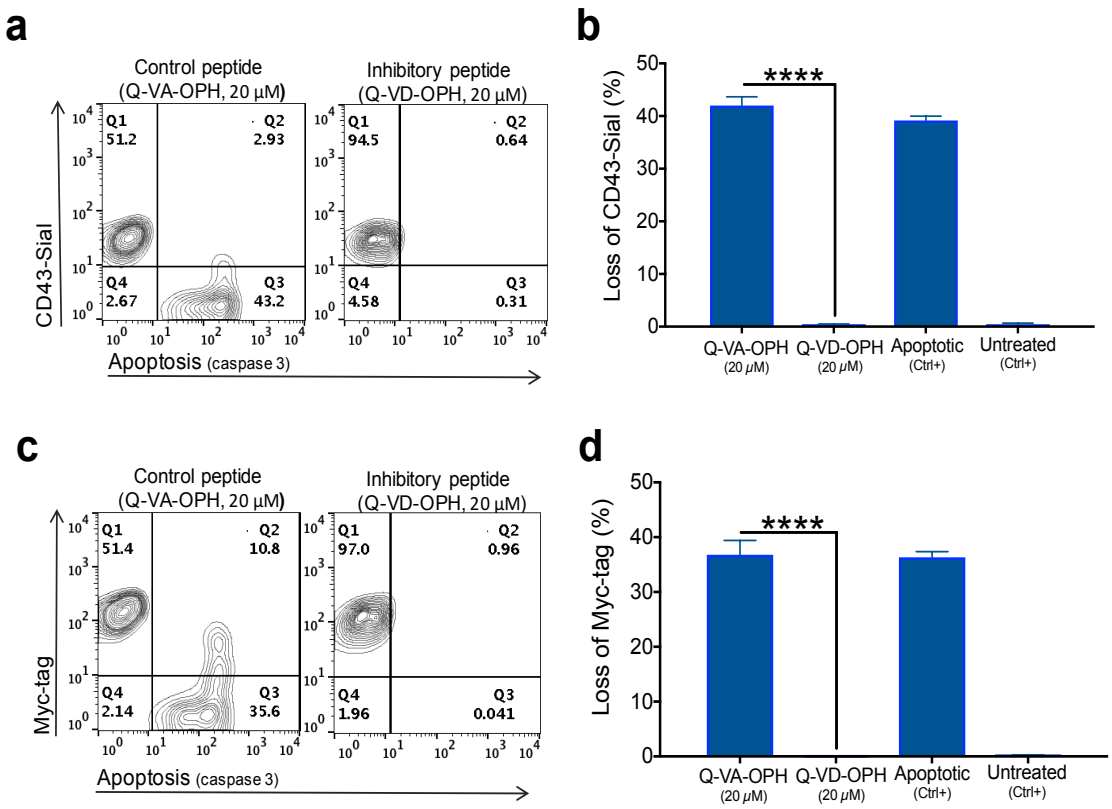


Figure 5.9. Effect of pan-caspase inhibition of staurosporine-treated CEM on proteolytic cleavage of CD43 . Myc-CD43 CEM were pre-treated with 20 µM of either control or inhibitory pan-caspase peptides for 45 min. Subsequently, T cells were treated with 1 µM staurosporine for 3 h in the presence of peptides followed by **4%** FA fixation. **a)** and **b) CD43-Sial staining:** Fixed cells were stained with DFT-1 and cleaved caspase 3 after permeabilisation. The FACS plot shows the gating strategy for defining apoptotic T cells (cleaved caspase 3 positive cells) used for graph **b**). **c)** and **d) Myc-tag staining.** As described in **a**, except instead of CD43-Sial, fixed cells were stained for N-terminal Myc-tag on CD43 with 9E10 mAb. The graphs represent the data obtained from 3 independent experiments. ns= not significant, and ****P < 0.0001 tested using one-way ANOVA multiple comparisons with Sidak post-test correction.

5.2.4.3. Detection of soluble supernatant CD43 MDD

To confirm the proteolytic cleavage of CD43 MDD during apoptosis, I developed a direct coating ELISA for detection of soluble CD43 in the supernatant of apoptotic T cells as described in Section 2.5. Briefly, Myc-CD43 and CD43-KO CEM were either untreated or treated with staurosporine for 3 h. Supernatants were collected and used to coat 96-well ELISA plates at different concentrations. Subsequently, biotinylated DFT-1 and 9E10 mAbs were used for detection of CD43-Sial and Myc-tag, respectively. As presented in Figure 5.10a and b, DFT-1 and 9E10 bound to the wells coated with the supernatants of apoptotic Myc-CD43 CEM in a dose-dependent manner in contrast to the supernatants of apoptotic CD43-KO and untreated CEM. The absorbance values obtained from the apoptotic and untreated CD43-KO CEM supernatants were used as the background and subtracted from the absorbance values obtained from the apoptotic and untreated Myc-CD43 CEM supernatants, respectively. Data pooled from 2 independent experiments showed a significant increase in soluble CD43-sial and Myc-tag in the supernatants of apoptotic Myc-CD43 CEM by comparison with the supernatants of untreated Myc-CD43 CEM (Figure 5.10c).

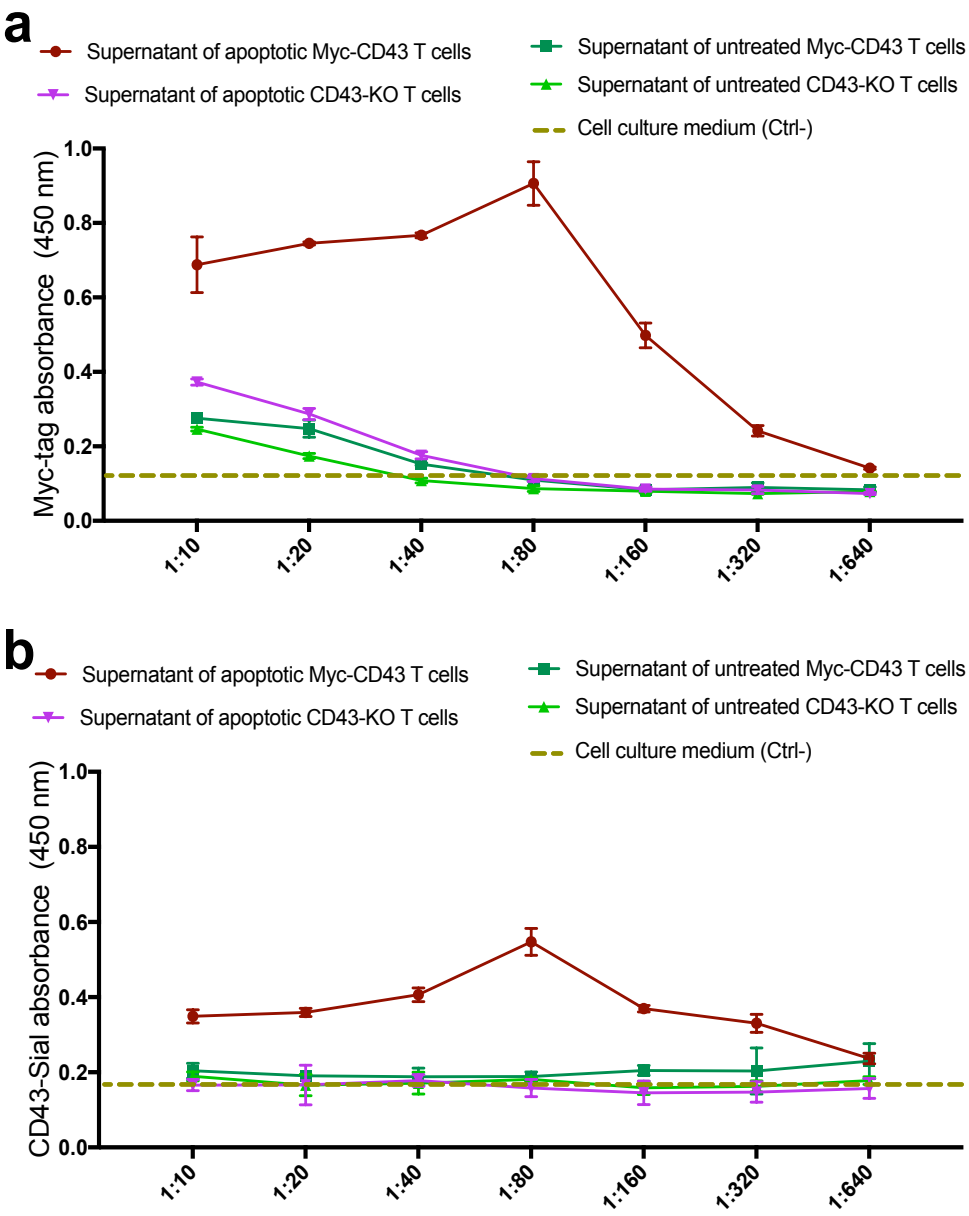

a
Supernatant of apoptotic Myc-CD43 T cells
Supernatant of apoptotic CD43-KO T cells
Supernatant of untreated Myc-CD43 T cells
Supernatant of untreated CD43-KO T cells
Cell culture medium (Ctrl-)
Myc-tag absorbance (450 nm)
1.0
0.8
0.6
0.4
0.2
0.0
1:10
1:20
1:40
1:80
1:160
1:320
1:640
b
Supernatant of apoptotic Myc-CD43 T cells
Supernatant of apoptotic CD43-KO T cells
Supernatant of untreated Myc-CD43 T cells
Supernatant of untreated CD43-KO T cells
Cell culture medium (Ctrl-)
CD43-Sial absorbance (450 nm)
1.0
0.8
0.6
0.4
0.2
0.0
1:10
1:20
1:40
1:80
1:160
1:320
1:640
c
Supernatant of untreated Myc-CD43 T cells
Supernatant of apoptotic Myc-CD43 T cells
Absorbance (450 nm)
1.5
1.0
0.5
0.0
**
****
CD43-Sial
Myc-tag

Figure 5.10. Soluble Myc-CD43 detection in the supernatant of apoptotic Myc-CD43 CEM. $1x10^8$ Myc-CD43 and CD43-KO CEM were treated in 1 mL RPMI containing 100 µM staurosporine for 3 h. Subsequently, supernatants were collected by pelleting cells using centrifugation at 500 g for 5 min at 4ºC. Tissue culture protease inhibitor cocktail was added at 1:100 and supernatants were aliquoted and stored at -20ºC. **a) Myc-tag detection:** Supernatants were thawed and diluted in 50 µL of 100 mM Na_2CO_3 buffer pH 8.5, for coating wells of 96-well ELISA plates overnight at 4ºC. Biotinylated 9E10 mAb was used to detect CD43 Myc-tag in the supernatants. The graph shows data obtained from triplicates. **b) CD43-Sial detection.** As described in **a**, except biotinylated DFT-1 mAb was used to detect CD43-Sial in the supernatants. **c) CD43-Sial and Myc-tag detection**. As described in **a** and **b**, except the supernatant dilution showing the highest value was chosen for coating. The graph represents SD for 2 independent experiments, each in triplicate. ****P < 0.0001 tested using two-way ANOVA with Sidak post-test correction.

5.2.4.4. Pyroptosis induced CD43 MDD cleavage

To evaluate whether CD43 MDD cleavage could also be observed during pyroptotic cell death, I treated Myc-CD43 CEM with 75 µM nigericin for 4 h followed by staining for cleaved caspase 1. Cells were fixed as described in Section 2.7.1 and labeled with C-20, DFT-1 and 9E10. As presented in Figure 5.11a, there was no significant difference between CD43 expression measured with C20 on the surface of pyroptotic and non-pyroptotic Myc-CD43 CEM based on data obtained from 3 independent experiments. However, both DFT-1 and 9E10 labeling were significantly reduced on the surface of Pop 2 compared to Pop 1, suggesting proteolytic cleavage of CD43 MDD during pyroptosis (Figure 5.11b and c). Interestingly, a population of caspase 1 negative cells (Q4) were also negative for DFT1 and 9E10 labeling, suggesting that CD43 DDM cleavage may occur prior to and/or independently of caspase 1 activation during pyroptotic cell death.

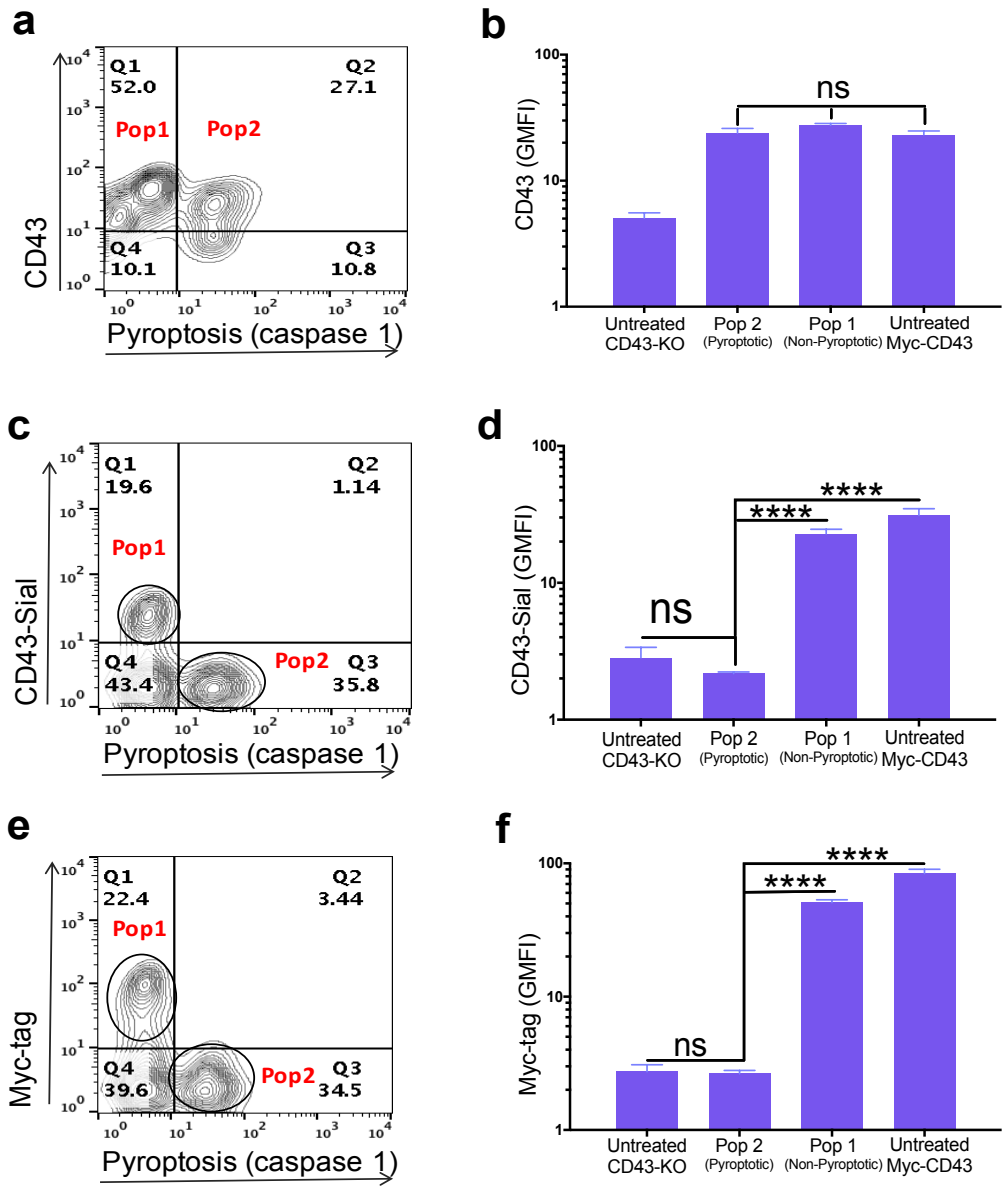


Figure 5.11. Pyroptosis induction of Myc-CD43 CEM results in proteolytic cleavage of CD43. a) and **b) CD43 staining:** Myc-CD43 CEM were treated with 75 µM nigericin for 4 h followed by cleaved caspase 1 staining. Afterwards, T cells were fixed and stained for CD43 with C-20 Ab representing CD43 expression on the T cell surface. The FACS plot shows the gating strategy for defining non-pyroptotic (Pop 1) and pyroptotic (Pop 2) T cells used for graph **b**). **c)** and **d) CD43-Sial staining.** As described in **a**, except CD43 was stained with DFT-1 mAb. **e)** and **f) Myc-tag staining:** As described in **a**, except instead of CD43 staining, fixed T cells were stained for CD43 N- terminal Myc-tag with 9E10 mAb. The graphs represent the data obtained from 3 independent experiments. ns = not-significant and ****P < 0.0001 tested using one-way ANOVA multiple comparisons with Sidak post-test correction.

5.2.5. Protease-mediated cleavage of CD43 MDD

In multiple studies, metalloproteases and serine proteases have been implicated in CD43 shedding upon PMA-treatment of granulocytes, neutrophils and mast cells [375, 379, 380, 398]. In one study, Bazil et al. demonstrated the involvement of metalloprotease and serine proteases in CD43 shedding from the surface of lymphocytes due to CD43 antibody crosslinking [380]. Therefore, I sought to investigate whether metalloproteases and/or serine proteases are involved in the cleavage of CD43 MDD during apoptotic cell death.

5.2.5.1. Role of serine and metalloproteases in apoptosis-induced CD43 MDD cleavage

WT-CEM were pre-treated with serine protease inhibitors [3,4-dichloroisocoumarin (3,4-DICH), α_1-antichymotrypsin ($\propto$Chymo) and α_1-antitrypsin ($\propto$Titry)] or metalloprotease inhibitors [1,10-Phenanthroline (1,10-Phen), Marimastat and GM6001] for 45 min before apoptosis induction using concentration ranges defined by those previously described in the literature [375, 406]. I labeled for caspase 3 activation to evaluate whether the protease inhibitors interfered with this process, and with DFT1 to evaluate CD43 MDD cleavage. As presented in Figure 5.12a and b, pre-treatment of WT-CEMs with either $\propto$Chymo or $\propto$Titry altered neither caspase 3 activation nor CD43 MDD cleavage during apoptosis. However, pre-treatment with 3,4-DICH reduced and completely abolished caspase 3 activation at 100 µM and 1 mM, respectively (Figure 5.12a). As shown earlier with the pan-caspase inhibitory peptide (Figure 5.2 and 9), blocking caspase activation prevented CD43 MDD cleavage.

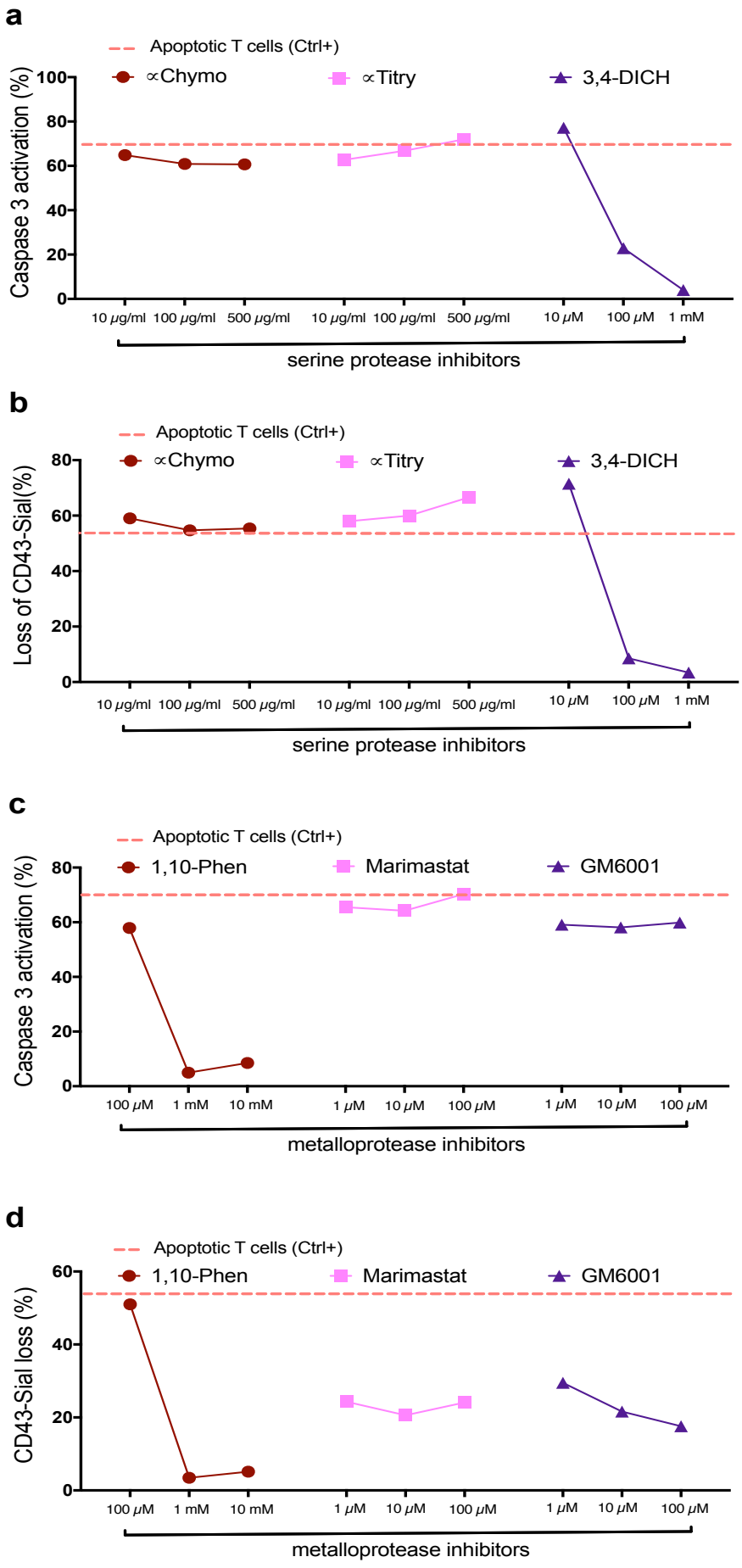

a
Apoptotic T cells (Ctrl+)
∝Chymo
∝Titry
3,4-DICH
Caspase 3 activation (%)
100
80
60
40
20
0
10 µg/ml
100 µg/ml
500 µg/ml
10 µg/ml
100 µg/ml
500 µg/ml
10 µM
100 µM
1 mM
serine protease inhibitors
b
Apoptotic T cells (Ctrl+)
∝Chymo
∝Titry
3,4-DICH
Loss of CD43-Sial(%)
80
60
40
20
0
10 µg/ml
100 µg/ml
500 µg/ml
10 µg/ml
100 µg/ml
500 µg/ml
10 µM
100 µM
1 mM
serine protease inhibitors
c
Apoptotic T cells (Ctrl+)
1,10-Phen
Marimastat
GM6001
Caspase 3 activation (%)
80
60
40
20
0
100 µM
1 mM
10 mM
1 µM
10 µM
100 µM
1 µM
10 µM
100 µM
metalloprotease inhibitors
d
Apoptotic T cells (Ctrl+)
1,10-Phen
Marimastat
GM6001
CD43-Sial loss (%)
60
40
20
0
100 µM
1 mM
10 mM
1 µM
10 µM
100 µM
1 µM
10 µM
100 µM
metalloprotease inhibitors

Figure 5.12. Effect of metalloprotease and serine protease inhibitors on caspase 3 activation and CD43 cleavage during apoptotic cell death. WT-CEMs were pre-treated with different concentrations of either metalloprotease or serine protease inhibitors for 45 min followed by 1 μM staurosporine treatment for 4 h in the absence or presence of inhibitors. Subsequently, cells were fixed with 4% FA and stained with DFT-1 mAb and were then permeabilised to stain cleaved caspase 3 representing apoptosis. **a)** and **b) 3,4-dichloroisocoumarin (3,4-DICH), α_1-antichymotrypsin (∝Chymo) and α_1-antitrypsin (∝Titry) used as serine protease inhibitors. a**) and **b**) show the effect of these serine protease inhibitors on caspase 3 activation and CD43 MDD status, respectively. **c) and d) 1,10-Phenanthroline (1,10-Phen), Marimastat and GM6001 used as metalloprotease inhibitors. c**) and **d**) show the effect of these serine protease inhibitors on caspase 3 activation and CD43 MDD status, respectively.

Similarly, 3,4-DICH treatment inhibited both caspase 3 activation and CD43 cleavage in a dose dependent-manner (Figure 5.12a and b). As shown in Figure 5.12c and d, 1 mM 1,10-Phen treatment also blocked caspase 3 activation and CD43 cleavage. However, treatment with different concentrations of Marimastat and GM6001 did not alter caspase 3 activation, but did reduce cleavage of CD43 MDD during apoptotic cell death (Figure 5.12c and d). These data support the involvement of caspase activation in apoptosis driving CD43 cleavage, and further suggest that a metalloprotease might be responsible for proteolytic cleavage of CD43 MDD on apoptotic CEM.

5.2.5.2. ADAM10 cleaves CD43 MDD during T cell death

Since 1,10-Phenanthroline, Marimastat and GM6001 are all broad-spectrum metalloprotease inhibitors, I decided to test more specific inhibitors of metalloproteases. A class of metalloproteases termed “A Desintegrin And Metalloprotease domain-containing protein” (ADAM) are well known for

cleaving cell surface proteins. Two members of this family, ADAM10 and ADAM17, were of particular potential relevance, since they are expressed on T cells and cleave molecules of immunological interest including diverse growth factors, cytokines, receptors and adhesion molecules [407].

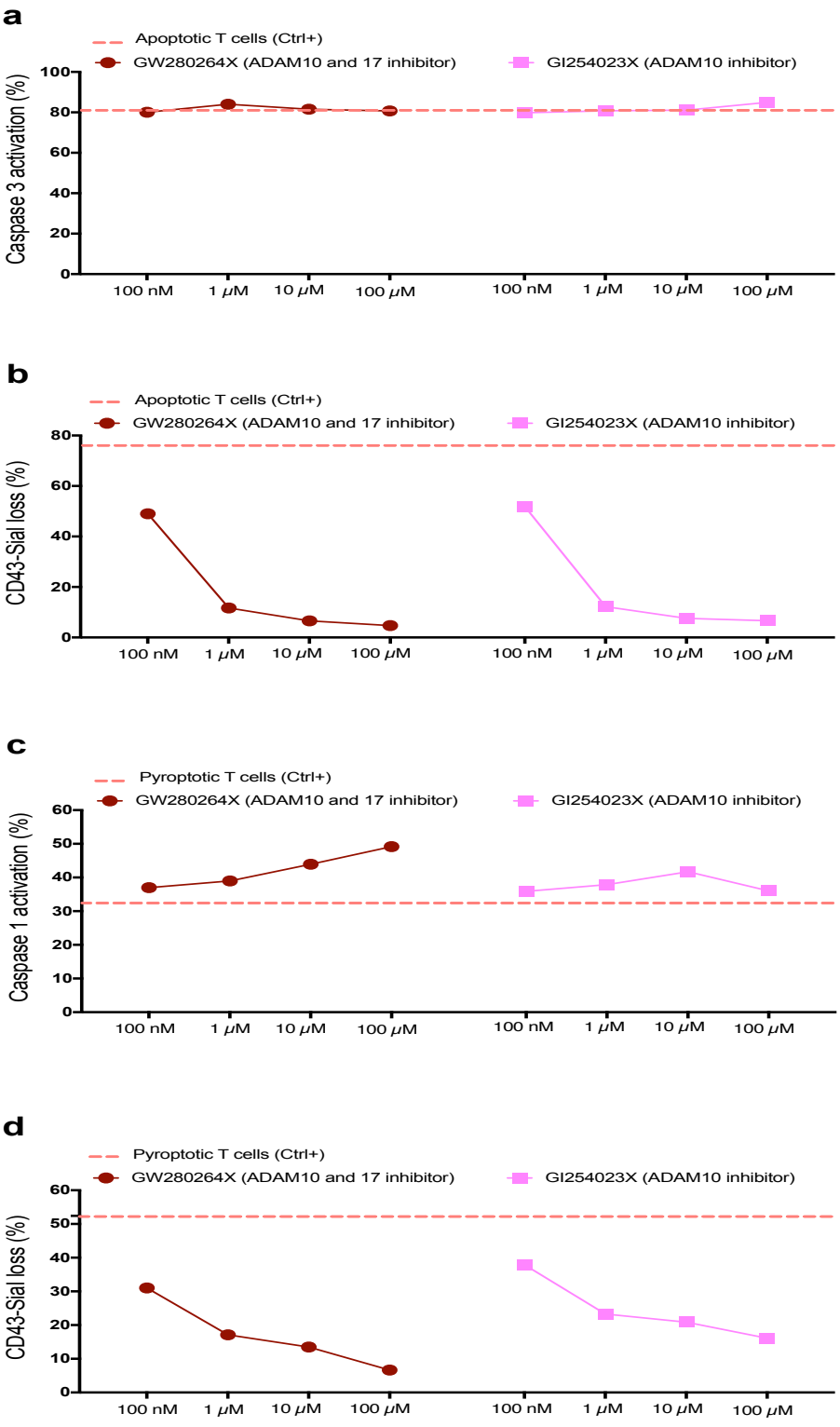


Figure 5.13. Effect of ADAM17 and 10 inhibitors on caspase 3 activation and CD43 cleavage during T cell death. WT-CEM were pre-treated with different concentrations of either GW280264X (ADAM 17 and 10 inhibitor) or GI254023X (ADAM10 inhibitor) for 45 min followed by either 1 µM staurosporine treatment to induce apoptosis or 75 µM nigericin treatment to induce pyroptosis in the presence of inhibitors for 4 h. Subsequently, apoptotic T cells were fixed with 4% FA and stained with DFT-1 mAb CD43 and for cleaved caspase 3 after permeabilisation. Pyroptotic T cells were stained for cleaved caspase 1 representing pyroptosis, and then fixed and stained with DFT-1. **a)** and **b) Effect of GW280264X and GI254023X on apoptotic T cells**. **a**) and **b**) show the effect of these inhibitors on caspase 3 activation and CD43 , respectively. **c) and d) Effect of GW280264X and GI254023X on pyroptotic T cells:** Graph c) and d) show the effect of these inhibitors on caspase 1 activation and CD43 MDD status, respectively.

5.2.5.2.1. ADAM10 inhibitors suggest ADAM10 as the protease cleaving CD43 MDD during cell death

Since specific inhibitors are available for ADAM10 and 17, I decided to investigate their role in proteolytic cleavage of CD43 MDD during apoptotic and pyroptotic cell death.

Initially, I pre-treated WT-CEMs for 45 min with different concentrations (100 nM - 100 µM) of either GW280264X (ADAM17 and 10 inhibitor) or GI254023X (ADAM10-specific inhibitor) before induction of apoptosis and pyroptosis in the presence of the inhibitors. As presented in Figure 5.13a and c, neither GW280264X nor GI254023X prevented cleavage of caspase 3 or 1, implying that they would not interfere with induction of apoptosis or pyroptosis. However, both inhibitors prevented loss of DFT-1 labeling during apoptotic and pyroptotic cell death in a dose dependent-manner (Figure 5.13b and d). Data from a single

experiment (Figure 5.14a, b) and pooled from 3 independent experiments (Figure 5.14c) showed that pre-treatment of WT-CEMs with 10 µM GI254023X significantly reduced DFT-1 labeling during apoptosis and pyroptosis. This result was confirmed using Myc-CD43 CEM pre-treated with 100 µM GI254023X before apoptosis induction and measurement of soluble supernatant CD43-Myc Figure 5.14d. Together, these data strongly support a major role for ADAM10 in the cleavage of CD43 MDD from the surface of apoptotic and pyroptotic CD4+ T cells. Moreover, The ADAM10/17 inhibitors could be used to uncouple the effects down stream processes of apoptosis/pyroptosis versus CD43 cleavage on the uptake of dying T cells by macrophages.

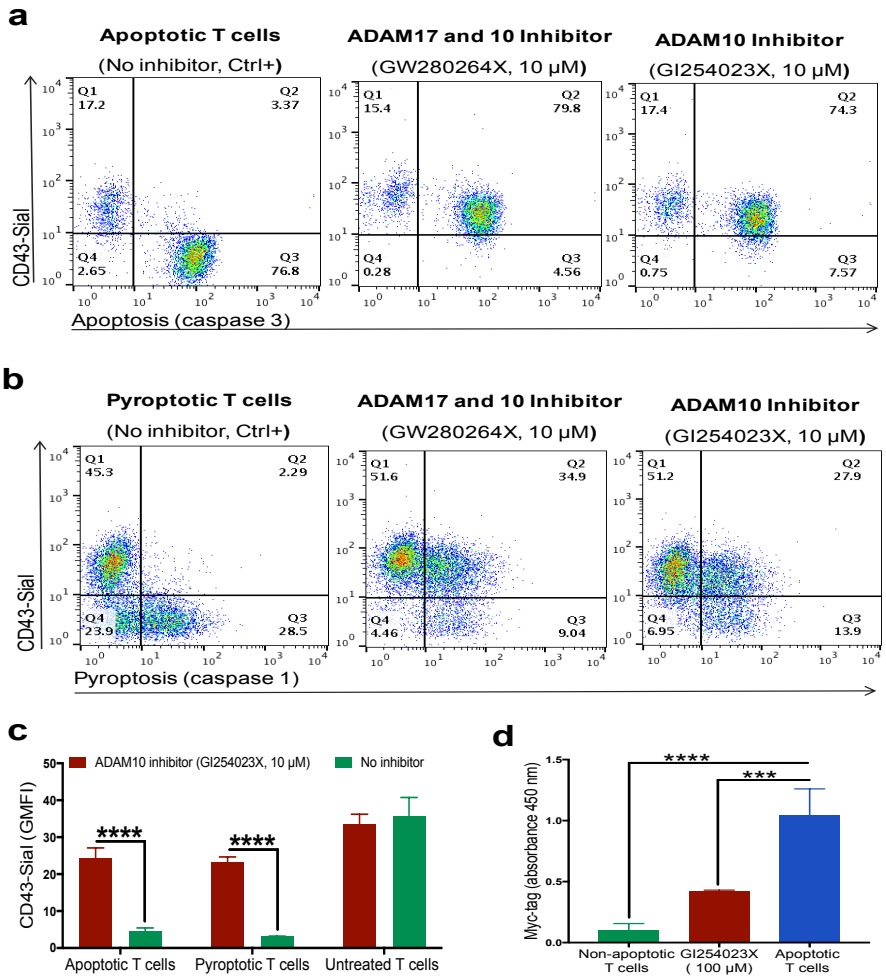


Figure 5.14. Effect of ADAM17 and 10 inhibitors on proteolytic cleavage of CD43 during T cell death. a), b) and **c) Effect of GI254023X on CD43 cleavage during apoptosis and pyroptosis.** WT-CEM were pre-treated with either 10 μM GW280264X or GI254023X for 45 min followed by either 1 μM staurosporine treatment to induce apoptosis or 75 μM nigericin treatment to induce pyroptosis in the presence of inhibitor for 4 h. In **a**), apoptotic T cells were fixed with 4% FA and stained with DFT-1 mAb and for cleaved caspase 3 after permeabilisation. In **b**), pyroptotic T cells were stained for cleaved caspase 1 and then fixed and stained with DFT-1. In **c**), the graph represents data obtained from 3 independent experiments. ****P < 0.0001 tested using two-way ANOVA with Sidak post-test correction. **d) Soluble Myc-CD43 detection in the supernatant of apoptotic Myc-CD43 CEM:** $1x10^8$ Myc-CD43 and CD43-KO CEM were incubated in 1 mL RPMI containing 100 μM GI254023X or remained untreated for 45 min before apoptosis induction with 100 μM staurosporine treatment for 4 h. Subsequently, supernatants were collected by pelleting cells using centrifugation at 500 g for 5 min at 4ºC. Tissue culture protease inhibitor cocktail was added at 1:100 and supernatants were aliquoted and stored at -20ºC. Supernatants were thawed and diluted in 50 μL of 100 mM Na_2CO_3 buffer pH 8.5 for coating wells of 96-well ELISA plates overnight at 4ºC. Biotinylated 9E10 mAb was used to detect CD43 C-terminal Myc-tag in the supernatants. The graph shows data obtained from triplicates. ***P < 0.001 and ****P < 0.0001 tested using one-way ANOVA multiple comparisons with Sidak post-test correction.

5.2.5.2.2. ADAM10-KO T cells reveal ADAM10 is the protease cleaving CD43 MDD during cell death

To further explore the role of ADAM10 in the proteolytic cleavage of CD43 MDD during HIV-1 infection and cell death, and to confirm data collected using ADAM10 inhibitors, I obtained ADAM10-KO CEM generated by Dr. R.A. Russell and Dr. M.D. Moore. Firstly, I investigated the expression of ADAM10 on the surface of WT-CEM and Myc-CD43 CEM KO for ADAM10 using antibody labelling (Figure 5.15).

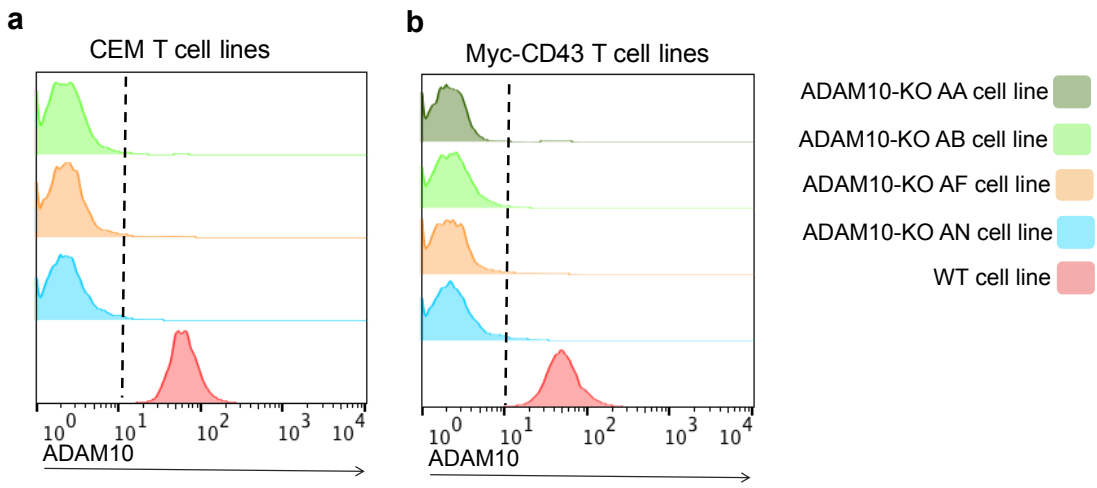


Figure 5.15. Characterisation of ADAM10-KO CEM lines. The histograms represent ADAM10-KO and WT CEM lines, which were fixed with **4%** FA and stained with 11G2 mAb that labels ADAM10 on the surface of CEM. **a) ADAM10-KO and WT- CEM lines. b) ADAM10-KO and Myc-CD43 CEM lines.**

I induced apoptotic and pyroptotic cell death in ADAM10-KO CEM lines including three ADAM10-KO WT-CEM lines (AB, AF and AN) and four ADAM10-KO Myc-CD43 CEM lines (AA, AB, AF and AN) generated using different guide RNAs targeting CRISPR-Cas9. Data from a single experiment (Figure 5.16a and c) and pooled from 4 independent experiments (Figure 5.16b and d) showed that the absence of ADAM10 on the surface of both WT-CEM and Myc-CD43 CEM significantly prevented DFT-1 epitope cleavage during apoptosis (Figure 5.16c). Also, C-20 antibody labeling showed that there was no significant difference between CD43 expression on the surface of apoptotic and non-apoptotic T lines cells (Figure 5.16e – h). Similar data were collected from 4 independent pyroptosis-induction experiments summarised in Figure 5.17.

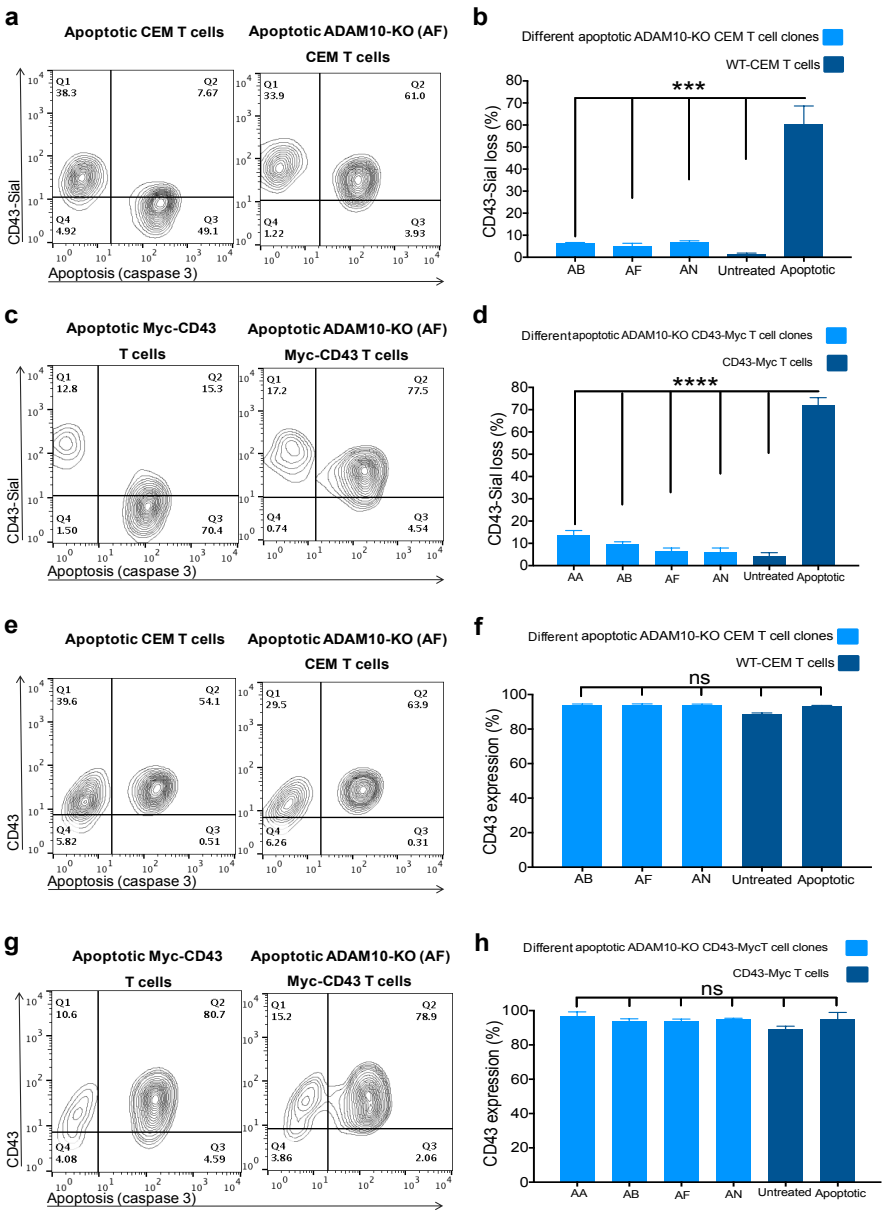


Figure 5.16. Role of ADAM10 in proteolytic cleavage of CD43 from the surface of apoptotic T cells. CEM were treated with 1 µM staurosporine for 4 h, and then fixed with 4% FA. CD43 on fixed cells was stained with either DFT-1 mAb or C-20 Ab followed by permeabilisation and cleaved caspase 3 staining. **a)** and **b) CD43-Sial staining of apoptotic ADAM10-KO and WT-CEMs. c)** and **d) CD43-Sial staining of apoptotic ADAM10-KO and WT Myc-CD43 CEM. e)** and **f) CD43 staining of apoptotic ADAM10-KO and WT-CEM. g) and h) CD43 staining of apoptotic ADAM10-KO and WT Myc-CD43 CEM.** The FACS plots show the gating strategy used to extract data for the following graph. The graphs represent the data obtained from 4 independent experiments. ns = not significant, ***P < 0.001 and ****P < 0.0001 tested using one-way ANOVA multiple comparisons with Sidak post-test correction.

These data together with data collected in the presence of the ADAM10-specific inhibitor (Section 5.2.5.2.1), confirm the role of ADAM10 as the principal metalloprotease cleaving CD43 MDD from the surface of apoptotic and pyroptotic CD4+ T cells.

5.2.5.2.3. Generation of ADAM10-KO and WT HEK cells expressing Myc-CD43

Human embryonic kidney (HEK) cells do not naturally express CD43 on the surface, whereas they do express ADAM10. Therefore, I decided to generate Myc-CD43 transgenic HEK cells allowing me to further investigate the role of ADAM10 in the cleavage of CD43 MDD during cell death. As described in Section 2.1.8.1, I transduced ADAM10-KO and WT HEK cells with lentiviral vectors encoding CD43 with an N-terminal Myc-tag and puromycin-resistance selectable marker. After puromycin selection, I investigated the expression of CD43 on the surface of HEK cells by DFT-1 labeling.

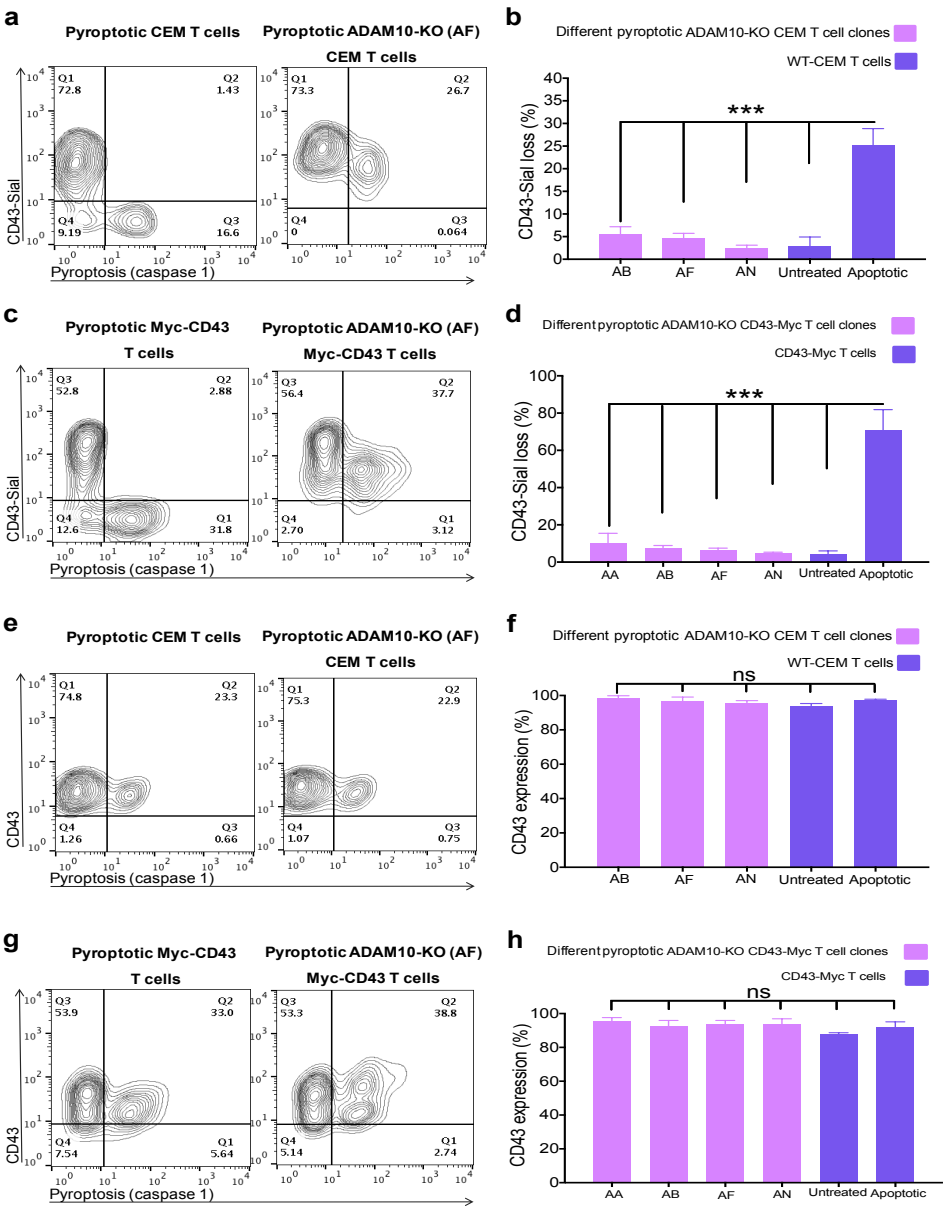


Figure 5.17. Role of ADAM10 in proteolytic cleavage of CD43 from the surface of pyroptotic T cells. CEM were treated with 75 μM nigericin for 4 h followed by cleaved caspase 1 staining representing pyroptosis. Afterwards, cells were fixed and stained for CD43 with either DFT-1 mAb or C-20 Ab. **a)** and **b) CD43-Sial staining of pyroptotic ADAM10-KO and WT-CEM. c)** and **d) CD43-Sial staining of pyroptotic ADAM10-KO and WT Myc-CD43 CEM. e)** and **f) CD43 staining of pyroptotic ADAM10-KO and WT-CEM. g)** and **h) CD43 staining of pyroptotic ADAM10-KO and WT Myc-CD43 CEM.** The FACS plots show the gating strategy used to extract data for the following graphs. The graphs represent the data obtained from 4 independent experiments. ns = not significant and ***P < 0.001 tested using one-way ANOVA multiple comparisons with Sidak post-test correction.

As presented in Figure 5.18, Myc-CD43 transduction of ADAMA10-KO and WT HEK cells was successful. To induce apoptosis, I treated HEK cells with different concentrations of staurosporine (1-10 µM) over different incubation times (1-32 h) including that reported in the literature (1 µM for 12-24 h [408]), yet could only detect ~4% caspase 3 positive HEK cells. Therefore, apoptotic cell induction in HEK cells requires further optimisation.

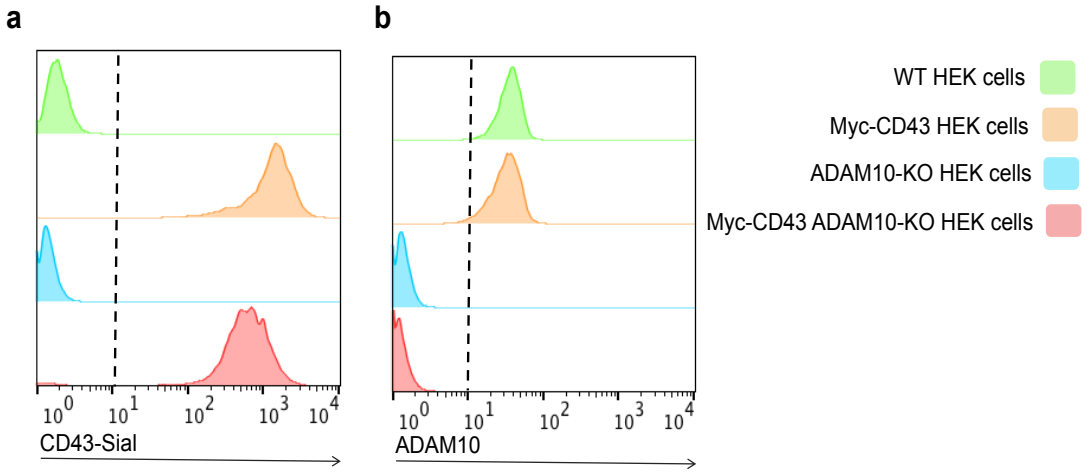


Figure 5.18. Characterisation of Myc-CD43 ADAM10-KO and WT HEK cell. a) CD43-Sial expression. The histograms show different HEK cell lines, which were fixed with **4%** FA and stained with DFT-1 mAb representing expression of sialylated CD43 on the surface of HEK cells. **b) ADAM10 expression:** The histograms show different HEK cell lines, which were fixed with **4%** FA and stained with 11G2 mAb representing expression of ADAM10 on the surface of HEK cells.

5.2.6. The role of CD43 in efferocytic uptake by macrophages

Meesmann et al. [309] reported that apoptotic cell death results in the general surface desialylation of lymphoblasts similar to that observed by Bilyy et al. [382] on apoptotic Jurkat T cells. Moreover, Meesmann et al. have shown that not only further surface desialylation of apoptotic lymphoblasts by neuraminidase treatment, but also desialylation of viable lymphoblasts, leads

to an increase in MDM uptake, implying the role of sialic acid as a don't eat me signal. However, these groups did not identify the specific sialylated molecules implicated in this effect.

From 2004 to 2012, the Beppu laboratory conducted a series of studies indicating that CD43 on the surface of early apoptotic Jurkat T cells forms a cap which interacts with nucleolin on THP-1-derived macrophages resulting in Jurkat uptake [409-411]. They also reported that this interaction is mediated by the sialylpolylactosaminyl chains on CD43 [409, 410, 412]. Moreover, in their most recent study regarding the role of CD43 in the clearance of T cells by macrophages, they reported that treatment of Jurkat T cells with 5 μM cytochalasin B for 30 min capped CD43 on the surface of T cells without apoptosis induction, and that this was sufficient for THP-1 macrophage uptake, suggesting CD43-capping as an eat-me signal [410]. However, I observed significant (~2-fold) increase in the MDM capture of HIV-1-infected CD43-KO CEM compared to the infected WT-CEM line by MDM (Figure 3.9), suggesting the absence of CD43 as an eat me signal on the surface of HIV-1-infected CD4+ T cells. The difference between my results and those of the Beppu lab may relate to the capping of CD43. If the CD43 cap is orientated away from the T cell contact site with the macrophage, then this may have the same effect as my observation of complete removal of the sialylated CD43 MDD.

5.2.6.1. Sialic acid residues on CD43 prevent efferocytic uptake of HIV-1 infected primary CD4+ T cells by MDM

Based on the literature outlined above and significant increases in the MDM uptake of HIV-1-infected CD43-KO CEM discussed in Chapter 3, I sought to investigate the role sialylated carbohydrate chains of CD43 in the MDM capture of HIV-1-infected cells. For this purpose, monocytes isolated from 4 donors were differentiated into MDM while the autologous CD4+ T cells were infected at MOI of 0.01 with HIV-$1_{Bal\text{-}Luc}$ for 7 days. In the meantime, CD43-KO and WT-CEMs were infected with HIV-$1_{NL4.3\text{-}Luc}$ at MOI of 0.01 for 2 and 3 days, respectively. As presented in Figure 5.19a, on day 10, infected T cells were pre-treated with 100 mU Vib. sialidase for 1 h at at 37ºC, and then washed to remove residual sialidase before co-culturing them with MDM. After 1 h, T cells were removed with vigorous washing, MDM were lysed, and luciferase measured. MDM uptake of sialidase-treated primary CD4+ and WT-CEMs was significantly increased by comparison with their untreated counterpart T cells (Figure 5.19b), demonstrating that removal of silaic acid can enhance efferocytosis. However, MDM capture of HIV-1-infected CD43-KO CEM did not significantly change after sialidase treatment (Figure 5.19b), suggesting CD43 as the major source of sialic acid on the surface of CD4+ T cells. These data imply that the modification or loss of the CD43 sialylated MDD on HIV-1-infected CD4+ T cells observed and discussed in this study may promote efferocytic uptake by MDM.

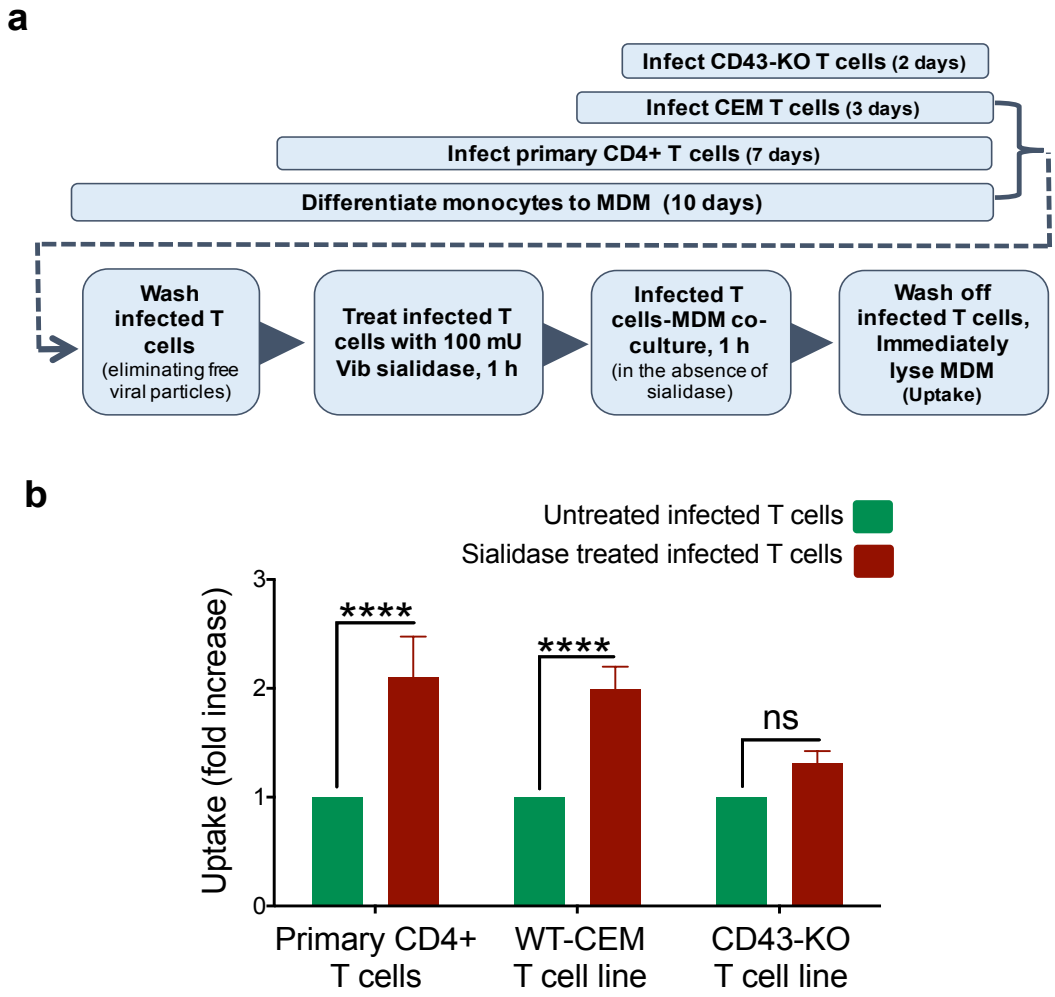


Figure 5.19. The effect of sialidase treatment on the engulfment of HIV-1-infected T cells by MDM. a) The schematic experimental strategy: Monocytes were differentiated into MDM for 10 days, while autologous CD4+ primary T cells were infected at MOI of 0.01 with HIV-$1_{Bal\text{-}Luc}$ for 7 days. Meanwhile, CD43-KO and WT-CEM were infected with HIV-$1_{NL4.3\text{-}Luc}$ at MOI of 0.01 for 2 and 3 days, respectively. On day 10, infected T cells were washed thoroughly to remove cell free viral particles and T cells were pre-treated with 100 mU Vib. sialidase for 1 h at 37ºC. T cells were then washed to remove residual sialidase and co-cultured with MDM for 1 h. Subsequently, infected T cells were removed with vigorous washing and MDM were lysed, and luciferase assayed. **b) Uptake:** The graph shows luciferase signal representing the uptake of infected T cells by MDM. Bars = Mean luciferase signal of MDM co-cultured with infected T cells divided by the mean luciferase signal of infected T cells with the relevant treatment (%). SD for 4 donors, each in triplicate. ns = not significant and ****$p < 0.0001$ tested using two-way ANOVA with Sidak post-test correction.

5.2.6.2. CD43 prevents efferocytosis of healthy CD4+ T cells

In order to explore the role of CD43 in the capture of healthy, desialylated and dying T cells by MDM, I decided to establish a high-throughput assay similar to that established in the lab by Dr. Duncan to investigate the MDM capture of T cells infected with HIV-1 encoding a luciferase reporter signal. As described in Section 2.1.8.2, I transduced CD43-KO and WT-CEM with lentiviral particles encoding a Renilla luciferase plasmid and blasticidin as a selection marker. After blasticidin selection and characterisation of these T cell lines, I used luciferase reporter CD43-KO (CD43-KO Luc) and WT-CEM (WT-CEM Luc) T cells to compare the MDM capture of healthy CD43-KO CEM with WT-CEMs. As shown in Figure 5.20a, isolated monocytes from 3 donors were differentiated into MDM in 10 days. On day 10, CD43-KO Luc and WT-CEM Luc T cells were co-cultured with MDM for 2 h. After removing T cells by vigorous washing, I lysed MDM and measured luciferase signal representing MDM uptake of T cells. As presented in Figure 5.20, healthy CD43-KO CEM were significantly more engulfed by MDM compared to the MDM capture of healthy WT-CEMs, demonstrating that CD43 on the surface healthy CD4+ T cells acts as a don't eat-me signal. However, the role of CD43, its sialic acid residues, the cleavage of its sialylated MDD by ADAM10 and the role of other factors such as phosphatidyl serine (PS) exposure during cell death require further investigation for their roles in efferocytosis.

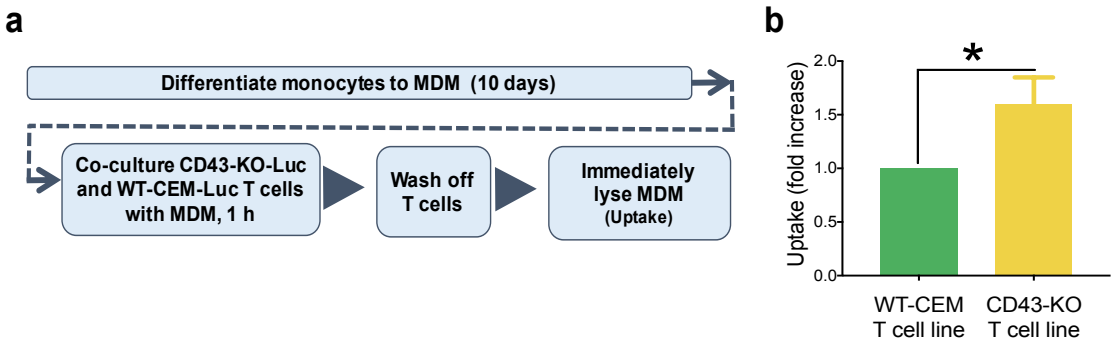


Figure 5.20. The role of CD43 in efferocytic uptake of healthy T cells by MDM. a) Schematic experimental strategy. Monocytes were differentiated into MDM for 10 days. On day 10, healthy CD43-KO Luc and WT-CEM Luc were co-cultured with MDM for 2 h. Afterwards, T cells were removed with vigorous washing and MDM were lysed, and luciferase assayed. **b) Uptake.** The graph shows luciferase signal representing the uptake of T cells by MDM. Bars = Mean luciferase signal of MDM co-cultured with T cells divided by the mean luciferase signal of relevant T cells (%). SD for 3 donors, each in triplicate. *p < 0.05 by one-sample t-test, comparing CD43-KO CEM uptake to a hypothetical value of 1.

5.3. Discussion

In this chapter, I investigated the mechanism of modification of CD43 sialylated MDD on CD4+ T cells during acute HIV-1 infection, and apoptotic and pyroptotic cell death. No studies have elucidated the mechanism underlying these phenomena. However, as outlined earlier in this chapter, the existing literature provided me with clues to design my experiments and navigate my study to uncover the mechanism underlying modification of CD43 sialylated MDD (summarised in Figure 5.21).

Based on my findings, I propose that pyroptotic and apoptotic cell death in CD4+ T cells triggers ADAM10-mediated proteolytic cleavage of the CD43 MDD. My data demonstrate the involvement of caspase activation in apoptosis

and pyroptosis that leads to the proteolytic cleavage of the CD43 MDD. Using specific caspase inhibitors, I ruled out a role for caspase 8 activation as an initiator caspase, and demonstrate the involvement of cleaved caspase 3 and 9 as effector and initiator caspases, respectively, in apoptotic cell death leading to the cleavage of CD43 MDD. By contrast, my demonstration that inhibition of cytoskeletal remodelling and Golgi to plasma membrane trafficking did not prevent CD43 MDD cleavage during apoptosis rules out a mechanism requiring cellular trafficking or recycling of CD43 in this process.

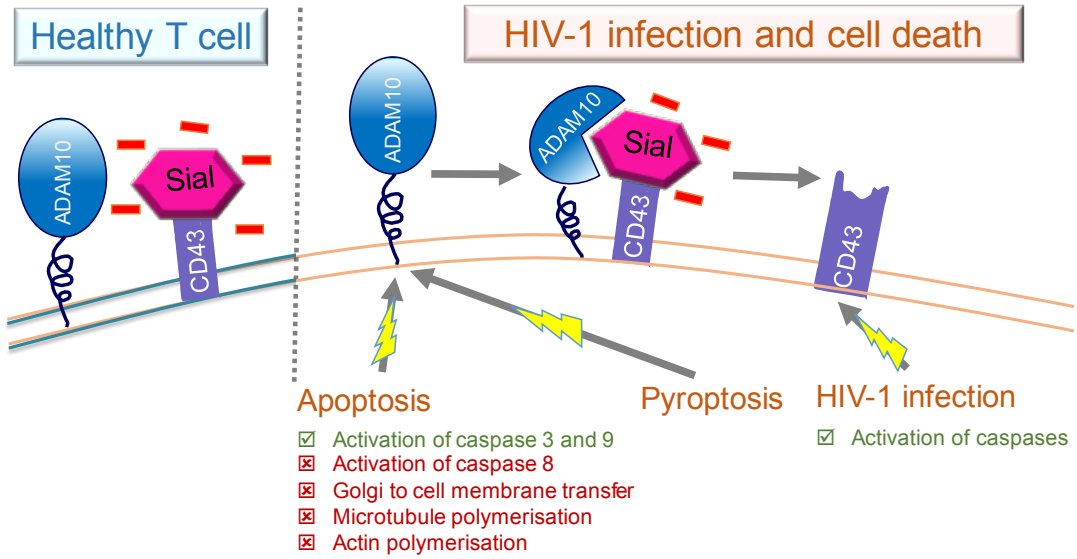


Figure 5.21. Schematic summary showing proposed mechanism of CD43 MDD cleavage on the surface of CD4+ T cells during apoptotic and pyroptotic cell death and HIV-1 infection. Apoptosis: cleavage of pro-caspase 3 and 9 trigger apoptotic cell death driving ADAM10 activation resulting in proteolytic cleavage of the CD43 MDD. **Pyroptosis:** cell death triggers ADAM10 mediated cleavage of the CD43 MDD. **HIV-1 infection:** Activation of caspases trigger modification of the CD43 MDD.

My results regarding the role of CD43 in MDM efferocytic uptake of HIV-1-infected and healthy CD4+ T cells are consistent with the model shown in

Figure 5.22. Inhibition of caspase activation significantly reduces efferocytosis of HIV-1-infected WT-CEMs by MDM, whereas it does not alter the MDM capture of infected CD43-KO CEM, suggesting that CD43 MDD cleavage during acute HIV-1 infection acts as an eat-me signal. Moreover, removing sialic acid residues from infected WT-CEM and primary CD4+ T cells significantly enhances their efferocytic uptake by MDM, while it does not change the uptake of infected CD43-KO CEM by MDM, implying sialic acid residues on CD43 act as a don't eat-me signal on the surface of HIV-1-infected T cells.

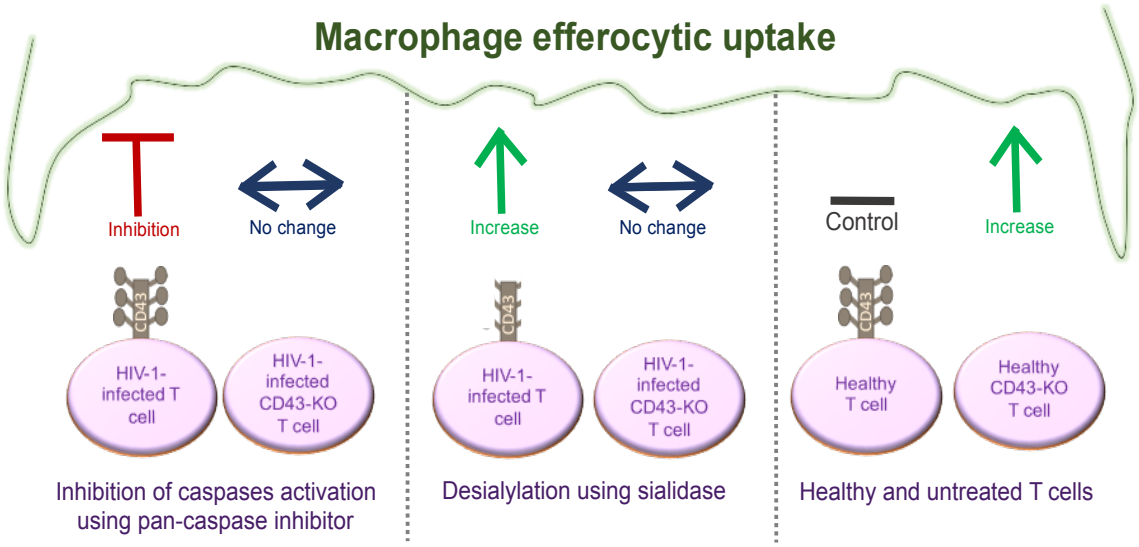


Figure 5.22. Schematic summary showing the role of CD43 on the surface of HIV-1-infected and healthy T cells in MDM efferocytic uptake. Left to right: Inhibition of caspase activation using pan-caspase peptide inhibitor significantly reduces the capture of HIV-1-infected WT-CEMs, whereas it does not alter the MDM capture of HIV-1-infected CD43-KO CEM, implicating cell death in HIV-1 infection-mediated efferocytosis. Removing sialic acid from the surface of HIV-1 infected T cells significantly enhances the uptake of infected WT-CEM and primary CD4+ T cells, whereas it does not alter the MDM uptake of CD43-KO CEM. The MDM efferocytic uptake of healthy CD43-KO CEM is significantly higher compared to their healthy WT-CEM counterparts.

Studying the role of CD43 on the surface of healthy CEM also revealed a significant increase in the MDM efferocytic uptake of CD43-KO CEM by comparison with WT-CEM, implying a role for CD43 as a don't eat-me signal on the surface of healthy CD4+ T cells.

The Beppu laboratory is the only laboratory which have investigated the role of CD43 in the MDM efferocytic uptake of apoptoic T cells. Based on their studies, CD43 forms a cap on early apoptotic T cell recognised by nucleolin on the macrophage resulting in the engulfment of dying T cells [409-411]. Eda et al. used DFT-1 labelling in their studies, similar to my study [409]. However, they reported that CD43 forms a transient cap in 8% of etoposide treated Jurkat T cells using fluorescent imaging [409]. The cap formation occurs 2 h into etoposide treatment of Jurkats followed by CD43 degradation after 4 h. It was suggested that the cap formation was caused by caspase activation and occurred prior to PS exposure [409]. As mentioned in Chapter 4, I supervised Miss Rachael Harrison for her FHS project in which she optimised the induction of apoptotic cell death in WT-CEM and Jurkat T cell lines using etoposide. Her data confirmed and extended my results showing a direct correlation between caspase 3 activation and CD43 MDD cleavage during apoptosis using another T cell line and an alternative inducer of apoptosis. Therefore, Miss Harrison's data and mine contradict what Eda et al. reported. However, live imaging of Jurkat T cells treated with 10 μM etoposide (used concentration by Eda et al.) and labeled with C-20 will allow us to investigate whether CD43 on the surface of apoptotic T cells may form a cap prior to the CD43 MDD cleavage.

As mentioned above, the Beppu lab proposed that nucleolin, a nuclear receptor expressed on MDM, binds CD43 on dying Jurkats triggering their uptake by MDM [410]. I have not investigated the potential for specific macrophage receptors in the uptake of dying or HIV-1-infected T cells, as my model is based on the loss of electrostatic and steric inhibition when CD43 MDD is removed. However, at this stage I cannot rule out the possibility that CD43 MDD cleavage exposes a specific ligand or ligands for a macrophage receptor that can mediate phagocytosis. Further study will be required to interrogate this.

Chapter 6: Concluding remarks

6.1. Summary

Macrophages play an essential role in the maintenance of tissue homeostasis and regulation of immune responses by efferocytic uptake of dying and pathogen-infected cells [209, 245, 413]. Moreover, macrophages have a key role in the pathogenesis of HIV-1 infection as they form long-lived viral reservoirs and disseminate the infection to the CNS [114]. Baxter et al. recently reported that macrophages selectively recognise and engulf HIV-1-infected T cells resulting in the efficient and productive infection of macrophages [339]. However, the signals for the macrophage efferocytic capture of the infected T cell remain undefined, but cell death appears to be an important component of this recognition. Thus, in this thesis, the loss of CD43 membrane distal domain (MDD) from the surface of dying and HIV-1 infected CD4+ T cells as a putative new eat-me signal has been studied. Furthermore, the mechanism of CD43 MDD cleavage during apoptotic and pyroptotic cell death, and HIV-1 infection, has been described. Results presented here provide evidence that:

i) Efferocytic capture of HIV-1-infected CD4+ T cells by macrophages is independent of HIV-1 Env interactions with macrophage receptor(s);
ii) Macrophage ICAM-1 is involved in the efferocytic uptake of HIV-1-infected CD4+ T cells, however neither LFA-1 or Mac-1 (ICAM-1 conventional ligands) nor CD43 (ICAM-1 unconventional ligand) on the infected T cell appear to acts as the counterpart to ICAM-1 in this process;
iii) CD43 on the surface of HIV-1-infected and healthy CD4+ T cells acts as a don’t eat-me signal;

iv) CD43 is the main sialic acid source on the surface of CD4+ T cells, and the removal of sialic acid residues from the surface of HIV-1-infected CD4+ T cells acts as an eat-me signal;
v) The CD43 MDD on CD4+ T cells is modified during HIV-1 infection and is linked to caspase activation; and the inhibition of caspase activation reduces macrophage efferocytic uptake of HIV-1-infected CD4+ T cells;
vi) Activation of caspase 3 and 9 during apoptotic cell death is associated with the proteolytic cleavage of CD43 MDD
vii) ADAM10 proteolytically cleaves the CD43 MDD from the surface of apoptotic and pyroptotic CD4+ T cells.

To ensure that the T cell-macrophage co-culture model used in my study was as representative as possible of in vivo HIV-1 infection and cell death, primary macrophages and autologous CD4+ T cells were utilised wherever feasible. In addition to the well-established assay used for investigation of macrophage capture of infected T cells, a novel high-throughput cell-based assay was designed by generation of reporter T cell lines in this thesis to investigate macrophage efferocytic uptake of healthy and dying T cells. Immunofluorescent labelling and flow cytometry technology were utilised extensively to characterise CD43 MDD modification of multiple transgenic cell lines generated in this study including Myc-tag CD43 CEM T cells and HEK cells. In addition, ADAM10-KO T cell lines were used to probe the role of ADAM10 as the sheddase cleaving CD43 MDD from the surface of dying T cells.

6.2. Future perspectives

6.2.1. CD43 shedding during cell death

Data presented in this thesis show the proteolytic cleavage of CD43 MDD by ADAM10 from the surface of apoptotic and pyroptotic CD4+ T cells, which were collected using antibody labelling of dying cells and direct ELISA detecting soluble CD43 MDD in the supernatant of dying cells. However, to further validate these data and define the molecular weight of soluble CD43 MDD, western blotting ought to be conducted on the soluble MDD.

6.2.2. ADAM10 activity in CD43 shedding during HIV-1 infection and cell death

In this study, I successfully showed that ADAM10 proteolytically cleaves the CD43 MDD from the surface of a CD4+ T cell line undergoing apoptotic and pyroptotic cell death. However, the role of ADAM10 in CD43 MDD modification during HIV-1 infection needs to be studied, and the ADAM10-KO WT-CEM line provides a great tool for future investigation. Moreover, Myc-CD43 ADAM10-KO and WT HEK cell lines generated in this study will allow me to probe CD43 shedding and the role of ADAM10 as the sheddase in non-hematopoietic lineage cells, not expressing CD43 naturally.

Using primary CD4+ T cells, I was able to confirm my findings regarding CD43 MDD modification during apoptotic and pyroptotic cell death. Based on the results presented in this thesis, CD43 MDD is modified on the surface of HIV-1-infected T cell lines. So as to translate this finding into a more physiologically-

relevant model, modification of CD43 MDD shall be studied using dying and HIV-1-infected primary CD4+ T cells.

6.2.3. PS as a potential trigger of ADAM10 activation

The triggers that activate ADAM10 are not fully understood [335], and are unknown in the context of CD43 cleavage on dying and HIV-1 infected cells. However, recently it has been proposed that surface-PS exposure regulates ADAM17 shedding activity by deactivating the inhibitory cysteine-rich domain using close-range electrostatic interactions [414].

Since ADAM10 is a close structural relative of ADAM17 and containes an inhibitory cysteine-rich domain [415], and PS exposure is the common surface-signal on HIV-1-infected and dying (apoptotic and pyroptotic) T cells, the role of PS exposure as an ADAM10 trigger in the proteolytic cleavage of CD43 is worthy of investigation. To interrogate this, myeloid-lineage cell lines such as the Raji human B cell line and the HL-60 human promyelocytic line that fail to translocate PS to the outer leaflet of the plasma membrane during apoptosis due to low scamblase expression can be used [414]. Using these cell lines, one can investigate surface expression of ADAM10, and the cleavage of CD43 MDD during apoptotic and pyroptotic cell death. If no or low CD43 shedding phenotype is observed in these cells, one can transduce ADAM10-KO CEM cells with lentiviral particles encoding ADAM10 mutated in the inhibitory cysteine-rich domain, which by analogy with ADAM17 should prevent PS activation of ADAM10 catalysis [414].

As the common leading feature of apoptotic and pyroptotic cell death is activation of different caspases, the role of caspase activation was studied in the cleavage of CD43 MDD. However, the correlation between caspase activation and CD43 MDD cleavage was only observed during apoptosis, and whether caspases play a direct or indirect role in ADAM10 activation remains to be seen.

6.2.4. ADAM10 and CD43 membrane localisation during HIV-1 infection, cell death and efferocytosis

As discussed in Chapter 5, studies conducted by the Beppu laboratory reported that CD43 forms a cap on the apoptotic T cell that may interact with nucleolin on the macrophage leading to the efferocytic uptake of apoptotic T cells. To probe whether CD43 molecules form a cap before being proteolytically cleaved by ADAM10, and to investigate the T cell-macrophage efferocytic synapse, one can utilise live fluorescence microscopy and high-resolution fluorescence imaging to track the localisation of ADAM10 and CD43 on the T cell membrane during regulated cell death and HIV-1 infection. Moreover, if the role of PS exposure as an ADAM10 activator is implicated, one can investigate the dynamics of PS exposure in relation to CD43 shedding by ADAM10 using annexin-V labelling, a specific probe for PS exposure, and live cell imaging.

6.2.5. CD43 membrane proximal domain and efferocytosis

Results presented in this thesis suggest that CD43 and its sialic acid residues may act as a don’t eat-me signal due to imparting steric and electrostatic barriers between the T cell and the efferocyte. However, the potential role of CD43 membrane proximal domain (MPD) on the surface of HIV-1-infected and

dying CD4+ T cells as a ligand for macrophage efferocytic receptor(s) needs to be investigated. To probe this, ADAM10 cleavage site(s) on CD43 can be predicted using websites such as PROSPER and PeptideCutter, and CD43-KO CEM can be transduced by lentiviral particles encoding CD43 with mutation(s) in predicted cleavage site(s). If the cleavage site is discovered, transgenic CD43-KO CEM expressing CD43 MPD can be used to investigate; i) surface binding of potential macrophage soluble receptors including ICAM-1 and nucleolin, and ii) the effect of CD43 MPD on the efferocytic uptake of HIV-1-infected and dying T cells.

Lastly, as described earlier, CD47 is one of the major don't eat-me signals expressed not only on the surface of most normal cells, but frequently over-expressed on cancerous cells as a mechanism to prevent their clearance by phagocytes [305]. This inhibitory effect is the result of CD47 interaction with SIRPa on the efferocyte [306]. However, data presented in this study suggest that, unlike CD47, the potential role of CD43 as a don't eat-me signal is due to its biophysical features including it is long negatively charged extracellular domain (~45 nm) and abundance on the T cell surface (~20%) [319, 320]. Moreover, results presented in this study imply that the absence/cleavage of CD43 on/from the surface of HIV-1-infected T cells can trigger their efficient efferocytic uptake by macrophages suggesting that the absence of CD43 MDD is an eat-me signal. Interestingly, a study conducted by Seo et al. [325] has reported that after the shedding of CD43 MDD from the surface of activated murine T cells, the CD43 MPD is translocated to the nucleolus. Altogether, these findings suggest that the potential efferocytic uptake triggered by the

CD43 MDD shedding from the surface of HIV-1 infected or dying T cells is unlikely to be due to the interaction of CD43 MPD with an efferocytic receptor on the macrophage. Furthermore, antibodies against CD47 have been shown to lead to the uptake and clearance of leukaemic cells by macrophages in vitro and inhibition of tumour engraftment in vivo [307]. Whereas, it has been shown that antibodies against CD43 [368] and the absence of CD43 on CD43-KO cells [369] induce homotypic adhesion, highlighting the regulatory role of CD43's biophysical features in the pro- and anti-adhesive intracellular interactions between leukocytes. Taken together, these findings and observations suggest that the potential role of CD43 as a don't eat-me signal medically can not be exploited like CD47.

6.3. Contribution to the field

Based on the results presented in this thesis and points discussed in Section 6.2, I propose the following model for CD43 shedding from HIV-1-infected and dying CD4+ T cells and its implication on macrophage efferocytic uptake (Figure 6.1).

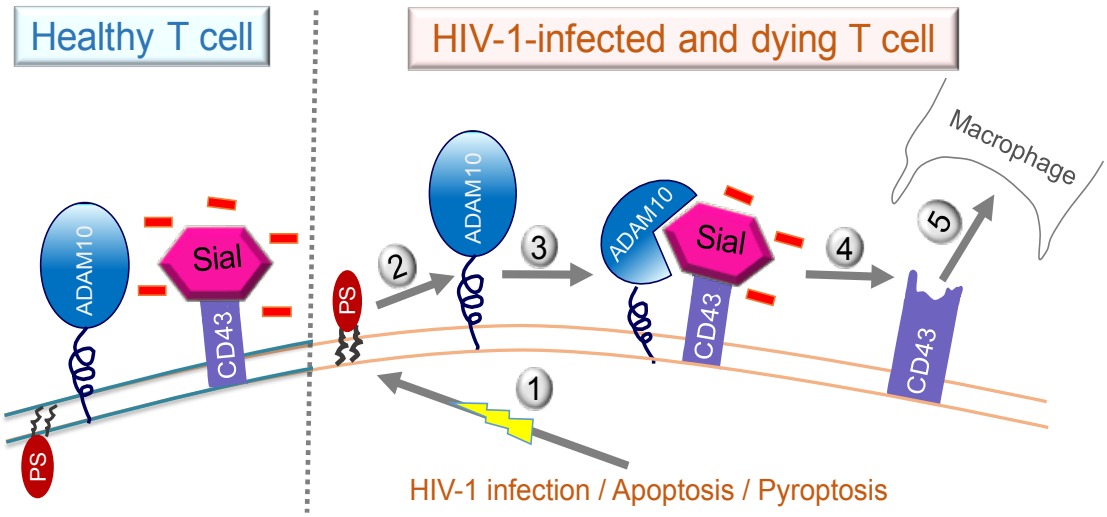


Figure 6.1. Schematic model for CD43 shedding by ADAM10 from the surface of HIV-1-infected and dying T cells and its effect on efferocytosis: 1) HIV-1 infection and apoptotic and pyroptotic cell death leads to the exposure of PS on the T cell surface; 2) PS-exposure may deactivate the ADAM10 inhibitory cysteine-rich domain using close-range electrostatic interactions; 3), Activated ADAM10 proteolytically cleaves the CD43 MDD 4) Exposure of the non-sialylated CD43 MPD domain may participate in macrophage efferocytic capture of infected and dying T cells.

An important question that follows on from this work is the role of CD43 and its cleavage by ADAM10 sheddase in the clearance of HIV-1 infected and dying T cells in vivo. Results presented here suggest that HIV-1 infection and cell death (apoptosis and pyroptosis) trigger the proteolytic cleavage of CD43 MDD by

ADAM10 sheddase mediating macrophage efferocytic uptake. Unravelling the CD43 shedding mechanism during HIV-1 infection and cell death, and its role in macrophage efferocytic uptake may have important implications for intervention in:

i) A cell-to-cell mode of T cell and macrophage infection by HIV-1;
ii) A fundamental mechanism regulating efferocytosis of dying T cells by macrophages;
iii) The role of ADAM10 in several inflammatory and autoimmune diseases that may be associated with defective efferocytosis.

References

1. Bella, J., et al., *The structure of the two amino-terminal domains of human ICAM-1 suggests how it functions as a rhinovirus receptor and as an LFA-1 integrin ligand.* Proceedings of the National Academy of Sciences of the United States of America, 1998. **95**(8): p. 4140-5.
2. Girum, T., A. Wasie, and A. Worku, *Trend of HIV/AIDS for the last 26 years and predicting achievement of the 90-90-90 HIV prevention targets by 2020 in Ethiopia: a time series analysis.* Bmc Infectious Diseases, 2018. **18**.
3. *Pneumocystis pneumonia--Los Angeles.* MMWR. Morbidity and mortality weekly report, 1981. **30**(21): p. 250-2.
4. Gottlieb, M.S., et al., *Pneumocystis carinii pneumonia and mucosal candidiasis in previously healthy homosexual men: evidence of a new acquired cellular immunodeficiency.* N Engl J Med, 1981. **305**(24): p. 1425-31.
5. Masur, H., et al., *Opportunistic infection in previously healthy women. Initial manifestations of a community-acquired cellular immunodeficiency.* Ann Intern Med, 1982. **97**(4): p. 533-9.
6. Centers for Disease, C., *Pneumocystis carinii pneumonia among persons with hemophilia A.* MMWR Morb Mortal Wkly Rep, 1982. **31**(27): p. 365-7.
7. Van de Perre, P., et al., *Acquired immunodeficiency syndrome in Rwanda.* Lancet, 1984. **2**(8394): p. 62-5.
8. Piot, P., et al., *Acquired immunodeficiency syndrome in a heterosexual population in Zaire.* Lancet, 1984. **2**(8394): p. 65-9.
9. De Cock, K.M., H.W. Jaffe, and J.W. Curran, *The evolving epidemiology of HIV/AIDS.* AIDS, 2012. **26**(10): p. 1205-13.
10. El-Sadr, W.M., et al., *Scale-up of HIV treatment through PEPFAR: a historic public health achievement.* Journal of acquired immune deficiency syndromes, 2012. **60 Suppl 3**: p. S96-104.
11. Beyrer, C., et al., *Global epidemiology of HIV infection in men who have sex with men.* Lancet, 2012. **380**(9839): p. 367-77.
12. Alizon, M., et al., *Molecular cloning of lymphadenopathy-associated virus.* Nature, 1984. **312**(5996): p. 757-60.
13. Wain-Hobson, S., M. Alizon, and L. Montagnier, *Relationship of AIDS to other retroviruses.* Nature, 1985. **313**(6005): p. 743.
14. Wain-Hobson, S., et al., *Nucleotide sequence of the AIDS virus, LAV.* Cell, 1985. **40**(1): p. 9-17.
15. Tebit, D.M. and E.J. Arts, *Tracking a century of global expansion and evolution of HIV to drive understanding and to combat disease.* The Lancet infectious diseases, 2011. **11**(1): p. 45-56.
16. Sharp, P.M. and B.H. Hahn, *Origins of HIV and the AIDS pandemic.* Cold Spring Harbor perspectives in medicine, 2011. **1**(1): p. a006841.
17. Peeters, M., et al., *Risk to human health from a plethora of Simian immunodeficiency viruses in primate bushmeat.* Emerging Infectious Diseases, 2002. **8**(5): p. 451-457.
18. Worobey, M., et al., *Direct evidence of extensive diversity of HIV-1 in Kinshasa by 1960.* Nature, 2008. **455**(7213): p. 661-U57.

19. Zhu, T.F., et al., *An African HIV-1 sequence from 1959 and implications for the origin of the epidemic.* Nature, 1998. **391**(6667): p. 594-597.
20. Sharp, P.M. and B.H. Hahn, *Origins of HIV and the AIDS Pandemic.* Cold Spring Harbor Perspectives in Medicine, 2011. **1**(1).
21. Kiwanuka, N., et al., *Effect of human immunodeficiency virus Type 1 (HIV-1) subtype on disease progression in persons from Rakai, Uganda, with incident HIV-1 infection.* J Infect Dis, 2008. **197**(5): p. 707-13.
22. Vermund, S.H. and A.J. Leigh-Brown, *The HIV Epidemic: High-Income Countries.* Cold Spring Harb Perspect Med, 2012. **2**(5): p. a007195.
23. Hu, W.S. and S.H. Hughes, *HIV-1 reverse transcription.* Cold Spring Harbor perspectives in medicine, 2012. **2**(10).
24. Collins, D.R. and K.L. Collins, *HIV-1 accessory proteins adapt cellular adaptors to facilitate immune evasion.* PLoS Pathog, 2014. **10**(1): p. e1003851.
25. Merk, A. and S. Subramaniam, *HIV-1 envelope glycoprotein structure.* Current Opinion in Structural Biology, 2013. **23**(2): p. 268-276.
26. Ott, D.E., et al., *Actin-binding cellular proteins inside human immunodeficiency virus type 1.* Virology, 2000. **266**(1): p. 42-51.
27. Zanetti, G., et al., *Cryo-electron tomographic structure of an immunodeficiency virus envelope complex in situ.* PLoS Pathog, 2006. **2**(8): p. e83.
28. Liu, J., et al., *Molecular architecture of native HIV-1 gp120 trimers.* Nature, 2008. **455**(7209): p. 109-13.
29. Hu, G., et al., *Structural Comparison of HIV-1 Envelope Spikes with and without the V1/V2 Loop.* J Virol, 2010.
30. White, T.A., et al., *Molecular architectures of trimeric SIV and HIV-1 envelope glycoproteins on intact viruses: strain-dependent variation in quaternary structure.* PLoS Pathog, 2010. **6**(12): p. e1001249.
31. Lee, J.H., G. Ozorowski, and A.B. Ward, *Cryo-EM structure of a native, fully glycosylated, cleaved HIV-1 envelope trimer.* Science, 2016. **351**(6277): p. 1043-1048.
32. Sundquist, W.I. and H.G. Krausslich, *HIV-1 assembly, budding, and maturation.* Cold Spring Harbor perspectives in medicine, 2012. **2**(7): p. a006924.
33. Perelson, A.S., et al., *HIV-1 dynamics in vivo: Virion clearance rate, infected cell life-span, and viral generation time.* Science, 1996. **271**(5255): p. 1582-1586.
34. Saphire, A.C., et al., *Syndecans serve as attachment receptors for human immunodeficiency virus type 1 on macrophages.* Journal of virology, 2001. **75**(19): p. 9187-200.
35. Mondor, I., S. Ugolini, and Q.J. Sattentau, *Human immunodeficiency virus type 1 attachment to HeLa CD4 cells is CD4 independent and gp120 dependent and requires cell surface heparans.* Journal of virology, 1998. **72**(5): p. 3623-34.
36. Ugolini, S., I. Mondor, and Q.J. Sattentau, *HIV-1 attachment: another look.* Trends in Microbiology, 1999. **7**(4): p. 144-149.
37. Geijtenbeek, T.B., et al., *DC-SIGN, a dendritic cell-specific HIV-1-binding protein that enhances trans-infection of T cells.* Cell, 2000. **100**(5): p. 587-97.
38. Ballana, E., et al., *Cell adhesion through alphaV-containing integrins is required for efficient HIV-1 infection in macrophages.* Blood, 2009. **113**(6): p. 1278-86.

39. Arthos, J., et al., *HIV-1 envelope protein binds to and signals through integrin alpha4beta7, the gut mucosal homing receptor for peripheral T cells.* Nature immunology, 2008. **9**(3): p. 301-9.
40. Dalgleish, A.G., et al., *The CD4 (T4) antigen is an essential component of the receptor for the AIDS retrovirus.* Nature, 1984. **312**(5996): p. 763-7.
41. Klatzmann, D., et al., *Selective tropism of lymphadenopathy associated virus (LAV) for helper-inducer T lymphocytes.* Science, 1984. **225**(4657): p. 59-63.
42. Dragic, T., et al., *HIV-1 entry into CD4+ cells is mediated by the chemokine receptor CC-CKR-5.* Nature, 1996. **381**(6584): p. 667-73.
43. Deng, H., et al., *Identification of a major co-receptor for primary isolates of HIV-1.* Nature, 1996. **381**(6584): p. 661-6.
44. Feng, Y., et al., *HIV-1 entry cofactor: functional cDNA cloning of a seven-transmembrane, G protein-coupled receptor.* Science, 1996. **272**(5263): p. 872-7.
45. Wilen, C.B., J.C. Tilton, and R.W. Doms, *HIV: cell binding and entry.* Cold Spring Harbor perspectives in medicine, 2012. **2**(8).
46. Engelman, A. and P. Cherepanov, *The structural biology of HIV-1: mechanistic and therapeutic insights.* Nat Rev Microbiol, 2012. **10**(4): p. 279-90.
47. Berger, E.A., et al., *A new classification for HIV-1.* Nature, 1998. **391**(6664): p. 240-240.
48. Mercer, J. and A. Helenius, *Virus entry by macropinocytosis.* Nat Cell Biol, 2009. **11**(5): p. 510-20.
49. Miyauchi, K., et al., *HIV enters cells via endocytosis and dynamin-dependent fusion with endosomes.* Cell, 2009. **137**(3): p. 433-44.
50. Dragic, T., et al., *A binding pocket for a small molecule inhibitor of HIV-1 entry within the transmembrane helices of CCR5.* Proceedings of the National Academy of Sciences of the United States of America, 2000. **97**(10): p. 5639-44.
51. Kilby, J.M., et al., *Potent suppression of HIV-1 replication in humans by T-20, a peptide inhibitor of gp41-mediated virus entry.* Nature medicine, 1998. **4**(11): p. 1302-7.
52. Goldstone, D.C., et al., *HIV-1 restriction factor SAMHD1 is a deoxynucleoside triphosphate triphosphohydrolase.* Nature, 2011. **480**(7377): p. 379-82.
53. Stremlau, M., et al., *Specific recognition and accelerated uncoating of retroviral capsids by the TRIM5alpha restriction factor.* Proceedings of the National Academy of Sciences of the United States of America, 2006. **103**(14): p. 5514-9.
54. Sheehy, A.M., et al., *Isolation of a human gene that inhibits HIV-1 infection and is suppressed by the viral Vif protein.* Nature, 2002. **418**(6898): p. 646-50.
55. Malim, M.H. and P.D. Bieniasz, *HIV Restriction Factors and Mechanisms of Evasion.* Cold Spring Harbor perspectives in medicine, 2012. **2**(5): p. a006940.
56. Sheehy, A.M., N.C. Gaddis, and M.H. Malim, *The antiretroviral enzyme APOBEC3G is degraded by the proteasome in response to HIV-1 Vif.* Nature medicine, 2003. **9**(11): p. 1404-7.
57. Marin, M., et al., *HIV-1 Vif protein binds the editing enzyme APOBEC3G and induces its degradation.* Nature medicine, 2003. **9**(11): p. 1398-403.
58. Baltimore, D., *RNA-dependent DNA polymerase in virions of RNA tumour viruses.* Nature, 1970. **226**(5252): p. 1209-11.
59. Arts, E.J. and D.J. Hazuda, *HIV-1 antiretroviral drug therapy.* Cold Spring Harbor perspectives in medicine, 2012. **2**(4): p. a007161.

60. Merluzzi, V.J., et al., *Inhibition of HIV-1 replication by a nonnucleoside reverse transcriptase inhibitor.* Science, 1990. **250**(4986): p. 1411-3.
61. Craigie, R. and F.D. Bushman, *HIV DNA Integration.* Cold Spring Harbor perspectives in medicine, 2012. **2**(7): p. a006890.
62. Schroder, A.R., et al., *HIV-1 integration in the human genome favors active genes and local hotspots.* Cell, 2002. **110**(4): p. 521-9.
63. Bushman, F.D. and R. Craigie, *Integration of Human-Immunodeficiency-Virus DNA - Adduct Interference Analysis of Required DNA Sites.* Proceedings of the National Academy of Sciences of the United States of America, 1992. **89**(8): p. 3458-3462.
64. Ciuffi, A., et al., *A role for LEDGF/p75 in targeting HIV DNA integration.* Nature medicine, 2005. **11**(12): p. 1287-9.
65. Hazuda, D.J., et al., *Inhibitors of strand transfer that prevent integration and inhibit HIV-1 replication in cells.* Science, 2000. **287**(5453): p. 646-50.
66. Liu, J., et al., *Specific NF-kappa B subunits act in concert with Tat to stimulate human immunodeficiency virus type 1 transcription.* Journal of virology, 1992. **66**(6): p. 3883-7.
67. Kinoshita, S., et al., *Host control of HIV-1 parasitism in T cells by the nuclear factor of activated T cells.* Cell, 1998. **95**(5): p. 595-604.
68. Zhu, Y., et al., *Transcription elongation factor P-TEFb is required for HIV-1 tat transactivation in vitro.* Genes & development, 1997. **11**(20): p. 2622-32.
69. Wei, P., et al., *A novel CDK9-associated C-type cyclin interacts directly with HIV-1 Tat and mediates its high-affinity, loop-specific binding to TAR RNA.* Cell, 1998. **92**(4): p. 451-62.
70. Bieniasz, P.D., et al., *Recruitment of a protein complex containing Tat and cyclin T1 to TAR governs the species specificity of HIV-1 Tat.* The EMBO journal, 1998. **17**(23): p. 7056-65.
71. Siliciano, R.F. and W.C. Greene, *HIV latency.* Cold Spring Harbor perspectives in medicine, 2011. **1**(1): p. a007096.
72. Rittner, K., et al., *The human immunodeficiency virus long terminal repeat includes a specialised initiator element which is required for Tat-responsive transcription.* Journal of molecular biology, 1995. **248**(3): p. 562-80.
73. Sodroski, J., et al., *Trans-acting transcriptional regulation of human T-cell leukemia virus type III long terminal repeat.* Science, 1985. **227**(4683): p. 171-3.
74. Sodroski, J., et al., *A transcriptional activator protein encoded by the x-lor region of the human T-cell leukemia virus.* Science, 1985. **228**(4706): p. 1430-4.
75. Weinberger, L.S., et al., *Stochastic gene expression in a lentiviral positive-feedback loop: HIV-1 Tat fluctuations drive phenotypic diversity.* Cell, 2005. **122**(2): p. 169-82.
76. Burnett, J.C., et al., *Control of stochastic gene expression by host factors at the HIV promoter.* PLoS pathogens, 2009. **5**(1): p. e1000260.
77. Karn, J. and C.M. Stoltzfus, *Transcriptional and posttranscriptional regulation of HIV-1 gene expression.* Cold Spring Harbor perspectives in medicine, 2012. **2**(2): p. a006916.
78. Karn, J. and C.M. Stoltzfus, *Transcriptional and posttranscriptional regulation of HIV-1 gene expression.* Cold Spring Harb Perspect Med, 2012. **2**(2): p. a006916.

79. Spearman, P., et al., *Membrane binding of human immunodeficiency virus type 1 matrix protein in vivo supports a conformational myristyl switch mechanism.* Journal of Virology, 1997. **71**(9): p. 6582-6592.
80. Freed, E.O., et al., *Single Amino-Acid Changes in the Human-Immunodeficiency-Virus Type-1 Matrix Protein Block Virus Particle-Production.* Journal of Virology, 1994. **68**(8): p. 5311-5320.
81. Ono, A., J.M. Orenstein, and E.O. Freed, *Role of the gag matrix domain in targeting human immunodeficiency virus type 1 assembly.* Journal of Virology, 2000. **74**(6): p. 2855-2866.
82. Ono, A., et al., *Phosphatidylinositol (4,5) bisphosphate regulates HIV-1 gag targeting to the plasma membrane.* Molecular Biology of the Cell, 2004. **15**: p. 122a-123a.
83. Saad, J.S., et al., *Structural basis for targeting HIV-1 Gag proteins to the plasma membrane for virus assembly.* Proceedings of the National Academy of Sciences of the United States of America, 2006. **103**(30): p. 11364-11369.
84. Freed, E.O., *HIV-1 replication.* Somat Cell Mol Genet, 2001. **26**(1-6): p. 13-33.
85. Brugger, B., et al., *The HIV lipidome: a raft with an unusual composition.* Proceedings of the National Academy of Sciences of the United States of America, 2006. **103**(8): p. 2641-6.
86. Lv, Z.T., Y. Chu, and Y. Wang, *HIV protease inhibitors: a review of molecular selectivity and toxicity.* Hiv Aids-Research and Palliative Care, 2015. **7**: p. 95-104.
87. Van Damme, N., et al., *The interferon-induced protein BST-2 restricts HIV-1 release and is downregulated from the cell surface by the viral Vpu protein.* Cell host & microbe, 2008. **3**(4): p. 245-52.
88. Neil, S.J., T. Zang, and P.D. Bieniasz, *Tetherin inhibits retrovirus release and is antagonized by HIV-1 Vpu.* Nature, 2008. **451**(7177): p. 425-30.
89. Picker, L.J. and D.I. Watkins, *HIV pathogenesis: the first cut is the deepest.* Nat Immunol, 2005. **6**(5): p. 430-2.
90. Keele, B.F., *Identifying and characterizing recently transmitted viruses.* Current opinion in HIV and AIDS, 2010. **5**(4): p. 327-34.
91. Shaw, G.M. and E. Hunter, *HIV transmission.* Cold Spring Harbor perspectives in medicine, 2012. **2**(11).
92. Haase, A.T., *Targeting early infection to prevent HIV-1 mucosal transmission.* Nature, 2010. **464**(7286): p. 217-23.
93. Walker, B. and A. McMichael, *The T-cell response to HIV.* Cold Spring Harbor perspectives in medicine, 2012. **2**(11).
94. Schnell, G., et al., *Compartmentalization and clonal amplification of HIV-1 variants in the cerebrospinal fluid during primary infection.* Journal of virology, 2010. **84**(5): p. 2395-407.
95. McMichael, A.J., et al., *The immune response during acute HIV-1 infection: clues for vaccine development.* Nature reviews. Immunology, 2010. **10**(1): p. 11-23.
96. Whitney, J.B., et al., *Rapid seeding of the viral reservoir prior to SIV viraemia in rhesus monkeys.* Nature, 2014. **512**(7512): p. 74-7.
97. Igarashi, T., et al., *Macrophage are the principal reservoir and sustain high virus loads in rhesus macaques after the depletion of CD4+ T cells by a highly pathogenic simian immunodeficiency virus/HIV type 1 chimera (SHIV): Implications for HIV-1 infections of humans.* Proc Natl Acad Sci U S A, 2001. **98**(2): p. 658-63.

98. Veazey, R.S., et al., *Gastrointestinal tract as a major site of CD4+ T cell depletion and viral replication in SIV infection.* Science, 1998. **280**(5362): p. 427-31.
99. Gartner, S., et al., *The role of mononuclear phagocytes in HTLV-III/LAV infection.* Science, 1986. **233**(4760): p. 215-9.
100. Rodriguez, B., et al., *Predictive value of plasma HIV RNA level on rate of CD4 T-cell decline in untreated HIV infection.* JAMA, 2006. **296**(12): p. 1498-506.
101. Schuitemaker, H., et al., *Biological phenotype of human immunodeficiency virus type 1 clones at different stages of infection: progression of disease is associated with a shift from monocytotropic to T-cell-tropic virus population.* J Virol, 1992. **66**(3): p. 1354-60.
102. Sant, A.J. and A. McMichael, *Revealing the role of CD4(+) T cells in viral immunity.* The Journal of experimental medicine, 2012. **209**(8): p. 1391-5.
103. Lackner, A.A., M.M. Lederman, and B. Rodriguez, *HIV pathogenesis: the host.* Cold Spring Harbor perspectives in medicine, 2012. **2**(9): p. a007005.
104. Sasseville, V.G., et al., *Induction of lymphocyte proliferation and severe gastrointestinal disease in macaques by a nef gene variant SIVmac239.* Am J Pathol, 1996. **149**(1): p. 163-76.
105. Costin, J.M., *Cytopathic mechanisms of HIV-1.* Virology journal, 2007. **4**: p. 100.
106. Doitsh, G., et al., *Abortive HIV infection mediates CD4 T cell depletion and inflammation in human lymphoid tissue.* Cell, 2010. **143**(5): p. 789-801.
107. Garg, H., J. Mohl, and A. Joshi, *HIV-1 induced bystander apoptosis.* Viruses, 2012. **4**(11): p. 3020-43.
108. Alimonti, J.B., T.B. Ball, and K.R. Fowke, *Mechanisms of CD4+ T lymphocyte cell death in human immunodeficiency virus infection and AIDS.* The Journal of general virology, 2003. **84**(Pt 7): p. 1649-61.
109. Swanstrom, R. and J. Coffin, *HIV-1 pathogenesis: the virus.* Cold Spring Harbor perspectives in medicine, 2012. **2**(12): p. a007443.
110. Stevenson, M., et al., *HIV-1 replication is controlled at the level of T cell activation and proviral integration.* The EMBO journal, 1990. **9**(5): p. 1551-60.
111. Okabe, Y. and R. Medzhitov, *Tissue biology perspective on macrophages.* Nature Immunology, 2016. **17**(1): p. 9-17.
112. Wynn, T.A., A. Chawla, and J.W. Pollard, *Macrophage biology in development, homeostasis and disease.* Nature, 2013. **496**(7446): p. 445-55.
113. Haldar, M. and K.M. Murphy, *Origin, development, and homeostasis of tissue-resident macrophages.* Immunological Reviews, 2014. **262**(1): p. 25-35.
114. Sattentau, Q.J. and M. Stevenson, *Macrophages and HIV-1: An Unhealthy Constellation.* Cell Host & Microbe, 2016. **19**(3): p. 304-310.
115. Raposo, R.A., et al., *Proteomic-based identification of CD4-interacting proteins in human primary macrophages.* PLoS One, 2011. **6**(4): p. e18690.
116. Arrildt, K.T., et al., *Phenotypic Correlates of HIV-1 Macrophage Tropism.* Journal of Virology, 2015. **89**(22): p. 11294-11311.
117. Amie, S.M., E. Noble, and B. Kim, *Intracellular nucleotide levels and the control of retroviral infections.* Virology, 2013. **436**(2): p. 247-54.
118. Laguette, N., et al., *SAMHD1 is the dendritic- and myeloid-cell-specific HIV-1 restriction factor counteracted by Vpx.* Nature, 2011. **474**(7353): p. 654-U132.
119. Lackner, A.A., M.M. Lederman, and B. Rodriguez, *HIV pathogenesis: the host.* Cold Spring Harb Perspect Med, 2012. **2**(9): p. a007005.

120. Gordon, S. and F.O. Martinez, *Alternative activation of macrophages: mechanism and functions.* Immunity, 2010. **32**(5): p. 593-604.
121. Shen, R., et al., *Macrophages in vaginal but not intestinal mucosa are monocyte-like and permissive to human immunodeficiency virus type 1 infection.* J Virol, 2009. **83**(7): p. 3258-67.
122. Shen, R., et al., *Stromal down-regulation of macrophage CD4/CCR5 expression and NF-kappaB activation mediates HIV-1 non-permissiveness in intestinal macrophages.* PLoS pathogens, 2011. **7**(5): p. e1002060.
123. Bergamaschi, A. and G. Pancino, *Host hindrance to HIV-1 replication in monocytes and macrophages.* Retrovirology, 2010. **7**: p. 31.
124. King, D.F.L., et al., *Mucosal Tissue Tropism and Dissemination of HIV-1 Subtype B Acute Envelope-Expressing Chimeric Virus.* Journal of Virology, 2013. **87**(2): p. 890-899.
125. Rappaport, J. and D.J. Volsky, *Role of the macrophage in HIV-associated neurocognitive disorders and other comorbidities in patients on effective antiretroviral treatment.* Journal of Neurovirology, 2015. **21**(3): p. 235-241.
126. Costiniuk, C.T. and M.A. Jenabian, *The lungs as anatomical reservoirs of HIV infection.* Reviews in Medical Virology, 2014. **24**(1): p. 35-54.
127. Deleage, C., et al., *Human immunodeficiency virus infects human seminal vesicles in vitro and in vivo.* The American journal of pathology, 2011. **179**(5): p. 2397-408.
128. Zalar, A., et al., *Macrophage HIV-1 infection in duodenal tissue of patients on long term HAART.* Antiviral research, 2010. **87**(2): p. 269-71.
129. Cory, T.J., et al., *Overcoming pharmacologic sanctuaries.* Current Opinion in Hiv and Aids, 2013. **8**(3): p. 190-195.
130. Cribbs, S.K., et al., *Healthy HIV-1-Infected Individuals on Highly Active Antiretroviral Therapy Harbor HIV-1 in Their Alveolar Macrophages.* Aids Research and Human Retroviruses, 2015. **31**(1): p. 64-70.
131. Cassol, E., et al., *CD14(+) macrophages that accumulate in the colon of African AIDS patients express pro-inflammatory cytokines and are responsive to lipopolysaccharide.* Bmc Infectious Diseases, 2015. **15**.
132. Crowe, S.M., et al., *The Macrophage: the intersection between HIV infection and atherosclerosis (vol 87, pg 589, 2010).* Journal of Leukocyte Biology, 2010. **87**(6): p. 1167-1167.
133. Gohda, J., et al., *HIV-1 replicates in human osteoclasts and enhances their differentiation in vitro.* Retrovirology, 2015. **12**.
134. Phillips, D.M. and A.S. Bourinbaiar, *Mechanism of Hiv Spread from Lymphocytes to Epithelia.* Virology, 1992. **186**(1): p. 261-273.
135. Igakura, T., et al., *Spread of HTLV-I between lymphocytes by virus-induced polarization of the cytoskeleton.* Science, 2003. **299**(5613): p. 1713-1716.
136. Jolly, C., et al., *HIV-1 cell to cell transfer across an Env-induced, actin-dependent synapse.* The Journal of experimental medicine, 2004. **199**(2): p. 283-93.
137. Groot, F., S. Welsch, and Q.J. Sattentau, *Efficient HIV-1 transmission from macrophages to T cells across transient virological synapses.* Blood, 2008. **111**(9): p. 4660-3.
138. Jolly, C., et al., *The Regulated Secretory Pathway in CD4(+) T cells Contributes to Human Immunodeficiency Virus Type-1 Cell-to-Cell Spread at the Virological Synapse.* Plos Pathogens, 2011. **7**(9).

139. Martin, N. and Q. Sattentau, *Cell-to-cell HIV-1 spread and its implications for immune evasion.* Current Opinion in Hiv and Aids, 2009. **4**(2): p. 143-149.
140. Jolly, C., I. Mitar, and Q.J. Sattentau, *Adhesion molecule interactions facilitate human immunodeficiency virus type 1-induced virological synapse formation between T cells.* Journal of Virology, 2007. **81**(24): p. 13916-13921.
141. Sattentau, Q., *Avoiding the void: cell-to-cell spread of human viruses.* Nature reviews. Microbiology, 2008. **6**(11): p. 815-26.
142. Del Portillo, A., et al., *Multiploid inheritance of HIV-1 during cell-to-cell infection.* Journal of virology, 2011. **85**(14): p. 7169-76.
143. Sigal, A., et al., *Cell-to-cell spread of HIV permits ongoing replication despite antiretroviral therapy.* Nature, 2011. **477**(7362): p. 95-8.
144. Sundquist, W.I. and H.G. Krausslich, *HIV-1 Assembly, Budding, and Maturation.* Cold Spring Harbor Perspectives in Medicine, 2012. **2**(7).
145. Sourisseau, M., et al., *Inefficient human immunodeficiency virus replication in mobile lymphocytes.* Journal of Virology, 2007. **81**(2): p. 1000-1012.
146. Mazurov, D., et al., *Quantitative Comparison of HTLV-1 and HIV-1 Cell-to-Cell Infection with New Replication Dependent Vectors.* Plos Pathogens, 2010. **6**(2).
147. Chen, P., et al., *Predominant mode of human immunodeficiency virus transfer between T cells is mediated by sustained Env-dependent neutralization-resistant virological synapses.* Journal of Virology, 2007. **81**(22): p. 12582-12595.
148. McDonald, D., *Dendritic Cells and HIV-1 Trans-Infection.* Viruses, 2010. **2**(8): p. 1704-17.
149. Cameron, P.U., et al., *Dendritic Cells Exposed to Human-Immunodeficiency-Virus Type-1 Transmit a Vigorous Cytopathic Infection to Cd4+ T-Cells.* Science, 1992. **257**(5068): p. 383-386.
150. McDonald, D., et al., *Recruitment of HIV and its receptors to dendritic cell-T cell junctions.* Science (New York, N.Y.), 2003. **300**(5623): p. 1295-7.
151. Geijtenbeek, T.B.H., et al., *DC-SIGN, a dendritic cell-specific HIV-1-binding protein that enhances trans-infection of T cells.* Cell, 2000. **100**(5): p. 587-597.
152. Ménager, Mickaël M. and Dan R. Littman, *Actin Dynamics Regulates Dendritic Cell-Mediated Transfer of HIV-1 to T Cells.* Cell, 2016. **164**(4): p. 695-709.
153. Abela, I.A., et al., *Cell-Cell Transmission Enables HIV-1 to Evade Inhibition by Potent CD4bs Directed Antibodies.* Plos Pathogens, 2012. **8**(4).
154. Schiffner, T., Q.J. Sattentau, and C.J.A. Duncan, *Cell-to-cell spread of HIV-1 and evasion of neutralizing antibodies.* Vaccine, 2013. **31**(49): p. 5789-5797.
155. Duncan, C.J.A., et al., *High-Multiplicity HIV-1 Infection and Neutralizing Antibody Evasion Mediated by the Macrophage-T Cell Virological Synapse.* Journal of Virology, 2014. **88**(4): p. 2025-2034.
156. Reh, L., et al., *Capacity of Broadly Neutralizing Antibodies to Inhibit HIV-1 Cell-Cell Transmission Is Strain- and Epitope-Dependent.* Plos Pathogens, 2015. **11**(7).
157. Doitsh, G. and W.C. Greene, *Dissecting How CD4 T Cells Are Lost During HIV Infection.* Cell Host & Microbe, 2016. **19**(3): p. 280-291.
158. Hochreiter-Hufford, A. and K.S. Ravichandran, *Clearing the dead: apoptotic cell sensing, recognition, engulfment, and digestion.* Cold Spring Harbor perspectives in biology, 2013. **5**(1): p. a008748-a008748.
159. Ho, D.D., et al., *Rapid Turnover of Plasma Virions and Cd4 Lymphocytes in Hiv-1 Infection.* Nature, 1995. **373**(6510): p. 123-126.

160. Zagury, D., et al., *Long-Term Cultures of Htlv-Iii Infected T-Cells - a Model of Cytopathology of T-Cell Depletion in Aids.* Science, 1986. **231**(4740): p. 850-853.
161. Gandhi, R.T., et al., *HIV-1 directly kills CD4(+) T cells by a Fas-independent mechanism.* Journal of Experimental Medicine, 1998. **187**(7): p. 1113-1122.
162. Jekle, A., et al., *In vivo evolution of human immunodeficiency virus type 1 toward increased pathogenicity through CXCR4-mediated killing of uninfected CD4 T cells.* Journal of Virology, 2003. **77**(10): p. 5846-5854.
163. Levy, J.A., *Pathogenesis of Human-Immunodeficiency-Virus Infection.* Microbiological Reviews, 1993. **57**(1): p. 183-289.
164. Shaw, G.M., et al., *Molecular Characterization of Human T-Cell Leukemia (Lymphotropic) Virus Type-Iii in the Acquired Immune-Deficiency Syndrome.* Science, 1984. **226**(4679): p. 1165-1171.
165. Arokium, H., M. Kamata, and I. Chen, *Virion-Associated Vpr of Human Immunodeficiency Virus Type 1 Triggers Activation of Apoptotic Events and Enhances Fas-Induced Apoptosis in Human T Cells.* Journal of Virology, 2009. **83**(21): p. 11283-11297.
166. Zauli, G., et al., *Human immunodeficiency virus type 1 Nef protein sensitizes CD4(+) T lymphoid cells to apoptosis via functional upregulation of the CD95/CD95 ligand pathway.* Blood, 1999. **93**(3): p. 1000-1010.
167. Sainski, A.M., et al., *The HIV-1-Specific Protein Casp8p41 Induces Death of Infected Cells through Bax/Bak.* Journal of Virology, 2011. **85**(16): p. 7965-7975.
168. Cooper, A., et al., *HIV-1 causes CD4 cell death through DNA-dependent protein kinase during viral integration.* Nature, 2013. **498**(7454): p. 376-+.
169. Doitsh, G., et al., *Cell death by pyroptosis drives CD4 T-cell depletion in HIV-1 infection.* Nature, 2014. **505**(7484): p. 509-+.
170. Finkel, T.H., et al., *Apoptosis occurs predominantly in bystander cells and not in productively infected cells of HIV- and SIV-infected lymph nodes.* Nat Med, 1995. **1**(2): p. 129-34.
171. Doitsh, G., et al., *Abortive HIV Infection Mediates CD4 T Cell Depletion and Inflammation in Human Lymphoid Tissue.* Cell, 2010. **143**(5): p. 789-801.
172. Galloway, N.L.K., et al., *Cell-to-Cell Transmission of HIV-1 Is Required to Trigger Pyroptotic Death of Lymphoid-Tissue-Derived CD4 T Cells.* Cell Reports, 2015. **12**(10): p. 1555-1563.
173. Munoz-Arias, I., et al., *Blood-Derived CD4 T Cells Naturally Resist Pyroptosis during Abortive HIV-1 Infection.* Cell Host & Microbe, 2015. **18**(4): p. 463-470.
174. Galluzzi, L., et al., *Necroptosis: Mechanisms and Relevance to Disease.* Annu Rev Pathol, 2017. **12**: p. 103-130.
175. Ichim, G. and S.W. Tait, *Necroptosis: Fifty shades of RIPKs.* Mol Cell Oncol, 2015. **2**(2): p. e965638.
176. Pan, T., et al., *Necroptosis takes place in human immunodeficiency virus type-1 (HIV-1)-infected CD4+ T lymphocytes.* PLoS One, 2014. **9**(4): p. e93944.
177. Gaiha, G.D., et al., *Dysfunctional HIV-Specific CD8(+) T Cell Proliferation Is Associated with Increased Caspase-8 Activity and Mediated by Necroptosis.* Immunity, 2014. **41**(6): p. 1001-1012.
178. Deeks, S.G., R. Tracy, and D.C. Douek, *Systemic Effects of Inflammation on Health during Chronic HIV Infection.* Immunity, 2013. **39**(4): p. 633-645.

179. Galluzzi, L., et al., *Molecular mechanisms of cell death: recommendations of the Nomenclature Committee on Cell Death 2018.* Cell Death Differ, 2018. **25**(3): p. 486-541.
180. Green, D.R., T.H. Oguin, and J. Martinez, *The clearance of dying cells: table for two.* Cell Death Differ, 2016. **23**(6): p. 915-26.
181. Weinlich, R., et al., *Necroptosis in development, inflammation and disease.* Nature Reviews Molecular Cell Biology, 2017. **18**(2): p. 127-136.
182. Green, D.R., et al., *Immunogenic and tolerogenic cell death.* Nature Reviews Immunology, 2009. **9**(5): p. 353-363.
183. Yatim, N., S. Cullen, and M.L. Albert, *Dying cells actively regulate adaptive immune responses.* Nature Reviews Immunology, 2017. **17**(4): p. 262-275.
184. Tait, S.W. and D.R. Green, *Mitochondria and cell death: outer membrane permeabilization and beyond.* Nat Rev Mol Cell Biol, 2010. **11**(9): p. 621-32.
185. Igney, F.H. and P.H. Krammer, *Death and anti-death: tumour resistance to apoptosis.* Nat Rev Cancer, 2002. **2**(4): p. 277-88.
186. Czabotar, P.E., et al., *Control of apoptosis by the BCL-2 protein family: implications for physiology and therapy.* Nat Rev Mol Cell Biol, 2014. **15**(1): p. 49-63.
187. Ichim, G. and S.W.G. Tait, *A fate worse than death: apoptosis as an oncogenic process.* Nature Reviews Cancer, 2016. **16**(8): p. 539-548.
188. Galluzzi, L., et al., *Essential versus accessory aspects of cell death: recommendations of the NCCD 2015.* Cell Death and Differentiation, 2015. **22**(1): p. 58-73.
189. Marsden, V.S., et al., *Apoptosis initiated by Bcl-2-regulated caspase activation independently of the cytochrome c/Apaf-1/caspase-9 apoptosome.* Nature, 2002. **419**(6907): p. 634-637.
190. Strasser, A., P.J. Jost, and S. Nagata, *The many roles of FAS receptor signaling in the immune system.* Immunity, 2009. **30**(2): p. 180-92.
191. Aggarwal, B.B., S.C. Gupta, and J.H. Kim, *Historical perspectives on tumor necrosis factor and its superfamily: 25 years later, a golden journey.* Blood, 2012. **119**(3): p. 651-65.
192. Mehlen, P. and S. Tauszig-Delamasure, *Dependence receptors and colorectal cancer.* Gut, 2014. **63**(11): p. 1821-9.
193. Cookson, B.T. and M.A. Brennan, *Pro-inflammatory programmed cell death.* Trends in Microbiology, 2001. **9**(3): p. 113-114.
194. Bergsbaken, T., S.L. Fink, and B.T. Cookson, *Pyroptosis: host cell death and inflammation.* Nature Reviews Microbiology, 2009. **7**(2): p. 99-109.
195. Jorgensen, I. and E.A. Miao, *Pyroptotic cell death defends against intracellular pathogens.* Immunological Reviews, 2015. **265**(1): p. 130-142.
196. Shi, J.J., W.Q. Gao, and F. Shao, *Pyroptosis: Gasdermin-Mediated Programmed Necrotic Cell Death.* Trends in Biochemical Sciences, 2017. **42**(4): p. 245-254.
197. Wang, Y.P., et al., *Chemotherapy drugs induce pyroptosis through caspase-3 cleavage of a gasdermin.* Nature, 2017. **547**(7661): p. 99-+.
198. Shi, J.J., et al., *Inflammatory caspases are innate immune receptors for intracellular LPS.* Nature, 2014. **514**(7521): p. 187-+.
199. Olivares-Zavaleta, N., et al., *Chlamydia pneumoniae Inhibits Activated Human T Lymphocyte Proliferation by the Induction of Apoptotic and Pyroptotic Pathways.* Journal of Immunology, 2011. **186**(12): p. 7120-7126.

200. Aachoui, Y., et al., *Inflammasome-mediated pyroptotic and apoptotic cell death, and defense against infection.* Current Opinion in Microbiology, 2013. **16**(3): p. 319-326.
201. Franchi, L., et al., *The inflammasome: a caspase-1-activation platform that regulates immune responses and disease pathogenesis.* Nature Immunology, 2009. **10**(3): p. 241-247.
202. Broz, P. and V.M. Dixit, *Inflammasomes: mechanism of assembly, regulation and signalling.* Nature Reviews Immunology, 2016. **16**(7): p. 407-420.
203. Shi, J., W. Gao, and F. Shao, *Pyroptosis: Gasdermin-Mediated Programmed Necrotic Cell Death.* Trends Biochem Sci, 2017. **42**(4): p. 245-254.
204. Shi, C. and E.G. Pamer, *Monocyte recruitment during infection and inflammation.* Nature Reviews Immunology, 2011. **11**(11): p. 762-774.
205. Baehrecke, E.H., *How death shapes life during development.* Nature reviews. Molecular cell biology, 2002. **3**(10): p. 779-87.
206. Scott, R.S., et al., *Phagocytosis and clearance of apoptotic cells is mediated by MER.* Nature, 2001. **411**(6834): p. 207-11.
207. Elliott, M.R. and K.S. Ravichandran, *The Dynamics of Apoptotic Cell Clearance.* Dev Cell, 2016. **38**(2): p. 147-60.
208. Zent, C.S. and M.R. Elliott, *Maxed out macs: physiologic cell clearance as a function of macrophage phagocytic capacity.* FEBS J, 2017. **284**(7): p. 1021-1039.
209. Ravichandran, K.S., *Find-me and eat-me signals in apoptotic cell clearance: progress and conundrums.* The Journal of experimental medicine, 2010. **207**(9): p. 1807-17.
210. Karnovsky, M.L., *Metchnikoff in Messina: a century of studies on phagocytosis.* The New England journal of medicine, 1981. **304**(19): p. 1178-80.
211. Gordon, S., *Phagocytosis: An Immunobiologic Process.* Immunity, 2016. **44**(3): p. 463-75.
212. Underhill, D.M. and H.S. Goodridge, *Information processing during phagocytosis.* Nature reviews. Immunology, 2012. **12**(7): p. 492-502.
213. Gregory, C., *Cell biology: Sent by the scent of death.* Nature, 2009. **461**(7261): p. 181-2.
214. Monks, J., et al., *Epithelial cells remove apoptotic epithelial cells during post-lactation involution of the mouse mammary gland.* Biology of reproduction, 2008. **78**(4): p. 586-94.
215. Loov, C., et al., *Slow degradation in phagocytic astrocytes can be enhanced by lysosomal acidification.* Glia, 2015.
216. Kumar, S. and R.B. Birge, *Efferocytosis.* Curr Biol, 2016. **26**(13): p. R558-9.
217. Henson, P.M., *Cell Removal: Efferocytosis.* Annu Rev Cell Dev Biol, 2017.
218. Hoffmann, P.R., et al., *Phosphatidylserine (PS) induces PS receptor-mediated macropinocytosis and promotes clearance of apoptotic cells.* J Cell Biol, 2001. **155**(4): p. 649-59.
219. Martin, C.J., K.N. Peters, and S.M. Behar, *Macrophages clean up: efferocytosis and microbial control.* Curr Opin Microbiol, 2014. **17**: p. 17-23.
220. deCathelineau, A.M. and P.M. Henson, *The final step in programmed cell death: phagocytes carry apoptotic cells to the grave.* Essays in biochemistry, 2003. **39**: p. 105-17.
221. Galluzzi, L., et al., *Essential versus accessory aspects of cell death: recommendations of the NCCD 2015.* Cell Death Differ, 2015. **22**(1): p. 58-73.

222. Poon, I.K.H., et al., *Apoptotic cell clearance: basic biology and therapeutic potential.* Nature reviews. Immunology, 2014. **14**(3): p. 166-80.
223. Fond, A.M., K.S. Ravichandran, and C.D.G. Editor, *Clearance of Dying Cells by Phagocytes: Mechanisms and Implications for Disease Pathogenesis.* 2016. **930**: p. 133-149.
224. Peter, C., S. Wesselborg, and K. Lauber, *Molecular suicide notes: last call from apoptosing cells.* Journal of molecular cell biology, 2010. **2**(2): p. 78-80.
225. Kroemer, G., *Dying cell recognition shapes the pathophysiology of cell death.* Cell Death and Differentiation, 2016. **23**(6): p. 913-914.
226. Lauber, K., et al., *Apoptotic cells induce migration of phagocytes via caspase-3-mediated release of a lipid attraction signal.* Cell, 2003. **113**(6): p. 717-30.
227. Truman, L.A., et al., *CX3CL1/fractalkine is released from apoptotic lymphocytes to stimulate macrophage chemotaxis.* Blood, 2008. **112**(13): p. 5026-5036.
228. Elliott, M.R., et al., *Nucleotides released by apoptotic cells act as a find-me signal to promote phagocytic clearance.* Nature, 2009. **461**(7261): p. 282-286.
229. Gude, D.R., et al., *Apoptosis induces expression of sphingosine kinase 1 to release sphingosine-1-phosphate as a "come-and-get-me" signal.* The FASEB Journal, 2008. **22**(8): p. 2629-2638.
230. Li, W., *Eat-me signals: keys to molecular phagocyte biology and "appetite" control.* J Cell Physiol, 2012. **227**(4): p. 1291-7.
231. Segawa, K. and S. Nagata, *An Apoptotic 'Eat Me' Signal: Phosphatidylserine Exposure.* Trends Cell Biol, 2015. **25**(11): p. 639-50.
232. Brown, G.C. and J.J. Neher, *Eaten alive! Cell death by primary phagocytosis: 'phagoptosis'.* Trends in biochemical sciences, 2012. **37**(8): p. 325-32.
233. Gardai, S.J., et al., *Recognition ligands on apoptotic cells: a perspective.* Journal of leukocyte biology, 2006. **79**(5): p. 896-903.
234. Overholtzer, M., et al., *A nonapoptotic cell death process, entosis, that occurs by cell-in-cell invasion.* Cell, 2007. **131**(5): p. 966-79.
235. Flannagan, R.S., V. Jaumouille, and S. Grinstein, *The cell biology of phagocytosis.* Annu Rev Pathol, 2012. **7**: p. 61-98.
236. Pauwels, A.M., et al., *Patterns, Receptors, and Signals: Regulation of Phagosome Maturation.* Trends Immunol, 2017. **38**(6): p. 407-422.
237. Brewer, J.M., et al., *Vesicle size influences the trafficking, processing, and presentation of antigens in lipid vesicles.* Journal of immunology (Baltimore, Md. : 1950), 2004. **173**(10): p. 6143-50.
238. Doshi, N. and S. Mitragotri, *Macrophages recognize size and shape of their targets.* PloS one, 2010. **5**(4): p. e10051-e10051.
239. Champion, J.A. and S. Mitragotri, *Role of target geometry in phagocytosis.* Proceedings of the National Academy of Sciences of the United States of America, 2006. **103**(13): p. 4930-4.
240. Branzk, N., et al., *Neutrophils sense microbe size and selectively release neutrophil extracellular traps in response to large pathogens.* Nat Immunol, 2014. **15**(11): p. 1017-25.
241. Greenlee-Wacker, M.C., *Clearance of apoptotic neutrophils and resolution of inflammation.* Immunol Rev, 2016. **273**(1): p. 357-70.
242. Birge, R.B., et al., *Phosphatidylserine is a global immunosuppressive signal in efferocytosis, infectious disease, and cancer.* Cell Death Differ, 2016. **23**(6): p. 962-78.

243. Yatim, N., S. Cullen, and M.L. Albert, *Dying cells actively regulate adaptive immune responses.* Nature reviews. Immunology, 2017. **17**(4): p. 262-275.
244. Blander, J.M., *The many ways tissue phagocytes respond to dying cells.* Immunol Rev, 2017. **277**(1): p. 158-173.
245. Karaji, N. and Q.J. Sattentau, *Efferocytosis of Pathogen-Infected Cells.* Front Immunol, 2017. **8**: p. 1863.
246. Bevers, E.M., et al., *Generation of prothrombin-converting activity and the exposure of phosphatidylserine at the outer surface of platelets.* European journal of biochemistry, 1982. **122**(2): p. 429-36.
247. Bevers, E.M. and P.L. Williamson, *Getting to the Outer Leaflet: Physiology of Phosphatidylserine Exposure at the Plasma Membrane.* Physiological Reviews, 2016. **96**(2).
248. Callahan, M.K., P. Williamson, and R.A. Schlegel, *Surface expression of phosphatidylserine on macrophages is required for phagocytosis of apoptotic thymocytes.* Cell Death and Differentiation, 2000. **7**(7): p. 645-653.
249. Elliott, J.I., et al., *Membrane phosphatidylserine distribution as a non-apoptotic signalling mechanism in lymphocytes.* Nature Cell Biology, 2005. **7**(8): p. 808-U76.
250. Borisenko, G.G., et al., *Macrophage recognition of externalized phosphatidylserine and phagocytosis of apoptotic Jurkat cells--existence of a threshold.* Archives of biochemistry and biophysics, 2003. **413**(1): p. 41-52.
251. Segawa, K., J. Suzuki, and S. Nagata, *Constitutive exposure of phosphatidylserine on viable cells.* Proceedings of the National Academy of Sciences of the United States of America, 2011. **108**(48): p. 19246-19251.
252. Fadok, V.A., et al., *Loss of phospholipid asymmetry and surface exposure of phosphatidylserine is required for phagocytosis of apoptotic cells by macrophages and fibroblasts.* The Journal of biological chemistry, 2001. **276**(2): p. 1071-7.
253. Böse, J., et al., *The phosphatidylserine receptor has essential functions during embryogenesis but not in apoptotic cell removal.* Journal of biology, 2004. **3**(4): p. 15-15.
254. Bratton, D.L. and P.M. Henson, *Apoptotic cell recognition: will the real phosphatidylserine receptor(s) please stand up?* Current biology : CB, 2008. **18**(2): p. R76-9.
255. Park, D., et al., *BAI1 is an engulfment receptor for apoptotic cells upstream of the ELMO/Dock180/Rac module.* Nature, 2007. **450**(7168): p. 430-434.
256. Mazaheri, F., et al., *Distinct roles for BAI1 and TIM-4 in the engulfment of dying neurons by microglia.* Nature Communications, 2014. **5**: p. 4046-4046.
257. Park, S.Y., et al., *Rapid cell corpse clearance by stabilin-2, a membrane phosphatidylserine receptor.* Cell Death and Differentiation, 2008. **15**(1): p. 192-201.
258. Zhou, B., et al., *Identification of the hyaluronan receptor for endocytosis (HARE).* The Journal of biological chemistry, 2000. **275**(48): p. 37733-41.
259. Park, S.-Y., et al., *Epidermal growth factor-like domain repeat of stabilin-2 recognizes phosphatidylserine during cell corpse clearance.* Molecular and cellular biology, 2008. **28**(17): p. 5288-98.
260. Park, S.-Y., et al., *Stabilin-1 mediates phosphatidylserine-dependent clearance of cell corpses in alternatively activated macrophages.* Journal of Cell Science, 2009. **122**(18).

261. Kobayashi, N., et al., *TIM-1 and TIM-4 glycoproteins bind phosphatidylserine and mediate uptake of apoptotic cells.* Immunity, 2007. **27**(6): p. 927-40.
262. DeKruyff, R.H., et al., *T cell/transmembrane, Ig, and mucin-3 allelic variants differentially recognize phosphatidylserine and mediate phagocytosis of apoptotic cells.* Journal of immunology (Baltimore, Md. : 1950), 2010. **184**(4): p. 1918-30.
263. Park, D., A. Hochreiter-Hufford, and K.S. Ravichandran, *The phosphatidylserine receptor TIM-4 does not mediate direct signaling.* Current biology : CB, 2009. **19**(4): p. 346-51.
264. Raucci, A., et al., *A soluble form of the receptor for advanced glycation endproducts (RAGE) is produced by proteolytic cleavage of the membrane-bound form by the sheddase a disintegrin and metalloprotease 10 (ADAM10).* FASEB journal : official publication of the Federation of American Societies for Experimental Biology, 2008. **22**(10): p. 3716-27.
265. Brett, J., et al., *Survey of the distribution of a newly characterized receptor for advanced glycation end products in tissues.* The American journal of pathology, 1993. **143**(6): p. 1699-712.
266. He, M., et al., *Receptor for advanced glycation end products binds to phosphatidylserine and assists in the clearance of apoptotic cells.* EMBO reports, 2011. **12**(4): p. 358-64.
267. Simhadri, V.R., et al., *Human CD300a binds to phosphatidylethanolamine and phosphatidylserine, and modulates the phagocytosis of dead cells.* Blood, 2012. **119**(12).
268. Murakami, Y., et al., *CD300b regulates the phagocytosis of apoptotic cells via phosphatidylserine recognition.* Cell death and differentiation, 2014. **21**(11): p. 1746-57.
269. Tian, L., et al., *p85α recruitment by the CD300f phosphatidylserine receptor mediates apoptotic cell clearance required for autoimmunity suppression.* Nature communications, 2014. **5**: p. 3146-3146.
270. Choi, S.C., et al., *Cutting Edge: Mouse CD300f (CMRF-35-Like Molecule-1) Recognizes Outer Membrane-Exposed Phosphatidylserine and Can Promote Phagocytosis.* The Journal of Immunology, 2011. **187**(7): p. 3483-3487.
271. Oka, K., et al., *Lectin-like oxidized low-density lipoprotein receptor 1 mediates phagocytosis of aged/apoptotic cells in endothelial cells.* Proceedings of the National Academy of Sciences of the United States of America, 1998. **95**(16): p. 9535-40.
272. Gardai, S.J., et al., *Cell-Surface Calreticulin Initiates Clearance of Viable or Apoptotic Cells through trans-Activation of LRP on the Phagocyte.* Cell, 2005. **123**(2): p. 321-334.
273. Obeid, M., et al., *Calreticulin exposure dictates the immunogenicity of cancer cell death.* Nature medicine, 2007. **13**(1): p. 54-61.
274. Païdassi, H., et al., *C1q binds phosphatidylserine and likely acts as a multiligand-bridging molecule in apoptotic cell recognition.* Journal of immunology (Baltimore, Md. : 1950), 2008. **180**(4): p. 2329-38.
275. Vandivier, R.W., et al., *Role of Surfactant Proteins A, D, and C1q in the Clearance of Apoptotic Cells In Vivo and In Vitro: Calreticulin and CD91 as a Common Collectin Receptor Complex.* The Journal of Immunology, 2002. **169**(7): p. 3978-3986.

276. Tóth, B., et al., *Transglutaminase 2 Is Needed for the Formation of an Efficient Phagocyte Portal in Macrophages Engulfing Apoptotic Cells.* The Journal of Immunology, 2009. **182**(4).
277. Oshima, K., et al., *MFG-E8: Origin, Structure, Expression, Functions and Regulation*. 2014, Springer Netherlands: Dordrecht. p. 1-31.
278. Akakura, S., et al., *The opsonin MFG-E8 is a ligand for the alphavbeta5 integrin and triggers DOCK180-dependent Rac1 activation for the phagocytosis of apoptotic cells.* Experimental cell research, 2004. **292**(2): p. 403-16.
279. Albert, M.L., R.B. Birge, and J.-I. Kim, *|[alpha]|v|[beta]|5 integrin recruits the CrkII|[ndash]|Dock180|[ndash]|Rac1complex for phagocytosis of apoptotic cells.* Nature Cell Biology, 2000. **2**(12): p. 899-905.
280. Hanayama, R., et al., *Identification of a factor that links apoptotic cells to phagocytes.* Nature, 2002. **417**(6885): p. 182-187.
281. Anderson, H.A., et al., *Serum-derived protein S binds to phosphatidylserine and stimulates the phagocytosis of apoptotic cells.* Nature Immunology, 2003. **4**(1): p. 87-91.
282. Hafizi, S. and B. Dahlbäck, *Gas6 and protein S.* FEBS Journal, 2006. **273**(23): p. 5231-5244.
283. Ishimoto, Y., et al., *Promotion of the Uptake of PS Liposomes and Apoptotic Cells by a Product of Growth Arrest-Specific Gene, gas6.* Journal of Biochemistry, 2000. **127**(3): p. 411-417.
284. Lemke, G., *Biology of the TAM receptors.* Cold Spring Harbor perspectives in biology, 2013. **5**(11): p. a009076-a009076.
285. Kim, J., *Identification of a human monoclonal natural IgM antibody that recognizes early apoptotic cells and promotes phagocytosis.* Hybridoma (2005), 2010. **29**(4): p. 275-81.
286. Liu, G., et al., *High Mobility Group Protein-1 Inhibits Phagocytosis of Apoptotic Neutrophils through Binding to Phosphatidylserine.* The Journal of Immunology, 2008. **181**(6).
287. Friggeri, A., et al., *HMGB1 inhibits macrophage activity in efferocytosis through binding to the αvβ3-integrin.* American Journal of Physiology - Cell Physiology, 2010. **299**(6).
288. Balasubramanian, K., S.N. Maiti, and A.J. Schroit, *Recruitment of beta-2-glycoprotein 1 to cell surfaces in extrinsic and intrinsic apoptosis.* Apoptosis, 2005. **10**(2): p. 439-446.
289. Maiti, S.N., et al., *Beta-2-glycoprotein 1-dependent macrophage uptake of apoptotic cells. Binding to lipoprotein receptor-related protein receptor family members.* The Journal of biological chemistry, 2008. **283**(7): p. 3761-6.
290. Willems, G.M., et al., *Role of divalency in the high-affinity binding of anticardiolipin antibody-beta 2-glycoprotein I complexes to lipid membranes.* Biochemistry, 1996. **35**(43): p. 13833-42.
291. Largent, B.L., et al., *Carbohydrate-specific adhesion of alveolar macrophages to mannose-derivatized surfaces.* The Journal of biological chemistry, 1984. **259**(3): p. 1764-9.
292. Hodge, S., et al., *Azithromycin Improves Macrophage Phagocytic Function and Expression of Mannose Receptor in Chronic Obstructive Pulmonary Disease.* American Journal of Respiratory and Critical Care Medicine, 2008. **178**(2): p. 139-148.

293. Ezekowitz, R.A., et al., *Molecular characterization of the human macrophage mannose receptor: demonstration of multiple carbohydrate recognition-like domains and phagocytosis of yeasts in Cos-1 cells.* The Journal of experimental medicine, 1990. **172**(6): p. 1785-94.
294. Le Cabec, V., et al., *The human macrophage mannose receptor is not a professional phagocytic receptor.* Journal of leukocyte biology, 2005. **77**(6): p. 934-43.
295. Gregory, C.D., A. Devitt, and O. Moffatt, *Roles of ICAM-3 and CD14 in the recognition and phagocytosis of apoptotic cells by macrophages.* Biochemical Society transactions, 1998. **26**(4): p. 644-9.
296. Moffatt, O.D., et al., *Macrophage Recognition of ICAM-3 on Apoptotic Leukocytes.* The Journal of Immunology, 1999. **162**(11).
297. Rubartelli, A., A. Poggi, and M.R. Zocchi, *The selective engulfment of apoptotic bodies by dendritic cells is mediated by the alpha(v)beta3 integrin and requires intracellular and extracellular calcium.* European journal of immunology, 1997. **27**(8): p. 1893-900.
298. Savill, J., et al., *Vitronectin receptor-mediated phagocytosis of cells undergoing apoptosis.* Nature, 1990. **343**(6254): p. 170-3.
299. Ogden, C.A., et al., *C1q and mannose binding lectin engagement of cell surface calreticulin and CD91 initiates macropinocytosis and uptake of apoptotic cells.* The Journal of experimental medicine, 2001. **194**(6): p. 781-95.
300. Behrens, E.M., et al., *Apoptotic Cell-Mediated Immunoregulation of Dendritic Cells Does Not Require iC3b Opsonization.* The Journal of Immunology, 2008. **181**(5): p. 3018-3026.
301. Gu, B.J., et al., *P2X(7) is a scavenger receptor for apoptotic cells in the absence of its ligand, extracellular ATP.* Journal of immunology (Baltimore, Md. : 1950), 2011. **187**(5): p. 2365-75.
302. Marques-da-Silva, C., et al., *Purinergic receptor agonists modulate phagocytosis and clearance of apoptotic cells in macrophages.* Immunobiology, 2011. **216**(1-2): p. 1-11.
303. Frleta, D., et al., *HIV-1 infection-induced apoptotic microparticles inhibit human DCs via CD44.* The Journal of clinical investigation, 2012. **122**(12): p. 4685-97.
304. Wang, Q., et al., *Pyroptotic cells externalize eat-me and release find-me signals and are efficiently engulfed by macrophages.* International Immunology, 2013. **25**(2): p. 363-372.
305. Jaiswal, S., et al., *CD47 is upregulated on circulating hematopoietic stem cells and leukemia cells to avoid phagocytosis.* Cell, 2009. **138**(2): p. 271-85.
306. Chao, M.P., R. Majeti, and I.L. Weissman, *Programmed cell removal: a new obstacle in the road to developing cancer.* Nature reviews. Cancer, 2012. **12**(1): p. 58-67.
307. Chao, M.P., et al., *Therapeutic antibody targeting of CD47 eliminates human acute lymphoblastic leukemia.* Cancer research, 2011. **71**(4): p. 1374-84.
308. Stumpfova, M., et al., *The immunosuppressive surface ligand CD200 augments the metastatic capacity of squamous cell carcinoma.* Cancer research, 2010. **70**(7): p. 2962-72.
309. Meesmann, H.M., et al., *Decrease of sialic acid residues as an eat-me signal on the surface of apoptotic lymphocytes.* J Cell Sci, 2010. **123**(Pt 19): p. 3347-56.
310. Linnartz, B., et al., *Sialic acid on the neuronal glycocalyx prevents complement C1 binding and complement receptor-3-mediated removal by microglia.* The

Journal of neuroscience : the official journal of the Society for Neuroscience, 2012. **32**(3): p. 946-52.
311. Wang, Y. and H. Neumann, *Alleviation of neurotoxicity by microglial human Siglec-11.* The Journal of neuroscience : the official journal of the Society for Neuroscience, 2010. **30**(9): p. 3482-8.
312. Elward, K., et al., *CD46 plays a key role in tailoring innate immune recognition of apoptotic and necrotic cells.* The Journal of biological chemistry, 2005. **280**(43): p. 36342-54.
313. Brown, S., et al., *Apoptosis disables CD31-mediated cell detachment from phagocytes promoting binding and engulfment.* Nature, 2002. **418**(6894): p. 200-3.
314. Park, Y.-J., et al., *PAI-1 inhibits neutrophil efferocytosis.* Proceedings of the National Academy of Sciences of the United States of America, 2008. **105**(33): p. 11784-9.
315. Barkal, A.A., et al., *Engagement of MHC class I by the inhibitory receptor LILRB1 suppresses macrophages and is a target of cancer immunotherapy.* Nature Immunology, 2018. **19**(1): p. 76-+.
316. Clark, M.C. and L.G. Baum, *T cells modulate glycans on CD43 and CD45 during development and activation, signal regulation, and survival.* Ann N Y Acad Sci, 2012. **1253**: p. 58-67.
317. de Laurentiis, A., et al., *Mass spectrometry-based identification of the tumor antigen UN1 as the transmembrane CD43 sialoglycoprotein.* Mol Cell Proteomics, 2011. **10**(5): p. M111 007898.
318. Marth, J.D. and P.K. Grewal, *Mammalian glycosylation in immunity.* Nat Rev Immunol, 2008. **8**(11): p. 874-87.
319. Barran, P., et al., *Modification of CD43 and other lymphocyte O-glycoproteins by core 2 N-acetylglucosaminyltransferase.* Glycobiology, 1997. **7**(1): p. 129-36.
320. Cyster, J.G., D.M. Shotton, and A.F. Williams, *The dimensions of the T lymphocyte glycoprotein leukosialin and identification of linear protein epitopes that can be modified by glycosylation.* EMBO J, 1991. **10**(4): p. 893-902.
321. Shelley, C.S., et al., *Molecular Characterization of Sialophorin (Cd43), the Lymphocyte Surface Sialoglycoprotein Defective in Wiskott-Aldrich Syndrome.* Proceedings of the National Academy of Sciences of the United States of America, 1989. **86**(8): p. 2819-2823.
322. Cannon, J.L., et al., *CD43 interaction with ezrin-radixin-moesin (ERM) proteins regulates T-cell trafficking and CD43 phosphorylation.* Mol Biol Cell, 2011. **22**(7): p. 954-63.
323. Allenspach, E.J., et al., *ERM-dependent movement of CD43 defines a novel protein complex distal to the immunological synapse.* Immunity, 2001. **15**(5): p. 739-50.
324. Tong, J., et al., *CD43 regulation of T cell activation is not through steric inhibition of T cell-APC interactions but through an intracellular mechanism.* J Exp Med, 2004. **199**(9): p. 1277-83.
325. Seo, W. and H.J. Ziltener, *CD43 processing and nuclear translocation of CD43 cytoplasmic tail are required for cell homeostasis.* Blood, 2009. **114**(17): p. 3567-3577.
326. Ostberg, J.R., R.K. Barth, and J.G. Frelinger, *The Roman god Janus: a paradigm for the function of CD43.* Immunol Today, 1998. **19**(12): p. 546-50.

327. Sabri, S., et al., *Glycocalyx modulation is a physiological means of regulating cell adhesion.* J Cell Sci, 2000. **113 (Pt 9)**: p. 1589-600.
328. Saftig, P. and K. Reiss, *The "A Disintegrin And Metalloproteases" ADAM10 and ADAM17: Novel drug targets with therapeutic potential?* European Journal of Cell Biology, 2011. **90**(6-7): p. 527-535.
329. Seegar, T.C.M., et al., *Structural Basis for Regulated Proteolysis by the alpha-Secretase ADAM10.* Cell, 2017. **171**(7): p. 1638-1648 e7.
330. Stawikowska, R., et al., *Activity of ADAM17 (a Disintegrin and Metalloprotease 17) Is Regulated by Its Noncatalytic Domains and Secondary Structure of its Substrates.* Journal of Biological Chemistry, 2013. **288**(31): p. 22871-22879.
331. Janes, P.W., et al., *Adam meets Eph: An ADAM substrate recognition module acts as a molecular switch for ephrin cleavage in trans.* Cell, 2005. **123**(2): p. 291-304.
332. Hartmann, D., et al., *The disintegrin/metalloprotease ADAM 10 is essential for Notch signalling but not for alpha-secretase activity in fibroblasts.* Human Molecular Genetics, 2002. **11**(21): p. 2615-2624.
333. Wetzel, S., L. Seipold, and P. Saftig, *The metalloproteinase ADAM10: A useful therapeutic target?* Biochimica Et Biophysica Acta-Molecular Cell Research, 2017. **1864**(11): p. 2071-2081.
334. Maretzky, T., et al., *The Cytoplasmic Domain of A Disintegrin and Metalloproteinase 10 (ADAM10) Regulates Its Constitutive Activity but Is Dispensable for Stimulated ADAM10-dependent Shedding.* Journal of Biological Chemistry, 2015. **290**(12): p. 7416-7425.
335. Matthews, A.L., et al., *Regulation of A disintegrin and metalloproteinase (ADAM) family sheddases ADAM10 and ADAM17: The emerging role of tetraspanins and rhomboids.* Platelets, 2017. **28**(4): p. 333-341.
336. Dornier, E., et al., *TspanC8 tetraspanins regulate ADAM10/Kuzbanian trafficking and promote Notch activation in flies and mammals.* Journal of Cell Biology, 2012. **199**(3): p. 481-496.
337. Haining, E.J., et al., *The TspanC8 Subgroup of Tetraspanins Interacts with A Disintegrin and Metalloprotease 10 (ADAM10) and Regulates Its Maturation and Cell Surface Expression.* Journal of Biological Chemistry, 2012. **287**(47).
338. Prox, J., et al., *Tetraspanin15 regulates cellular trafficking and activity of the ectodomain sheddase ADAM10.* Cellular and Molecular Life Sciences, 2012. **69**(17): p. 2919-2932.
339. Baxter, A.E., et al., *Macrophage infection via selective capture of HIV-1-infected CD4+ T cells.* Cell Host Microbe, 2014. **16**(6): p. 711-21.
340. Seaman, M.S., et al., *Tiered categorization of a diverse panel of HIV-1 Env pseudoviruses for assessment of neutralizing antibodies.* J Virol, 2010. **84**(3): p. 1439-52.
341. McCoy, L.E., et al., *Potent and broad neutralization of HIV-1 by a llama antibody elicited by immunization.* The Journal of experimental medicine, 2012. **209**(6): p. 1091-103.
342. Lefebvre, J.C., et al., *Altered glycosylation of leukosialin, CD43, in HIV-1-infected cells of the CEM line.* The Journal of experimental medicine, 1994. **180**(5): p. 1609-17.
343. Descheny, L., et al., *Ameliorating skin-homing receptors on malignant T cells with a fluorosugar analog of N-acetylglucosamine: P-selectin ligand is a more*

sensitive target than E-selectin ligand. J Invest Dermatol, 2006. **126**(9): p. 2065-73.
344. Agarwal, K., et al., *Inhibition of mucin-type O-glycosylation through metabolic processing and incorporation of N-thioglycolyl-D-galactosamine peracetate (Ac5GalNTGc).* J Am Chem Soc, 2013. **135**(38): p. 14189-97.
345. Alsinet, E., et al., *Differential effects of anti-CD45 monoclonal antibody on human B cell proliferation: a monoclonal antibody recognizing a neuraminidase-sensitive epitope of the T200 molecule enhances anti-immunoglobulin-induced proliferation.* Eur J Immunol, 1990. **20**(12): p. 2801-4.
346. Huang, J., et al., *Broad and potent neutralization of HIV-1 by a gp41-specific human antibody.* Nature, 2012. **491**(7424): p. 406-12.
347. Buchacher, A., et al., *Generation of human monoclonal antibodies against HIV-1 proteins; electrofusion and Epstein-Barr virus transformation for peripheral blood lymphocyte immortalization.* AIDS research and human retroviruses, 1994. **10**(4): p. 359-69.
348. Verkoczy, L., G. Kelsoe, and B.F. Haynes, *HIV-1 envelope gp41 broadly neutralizing antibodies: hurdles for vaccine development.* PLoS pathogens, 2014. **10**(5): p. e1004073-e1004073.
349. Sanders, R.W., et al., *A next-generation cleaved, soluble HIV-1 Env trimer, BG505 SOSIP.664 gp140, expresses multiple epitopes for broadly neutralizing but not non-neutralizing antibodies.* PLoS pathogens, 2013. **9**(9): p. e1003618-e1003618.
350. Huang, J., et al., *Broad and potent HIV-1 neutralization by a human antibody that binds the gp41-gp120 interface.* Nature, 2014. **515**(7525): p. 138-42.
351. Falkowska, E., et al., *Broadly neutralizing HIV antibodies define a glycan-dependent epitope on the prefusion conformation of gp41 on cleaved envelope trimers.* Immunity, 2014. **40**(5): p. 657-68.
352. Lee, J.H., et al., *Antibodies to a conformational epitope on gp41 neutralize HIV-1 by destabilizing the Env spike.* Nature communications, 2015. **6**: p. 8167-8167.
353. Ferguson, A.L., et al., *Computational prediction of broadly neutralizing HIV-1 antibody epitopes from neutralization activity data.* PloS one, 2013. **8**(12): p. e80562-e80562.
354. Walker, L.M., et al., *Broad neutralization coverage of HIV by multiple highly potent antibodies.* Nature, 2011. **477**(7365): p. 466-70.
355. Wu, X., et al., *Rational design of envelope identifies broadly neutralizing human monoclonal antibodies to HIV-1.* Science (New York, N.Y.), 2010. **329**(5993): p. 856-61.
356. Thali, M., et al., *Characterization of conserved human immunodeficiency virus type 1 gp120 neutralization epitopes exposed upon gp120-CD4 binding.* Journal of virology, 1993. **67**(7): p. 3978-88.
357. Moore, J.P., et al., *Immunochemical analysis of the gp120 surface glycoprotein of human immunodeficiency virus type 1: probing the structure of the C4 and V4 domains and the interaction of the C4 domain with the V3 loop.* Journal of virology, 1993. **67**(8): p. 4785-96.
358. Sanders, R.W., et al., *The mannose-dependent epitope for neutralizing antibody 2G12 on human immunodeficiency virus type 1 glycoprotein gp120.* Journal of virology, 2002. **76**(14): p. 7293-305.

359. Blankson, J.N., D. Persaud, and R.F. Siliciano, *The challenge of viral reservoirs in HIV-1 infection.* Annual review of medicine, 2002. **53**(November): p. 557-93.
360. Bol, S.M., et al., *Donor variation in in vitro HIV-1 susceptibility of monocyte-derived macrophages.* Virology, 2009. **390**(2): p. 205-11.
361. Kumar, A. and G. Herbein, *The macrophage: a therapeutic target in HIV-1 infection.* Mol Cell Ther, 2014. **2**: p. 10.
362. Schacker, T., et al., *Productive infection of T cells in lymphoid tissues during primary and early human immunodeficiency virus infection.* Journal of Infectious Diseases, 2001. **183**(4): p. 555-562.
363. Zhang, Z.Q., et al., *Sexual transmission and propagation of SIV and HIV in resting and activated CD4(+) T cells.* Science, 1999. **286**(5443): p. 1353-1357.
364. Cenker, J.J., R.D. Stultz, and D. McDonald, *Brain Microglial Cells Are Highly Susceptible to HIV-1 Infection and Spread.* AIDS Res Hum Retroviruses, 2017. **33**(11): p. 1155-1165.
365. Dunne, J.L., et al., *Mac-1, but not LFA-1, uses intercellular adhesion molecule-1 to mediate slow leukocyte rolling in TNF-alpha-induced inflammation.* Journal of Immunology, 2003. **171**(11): p. 6105-6111.
366. Rosenstein, Y., et al., *CD43, a molecule defective in Wiskott-Aldrich syndrome, binds ICAM-1.* Nature, 1991. **354**(6350): p. 56-58.
367. Axelsson, B., et al., *Induction of Aggregation and Enhancement of Proliferation and Il-2 Secretion in Human T-Cells by Antibodies to Cd43.* Journal of Immunology, 1988. **141**(9): p. 2912-2917.
368. Nong, Y.H., et al., *A Monoclonal-Antibody to Sialophorin (CD43) Induces Homotypic Adhesion and Activation of Human-Monocytes.* Journal of Experimental Medicine, 1989. **170**(1): p. 259-267.
369. Manjunath, N., et al., *Targeted Disruption of Cd43 Gene Enhances T-Lymphocyte Adhesion.* Journal of Immunology, 1993. **151**(3): p. 1528-1534.
370. Srinivas, R.V., et al., *Enhanced susceptibility to human immunodeficiency virus infection in CD4+ T lymphocytes genetically deficient in CD43.* AIDS Res Hum Retroviruses, 1995. **11**(9): p. 1015-21.
371. Meyerhoff, R.R., et al., *HIV-1 Consensus Envelope-Induced Broadly Binding Antibodies.* AIDS Res Hum Retroviruses, 2017. **33**(8): p. 859-868.
372. Pejchal, R., et al., *A potent and broad neutralizing antibody recognizes and penetrates the HIV glycan shield.* Science, 2011. **334**(6059): p. 1097-103.
373. *database of broadly neutralizing antibodies to HIV-1 | bNAber*.
374. Sabri, S., et al., *Glycocalyx modulation is a physiological means of regulating cell adhesion.* Journal of Cell Science, 2000. **113**(9): p. 1589-1600.
375. Bazil, V. and J.L. Strominger, *Metalloprotease and Serine-Protease Are Involved in Cleavage of CD43, CD44, and CD16 from Stimulated Human Granulocytes - Induction of Cleavage of L-Selectin Via CD16.* Journal of Immunology, 1994. **152**(3): p. 1314-1322.
376. Campanero, M.R., et al., *Down-regulation by tumor necrosis factor-alpha of neutrophil cell surface expression of the sialophorin CD43 and the hyaluronate receptor CD44 through a proteolytic mechanism.* Eur J Immunol, 1991. **21**(12): p. 3045-8.
377. Lopez, S., et al., *CD43 (sialophorin, leukosialin) shedding is an initial event during neutrophil migration, which could be closely related to the spreading of adherent cells.* Cell Adhes Commun, 1998. **5**(2): p. 151-60.

378. Nathan, C., et al., *Albumin Inhibits Neutrophil Spreading and Hydrogen-Peroxide Release by Blocking the Shedding of Cd43 (Sialophorin, Leukosialin).* Journal of Cell Biology, 1993. **122**(1): p. 243-256.
379. Rieu, P., et al., *Human neutrophils release their major membrane sialoprotein, leukosialin (CD43), during cell activation.* Eur J Immunol, 1992. **22**(11): p. 3021-6.
380. Bazil, V. and J.L. Strominger, *CD43, the major sialoglycoprotein of human leukocytes, is proteolytically cleaved from the surface of stimulated lymphocytes and granulocytes.* Proc Natl Acad Sci U S A, 1993. **90**(9): p. 3792-6.
381. Onami, T.M., et al., *Dynamic regulation of T cell immunity by CD43.* Journal of Immunology, 2002. **168**(12): p. 6022-6031.
382. Bilyy, R.O., et al., *Macrophages discriminate glycosylation patterns of apoptotic cell-derived microparticles.* J Biol Chem, 2012. **287**(1): p. 496-503.
383. Miterski, B., et al., *PTPRC (CD45) is not associated with multiple sclerosis in a large cohort of German patients.* BMC Med Genet, 2002. **3**: p. 3.
384. Saga, Y., et al., *Sequences of Ly-5 cDNA: isoform-related diversity of Ly-5 mRNA.* Proc Natl Acad Sci U S A, 1986. **83**(18): p. 6940-4.
385. Streuli, M., et al., *Differential usage of three exons generates at least five different mRNAs encoding human leukocyte common antigens.* J Exp Med, 1987. **166**(5): p. 1548-66.
386. Lefebvre, J.C., et al., *Altered sialylation of CD45 in HIV-1-infected T lymphocytes.* Virology, 1994. **199**(2): p. 265-74.
387. Doitsh, G., et al., *Cell death by pyroptosis drives CD4 T-cell depletion in HIV-1 infection.* Nature, 2014. **505**(7484): p. 509-14.
388. Grivel, J.C., N. Malkevitch, and L. Margolis, *Human immunodeficiency virus type 1 induces apoptosis in CD4(+) but not in CD8(+) T cells in ex vivo-infected human lymphoid tissue.* J Virol, 2000. **74**(17): p. 8077-84.
389. Feng, G. and N. Kaplowitz, *Mechanism of staurosporine-induced apoptosis in murine hepatocytes.* Am J Physiol Gastrointest Liver Physiol, 2002. **282**(5): p. G825-34.
390. Perez, B., et al., *Apoptotic cells can deliver chemotherapeutics to engulfing macrophages and suppress inflammatory cytokine production.* J Biol Chem, 2012. **287**(19): p. 16029-36.
391. McKenzie, B.A., et al., *Caspase-1 inhibition prevents glial inflammasome activation and pyroptosis in models of multiple sclerosis.* Proc Natl Acad Sci U S A, 2018. **115**(26): p. E6065-E6074.
392. Ellies, L.G., et al., *The CD43 130-kD peripheral T-cell activation antigen is downregulated in thymic positive selection.* Blood, 1996. **88**(5): p. 1725-1732.
393. Jones, A.T., et al., *Characterization of the Activation-Associated Isoform of Cd43 on Murine T-Lymphocytes.* Journal of Immunology, 1994. **153**(8): p. 3426-3439.
394. Alcaide, P., et al., *The 130-kDa glycoform of CD43 functions as an E-selectin ligand for activated th1 cells In Vitro and in delayed-type hypersensitivity reactions In Vivo.* Journal of Investigative Dermatology, 2007. **127**(8): p. 1964-1972.
395. Matsumoto, M., et al., *CD43 functions as a ligand for E-selectin on activated T cells.* Journal of Immunology, 2005. **175**(12): p. 8042-8050.

396. Piller, F., et al., *Human Lymphocyte-T Activation Is Associated with Changes in O-Glycan Biosynthesis.* Journal of Biological Chemistry, 1988. **263**(29): p. 15146-15150.
397. Giordanengo, V., et al., *Epigenetic reprogramming of UDP-N-acetylglucosamine 2-epimerase/N-acetylmannosamine kinase (GNE) in HIV-1-infected CEM T cells.* FASEB J, 2004. **18**(15): p. 1961-3.
398. Weber, S., et al., *Leukosialin (CD43) is proteolytically cleaved from stimulated HMC-1 cells.* Immunobiology, 1997. **197**(1): p. 82-96.
399. Chauvier, D., et al., *Broad-spectrum caspase inhibitors: from myth to reality?* Cell Death and Differentiation, 2007. **14**(2): p. 387-391.
400. McIlwain, D.R., T. Berger, and T.W. Mak, *Caspase Functions in Cell Death and Disease.* Cold Spring Harbor Perspectives in Biology, 2013. **5**(4).
401. Slee, E.A., C. Adrain, and S.J. Martin, *Executioner caspase-3,-6, and-7 perform distinct, non-redundant roles during the demolition phase of apoptosis.* Journal of Biological Chemistry, 2001. **276**(10): p. 7320-7326.
402. Terlizzi, M., et al., *Pharmacological inhibition of caspase-8 limits lung tumour outgrowth.* British Journal of Pharmacology, 2015. **172**(15): p. 3917-3928.
403. Kim, J.Y. and J.H. Park, *ROS-dependent caspase-9 activation in hypoxic cell death.* Febs Letters, 2003. **549**(1-3): p. 94-98.
404. Duncan, C.J., et al., *High-multiplicity HIV-1 infection and neutralizing antibody evasion mediated by the macrophage-T cell virological synapse.* J Virol, 2014. **88**(4): p. 2025-34.
405. O'Neil-Andersen, N.J. and D.A. Lawrence, *Differential modulation of surface and intracellular protein expression by T cells after stimulation in the presence of monensin or brefeldin A.* Clin Diagn Lab Immunol, 2002. **9**(2): p. 243-50.
406. Mambole, A.S., et al., *The cleavage of neutrophil leukosialin (CD43) by cathepsin G releases its extracellular domain and triggers its intramembrane proteolysis by presenilin/gamma-secretase.* Journal of Biological Chemistry, 2008. **283**(35): p. 23627-23635.
407. Edwards, D.R., M.M. Handsley, and C.J. Pennington, *The ADAM metalloproteinases.* Mol Aspects Med, 2008. **29**(5): p. 258-89.
408. Nagata, E., et al., *Inositol hexakisphosphate kinase-2, a physiologic mediator of cell death.* J Biol Chem, 2005. **280**(2): p. 1634-40.
409. Eda, S., M. Yamanaka, and M. Beppu, *Carbohydrate-mediated phagocytic recognition of early apoptotic cells undergoing transient capping of CD43 glycoprotein.* The Journal of biological chemistry, 2004. **279**(7): p. 5967-74.
410. Oguri, E., et al., *Clearance of CD43-capped cells by macrophages: capping alone leads to phagocytosis.* Biol Pharm Bull, 2012. **35**(4): p. 551-8.
411. Yamanaka, M., S. Eda, and M. Beppu, *Carbohydrate chains and phosphatidylserine successively work as signals for apoptotic cell removal.* Biochemical and Biophysical Research Communications, 2005. **328**(1): p. 273-280.
412. Miki, Y., K. Hirano, and M. Beppu, *Macrophage recognition of thiol-group oxidized cells: recognition of carbohydrate chains by macrophage surface nucleolin as apoptotic cells.* Biosci Biotechnol Biochem, 2012. **76**(11): p. 2068-74.
413. Ravichandran, K.S., *Beginnings of a good apoptotic meal: the find-me and eat-me signaling pathways.* Immunity, 2011. **35**(4): p. 445-55.
414. Sommer, A., et al., *Phosphatidylserine exposure is required for ADAM17 sheddase function.* Nature Communications, 2016. **7**.

415. Seegar, T.C.M., et al., *Structural Basis for Regulated Proteolysis by the alpha-Secretase ADAM10.* Cell, 2017. **171**(7): p. 1638-+.